



# IBCM

V International Baltic  
Conference on Magnetism

2023

# Book of Abstracts

# IBCM-2023

## CONTENTS

Plenary lectures .....	3
Invited talks .....	10
Oral talks .....	34
Poster presentations .....	113
Author index.....	195

# Plenary lectures

# **3D-Direct laser writing for dielectric photonics based on Bloch surface waves**

Fedyanin A.

Faculty of Physics, Lomonosov Moscow State University, Russia

Modern integrated photonic platforms should combine low-loss guiding, spectral flexibility, high light confinement, and close packing of optical components. One of the prominent platforms represents dielectric nanostructures combined with photonic band gap media that manipulate low-loss Bloch surface waves (BSW). BSW platform is all-dielectric counterpart to surface plasmon-polariton one, but it has the advantages of long propagation length (up to cm in visible), ultrawide spectral range of operation (from UV to mid-IR and THz), and access to the confined electromagnetic field making BSW applicable for integrated photonics, sensing, and other fields. Here, we reviewed several ways for directed and highly efficient BSW excitation using dielectric nanostructures of various designs on the photonic crystal (PC) surface. First, we achieve color-selective directional excitation of BSW mediated by Mie resonances in a semiconductor nanoparticle printed on the PC surface using laser-induced backward transfer technique. We show that a single silicon nanoparticle can be used as a subwavelength multiplexer switching the BSW excitation direction from forward to backward within the 30 nm spectral range with its central wavelength governed by the nanoparticle size. Numerical simulation gives an estimate of 8% BSW excitation efficiency with a single nanoparticle. Second, we show a new concept of 3D out-of-plane coupler which is a microscale prism exploiting frustrated total internal reflection in the Otto configuration for unidirectional excitation of waveguide modes with efficiency up to 100%. Polymer microprisms are printed using two-photon laser lithography and allow transferring more than 40% of the incident light energy into BSWs. The couplers enable focusing BSWs simultaneously with their excitation. Finally, halide perovskite micro- and nanolasers were integrated with BSW platform and demonstrated directional BSW excitation with the efficiency of over 16%. A pronounced BSW beam steering effect is shown.

# Flexomagnetism: “bending horseshoe magnets” at nanoscale

Pyatakov A. \*, Kaminskiy A.

Lomonosov Moscow State University, 119991, Leninskie gory 1, Moscow, Russia

\*Pyatakov@physics.msu.ru

Films of magnetic materials are widely used in magnetic memory and spintronics. In epitaxial films the strain due to the lattice misfit with the substrate amounts to several percent, well above the strength limit of bulk materials that gives a way for strain engineering of material properties. With the advent of two- dimensional (2D) graphene-like materials, and, quite recently, the magnetic 2D materials found in 2017 [1,2], the idea of a thin film and its flexibility came to its ultimate limit and gave rise to the special strain-related fundamental and applied research areas of straintronics [3].

Among various types of deformation the *flexural* one is of special interest. Flexure or bending is a special type of deformation characterized by strain gradient. In contrast to the quite common flexoelectric phenomena (the strain-gradient induced electric polarization) the flexomagnetic effects [4,5] are nontrivial and occur only in media with special symmetry of magnetic ordering.

In this report the mechanism of flexomagnetism as well as major factors of flexomagnetic effect enhancement in van der Waals magnets is discussed. The vivid illustration of such a mechanism can be the decompensation of layer magnetizations in an antiferromagnetic bilayer material (fig.1): the exchange interaction in the stretched bottom layer is weaker than in the top one.

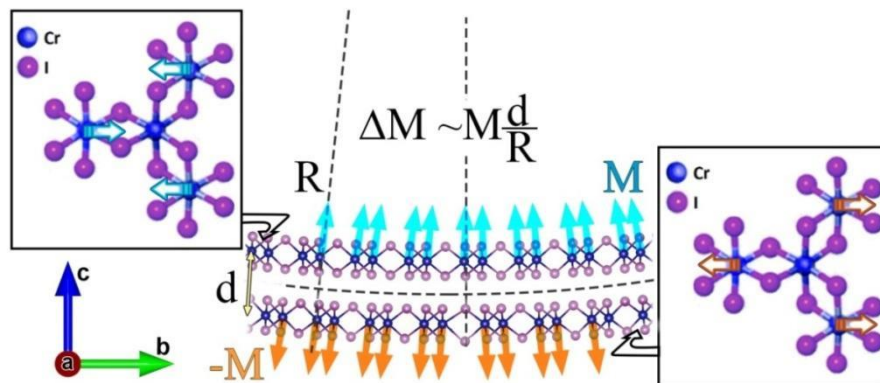


Fig. 1 The flexomagnetic effect in antiferromagnetic bilayer material:  $\mathbf{M}$  is a moment of a single ion in the antiferromagnetic sublattice,  $d$  is the distance between the middle lines of the top and bottom,  $R$  is the curvature radius that is inversely proportional to a strain gradient along  $c$ -axis. The top views of relative displacements of magnetic ions in the top and the bottom layers are shown in the insets.

A. Pyatakov and A. Kaminskiy acknowledge the support of Basis Foundation (Junior Leader Program).

[1] B. Huang *et al.*, Nature, 546, 270 (2017).

[2] C. Gong *et al.*, Nature, 546, 265 (2017).

[3] A.A. Bukharaev, A.K. Zvezdin, A.P. Pyatakov, Yu.K. Fetisov, Phys. Usp., 61, 1288 (2018).

[4] E. A. Eliseev *et al* Phys. Rev. B, 79 165433 (2009).

[5] P. Lukashev R. F. Sabirianov, Phys. Rev. B 82 94417 (2010).

# Laser-induced spin waves in the center and at the edge of the Brillouin zone

Kalashnikova A. \*

Ioffe Institute, 194021, Politekhnikeskaya 26, St. Petersburg, Russia

\*kalashnikova@mail.ioffe.ru

Magnonics studies generation, propagation, control, and detection of spin waves, as well as the corresponding media and structures for efficient spin wave transducers, waveguides etc. Magnon wavelengths range from tens of microns to nanometers, while their frequencies range from giga- to terahertz, and their propagation can be free from accompanying Joule losses. Therefore, magnonics is considered as a promising direction for development of a component base for future information processing devices [1]. However, magnonics faces several challenges such as generation of waves with large wave vectors and frequencies, controlling their propagation, and integration of magnonic elements with components of electronics or photonics.

In this talk, we show how femtosecond laser pulses can facilitate development of magnonics by tackling some of these challenges. We present a brief overview of femtomagnetic phenomena [2,3] leading to the generation of spin waves, discuss limitations for their frequencies and wavevectors [4], and show how features of the interaction of short laser pulses with magnetic materials can be used to control the properties of spin waves [5].

Specifically, we consider laser-induced generation of magnetostatic waves – spin waves near the centre of the Brillouin zone – in anisotropic magnetic metallic films [4-6], which are already used in magnonics. We also suggest implementation of a tuneable source of magnetostatic packets [7] and of waves with unidirectional propagation [8].

We also consider the laser-induced excitation of coherent two-magnon modes characterized by highest possible wavevectors and frequencies at the edge of the Brillouin zone. We analyse how such excitation is related to the ultrafast control of the exchange interaction [9,10]. We show that such spin dynamics, although not manifested as macroscopic magnetization dynamics, can be detected optically. This raises an interesting question on the possibility of using such spin excitations at the edge of the Brillouin zone for ultrafast information processing.

Author is extremely grateful to the members of the Ferroics Physics Laboratory at Ioffe Institute for fruitful collaboration. Support by RFBR grant No. 19-52-12065 is acknowledged.

- [1] A. Barman et al., *J. Phys.: Condens. Matter*, **33** (2021) 413001.
- [2] A. V. Kimel et al., *Phys. Rep.* **852**, 1 (2020).
- [3] N. E. Khokhlov et al., *Tech. Phys. Lett.*, **67** (2022) 2335.
- [4] N. E. Khokhlov et al., *Phys. Rev. Appl.*, **12** (2019) 044044.
- [5] Ia. A. Filatov et al., *Appl. Phys. Lett.*, **120** (2022) 112404.
- [6] L. A. Shelukhin et al., *Phys. Rev. Appl.*, **14** (2020) 034061.
- [7] N. E. Khokhlov et al., *J. Magn. Magn. Mater.*, **534** (2021) 168018.
- [8] P. I. Gerevenkov et al., *Phys. Rev. Appl.*, **19** (2023) 024062.
- [9] A. E. Fedianin et al., *Phys. Rev. B*, **107** (2023) 144430.
- [10] F. Formisano et al., arXiv:2303.06996.

# Magnetic Phase Transitions in $RMn_2Si_2$ Intermetallics

Mushnikov N. \*, Gerasimov E.

Institute of Metal Physics, Ural Branch of RAS, S. Kovalevskaya 18, 620108, Ekaterinburg, Russia

\*corresponding author [mushnikov@imp.uran.ru](mailto:mushnikov@imp.uran.ru)

The ternary  $RMn_2X_2$  ( $R$  is a rare-earth metal;  $X$  - Si or Ge) compounds crystallize in the layered tetragonal  $ThCr_2Si_2$ -type (space group  $I4mmm$ ) structure in which each type of the atoms occupy separate layers stacked along the  $c$ -axis in the sequence  $-R-X-Mn-X-R-$ . Mn atoms form a ferromagnetic ordering within the Mn layer. Relatively weak interlayer exchange interaction can be negative or positive. The compounds demonstrate an unusual variation of the interlayer Mn-Mn ordering from antiferromagnetic (AF) to ferromagnetic (FM) when the distance between Mn ions in the layer increases. The ordering is also affected by the  $R$ -Mn exchange interaction. Therefore, the compounds exhibit unique set of magnetic structures and magnetic phase transitions, which attracts significant attention of the researchers.

We studied magnetic, magnetovolume, thermal and magnetotransport properties of quasi-ternary compounds  $La_{1-x}R_xMn_2Si_2$ , ( $R$ = Sm, Gd, Tb, Dy). In these systems, substitution of different  $R$  atoms allows us to change gradually the interatomic distances, interlayer exchange interactions and contributions of  $R$  and Mn magnetic subsystems to the magnetic anisotropy of the compounds. For  $La_{1-x}Sm_xMn_2Si_2$ , large linear and volume magnetostrictions and positive magnetoresistance were observed at the field-induced AF-FM transition.

For the  $La_{1-x}Gd_xMn_2Si_2$  and  $La_{1-x}Tb_xMn_2Si_2$  compounds in the low-temperature region, negative Mn-Mn interlayer exchange interactions and the easy-axis type magnetocrystalline anisotropy of the manganese sublattice leads to the appearance of an unexpected magnetic structures. For the compounds with Gd, the resulting magnetic moment is oriented perpendicular to the direction of the easy  $c$ -axis of the Mn sublattice. For the Tb-containing compounds, a competition of the negative Tb-Mn and Mn-Mn interlayer exchange interactions and strong uniaxial magnetic anisotropy of both Tb and Mn sublattices lead to formation of a frustrated magnetic state of Tb ions, which prevents magnetic ordering in the Tb sublattice.

The origin of the magnetic phase transition in  $RMn_2Si_2$  intermetallics was explored within the *ab initio* DFT-based approach. The calculated exchange interaction parameters indicate that the antiferromagnetic interlayer ordering is stabilized by a dominant negative interaction via Si-Si dimer, which forms the bonding molecular orbital acting as a mediator in the Mn  $d$  superexchange mechanism.

The obtained results show a significant role of the Mn-Mn and Mn- $R$  exchange interactions and magnetic anisotropy in formation of magnetic structures and realization of magnetic phase transitions in layered intermetallic compounds.

Support by Russian Science Foundation (project No. 23-12-00265) is acknowledged.

# Programming of the mechanical properties and magnetic response of magnetoactive elastomers

Kramarenko E. \*

Faculty of Physics, Lomonosov Moscow State University, 119991, Leninskie gory 1, Moscow, Russia

\*kram@polly.phys.msu.ru

Magnetoactive elastomers (MAEs) are composite materials consisting of soft polymer networks filled with magnetic microparticles [1-3]. Belonging to the class of smart materials, they are attracting ever-increasing interest nowadays. A complex magneto-mechanical coupling induced in these materials in magnetic fields gives us an effective tool to significantly alter and to control a number of physical properties of these composites by the application of a magnetic field. Among the most prominent effects observed in MAEs are magnetorheological and magnetodeformation effects, magnetically controlled dielectric and electric properties [1,2]. The high magnetic response of these materials is vital for many practical applications such as peristaltic systems, magnetic field sensors and soft robotics.

Rearrangement of magnetic particles in a soft polymer matrix caused by magnetic interactions in magnetic fields is the key reason of MAE's magnetic response. Its magnitude depends on the elastic modulus of the polymer matrix as well as the magnetic properties, concentration, and distribution of the magnetic particles. The softer is the matrix, the larger displacements of the particles from their initial equilibrium positions are available in magnetic fields, leading to larger magnetic effects. Anisotropic distribution of the magnetic particles produces larger magnetic response.

In this talk, we report on magnetically controlled properties of MAEs, discuss the possible ways to tune the mechanical properties of these composites and their magnetic response by altering properties of two main components, i.e., polymer matrix and magnetic particles. We demonstrate, how "magnetic activity" of the filler particles allows to use the magnetic field as a tool to produce anisotropic MAEs and how additional "thermal activity" of new polymer matrices allows to program magneto-mechanical coupling in a complex way by tuning temperature and magnetic field. Finally, prospects for practical application are discussed.

Financial support of the Russian Science Foundation (project No. 19-13-00340-II) is gratefully acknowledged.

[1] M. Shamonin, E.Y. Kramarenko, In: Novel Magnetic Nanostructures, Elsevier, 221 (2018).

[2] E.Yu. Kramarenko, G.V. Stepanov, A.R. Khokhlov, INEOS OPEN, 2, 178 (2020).

[3] Iu. Alekhina, E. Kramarenko, L. Makarova, N. Perov. In: Magnetic Materials and Technologies for Medical Applications. Ed.A.M. Tishin, Elsevier Ltd., 501 (2022).



# Ultrasensitive Magnetic Methods for Biomedical Applications, Targeted Drug Delivery and *in vitro* Diagnostics

Nikitin P.

Prokhorov General Physics of the Russian Academy of Sciences, 119991, Vavilov str 38, Moscow, Russia

Email: nikitin@kapella.gpi.ru

Magnetic nanoparticles (MP) based on iron oxides possess a wide array of unique properties and are promising for many biomedical applications. Iron is present in the human body in various forms (about 5 g total) that are vital for the organism's functioning. Iron nanooxides feature low toxicity and are approved in many countries for intravenous injecting to humans. For MP applications in life science research, the author developed several original ultrasensitive magnetic and optical methods. The related devices were effectively used for development of new hybrid magnetic agents for suppression of tumors in animals, as well as for biochemical diagnostics.

Promising nanoagents, which perfectly work *in vitro*, nearly always become therapeutically inconsistent *in vivo* because of rapid elimination from the bloodstream by the mononuclear phagocyte system (MPS). We have developed a breakthrough technology in nanomedicine called "MPS-cytoblockade", which enables considerable (32-fold) prolongation of blood circulation time of almost any nanoagent to enhance its therapeutic efficacy [1]. It was demonstrated that MPS-cytoblockade considerably improved drug delivery to five types of tumors of various nature: from melanoma to breast cancer, including two types of human tumors inoculated into mice. In particular, the efficiency of "active" magnetic delivery of drugs to cancerous tumors in animals increased 23-fold. Significant suppression of tumors was achieved while minimizing side effects [2]. For the first time, it was shown that targeting hybrid (magnetic and polymeric with IR775 dye) nanoparticles with lectins to the glycosylation profile of cancer cells, followed by a photodynamic therapy, represents a promising strategy for the treatment of aggressive tumors. Such hybrid resulted in 100% inhibition of tumor growth in mice and has great potential to become a highly effective oncotheranostic agent [3].

An important part of these studies was the investigation of the toxicity of magnetic nanocarriers and products of their *in vivo* biodegradation [4,5]. It was found that MP biodegradation in animals enhances gene expression of iron-associated proteins, increases the levels of erythrocytes and hemoglobin in the blood of animals, and also does not cause significant toxicity of MP.

Based on the use of MPs as labels for immunoreactions, a variety of express methods were developed for *in vitro* measuring in human biological fluids the concentrations of small molecules, protein markers of diseases, and extracellular vesicles (EV). The latter, being carriers of protein and DNA fragments of cancer cells, are promising for non-invasive "liquid biopsy". The limit of EV detection in clinical samples of patients with breast cancer was  $3.7 \cdot 10^5$  pcs/ $\mu$ L [6]. That is 1-2 orders of magnitude better than that of the most sensitive commercial tests. Another developed method enables rapid (20 min) measuring concentrations of small molecules, in particular ochratoxin A, in foods from 11 pg/ml in a dynamic range of 5 orders of magnitude [7]. That is at the level of the best reference analytical techniques, which are much more laborious and time consuming.

[1] M.P. Nikitin, et al. Nature Biomedical Engineering, 4, 717 (2020).

[2] E.N. Mochalova, et al. Int. J. Mol. Sci., 24, 10623 (2023).

[3] V.L. Kovalenko, et al. Pharmaceutics, 15, 92 (2023).

[4] I.V. Zelepukin, et al. ACS Nano, 15, 11341 (2021).

[5] A.V. Yaremenko, et al. Journal of Nanobiotechnology, 20, 535. (2022).

[6]. V.A. Bragina, et al. Nanomaterials, 12, 1579 (2022).

[7]. A.V. Orlov, et al. Food Chemistry, 383, 132427 (2022).

# Invited talks

## A few stories on artificial magnetism

Lapine M. <sup>a,b,c,\*</sup>

<sup>a</sup>*ITMO University, Saint Petersburg, 197101 Russia*

<sup>b</sup>*University of Technology Sydney, 2007 NSW, Australia*

<sup>c</sup>*Harbin Engineering University, Harbin 150001, China*

\*mikhail.lapine@gmail.com

Even if the emergence of metamaterials is typically attributed to the quest for negative refraction, one of the key initial aspects was set in the creation of artificial magnetic response [1], which essentially relies on inducing loop currents in artificial resonators of an appropriate scale [2]. Analytical theory for the effective permeability of such systems was developed two decades ago [3], and gave rise to a range of subsequent studies. I will review a few of these latter achievements, including light-weight artificial diamagnetism [4], interaction of magnetic and mechanical properties in metamaterials [5], wide-band negative permeability in nonlinear systems [6], as well as application of metamaterials for magnetic resonance imaging [7-8]. Further on, the ongoing drive towards optical magnetism has renewed interest in magnetic properties of dielectric Mie-resonators, which has inspired research on optical sorting of nanoparticles [9], and its continuation into acoustics. This overview will naturally lead into an outlook of the unresolved issues and collaboration prospects.

Research on the discrete metamaterials was supported by the Russian Science Foundation (grant no. 22-11-00153).

- [1] M. Gorkunov, M. Lapine and S. A. Tretyakov, *Crystallography Reports*, 51(6), 1048–1062 (2006)
- [2] R. Marqués, L. Jelinek, M. J. Freire, J. D. Baena and M. Lapine, *Proc. IEEE*, 99, 1660–1668 (2011)
- [3] M. Gorkunov, M. Lapine, E. Shamonina, and K. H. Ringhofer, *Eur. Phys. J. B*, 28, 263–269 (2002)
- [4] M. Lapine, A. K. Krylova, P. A. Belov, C. G. Poulton, R. C. McPhedran and Yu. S. Kivshar, *Phys. Rev. B*, 87, 024408 (2013)
- [5] M. Lapine, I. V. Shadrivov, D. A. Powell and Yu. S. Kivshar, *Nature Materials*, 11, 30–33 (2012)
- [6] M. Lapine, I. V. Shadrivov and Yu. S. Kivshar, *Sci. Rep.*, 2, 412 (2012)
- [7] M. J. Freire, L. Jelinek, R. Marqués, and M. Lapine, *J. Magn. Resonance* 203, 81–90 (2010)
- [8] A. P. Slobozhanyuk, A. V. Shchelokova, D. A. Dobrykh, P. S. Seregin, D. A. Powell, I. V. Shadrivov, A. G. Webb, P. A. Belov, and M. Lapine, *RAS Bulletin Physics* 86, S216–S221 (2022)
- [9] D. A. Shilkin, E. V. Lyubin, M. R. Shcherbakov, M. Lapine, and A. A. Fedyanin, *ACS Photonics* 4(9), 2312–2319 (2017)

## **Aptamer modified Au/Ni/Au nanodiscs for magnetomechanical cell surgery**

Sokolov A.<sup>a,\*</sup>, Lukyanenko A.<sup>a</sup>, Zabluda V.<sup>a</sup>, Borus A.<sup>a</sup>, Zamay G.<sup>b</sup>, Zamay T.<sup>b,c</sup>, Luzan N.<sup>b,c</sup>,  
Zamay S.<sup>c</sup>

<sup>a</sup> Kirensky Institute of Physics, Federal Research Center KSC SB RAS, 660036, Akademgorodok 50/38,  
Krasnoyarsk, Russia

<sup>b</sup> Krasnoyarsk State Medical University, Laboratory for Biomolecular and Medical Technologies, 660022,  
P. Zheleznyaka 1, Krasnoyarsk, Russia

<sup>c</sup> Federal Research Center KSC SB RAS, 660036, Akademgorodok 50, Krasnoyarsk, Russia

\* alexeys@iph.krasn.ru

One of the main problems of cancer treatment is the fight against metastases and individual cancer cells. In 2010, Kim et al proposed to use permalloy nanodiscs with a vortex magnetization structure to fight brain glioma cancer cells [1]. In a previous study, we have already shown an antitumor effect of nanodisks in vitro in cultured ascites cells and in vivo in mice with Ehrlich ascites carcinoma [2] and for Glioblastoma [3] when using magnetic nickel nanodiscs, 500 nm diameter and 50 nm thick, were coated with a gold layer in alternating magnetic field less than 100 Oe.

In this paper, we consider the technology of obtaining of magnetic nanodisks up to 1  $\mu\text{m}$  in diameter by optical lithography and electron beam deposition.

Three-layer Au/Ni/Au magnetic nanodisks with a quasi-dipole magnetization structure, immobilized by fluorescent dye molecules and DNA aptamers to human glioblastoma cells, and a software and hardware complex for remote control of the process of magnetomechanical microsurgery by exposure to alternating magnetic fields (up to 100 Hz) intensity (up to 200 Oe) demonstrate excellent prospects for use in medicine.

As a result of experimental and theoretical studies, the following were selected:

- (1) waveform, frequency, strength and duration of magnetic field exposure,
- (2) diameter, layer thickness, magnetic properties and nanodisc technology;
- (3) the mechanisms of interaction of magnetic nanodisks with molecular-cellular targets have been studied.

We are looking for physical-technical and chemical-technological and engineering solutions for magnetomechanical microsurgery of human brain glioblastoma. The signal shape, frequency, intensity and duration of the magnetic field are selected. The dimensions, magnetic properties and technology for obtaining magnetic nanodisks and their preparations with DNA aptamers are determined.

The efficiency of the presented solutions has been demonstrated in vitro on ascitic Ehrlich carcinoma cells and primary cultures of human lung cancer and glioblastoma, and in vivo on mice with ascitic and solid Ehrlich carcinoma and mice with drug immunosuppression, which underwent xenotransplantation of human brain glioblastoma cells. The proposed solutions can be used to develop tools and methods for microsurgery of other malignant neoplasms and their metastases.

This research was funded by the Regional State Autonomous Institution "Krasnoyarsk Regional Fund for Support of Scientific and Scientific and Technical Activities", (application code № 2022060108781) and with the support of a partner company JSC «NPP «Radiosviaz».

[1] D. Kim, Nat. Mater. 9, 165-171, (2010)

[2] P. Kim, Dokl Biochem Biophys, 466, 66–69, (2016)

[3] T. Zamay, Nucleic Acid Ther. 27, 2, 105-114 (2017)

## Biomimetic materials and tissue engineering

F. Senatov, P. Kovaleva, A. Zimina, A. Levin, S. Petrov,

S. Karshieva, E. Koudan

National University of Science and Technology “MISIS”, Center for Biomedical Engineering,

119049, Leninskiy 6s7, Moscow, Russia

\*Senatov@misis.ru

Over the past decade, we have seen the emergence and transition to new modern trends, such as 3D and 4D printing, smart prostheses, biomimetic materials and bioprinting.

Biomimetic polymer materials are widely used in different medical applications, especially as scaffolds in tissue engineering. Reverse engineering approaches, which include the study of native tissue and polymer using high-resolution microscopy and CT, combined with 3D bioprinting methods, allows the formation of biomimetic anisotropic structures that repeat the architecture of native tissue.

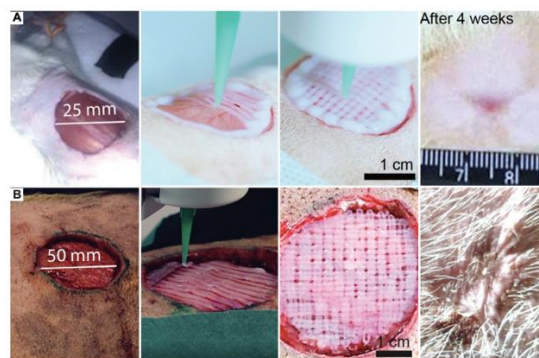


Figure 1 – In vivo bioprinting in animal experiments: (A) Rats and (B) minipigs. High levels of bioprinting fidelity have been demonstrated both in rats and in minipigs [5]

The in vivo experiments demonstrated that the employed original bioinks based on collagen hydrogel, platelet lysate, and dermal fibroblasts significantly improve the quality of wound healing processes in rat and minipig skin wounds. Further development and successful clinical applications of commercial in situ bioprinters are highly desirable.

SMP studies were funded by the Russian Science Foundation (RSF), project No. 21-73-20205; bio studies were funded by the Ministry of Science and Higher Education of the Russian Federation under the strategic academic Not acceptable leadership program “Priority 2030” (NUST MISIS).

[1] F. Senatov, et al., Effect of recombinant BMP-2 and erythropoietin on osteogenic properties of biomimetic PLA/PCL/HA and PHB/HA scaffolds in critical-size cranial defects model, *Materials Science & Engineering C* (2021)

[2] Fedor Senatov, et al. Biomimetic UHMWPE/HA scaffolds with rhBMP-2 and erythropoietin for reconstructive surgery. *Materials Science and Engineering: C*, 2020, Vol. 111, 110750

[3] Zhukova, P.A. et al. Polymer Composite Materials Based on Polylactide with a Shape Memory Effect for “Self-Fitting” Bone Implants. *Polymers* 2021, 13, 2367

[4] Senatov, F. et al. Osseointegration evaluation of UHMWPE and PEEK-based scaffolds with BMP-2 using model of critical-size cranial defect in mice and push-out test / *Journal of the Mechanical Behavior of Biomedical Materials*, 2021, 119, 104477

[5] : Levin AA, et al. 2023, Commercial articulated collaborative in situ 3D bioprinter for skin wound healing. *Int J Bioprint*. 9(2): 675

# Crystal Structure and Magnetic Properties of Iron Polyhydrides at Ultra High Pressures

I. Lyubutin<sup>a\*</sup>, A. Gavriiliuk<sup>a,b,c</sup>, V. Struzhkin<sup>d</sup>, S. Aksenov<sup>a</sup>,  
A. Ivanova<sup>a</sup>, A. Mironovich<sup>b</sup>, M. Lyubutina<sup>a</sup>, I. Troyan<sup>a</sup>

<sup>a</sup> Shubnikov Institute of Crystallography, Federal Scientific Research Centre “Crystallography and Photonics”, Russian Academy of Sciences, Moscow, 119333 Russia

<sup>b</sup> Institute for Nuclear Research, Russian Academy of Sciences, Troitsk, Moscow, 108840 Russia

<sup>c</sup> Immanuel Kant Baltic Federal University, Kaliningrad, 236041 Russia

<sup>d</sup> Center for High Pressure Science and Technology Advanced Research (HPSTAR), Pudong, 201203 Shanghai, People’s Republic of China

\* corresponding author e-mail: lyubutinig@mail.ru

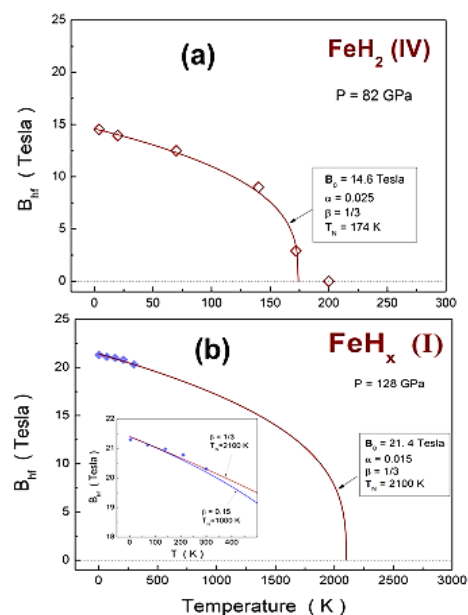
It is known that ferromagnetic  $\alpha$ -Fe at a pressure of about 15 GPa transforms into the *hcp* phase of  $\epsilon$ -Fe, which is nonmagnetic down to 4 K [1]. The properties of iron hydrides have not been experimentally studied, but theory predicts that some iron hydrides may be superconductors.

In our work, iron polyhydrides were synthesized at pressures of 77–157 GPa and temperatures up to 2000 K by the laser heating of an iron–borazane ( $\text{NH}_3\text{BH}_3$ ) sample in diamond anvil cells. X-ray spectra of the synthesized products indicate the formation of several  $\text{FeH}_x$  phases, in which reflections of  $\text{FeH}_2$  iron hydride with the tetragonal crystal structure  $I4/mmm$  are reliably detected. The magnetic and electronic properties of  $\text{FeH}_x$  compounds have been studied by nuclear forward scattering spectroscopy on Fe-57 nuclei (NFS – synchrotron Mössbauer spectroscopy) at high pressures in the temperature range of 4–300 K in external magnetic fields up to 5 T [2].

The NFS data indicate creation seven  $\text{FeH}_x$  compounds with very different electronic and magnetic properties. The Neel temperature  $T_N$  determined for the  $\text{FeH}_2$  phase at a pressure of 82 GPa is about 174 K (Fig. 1a). Another surprising result is the discovery of one of the  $\text{FeH}_x$  phases, of unknown composition, which at a pressure of 128 GPa remains magnetically ordered in the temperature range from 4 to 300 K, and the extrapolated value of  $T_N$  can reach ~ 2100 K! (Fig. 1b). Such a high pressure is characteristic of the boundary between the lower mantle and the outer core of the Earth. The existence of a magnetic phase of an iron compound at such a record high pressure is unique and has not yet been observed to date. The obtained experimental data are very important both from the fundamental physics of metals and their magnetism, and also from the point of view of the physics of the Earth and terrestrial magnetism.

**Figure 1.** Temperature dependence of the magnetic hyperfine field  $B_{\text{hf}}$  at Fe-57 nuclei in the  $\text{FeH}_2$  phase at a pressure of 82 GPa (a); estimated Néel temperature is ~174 K; and in the  $\text{FeH}_x(\text{I})$  phase at a pressure of 128 GPa. Extrapolated value of the Neel temperature is ~ 2100 K (b).

This work was carried out with the financial support of the Russian Science Foundation (grant # 22-12-00163). X-ray diffraction studies were performed within the State Assignment of FSRC "Crystallography and Photonics" RAS.



[1] A. G. Gavriiliuk, *et al.* *JETP Letters* 117, 126 (2023). DOI: 10.1134/S0021364022602986

[2] A.G. Gavriiliuk, *et al.* *JETP Letters* 116, 804 (2022). DOI: 10.1134/S0021364022602433

# Design of g-C<sub>3</sub>N<sub>4</sub>-based photocatalysts for hydrogen production and reduction of carbon dioxide under visible light

A. Zhurenok<sup>a</sup>, D. Vasilchenko<sup>a,b</sup>, E. Kozlova<sup>a,\*</sup>

<sup>a</sup> Boreskov Institute of Catalysis, 630090, pr. Ak. Lavrentieva 5, Novosibirsk, Russia

<sup>b</sup> Nikolaev Institute of Inorganic Chemistry, 630090, pr. Ak. Lavrentieva 3, Novosibirsk, Russia

\*kozlova@catalysis.ru

The trend towards an increase in consumption and a reduction in hydrocarbon reserves determines the need for the development of affordable alternative and, above all, renewable energy sources. In addition, a natural consequence of the increase in fossil fuel consumption is a multiple increase in carbon dioxide (CO<sub>2</sub>) emissions into the atmosphere. The areas of alternative energy based on the use of solar energy have paramount scientific significance and, in the future, significant practical prospects. The process of photocatalytic production of hydrogen under the visible light irradiation is considered to be especially attractive in this area, since in this case the transformation of solar energy into the energy of chemical bonds is carried out. The unique properties of hydrogen make it possible to consider it a universal and most environmentally friendly chemical energy carrier, suitable for use in almost all types of heat engines and many other types of power generating devices. From this point of view, the development of new efficient technologies for hydrogen production is relevant for solving, at least, local problems of hydrogen energy [1].

The capture and involvement of CO<sub>2</sub> in chemical transformations is an urgent task not only from the point of view of using CO<sub>2</sub> as a source of carbon, but also for reducing its concentration in the atmosphere. The reduction of CO<sub>2</sub> under mild conditions, as a rule, proceeds under the action of additional physical influences, such as light irradiation. Photocatalytic reduction of CO<sub>2</sub> is a promising process that mimics the function of natural photosynthesis. In this case, the products of the joint photocatalytic conversion of CO<sub>2</sub> and water can be alcohols and hydrocarbons [2].

The main factor hindering the practical use of photocatalytic processes such as hydrogen production and CO<sub>2</sub> reduction is the lack of efficient and at the same time stable heterogeneous photocatalysts functioning under the visible light irradiation, which makes up about 43% of the solar spectrum. Recently, more attention of researchers has been attracted by the graphitic carbon nitride g-C<sub>3</sub>N<sub>4</sub>. This material has the properties of a semiconductor with a band gap of 2.7 eV, and the positions of the valence and conduction bands are suitable for the photocatalytic water splitting and CO<sub>2</sub> reduction. Traditionally, g-C<sub>3</sub>N<sub>4</sub> is synthesized by thermal condensation of nitrogen-enriched organic precursors – cyanamides, melamine, and urea. Nevertheless, the photocatalytic activity of g-C<sub>3</sub>N<sub>4</sub> synthesized by this method is usually low due to the rapid recombination of photogenerated electron-hole pairs. Various approaches are being developed to increase the activity of photocatalysts based on g-C<sub>3</sub>N<sub>4</sub>.

This lecture systematizes data on the approaches applied to the synthesis of graphite-like carbon nitride at the Boreskov Institute of Catalysis. In particular, such synthetic approaches as the creation of heterostructures, the deposition of cocatalysts, and various template synthesis techniques will be considered. The relationship between the characteristics of synthesizing g-C<sub>3</sub>N<sub>4</sub> and its activity in the targeted processes of photocatalytic hydrogen production and carbon dioxide reduction under visible light will be discussed.

This work was supported by Russian Science Foundation Grant 21-13-00314.

[1] E.A. Kozlova, V.N. Parmon, Russ. Chem. Rev. 86, 870 (2017)

[2] E.A. Kozlova, M.N. Lyulyukin, D.V. Kozlov, V.N. Parmon, Russ. Chem. Rev. 90, 1520 (2021)

## Design of novel PDMS magnetic nanocomposites

S. Alberti<sup>a,\*</sup>, I. Sidane<sup>a</sup>, S. Slimani<sup>a,b</sup>, M. Ferretti<sup>a</sup>, D. Peddis<sup>a,b</sup>

<sup>a</sup> Chemistry and Industrial Chemistry Department, University of Genoa, via Dodecaneso 31, 16146, Genova (Ge), Italy

<sup>b</sup> Institute of Structure of Matter, National Research Council, nM<sup>2</sup>-Lab, via Salaria km 29.300, Monterotondo Scalo 00015, Roma, Italy

\*stefano.alberti@unige.it

Research into novel nanocomposites has attracted great interest in recent years for the possibility to combine the properties of structural materials with those of the nanoscale filler, to create ingenious and useful materials meeting the requirements of specific applications [1].

In this work, the synthesis of magnetic nanocomposites based on spinel iron oxide nanostructures (MeFe<sub>2</sub>O<sub>4</sub>; Me: Fe<sup>2+</sup> and Co<sup>2+</sup>), functionalized with an organic capping (oleic acid), and silicon-based polymer (polydimethylsiloxane, PDMS) has been optimized. Spinel ferrite nanoparticles are particularly attractive for biomedical applications due to their tunable magnetic properties (i.e., saturation magnetization and magnetic anisotropy). In addition, the synthesis of the proposed nanocomposite was carried out with the electrospinning technique, which is an innovative method that exploits a high electric potential to create a solid material out of viscous solutions. Fibers are withdrawn towards a metallic collector, creating a membrane with a three-dimensional fibrous network (Fig. 1) [2].

The aim of this work is to compare the magnetic and physical-chemical properties of different synthesized samples, where different types of magnetic nanoparticles were embedded in different concentrations. The characterization is carried out by means of morpho-structural (X-ray diffraction, XRD, Transmission electron microscopy, TEM) and magnetic measurements (Vibrating Sample Magnetometer, VSM). In addition, other methods (Fourier Transform Infrared Spectroscopy, FTIR, Thermogravimetric analysis, TGA, and Dynamic light scattering, DLS) have been used to determine the presence of magnetic nanoparticles within the polymer matrix as well as their stability.

The results of this study could provide valuable insights into the synthesis and optimization of magnetic hybrid nanocomposites for numerous applications.

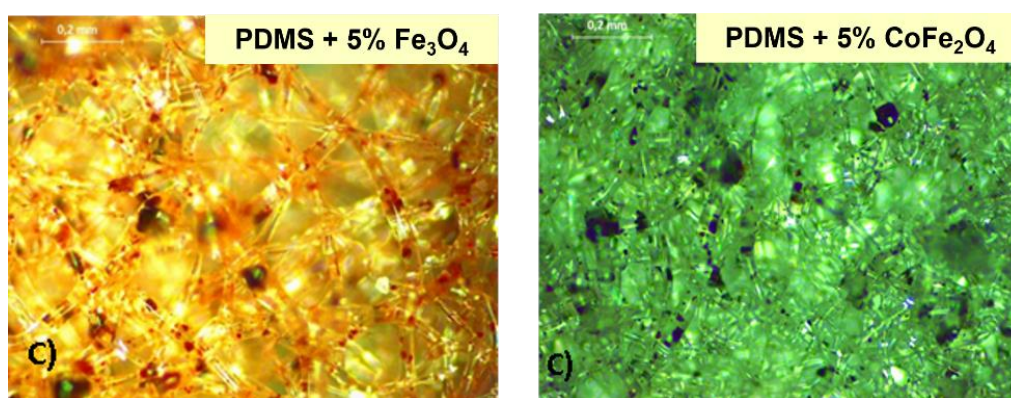


Figure 1: LOM images of magnetic nanocomposites

[1] S. Behrens and I. Appel. *Current Opinion in Biotechnology*, 39 (2016) 89-96

[2] S. Alberti et al., *J Mater Sci* 54 (2019) 1665–1676



# Doping-induced changes in the electronic and magnetic properties of Mn- and Cr-based MAX phases

V.Zhandun<sup>1,\*</sup>, O. Draganyuk<sup>1</sup>, N. Zamkova<sup>1,2</sup>

<sup>1</sup>Kirensky Institute of Physics, Federal Research Center KSC SB RAS, Krasnoyarsk, Russia

<sup>2</sup>Siberian Federal University, Krasnoyarsk, Russia

\*e-mail: [jvc@iph.krasn.ru](mailto:jvc@iph.krasn.ru)

First-principle study of the functional materials makes it possible to predict the existence of new materials with promising properties. This allows to reduce research costs and to provide some recommendations regarding promising compositions and synthesis conditions to experimenters. MAX phases of  $Mn_2AX$  [1] are atomic layered materials where M is a transition metal, A is an A-group element, and X is carbon and/or nitrogen. MAX phases are actively used in spintronic and magnetic cooling devices. Recently much attention has been paid to the study of magnetic MAX phases, including those based on the Fe and Mn atoms. In the present study the effect of the doping on the magnetic and electronic structures of  $Mn_2GaC$  and  $Cr_2GaC$  MAX phases was studied.

It is experimentally known that pure  $Mn_2GaC$  is metal with canted antiferromagnetic structure [2]. We have showed via DFT-GGA calculations that the substitution of 12.5% Ga atoms in  $Mn_2GaC$  by Fe (Fig.1) or Al atoms results in the formation of ferromagnetic order in the MAX phases. The obtained alloys are thermodynamically stable and their magnetization and Curie temperature have higher values than in pure MAX phase. Also we have found that doping of the  $Cr_2GaC$  and  $Mn_2GaC$  by oxygen atoms leads to the pronounced changes in the electronic structure, namely, appearance of the bandgap for the one of the spin channel. Thus, we predict the appearance of the half-metallicity in oxygen-doped magnetic MAX phases. These intriguing findings allow tuning magnetic and electronic properties of MAX phases and showing the way to fabricate new compounds with promising properties for further practical applications in microelectronics and spintronics.

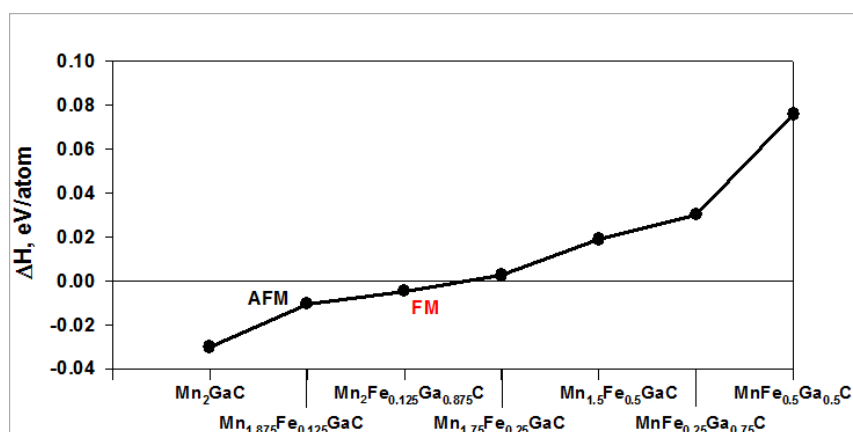


Fig. 1. Dependence of the enthalpy of formation on the composition of the Fe-doped MAX phase.

**Acknowledgements.** The study was funded by a grant from the Russian Science Foundation # 23-22-10020 <https://rscf.ru/project/22-22-20024/>, Krasnoyarsk Regional Fund of Science.

[1] Sokol, V. Natu, S. Kota and M. W. Barsoum, Trends in Chemistry 1 (2), 210-223 (2019).

[2] I. P. Novoselova, A. Petruhins, U. Wiedwald, A. S. Ingason, T. Hase, F. Magnus, V. Kapaklis, J. Palisaitis, M. Spasova, M. Farle, J. Rosen and R. Salikhov, , Sci. Rep., 2018, 8, 2637.

## Ferromagnetism in the Terminated $Mn_2C$ MXene

F. Tomilin<sup>a,b,\*</sup>, V. Kozak<sup>b</sup>, N. Fedorova<sup>b</sup>, A. Shubin<sup>b</sup>, A. Tarasov<sup>a,b</sup>, S. Varnakov<sup>a</sup>, S. Ovchinnikov<sup>a,b</sup>

<sup>a</sup> Kirensky Institute of Physics, FRC KSC SB RAS, 660036, Akademgorodok 50/38 Krasnoyarsk, Russia

<sup>b</sup> Siberian Federal University, 660041, Svobodny 79, Krasnoyarsk, Russia

\* felixnt@gmail.com

In the last 20 years, effective carrier injection, detection and control of spin current has been achieved in many spintronic devices based on magnetic tunnel junctions fabricated using both metallic and semiconductor fragments. Attention is now turning to the study of quantum, low-dimensional and topological materials, which have been successfully used in electronic and optical spintronic devices. A number of low-dimensional materials such as graphene, nitrides and chalcogenides exhibit unique properties that are promising for applications in spintronics. Recently, the family of low-dimensional materials has been joined by MXenes, i.e., 2D transition metal carbides and nitrides. These compounds can be synthesized by using chemical etching to cleave a hexagonal  $M_{n-1}AX_n$  (MAX) layered phase, where  $M$  is the transition metal,  $A$  is the group A element (e.g.,  $Si$ ,  $Al$  or  $Ga$ ) and  $X$  is carbon or nitrogen ( $n$  can vary from 1 to 4). In order to simulate different Mn-based MXene phases, carbon was chosen as element  $X$  and aluminum as element  $A$ , since they are relatively easy to etch from the parent MAX phases. Manganese was chosen as element  $M$  because of (i) a lack of publications on  $Mn$ -containing phases, (ii) its unique magnetic properties in the +2-oxidation state, and (iii) the possibility of obtaining a  $Mn$ -containing phase by substitution of  $Mn$  by  $Cr$ , since  $Cr$ -containing phases have been synthesized experimentally.

Density Functional Theory (DFT) within Periodic Boundary Conditions (PBC) has been used for electronic structure calculations of the crystalline structure and electronic properties of MAX and MXene phases using the CRYSTAL 17 code ([www.crystal.unito.it](http://www.crystal.unito.it)). The Perdew-Burke-Ernzerhof (PBE) DFT functional was used to calculate MXene phases. The equilibrium structure was determined using the quasi-Newton approach with the Broyden-Fletcher-Goldfarb-Shanno algorithm according to the Hessian matrix update scheme. The total spin magnetic moment per unit cell was set to the maximum possible value and, after optimization, took its equilibrium value for each lattice. To avoid artificial interactions between mirror partners of 2D lattices, a vacuum gap of 500 Å in the  $c$ -direction was introduced for all PBC calculations.

DFT-PBC calculations were used to study a series of low-dimensional  $Mn$ -based MXene phases with halogen ( $F$ ,  $Cl$ ),  $-OH$  and  $=O$  surface terminations with respect to the parent 2D  $Mn_2AlC$  MAX phase. It was shown that the MXene surface termination determines the spin and electronic properties of the phases. Surface passivation of  $Mn_2C$  by  $F$  and  $Cl$  ions results in maximum magnetic moments per unit cell of up to 5.63  $\mu_B$ , while hydroxylation leads to its half-metallicity, whereas oxygenation results in the appearance of flat bands, which could lead to strongly correlated electronic quantum phases with possible manifestation of quantum-related electron transport phenomena. The wide variation of challenging electronic and spin properties of  $Mn$ -based MXene phases makes them promising materials for advanced spin- and quantum-related applications. Following DFT simulations, novel low-dimensional MXene phases with advanced electronic and spin properties could be deliberately designed and synthesized experimentally [1].

The authors are grateful to JCSS Joint Super Computer Center of the Russian Academy of Sciences for providing supercomputers for the simulation. This study was supported by the Russian Science Foundation, project no. 21-12-00226.

[1] V. Kozak, CoCoM. Vol.35 (2023). DOI: 10.1016/j.cocom.2023.e00806

# Layered composite based on piezopolymer and magnetic elastomer for energy conversion

L. Makarova<sup>a,b,\*</sup>, Iu. Alekhina<sup>a,b</sup>, R. Makarin<sup>a</sup>, N. Perov<sup>a,b</sup>

<sup>a</sup>Lomonosov Moscow State University, 119991, Leninskie gory 1, Moscow, Russia

<sup>b</sup>Immanuel Kant Baltic Federal University, 236004, Nevskogo 14, Kaliningrad, Russia

\*la.loginova@physics.msu.ru

Multilayered magnetoelectric materials are of great interest for investigations due to their unique tunable properties and giant values of the magnetoelectric effect (MEE). Despite the intense investigations in the field of multilayer multiferroics, many issues such as property modification still require more detailed investigations and thus remain the focus of the research. The flexible layered structures consisting of soft components can reveal lower values of the resonant frequency for the dynamic magnetoelectric effect occurring in the bending deformation mode. The use of polymeric components in magnetoelectric structures should be promising for the development of flexible electronics including sensors and energy harvesting devices or biomedical devices. For this reason, the investigations of layered structures based on magnetic elastomers (MAE) and piezoelectric polymers (PEP) are of especial interest.

The investigations of the MEE of the layered structure MAE-PEP for the cantilever configuration were carried out. The investigations included the measurements of the dynamic magnetoelectric effect, namely, the detection of the resonant amplification of the induced signal at the applied gradient alternating magnetic field. The application of the gradient magnetic field makes it possible to observe pronounced bending deformations of the samples. The investigations were aimed at searching for the influence of an external load, such as a DC magnetic bias field or mechanical pressure, on the resonant frequency and also on the induced signal. The transverse configuration of the magnetic and electric signals (opposite to the plane of the multilayer) was used.

The frequency dependence of voltage induced under the influence of AC magnetic field shows the main resonance peak and several resonance-like peaks with lower amplitude at sub-multiple frequencies. The appearance of resonance-like peaks at multiplied frequencies means that the acting force applies 2, 3, etc., times less frequently than at the main resonance. More rare application of the acting force leads to the lower induced signal. However, all resonances observed in this frequency range are associated with the first bending mode of the sample. The resonant frequency slightly changed with the changes of amplitudes of the AC magnetic field and had the tendency to decrease with the increase of iron particles concentration in the MAE layer.

Under the applied external DC magnetic field - bias field - the Young's modulus of the MAE increases due to the magnetorheological effect, as well as the density of materials as well as the mass distribution changes due to magnetodeformation. The induced electrical voltage depended on the permeability of the MAE and the bias magnetic field.

The mean value of the magnetoelectric effect can be calculated as the induced voltage divided by the thickness of the piezopolymer layer between the conductive plates and the value of the magnetic field amplitude at the center of the free edge of the sample. The maximum value of the MEE (mean value) reaches 0.77 V/cm\*Oe at the resonant frequency 60 Hz for the sample with MAE layer of 3 mm thickness and 77 mass% iron particle concentration.

Support by RSF, grant number 22-72-10137 is acknowledged.

[1] L.A. Makarova et al., *Polymers*15, 11 (2023).

# Low-temperature Peculiarities of Magnetoresistance and Hall Effect in Nanocomposites $(\text{CoFeB})_x(\text{LiNbO}_3)_{100-x}$ below the Percolation Threshold

A. Granovsky<sup>a,b,c\*</sup>, S. Nikolaev<sup>d</sup>, A. Sitnikov<sup>e</sup>, V. Rylkov<sup>b,d</sup>

<sup>a</sup> Lomonosov Moscow State University, 119991 Moscow, Russia

<sup>b</sup> Institute for Theoretical and Applied Electrodynamics RAS, 124412 Moscow, Russia

<sup>c</sup> Samarkand State University, 140100 Samarkand, Uzbekistan

<sup>d</sup> National Research Center “Kurchatov Institute”, 123182 Moscow, Russia

<sup>e</sup> Voronezh State Technical University, 394026 Voronezh, Russia

\* granov@magn.ru

We present the results on magnetotransport properties of  $(\text{CoFeB})_x(\text{LiNbO}_3)_{100-x}$  film nanocomposites below the percolation threshold ( $x=40-48$  at.%) fabricated by ion beam sputtering of composite targets on silicon substrate. Magnetoresistance and Hall effect were studied at 3-250 K in magnetic fields up to 14 T.

The conductivity of nanocomposites with  $x \approx 44-48$  at.% in a wide temperature range is described by the relation  $\sigma \propto \ln T$ , characteristic for a strong tunneling coupling between granules [1]. For  $x < 44$  at.% this relation changes by the  $\ln \sigma \propto -(T_0/T)^{1/2}$  law, which is due to co-tunneling [1].

The samples with  $x \approx 44-48$  at.% demonstrate the anomalous Hall effect (AHE) with the scaling behavior  $\rho_{\text{AHE}} \propto \rho^n$ , where  $\rho_{\text{AHE}}$  is the AHE resistivity,  $\rho$  is the ordinary resistivity,  $n$  is the power-law index equal to  $\approx 0.4$ . This value  $n \approx 0.4$  is close to the index value corresponding to the tunneling AHE [2].

We observed the complicated non-monotonic behavior for the temperature dependence of magnetoresistance (MR). At  $T > 4$  K MR is negative and its absolute value exhibits minimum at  $\approx 40$  K. Above 40 K MR slightly increases with temperature that is unusual for MR of ferromagnetic materials. We attribute this anomaly with destroying superferromagnetic order. Below 40 K MR sharply increase with decrease of temperature. It was explained by resonance co-tunneling [3]. The unexpected behavior was observed below 4 K, where MR becomes positive and exhibits two minimums. It looks like a consequence of positive and negative contributions. In the presentation we discuss these peculiarities in the framework of existing theories of MR.

This work was financially supported by Russian Science Foundation, grant No. 22-19-00171.

[1] I.S. Beloborodov et al., Rev. Mod. Phys. 79, 416 (2007)

[2] V.V. Rylkov et al., Phys.Rev. B 95, 144202 (2017)

[3] S. Mitani et al., Phys.Rev. Lett. 81, 2799 (1998)

## Magnetic Nanoparticles for Improved Rapid Diagnostic Tests

M. Salvador<sup>a,\*</sup>, J. Marqués-Fernández<sup>a</sup>, A. Bunge<sup>b</sup>, V. Pilati<sup>a</sup>, J. Martínez-García<sup>a</sup>, R. Turcu<sup>b</sup>, D. Peddis<sup>c</sup>, M. García-Suárez<sup>d</sup>, M. Cima-Cabal<sup>d</sup>, M. Rivas<sup>a</sup>

<sup>a</sup> Department of Physics & IUTA, University of Oviedo, Spain

<sup>b</sup> National Institute for Research and Development of Isotopic and Molecular Technologies, Romania

<sup>c</sup> Department of Chemistry and Industrial Chemistry, Università degli Studi di Genova, Italy

<sup>d</sup> Escuela Superior de Ingeniería y Tecnología (ESIT), Universidad Internacional de la Rioja, Spain

\*salvadormaria@uniovi.es

Bioanalysis of a large number of samples, in short times, and at low cost is a challenge of modern times. COVID-19 showed us the need of detection tools that allow the *in situ* obtention of reliable results easily and in the shortest possible time to avoid the collapse of our society. Point-of-care devices do not depend on sophisticated equipment or qualified personnel, being very useful in emergencies, especially in remote areas and developing countries. Currently, lateral flow immunoassays (LFAs) are the most widely used point-of-care tests [1]. LFAs are chromatographic tests based on nitrocellulose strips, whose most relevant examples are the home pregnancy test or the rapid antigen tests used during the COVID-19 pandemic. However, some improvements such as increasing its sensitivity or the possibility of quantifying the analyte would allow a more extensive use. The use of magnetic nanoparticles as detection labels would allow both purposes [2].

In this talk I will discuss about magnetic LFAs, and its advantages and challenges for biomarker detection. I will analyze the characteristics and the advantages of the magnetic labels, and the reading out of the test, which should be addressed without adding excessive complexity to the method, eluding compromising its main advantages regarding costs, duration, and portability. To conclude, I will show some LFAs developed in our laboratory for applications of real interest: Detecting antibodies generated by SARS-CoV-2 and quantifying pneumolysin, the protein that indicates pneumococcal pneumonia when detected in the urine. For these applications, we have used magnetic clusters with mean sizes of 89 nm that are made of iron oxide nanoparticles of about 8 nm. The polyacrylic acid on their surface enables their biofunctionalization with a specific biorecognition biomolecule. An extraordinary advantage of the use of the magnetic clusters is their ability to concentrate diluted samples thanks to their magnetic character. Thanks to this simple technique, we have considerably improved the limit of detection of pneumolysin more than twenty times [3].

### Acknowledgments

We acknowledge support from the Spanish Ministry of Science and Innovation (EIN2020-112354), the Principality of Asturias (IDI/2018/000185 and BP19-141), and the IUTA (SV-20-GIJÓN-1-22). M.S. was supported by a “Severo Ochoa” fellowship (Consejería de Educación y Cultura del Gobierno del Principado de Asturias, grant BP19-141) and by the Margarita Salas fellowship financed by the European Union-NextGenerationEU and the Plan for Recovery, Transformation and Resilience.

[1] A. Sena-Torralba, et al. Chemical Reviews (2022)

[2] A. Moyano, et al. Diagnostics (2020)

[3] M. Salvador, et al. Nanomaterials (2022)

# Magnetism in Medicine: Old Problems and New Trends

Yu. Koksharov

Lomonosov Moscow State University, 119991, Leninskie gory 1, Moscow, Russia

yak@physics.msu.ru

Since ancient times, the magnetic field has inspired attempts to apply it in medicine. All human beings are constantly exposed to the Earth's magnetic field, but, as a rule, are unaware of its existence. Routine use of magnets for the whole body with a strength of up to 1.5 T in clinical MRI began in the early 1980s and introduced a new degree of exposure to magnetic fields on humans [1].

Hundreds of studies have shown that magnetic fields can affect various systems of the human body and that biomagnetic effects include changes in reactions of cells to various external influences [2]. However, the effect of the magnetic field on biological systems still arouses suspicion among many physicists, as well as among the medical community, since some common problems have not yet been satisfactorily solved. 1) Scientific reports contain many, at first glance, contradictory results. 2) The underlying mechanisms of biomagnetic effects remain elusive. 3) There are some strange features of these effects from the point of view of physics, for example, cells can react to the influx of energy, which is low compared to thermal energy (kT). The reasons for these difficulties are the following: 1) Biomagnetic effects are rather weak, since there is little interaction between magnetic fields and diamagnetic or paramagnetic substances of living bodies. 2) The systems of the human body are very complex and biomagnetic reactions are very selective, they depend on the state of activity of cells at the time of the beginning of the field effect. 3) The most relevant field variable is not always the field strength. Depending on the type of the biomagnetic reaction the frequency, the switching speed or the field gradient can be the determining factors of the response.

Water is an integral part of living organisms. The effect of magnetic field on water is still a controversial issue. It has been shown that magnetic treatment of water using very weak magnets with strong magnetic inhomogeneities ( $\nabla B \sim 0.1 \text{ T m}^{-1}$ ) accelerates the growth of nm-sized clusters. The problem is to explain how a magnetic field influences nucleation [3].

Nevertheless, despite the theoretical difficulties there are modern approved medical techniques using magnetic phenomena. Most of them can be grouped into the following types: (1) Magnetic fields are used indirectly to control (move) ferromagnetic (nano)materials or devices in the body. There is considerable interest in magnetic manipulation systems for current and future minimally invasive medical applications, including direct drug delivery systems based on nanotechnology. (2) Time varying magnetic fields produce electric currents in the body. The well-known application of this type is magnetic hyperthermia. (3) Static or slowly changing magnetic fields are measured with very high sensitivity and accuracy to study electrical activity in the human body (for example, a magnetoencephalogram of the brain). (4) Magnetic tomography methods make a breakthrough in diagnostics. The most well-known method is the MRI based on the nuclear magnetic resonance. However, other types of magnetic tomography based on the electron paramagnetic resonance or superparamagnetism of nanoparticles are also actively developing.

The potentially harmful nature of electromagnetic fields and static magnetic fields has become a major problem in recent years. Identification and prevention of possible harmful effects of technogenic magnetic fields is also a modern trend of the topic under consideration.

[1] W.Andrä and H.Nowak (Eds.) "Magnetism in Medicine: A Handbook" Willey-VCH (2007)

[2] X.Zhang, K.Yarema, A.Xu (Eds.) "Biological Effects of Static Magnetic Fields" Springer (2017)

[3] J.M.D.Coey "Philosophical Magazine" 92, 3857 (2012)

# Magneto-optical micro- and nanostructures for applications: Bi:YIG made by metal-organic decomposition and crystallized by laser annealing, and gasochromism in oxidized permalloy

D. Kulikova<sup>a,b</sup>, P. Tananaev<sup>a</sup>, E. Sgibnev<sup>a</sup>,  
A. Shelaev<sup>a</sup>, G. Yankovskii<sup>a</sup>, A. Baryshev<sup>a,\*</sup>

<sup>a</sup> Dukhov Automatics Research Institute (VNIIA), 127030, ul. Sushevskaya 22, Moscow, Russia

<sup>b</sup> Lomonosov Moscow State University, 119991, Leninskie gory 1, Moscow, Russia

\*baryshev@vniia.ru

Deposition of garnets on non-garnet elements of a waveguiding circuit or a nanostructure requires thin film fabrication technology compatible with other construction materials (dielectrics, semiconductors and metals) of miniaturized optical devices, including photonic integrated circuits. Such technology remains challenging because of the lattice mismatch between garnet and the above-mentioned materials. Also, rapid thermal annealing (RTA) needed for garnet crystallization can lead to exfoliation of the garnet film and various deteriorations of a circuit since thermal expansion coefficients of the materials are significantly different. All these technological problems are critical for magnetophotonic and plasmonic crystals based on Bi:YIG, resulting in worsening of their figure of merit. Thus, technologies for integrating garnets on photonic chips are desirable.

We present our research on synthesis of bismuth-substituted yttrium iron garnets (Bi:YIG) fabricated by a metal-organic decomposition (MOD) method with subsequent crystallization under *laser* irradiation (LRTA) [1, 2]. Micron- and sub-millimeter-sized Bi:YIG stripes and areas crystallized in air, oxygen and inert gas atmospheres are studied together with MOD-made Bi:YIG crystallized under conventional RTA. The demonstrated LRTA can be applicable for Bi:YIG monolithic integration on non-garnet substrates.

It is known that the redox reactions change optical properties of metal oxides (the effect of gasochromism). A number of researches demonstrate responses of binary systems as, for example, tungsten trioxide/catalyst metal for hydrogen sensing and smart windows, where the catalyst is responsible for dissociation of reducing (hydrogen) molecules and following transfer of atoms into the tungsten trioxide that results in the gasochromic effect through formation of oxygen vacancies. Magnetic metal (Co, Fe, Ni) oxides (spinel or garnets), to the best of our knowledge, have never been considered and applied as a material changing its magnetic birefringence or dichroism when reacting with a gas.

Applicability of oxidized permalloy nanofilms ( $\text{NiFeO}_x$ ) to hydrogen sensing will be discussed [3, 4]. Structural, magnetic, optical and magneto-optical properties of  $\text{NiFeO}_x$  significantly change versus the oxidation temperature&time. For optimal conditions, we show that the angle of Faraday rotation ( $\theta_F$ ) rise by an order of magnitude in the near IR wavelength range. This is likely due to formation of a mixture of oxides and spinels ( $\text{NiFe}_2\text{O}_4$ ) observed by the Raman spectroscopy. The as-deposited permalloy and  $\text{NiFeO}_x$  nanofilms with the largest  $\theta_F$  response were covered with a Pt catalyst layer and studied in a  $\text{H}_2$ -rich atmosphere. It is found that only the  $\text{NiFeO}_x/\text{Pt}$  bilayers irreversibly change their magnitude of  $\Delta\theta_F$ , and, being previously subjected to hydrogenation they recover sensitivity to hydrogen after heating. The gasochromic effect is detected via accumulation of  $\Delta\theta_F$  in a multipass-regime, thus stating its non-reciprocal nature.

[1] Y.M. Sgibnev *et al.*, *Crystal Growth & Design*. 22, 1196–1201 (2022).

[2] A.V. Shelaev *et al.*, *Optics and Laser Technology*. 155, 108411 (2022).

[3] D.P. Kulikova *et al.*, *Optical Materials* 107, 110067 (2020).

[4] D.P. Kulikova *et al.*, *Applied Surface Science* 613, 155937 (2023).

# Modelling the effect of particle arrangement on the magnetoelectric response of polymer-based composite films

O. Stolbov<sup>a,b</sup>, A. Ignatov<sup>b</sup>, V. Rodionova<sup>b</sup>, Yu. Raikher<sup>a,b\*</sup>,

<sup>a</sup> Institute of Continuous Media Mechanics, Russian Academy of Sciences, Ural Branch,  
614018, Korolyova 1, Perm, Russia

<sup>b</sup> Immanuel Kant Baltic Federal University, 236004, Nevskogo 14, Kaliningrad, Russia

\*sov@icmm.ru

Polymer composites materials capable of responding to an external magnetic field by generation of an electric field (multiferroics, MF) with prospects for tissue engineering do not require outstanding conversion characteristics. If their biocompatibility is granted, then quite moderate magnetoelectric efficiency of the films and scaffolds will do. However, a specific condition is the possibility to have the magnetoelectric effect at very low frequencies. For example, to accelerate osteogenesis of the stem cells adsorbed on such MF films, one may need the magnetic field – and, thus, the existence of surface electric field for the period from tens of seconds to many hours [1,2]. By those features the magnetoelectric units for tissue engineering differ greatly from industrial magnetoelectric transducers which work most at kHz or higher frequencies and do not need critically any substantial miniaturization.

As an attempt to understand the behavior of the materials of the afore-mentioned type, in our work we consider a model of the simplest scaffold—a thin film made of a three-component MF composite that is a polymer matrix filled with a mixture of piezoelectric and ferromagnet (or ferrite) micron-size particles. In particular, the films of this type are proposed for advanced muscle and bone engineering [3]. In the conventional Newnham classification of the magnetoelectric materials, this MF composite belongs to the 0-0-3 type.

The presence of a ferromagnetic phase, albeit the magnetic field has no direct effect on cell functioning, plays a key role. Indeed, in their vast majority, natural and artificial materials are ‘transparent’ for the magnetic field. Due to this, the field is experienced solely by the magnetic component of an MF film at a distance and independently of the presence of any organic substance (fabric, skin, etc.) in between. The driving mechanism of the magnetoelectric effect in question is the rotation of magnetically hard particles inside the matrix which, in turn, transfers the arisen mechanical stresses to the piezoelectric grains. The computer model of the MF film is built up as a periodic set of 2D cells each of which contains one piezoelectric and two ferromagnetic particles. The simulations are performed by means of finite element method on a single cell which, however, is incorporated in an infinite film by means of periodic boundary conditions. The problem of how the spatial arrangement of the particles and the orientation of the anisotropy axis of the piezoelectric one affect the magnetoelectric response is discussed. We argue that despite a quite particular scheme of the model, some important general conclusions may be drawn for the MF of the considered type [4].

Support by RSF grant # 21-72-30032 is gratefully acknowledged.

[1] B. Tang, J. Zhuang, L. Wang, B. Zhang, S. Lin, F. Jia, L. Dong, Q. Wang, K. Cheng, W.-J. Weng, *ACS Materials & Interfaces* 10, 7841 (2018)

[2] M. Guillot-Ferriols, M. I. García-Briega, L. Tolosa, C. M. Costa, S. Lanceros-Méndez, J. L. G. Ribelles, G. G. Ferrer, *Gels* 8, Art. no. 680 (2022)

[3] C. Ribeiro, V. Correia, P. Martins, F. M. Gama, S. Lanceros-Méndez, *Colloids & Surfaces B* 140, 430 (2016); S. Ribeiro, C. Ribeiro, E. O. Carvalho, C. R. Tubio, N. Castro, N. Pereira, V. Correia, A. Gomes and S. Lanceros-Méndez, *ACS Applied Bio Materials* 3, 4239 (2020)

[4] O. Stolbov, A. Ignatov, V. Rodionova, Yu. Raikher, *Soft Matter* 19, 4029 (2023)



# Non-heating alternating magnetic fields for the treatment of cancer with label-free imaging nanoobjects in vitro

M. Lomova

Saratov State University, Saratov, Russia.

Transformation of theranostics as an applied science, a gradual shift in the focus of the problem being solved in the field of oncological diseases, from cancer therapy to a multifactorial course of treatment and subsequent change in the body. For these purposes, agents that implement a wide range of antitumor tasks in theranostics are extremely important. The roadmap for the development of remotely controlled theranostic systems uses a clear path to the most convenient use in pharmaceuticals [1]. Magnetic nanorobots predetermine their further application in diagnostics (MRI, magnetic test systems), therapy (magnetic hyperthermia), targeted delivery (due to the use of an external magnetic field of a permanent magnet) [2-6]. Magnetic hyperthermia acquires a new round of its development, paying attention to the mechanically induced magnetic effect of objects in an alternating low-frequency magnetic field on a person [7]. The collective effect of cell death in a low-frequency magnetic field is possible only with a local change in the concentration of magnetic nanoparticles. The concentration of magnetic nanoparticles is possible by embedding them into porous submicron matrices, for example, based on mineral particles of calcium carbonate. The mineral carrier in the form of vaterite, being a self-dissolving platform (in this case, the parameters of the destruction process can be varied) in biological fluids, seems to be a promising drug delivery system. The most important properties for using calcium carbonate particles as drug carriers are: variability in shape and size, biocompatibility, biodegradability up to self-degradation, ease of preparation, rigidity. The anticancer use of calcium carbonate is based on the possibility of dissociation of calcium carbonate particles in biological fluids with subsequent leaching. The usage of Brillouin microscopy for the spatial study of biological objects and/or carriers is the only non-destructive, label-free tool for characterizing spatial structures. The development of biological technologies based on Brillouin spectroscopy is currently being carried out in several major world scientific groups [8-10]. In this case, the magnetic characteristic is not the main one and depends strongly on the types of lasers and recording systems used. Phonon interaction can provide valuable information about the spatial rigidity of biological objects with high resolution, which cannot be obtained by any other method, while the method remains label-free and non-invasive [11]. The multifactorial nature of studies using Brillouin spectroscopy puts this method on a par with the most popular methods for characterizing biological objects: fluorescence, photoacoustic, ultrasonic, etc.

A typical Brillouin spectrum is an intense central peak due to Rayleigh scattering and a set of equally shifted peaks that are the Stokes and anti-Stokes parts of the spectrum. From the spectral shift, the corresponding information about the elastic properties of the material can be obtained, in particular, the longitudinal modulus of elasticity  $M$  at frequencies of the order of units and tens of GHz. In this case, it should be taken into account that the spectrum accumulation time ( $\sim 1$  spectrum/0.5 s) does not allow one to take microphotographs of the sample surface, and spatial scanning is achieved using a system with spatial resolution, in which either the sample under study or the laser beam moves. Thus, it is possible to map with the creation of spatial distributions of the magnitude of the center frequency and/or amplitude of the inelastic scattering peak.

This research was funded by the Russian Science Foundation, grant number 23-13-00373.

## References:

- [1] Voronin, D. V.; Abalymov, A. A.; Svenskaya, Y. I.; Lomova, M. V. Key Points in Remote-Controlled Drug Delivery: From the Carrier Design to Clinical Trials. *Int. J. Mol. Sci.* 2021, 22 (17), 9149. <https://doi.org/10.3390/ijms22179149>.
- [2] Li, X.; Li, W.; Wang, M.; Liao, Z. Magnetic Nanoparticles for Cancer Theranostics: Advances and Prospects. *J. Controlled Release* 2021, 335, 437–448. <https://doi.org/10.1016/j.jconrel.2021.05.042>.
- [3] Gogoi, M. Magnetic Nanostructures for Cancer Theranostic Applications. *Curr. Pathobiol. Rep.* 2021, 9 (3), 71–78. <https://doi.org/10.1007/s40139-021-00224-2>.
- [4] Wang, S.; Wang, Z.; Hou, Y. Self-assembled Magnetic Nanomaterials: Versatile Theranostics Nanoplatforams for Cancer. *Aggregate* 2021, 2 (2). <https://doi.org/10.1002/agt2.18>.
- [5] Brito, B.; Price, T. W.; Gallo, J.; Bañobre-López, M.; Stasiuk, G. J. Smart Magnetic Resonance Imaging-Based Theranostics for Cancer. *Theranostics* 2021, 11 (18), 8706–8737. <https://doi.org/10.7150/thno.57004>.
- [6] Józefczak, A.; Kaczmarek, K.; Bielas, R. Magnetic Mediators for Ultrasound Theranostics. *Theranostics* 2021, 11 (20), 10091–10113. <https://doi.org/10.7150/thno.62218>.
- [7] Baskin, D. S.; Sharpe, M. A.; Nguyen, L.; Helekar, S. A. Case Report: End-Stage Recurrent Glioblastoma Treated With a New Noninvasive Non-Contact Oncomagnetic Device. *Front. Oncol.* 2021, 11, 708017. <https://doi.org/10.3389/fonc.2021.708017>.
- [8] Wu, P.-J.; Kabakova, I. V.; Ruberti, J. W.; Sherwood, J. M.; Dunlop, I. E.; Paterson, C.; Török, P.; Overby, D. R. Water Content, Not Stiffness, Dominates Brillouin Spectroscopy Measurements in Hydrated Materials. *Nat. Methods* 2018, 15 (8), 561–562. <https://doi.org/10.1038/s41592-018-0076-1>.
- [9] Antonacci, G.; Beck, T.; Bilenca, A.; Czarske, J.; Elsayad, K.; Guck, J.; Kim, K.; Krug, B.; Palombo, F.; Prevedel, R.; Scarcelli, G. Recent Progress and Current Opinions in Brillouin Microscopy for Life Science Applications. *Biophys. Rev.* 2020, 12 (3), 615–624. <https://doi.org/10.1007/s12551-020-00701-9>.
- [10] Bailey, M.; Alunni-Cardinali, M.; Correa, N.; Caponi, S.; Holsgrove, T.; Barr, H.; Stone, N.; Winlove, C. P.; Fioretto, D.; Palombo, F. Viscoelastic Properties of Biopolymer Hydrogels Determined by Brillouin Spectroscopy: A Probe of Tissue Micromechanics. *Sci. Adv.* 2020, 6 (44), eabc1937. <https://doi.org/10.1126/sciadv.abc1937>.
- [11] Palombo, F.; Fioretto, D. Brillouin Light Scattering: Applications in Biomedical Sciences. *Chem. Rev.* 2019, 119 (13), 7833–7847. <https://doi.org/10.1021/acs.chemrev.9b00019>.

## Nonlinear rheology of magnetic gels and elastomers

D. Chirikov, A. Zubarev\*

Ural Federal University, 620083, Lenina 51, Ekaterinburg, Russia

\*A.J.Zubarev@urfu.ru

Being placed in a magnetic field, magnetic gels and elastomers, very often demonstrate non-linear and hysteresis rheological behavior, as well as strong magnetorheological effects. It's interesting to note that, under the same conditions, deformation of the pure host polymer frequently, with high accuracy, corresponds to the linear Hook's law. Therefore, the internal nature of the observed non-linear, hysteresis and magnetorheological phenomena lie in transformations of internal morphology of the embedded particles disposition under the action of the applied field and/or macroscopic deformation of the composite. These macroscopic effects can be especially strong if the particles, under the applied field, form heterogeneous structures, ruptured at the composite deformation.

In this talk we present and discuss results of theoretical analysis of formation of the simplest type of the internal structures – linear chain-like aggregates and effect of these chains on macroscopic magnetic, magnetostriction and magnetoelastic properties of soft magneto-polymer composites with embedded non-Brownian magnetically soft particles. The hysteresis phenomena in these materials are also considered. It is taken into account that, in the field, the characteristic length of the chains is determined by competition between attraction of the magnetized particles and elastic resistance of the host medium to their displacement. The last point is the principal difference between the aggregate's formation in soft and liquid media. Appearance of the chains can induces strong, up to 2 orders of magnitude, increase of the composite rigidity, i.e. strong magnetoelastic effect. Macroscopic deformation of the sample provokes distraction of the chains, whose length exceeds some threshold value. This leads to decreasing dependence of the sample elastic modulus on its macroscopic shear.

Our analysis shows hysteresis dependence of the chain length on the applied field and macroscopic deformation of the composite. This provides the macroscopic hysteresis character of the composites magnetization, magnetostriction and deformation phenomena.

Despite its principal simplicity, the proposed model allows to explain, at least in the order of magnitude, serious of experimental results on rheophysical and magnetic phenomena in magneto-polymer composites. The comparison of the theoretical and experimental results is discussed.

# Peculiar magneto-optics: topological and asymmetric Faraday effects

V. Belotelov<sup>a,b,c\*</sup>

<sup>a</sup> Lomonosov Moscow State University, 119991, Leninskie gory 1, Moscow, Russia

<sup>b</sup> Russian Quantum Center, Skolkovo, Moscow Region 143025, Russia

<sup>c</sup> V.I. Vernadsky Crimean Federal University, Vernadsky Prospekt, 4, Simferopol, 295007, Crimea

\*belotelov@physics.msu.ru

Magneto-optical effects mediate interplay between optics and magnetism and provide efficient tools for a vast range of applications including imaging of magnetic patterns and control of light at gigahertz and even terahertz rates. The Faraday effect is the most well-known magneto-optical effect, which is rotation of linear polarization of light upon light propagation through a magnetized medium. Generally, the Faraday effect is considered for a plane wave and is odd in magnetization. However, the properties of the Faraday effect are modified if light propagates through a magnetophotonic structure or if the light carries orbital angular momentum.

The Faraday rotation is due to a phenomenon of magneto-optical circular birefringence—a difference of refractive indices of right- and left-handed circularly polarized light propagating through a transparent magnet along its magnetization. It is widely known that the magneto-optical Faraday effect is linear in magnetization and therefore the Faraday angles for the states with opposite magnetizations are of opposite sign but equal in modulus. Here we experimentally study propagation of light through a one-dimensional all-garnet magnetophotonic crystal to demonstrate an asymmetric Faraday effect (AFE) for which Faraday angles for opposite magnetic states differ not only in sign but in the absolute value as well [1]. AFE appears in the vicinity of the cavity resonance for an oblique incidence of light which plane of polarization is inclined to the incidence plane. Under proper incidence and polarization angles the magnitude of AFE could be very large reaching 30% of the absolute value of the Faraday effect. The effect originates from the difference in Q-factors for p- and s- polarized cavity modes that breaks the symmetry between the two opposite directions of polarization rotation. The discovered AFE is of prime importance for nanoscale magnonics and optomagnetism.

Apart from that we also experimentally demonstrate the topological Faraday effect—the polarization rotation caused by the orbital angular momentum of light [2]. It is found that the Faraday effect of the optical vortex beam passing through a transparent magnetic dielectric film differs from the Faraday effect for a plane wave. The additional contribution to the Faraday rotation depends linearly on the topological charge and radial number of the beam. The effect is explained in terms of the optical spin-orbit interaction. These findings underline the importance of using the optical vortex beams for studies of magnetically ordered materials.

This work was financially supported by the Ministry of Science and Higher Education of the Russian Federation, Megagrant project N 075-15-2022-1108.

[1] M.A. Yavorsky, M.A. Kozhaev, A.Yu. Fedorov, D.V. Vikulin, E.V., Barshak, V.N. Berzhansky, S.D. Lyashko, P.O. Kapralov, and V.I. Belotelov "Topological Faraday effect for optical vortices in magnetic films", *Physical Review Letters* 130, 166901 (2023).

[2] D.O. Ignatyeva, T.V. Mikhailova, P.O. Kapralov, S.D. Lyashko, V.N. Berzhansky, and V.I. Belotelov "Asymmetric Faraday Effect in a Magnetophotonic Crystal", arXiv:2211.14355.

[3] T.V. Mikhailova, D.O. Ignatyeva, S.D. Lyashko, V.N. Berzhansky, and V.I. Belotelov "Intensity Magneto-optical Faraday Effect in a Magnetophotonic Crystal", arXiv:2212.08457.

## Properties of Soft Magnetic Materials: from Experiment to Theory and Modeling

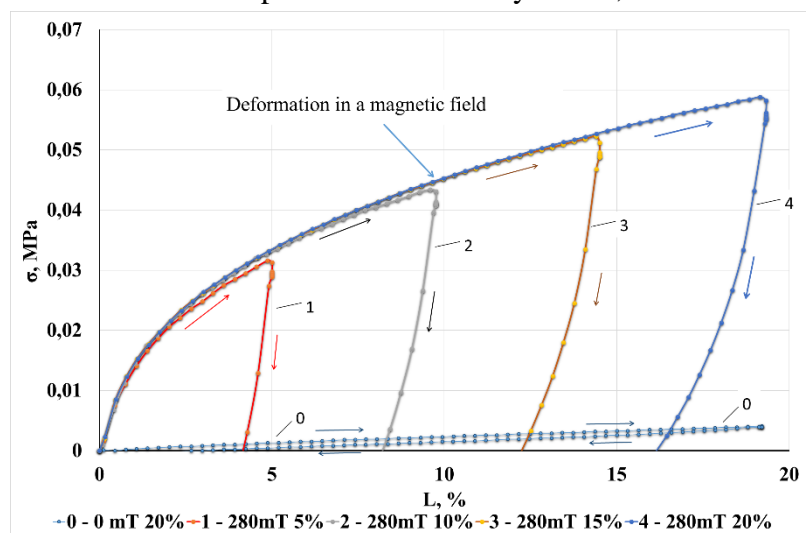
G. Stepanov\*, A. Bakhtiarov, D. Lobanov, P. Storozhenko

State Scientific Research Institute for Chemical Technologies of Organoelement Compounds, 105118, Shosse Entuziastov 38, Moscow, Russia.

\*gstepanov@mail.ru

Magnetoactive elastomer (MAE), a soft magnetic polymeric composite, has been in the focus of attention of Russian researchers for more than 25 years. A typical example of “smart material”, MAE possesses the capability to vary its parameters in magnetic fields reversibly. Nowadays, 12 properties, which may be changed in such a manner under the influence of external factors, are known. For instance, the capability to stiffen in magnetic fields is employed in controllable damping devices. Or, the way the material turns out of shape in homogeneous and non-homogeneous fields is used in micromotors. Alternatively, a multipolar magnetization pattern created in a strip of MAE filled with magnetically hard particles will give it the possibility to take complex shapes when placed in a magnetic field. This phenomenon may find use in soft grippers. In addition, the ability to change its conductivity in magnetic fields makes MAE a prospective material for employment in field sensors. The magnetic elastomer also exhibits the magnetopiezoresistive and magneto-optical effects. This set of properties is determined by the dipole interactions taking place among the magnetized particles filling the polymer matrix and capable of assembling reversibly into chain-like structures when influenced by a field. At the current moment, finding an adequate mathematical description for these properties is the key task.

Let's take the example of an MAE sample getting stiffer in magnetic field. The behavior of the material is clearly shown in the Figure demonstrating its stress-strain relationship. The measurements were carried out on a pull-test machine in the quasi-static regime using a cylinder-shaped specimen subjected to strain. As is suggested by the drawing, the stress-strain curve reveals a significant dependence on the strength of the magnetic field applied. For instance, line '0' shows the stress observed in the sample not influenced by a field, as a result of which its shape is practically that, which



would be seen in the classic Hook's law case. At the same time lines 1-4 correspond to different stress-strain relationships recorded at 280 mT and different strain degrees. The strain (load) move direction demonstrated by the sample is represented by the arrows. An important feature revealed by the curves is the magnitude of the residual deformation remaining in the sample still influenced by the field after load removal (the abscissa of the point at which the stress is zero and the curve intersects the x-axis). It is associated

with the shape memory of MAE and taken as the corresponding numerical characteristic. When the external influence is off, the sample will contract and regain its initial geometry. Such variations of properties appear as a result of the dipole interaction among the magnetized particles confined in the polymer and reversibly form chain-like structured under the influence of magnetic field. Giving these phenomena a description and modelling the processes taking place inside the magnetic elastomers is an important task of the present day.

## Second- and third-harmonics generation microscopy of magnetic garnet films

A. Maydykovskiy<sup>a</sup>, M. Temiryazeva<sup>b</sup>, A. Temiryazev<sup>b</sup>, T. Murzina<sup>a,\*</sup>

<sup>a</sup> Lomonosov Moscow State University, 119991, Leninskie gory 1, Moscow, Russia

<sup>b</sup> Kotel'nikov Institute of Radioengineering and Electronics of RAS, Fryazino Branch, Vvedensky Sq. 1, 141190 Fryazino, Russia

\*murzina@mail.ru

Magnetic iron garnet films being the main material for magneto-optical recording are continuously a subject of intensive studies. Functional properties of garnets are determined by a large range of parameters such as the film's crystalline quality, thickness, anisotropy etc., all of them being dependent on the interface domain structure, which makes its further investigation a challenging task [1]. Among others, the technique of optical second harmonic generation (SHG) has been shown as a powerful tool for the characterization of magnetic structures, providing high values of the magneto-optical SHG effects [2]. Here we demonstrate the efficiency of the nonlinear optical probe based on second- and third-harmonic generation (THG) for the visualization of magnetic domains at

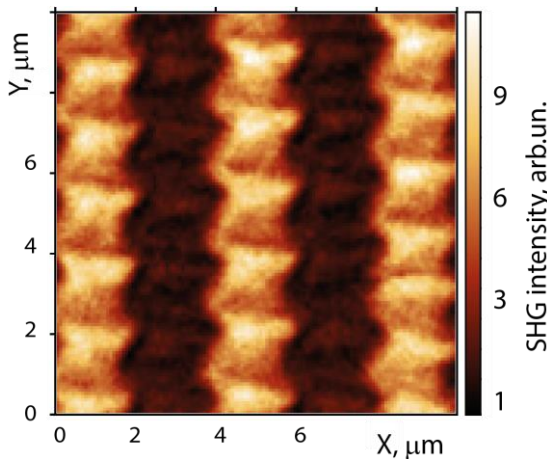


Figure 1. SHG microscopy image ( $\lambda_0=850$  nm) of the interface LuBiFeO/GGG interface layer.

the surface of  $(\text{LuBi})_3\text{Fe}_5\text{O}_{12}$  film as well as at its hidden interface with gallium gadolinium garnet (GGG) substrate. The experiments are performed using the nonlinear-optical microscopy setup based on the femtosecond OPO laser system tunable in the wavelength range from 800 nm up to 1600 nm, which correspond to the transparency range of garnet. Strong focusing of the laser beam by the immerse objective with high NA provided the submicron in-plane resolution of the method. At the same time, pronounced absorption at harmonics' wavelengths restricts the thickness of the garnet layer contributing to the nonlinear signal to about 2  $\mu\text{m}$  for the garnet film of 10  $\mu\text{m}$  in thickness. These factors allow for studying the surface and interface magnetic domains of the epitaxial garnet film; importantly, the magnetic

structure of hidden interface is a complicated object of investigation. Figure 1 shows the SHG intensity pattern of the  $(\text{LuBi})_3\text{Fe}_5\text{O}_{12}$ /GGG interface for the polarizations of the fundamental (at 850 nm wavelength) and SHG (at 425 nm) beams orthogonal to the magnetic stripe domains. Bright and dark bands correspond to magnetic stripe domains with the opposite orientation of residual magnetization oriented predominantly perpendicular to the films' surface. Besides, one can see the zigzag-type modulation with smaller period, which corresponds evidently to the interface blocking domains, their magnetization is expected to be mostly parallel to the interface. Similarly, strong magnetization-induced modulation of the THG intensity was obtained when using the pump wavelength of 1200 nm; in that case, even more pronounced zigzag pattern was obtained. Due to strong interface localization of the THG intensity we estimate the in-depth scale of the closing domains. To the best of our knowledge, third harmonic generation microscopy for the studies of magnetic structures has not been demonstrated up to now.

This research was funded by Russian Science Foundation, Grant 19-72-20103

[1] H. Alex, S. Rudolf, Magnetic Domains. Springer: Berlin/Heidelberg, Germany (1998).

[2] O. Aktsipetrov et al., JOSA B 22, 138 (2005)

## Milestones of Low-D Quantum Magnetism

A. Vasiliev<sup>a,b\*</sup>

<sup>a</sup> Lomonosov Moscow State University, 119991, Moscow, Russia

<sup>b</sup> National University of Science and Technology “MISIS”, 119049, Moscow, Russia

\*vasil@lt.phys.msu.ru

There is a long gap in time between the formulation of the basic theory of low-dimensional (low-D) magnetism as advanced by Ising, Heisenberg and Bethe and its experimental verification. The latter started not long before the discovery of high-TC superconductivity in cuprates and has been boosted by this discovery result in an impressive succession of newly observed physical phenomena. Milestones on this road were the compounds which reached their quantum ground states upon lowering the temperature either gradually or through different instabilities. The gapless and gapped ground states for spin excitations in these compounds are inherent for isolated half-integer spin and integer spin chains, respectively. The same is true for the compounds hosting odd and even leg spin ladders. Some complex oxides of transition metals reach gapped ground state by means of spin-Peierls transition, charge ordering or orbital ordering mechanisms. However, the overwhelming majority of low-dimensional systems arrive to a long-range ordered magnetic state, albeit quite exotic realizations. Finally, numerous square, triangular, kagome and honeycomb layered lattices, along with Shastry–Sutherland and Nersesyan–Tsvetlik patterns constitute the playground to check the basic concepts of two-dimensional magnetism, including resonating valence bond state, Berezinskii–Kosterlitz–Thouless transition and Kitaev model.

# Stress-dependent Magnetization Processes in CoFeSiBCr Amorphous Microwires

O. Lutsenko <sup>a</sup>, S. Evstigneeva<sup>a</sup>, N. Yudanov <sup>a</sup>, L. Panina<sup>a,b</sup>

<sup>a</sup> National University of Science and Technology, 119049, Leninskiy Avenue 4, Moscow, Russia

<sup>b</sup> Immanuel Kant Baltic Federal University, Kaliningrad, 236016 Russia

\*drlpanina@gmail.com

Amorphous ferromagnetic materials in the form of microwires are of interest for the development of various sensors. This paper analyses the magnetization processes in  $\text{Co}_{71}\text{Fe}_5\text{B}_{11}\text{Si}_{10}\text{Cr}_3$  microwires and gives the reasons why they can be used as stress/strain sensors. The following properties: miniature dimensions, small coercivity, low anisotropy, and magnetostriction, along with tuneable magnetic structure, make them suitable for innovative applications, for example, for testing internal stress/strain conditions of polymer composite materials. The sensing operation is based on the generation of higher frequency harmonics of the voltage pulse induced during the re-magnetization of the wire [1].

The wires are prepared by the modified Taylor-Ulitovskiy method [2] and when quenched in water they typically have an amorphous structure without crystalline phases. However, in Co-based compositions with small magnetostriction a short-range crystalline anisotropy can prevail, and such wires exhibit magnetic bistability. This is confirmed by measuring the hysteresis loops and axial domain wall (DW) velocity (Fig.1) The DW velocity increases with increasing the applied tensile stress until they destroy the axial domain structure. For higher stresses, the circumferential anisotropy is formed and remagnetization takes place mostly by rotation. This leads to the generation of a voltage signal with a stress-controllable amplitude and duration. The frequency spectrum of this signal contains higher harmonics of the excitation frequency, and their amplitudes are stress-dependent. The strongest dependence on stress is demonstrated by higher-number harmonics (17-23 in Fig.1.).

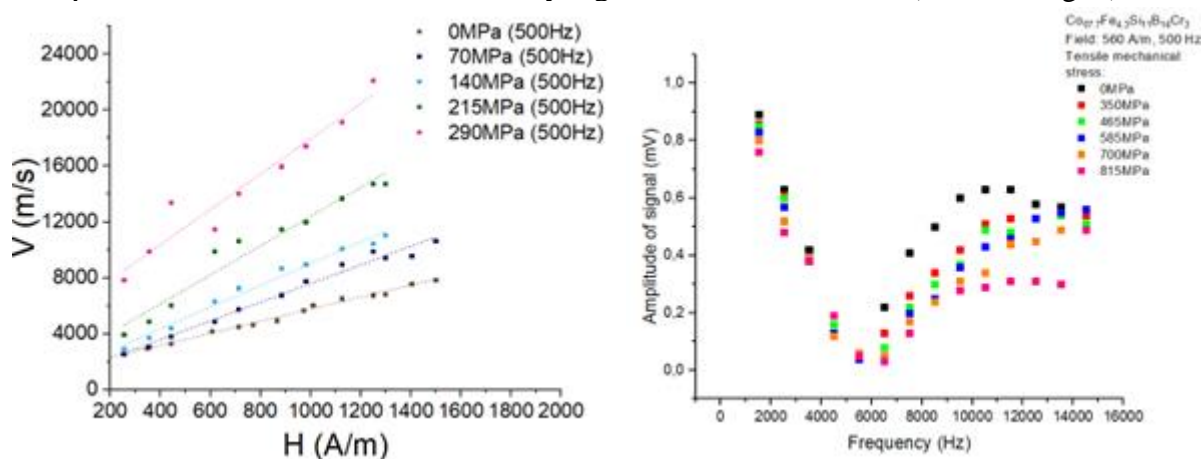


Fig.1. Domain wall velocity vs. driving magnetic field (left) and amplitudes of higher harmonics (right) for different tensile stress. Re-magnetization of the wire was done by plane coil creating a magnetic field of 325 A/m at its surface.

[1] M. G. Nematov et al, IEEE Trans. Magn. 53, 11, (2017)

[2] H. Chiriac, Mater. Sci. Eng. A 304–306, 166–171 (2001)

Acknowledgments. The work was supported by NUST MISIS (project K6-2022-043)

# Structural characterization of magnetic nanomaterials with biological activity

M. Avdeev<sup>a,b,\*</sup>

<sup>a</sup> Joint Institute for Nuclear Research, 141980, Joliot-Curie 6, Dubna, Moscow Reg., Russia

<sup>b</sup> Lomonosov Moscow State University, 119991, Leninskie gory 1, Moscow, Russia

\*avd@nf.jinr.ru

Magnetic iron oxide nanoparticles exhibit several types of responses to external magnetic fields, so they have a great potential in various bio-relevant areas including biochemistry, biotechnology, medicine, and environment. Different carriers for magnetic nanoparticles are used in applications. The interaction of the particles and carriers is the subject of intensive structural research, since this is a crucial point in the design of stable practical systems. The given report reviews and shows the importance of such kind of research for some magnetic nanomaterials with biological activity.

Thus, magnetoferritin represents a synthetic derivate of ferritin, iron storage protein, in which magnetite or maghemite substitute non-magnetic ferrihydrites inside the spherical protein shell – apoferritin (external diameter of 12 nm). While the magnetic core provides a magnetic response, the protein shell naturally provides biocompatibility of this complex. It should be mentioned that ferritin itself is known as an inflammatory biomarker of SARS-CoV-2 and, functionalized by the SARS-CoV-2 receptor-binding domain (or spike protein), is tested as an antiviral agent. The detailed structural research of magnetoferritin aqueous solutions revealed a number of effects related to physicochemical properties of the systems (iron loading, pH, synthesis temperature). These studies including ultraviolet and visible spectroscopy, dynamic light scattering, zeta potential measurements, SQUID magnetometry, magneto-optical, cryogenic transmission electron microscopy, X-ray diffraction and small-angle neutron scattering methods, showed to what extent the structure of magnetoferritin can be optimized regarding the iron loading and structural stability. [1]

Another example is related to the recently discovered biocatalytic activity of iron oxide nanoparticles themselves, which initiated their research for possible applications as artificial enzymes, or nanozymes. Such nanoparticles mimic the behavior of enzymes and can replace them in various applications. Due to the so-called peroxidase activity, iron oxide nanoparticles can be used, for example, in the creation of cheap chemical biosensors for immunoanalysis, which requires their incorporation into various artificial and cotton fabrics. For this purpose, deposition is used on products made of various textiles that are in contact with liquid suspensions of magnetic nanoparticles (ferrofluids), controlling the process using an external magnetic field and adjusting the required concentration and morphology of the deposited material. The production of magnetic textiles implies their thorough study, since any structural changes in nanoparticles affect the properties of new materials. The selection and optimization of the procedure for the synthesis of the most effective materials was carried out, taking into account the environmental friendliness of the synthesis. Again, the structure analysis explained the observed magnetic properties of tissues, as well as changes in their catalytic (peroxidase) activity, depending on the method of deposition of magnetic nanoparticles. [2]

[1] L. Balejíková, et al., *Molecules* 26, 6960 (2021)

[2] I. Safarik, et al., *ACS Appl. Mater. Interfaces* 13, 23627 (2021)



## Topological Hall effect in Co/Pt nanostructured films

M. Sapozhnikov<sup>a,\*</sup>, N. Gusev<sup>a</sup>, S. Gusev<sup>a</sup>, A. Fraerman<sup>c</sup>, D. Tatarskiy<sup>a</sup>, Yu. Petrov<sup>b</sup>, A. Temiryazev<sup>c</sup>

<sup>a</sup>Institute for Physics of Microstructures RAS, Nizhny Novgorod, 603950, Russia

<sup>b</sup>Physics Department, Saint Petersburg State University, Saint Petersburg, Russia

<sup>c</sup>Kotelnikov Institute of Radioengineering and Electronics RAS, Fryazino Branch, Fryazino, Russia

\*msap@ipmras.ru

A method consisting of simultaneous measurements of a Hall effect and a magneto-optic Kerr effect is used to study a topological Hall effect (THE) in thin ferromagnetic films. The method is based on the idea that the values of the topological effects are different at DC and optical frequencies. We calculate THE at the optical frequencies within the frameworks of Aharonov-Stern model [1] but taking into account the AC electric field. As the result it is shown that additional factor  $(\omega_R/\omega)^2 \sim 10^{-2} \div 10^{-4}$  ( $\omega_R$  is the frequency of the electron magnetic moment precession in the exchange field) appears in the comparison with the dc THE. So the topological effects in magneto-optics should be negligible.

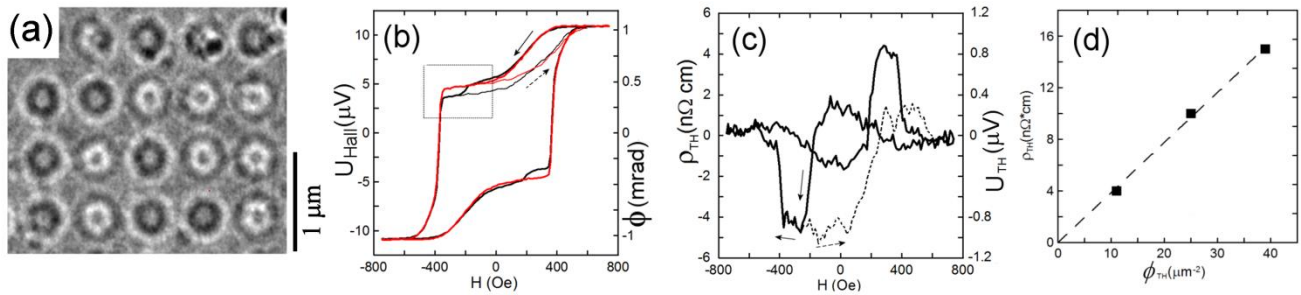


Fig. (a) LTEM image of a lattice of magnetic bubbles in a demagnetized state. The observed contrast corresponds to the distribution of magnetization for Bloch skyrmions. (b) MOKE (red line) and Hall (black line) hysteresis loops of the skyrmion lattice plotted on the same scale. Thinner lines are for minor loops. (c) The hysteresis curve of the THE. Dotted line is for minor loop. (d) Dependence of the THE on the value of the irradiated spot density in the system.

The samples are multilayer films of Co/Pt periodically locally irradiated with helium ions to form the array of the pinning centers for magnetic skyrmions. Such nanostructuring makes it possible to form dense lattices of magnetic skyrmions by simple magnetization reversal of the film in a uniform magnetic field (Fig. 1). Simultaneous measurement of the Hall effect and the Kerr effect of the samples are shown in the graph. At the moment of formation of a lattice of magnetic skyrmions, a step is observed in the Hall effect, which is absent in the Kerr effect. The difference between these signals is the sought-for THE. Its value, as it should be, is proportional to the density of the topological charge (density of magnetic skyrmions in the system).

The study of the samples structure is carried out within the framework of the scientific program of the National Center for Physics and Mathematics (project #6 "Nuclear and Radiation Physics")

[1] Y. Aharonov and A. Stern, , Phys. Rev. Lett. 69, 3593 (1992).

# Oral talks

# An influence of the Dzyaloshinskii-Moriya interaction on the magnetization reversal of the finite-size Co and Fe chains

S. Kolesnikov\*, E. Saprónova

Lomonosov Moscow State University, 119991, Leninskie gory 1, Moscow, Russia

\* kolesnikov@physics.msu.ru

In 1958 Dzyaloshinskii has suggested a new type of interaction between magnetic atoms in order to explain the weak ferromagnetism of antiferromagnetic crystals  $\alpha$ -Fe<sub>2</sub>O<sub>3</sub>, MnCO<sub>3</sub>, and CoCO<sub>3</sub> [1]. Latter Moriya has interpreted this interaction as an anisotropic superexchange interaction [2]. Now this interaction is called the Dzyaloshinskii-Moriya interaction (DMI). The interest to DMI has arisen after the observations of strong DMI in transition metal films [3]. DMI in layered structures can lead to formation of different magnetic structures like chiral domain walls, chiral bubbles and skyrmions. Strong DMI in atomic chains also can lead to some interesting phenomena. For example, biatomic Fe chains on the Ir(001)(5×1) surface have a DMI-induced noncollinear magnetic ground state [4]. Moreover, the DMI can significantly change the energies of excited states even if the ground state of an atomic chain is collinear. Using *ab initio* calculations the significant DMI in Co and Fe chains on Pt(664) surface has been predicted [5]. It has been shown that the infinitely long Co and Fe chains have the collinear ferromagnetic ground state, but DMI changes the energies of the excited states.

The magnetic properties of the atomic chains can be satisfactorily described in the framework of some effective theory including the exchange interaction, the magnetic anisotropy energy (MAE), DMI, and the interaction with the external fields. The parameters of the effective theory have been taken from Ref. [5]. For the numerical calculations the geodesic nudged elastic band (GNEB) method [6] is employed. For analytical calculations we use the continuous XY-model.

Energy barriers for magnetization reversal of the finite-size Co and Fe chains on Pt(664) surface are calculated with taking the Dzyaloshinskii-Moriya interaction into account. It has been found that the ground states of such atomic chains are noncollinear. The magnetization reversal of short atomic chains occurs without the formation of domain walls. At the same time, the magnetization reversal of longer atomic chains occurs via the formation of the clockwise domain wall (CDW) or the anticlockwise domain wall (ACDW). It is interesting that mechanisms of the magnetization reversal of the Co and Fe atomic chains are different. Knowing of the energy barriers allows to calculate the magnetization reversal times [7] both in zero and nonzero external magnetic fields. After that we calculate the magnetization curves and the coercivity of the finite-size Co and Fe chains. Here we focus on comparison of results for Co and Fe atomic chains.

The research is carried out using the equipment of the shared research facilities of HPC computing resources at Lomonosov Moscow State University [8]. The investigation is supported by the Russian Science Foundation (Project No. 21-72-20034).

[1] I. Dzyaloshinsky, J. Phys. Chem. Solids 4, 241 (1958).

[2] T. Moriya, Phys. Rev. Lett. 4, 228 (1960).

[3] H. T. Nembach, J. M. Shaw, M. Weiler, E. Jué, T. J. Silva, Nat. Phys. 11, 825 (2015).

[4] R. Mazzarello, E. Tosatti, Phys. Rev. B 79, 134402 (2009).

[5] B. Schweflinghaus, B. Zimmermann, M. Heide, G. Bihlmayer, S. Blugel, Phys. Rev. B 94, 024403 (2016).

[6] P. F. Bessarab, V. M. Uzdin, H. Jonsson, Comput. Phys. Commun. 196, 335 (2015).

[7] S.V. Kolesnikov, E.S. Saprónova, IEEE Magn. Lett. 13, 2505905 (2022).

[8] V. Voevodin, et. al., Supercomput. Front. Innov. 6, 4 (2019).

# **Anomalous behavior of the magnetocaloric effect in Ni<sub>49.3</sub>Mn<sub>40.4</sub>In<sub>10.3</sub> Heusler alloy in alternating magnetic fields**

A. Aliev\*, A. Gamzatov

Amirkhanov Institute of Physics. Dagestan Federal Research Centre of the Russian Academy of Sciences,  
367003, M. Yaragskogo 94, Makhachkala, Russia

\*lowtemp@mail.ru

The magnetocaloric effect is usually estimated by an indirect method from measurements of magnetization in constant magnetic fields, or is measured by a direct method with single cycles of applying a magnetic field. In real magnetic refrigeration machines, the magnetocaloric material will be exposed to an alternating (cyclic) magnetic field. Therefore, from a practical point of view, it is important to study the magnetocaloric properties of promising magnetocaloric materials in alternating magnetic fields. Relatively recently begun studies of the MCE in alternating magnetic fields show that in many Heusler alloys there is a strong dependence of the MCE on the frequency of the change in the magnetic field, degradation of the MCE under prolonged exposure to a cyclic magnetic field. The nature of the frequency dependence of the MCE at the moment does not have a generally accepted explanation, and the mechanisms responsible for degradation have been partially established.

This paper presents the results of a study of the magnetocaloric properties of the Ni<sub>49.3</sub>Mn<sub>40.4</sub>In<sub>10.3</sub> Heusler alloy. In this composition, three phase transitions are observed - a ferromagnetic-paramagnetic magnetic phase transition in the austenite phase, austenite-martensite magnetostructural phase transition, and a transition to a ferromagnetic state in the martensite phase. The magnetocaloric effect was directly measured in cyclic magnetic fields of various amplitudes (0.62, 1.2, and 1.8 T) and frequencies up to 30 Hz (in the case of a magnetic field of 1.8 T, the frequency was low, 0.3 Hz).

It has been found that in this composition, significant and comparable in modulus direct and inverse MCEs are observed in the region of magnetic and magnetostructural phase transitions, and this is observed in relatively low magnetic fields. This behavior is not typical for Heusler alloys, since high magnetic fields are usually required to induce a significant MCE in the region of the magnetostructural transition. With increasing frequency, the value of the MCE in the region of the magnetic phase transition decreases much more strongly in compared with that near the magnetostructural phase transition region. Although there are very few works on the study of the MCE in alternating fields, it can be said that the stronger dependence of the MCE value on the frequency of the magnetic field in the region of the magnetic transition is anomalous. Various mechanisms are proposed that are responsible for the observed anomalous behavior of the MCE in the studied Heusler alloy.

This work was supported by the Russian Science Foundation grant no. 22-19-00610.

# APPLICATION OF ION-SELECTIVE ELECTRODE FOR EXPRESS DETERMINATION OF CEFTRIAXONE IN BIOSYSTEMS

S. Tataeva<sup>a</sup>, R. Zeynalov<sup>a</sup>, K. Magomedov<sup>a,b,\*</sup>

<sup>a</sup> Dagestan State University, 367000, M.Gadzhieva 43A, Makhachkala, Russia

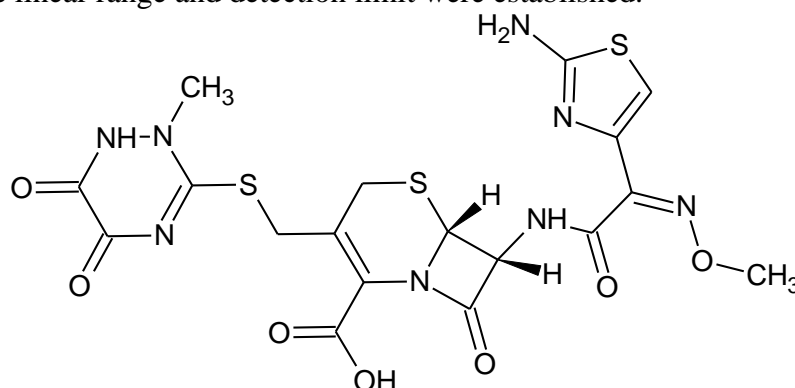
<sup>b</sup> Immanuel Kant Baltic Federal University, 236004, Nevskogo 14, Kaliningrad, Russia

\*corresponding author: [m\\_kurban@mail.ru](mailto:m_kurban@mail.ru)

Antibiotics are one of the most commonly prescribed drugs for seriously ill patients with significant individual pharmacokinetic variability. Non-invasive monitoring of antibiotic levels in relevant biological fluids, especially in polytherapy, makes a significant contribution to assessing the adequate effect of antibiotics, which is currently underutilized for identifying the relationship between antibiotic dosing and clinical effects. A number of chemical analyses have been developed using pharmaceutical dosage forms and their content determination.

Antibiotics enter the environment due to wastewater from pharmaceutical companies and clinics. Therefore, the determination of antibiotics, which belong to the group of medicinal compounds that have gained wide distribution but at the same time pose a potential danger to human health, is an especially relevant problem for modern analytical, clinical chemistry, pharmaceutical, and food industries.

The development and optimization of a ceftriaxone-selective electrode (Ceftr-SE) for accurate and rapid determination of ceftriaxone in biosystems is an important task in medical diagnostics. In this article, equilibria in the "membrane-solution" system were investigated as a function of pH and the amount of electroactive component (EAC). The electrochemical characteristics of Ceftr-SE were determined, and the linear range and detection limit were established.



Structural formula of ceftriaxone

To test the functionality of Ceftr-SE, experiments were conducted to determine ceftriaxone in the blood and saliva of COVID-19 patients in a flow injection mode. Optimal conditions for the flow injection system were found. The results were confirmed by atomic absorption spectroscopy (AAS) and the "spiked-recovery" method. The obtained data indicate high sensitivity and accuracy of Ceftr-SE.

This patent [1] may be useful for specialists involved in monitoring the levels of antibiotics in biological fluids.

[1] S. Tataeva, Patent. RU 2789107 C1 (30.01.2023 Bull. № 4)

# ASYMMETRY OF DOMAIN WALLS MOTION IN OUT OF PLANE AND IN-PLANE MAGNETIC FIELDS IN Pd/Co/Pd SYSTEM

A. Davydenko<sup>a</sup>, N. Chernousov<sup>a,\*</sup>, A. Pashenko<sup>a</sup>, A. Turpak<sup>a</sup>, A. Kozlov<sup>a</sup>

<sup>a</sup> Far Eastern Federal University, 690920,10 Ajax Bay, Russky Island,Vladivostok

\*nnchernousov@gmail.com

In this work, we study the dependencies of the velocity of domain walls (DWs) motion on the in-plane magnetic field  $v(H_x)$  at different values of the perpendicular magnetic field  $H_z$  in a sample Si/Cu(2 nm)/Pd(10 nm)/Co(0.7 nm)/Pd(3 nm) with perpendicular magnetic anisotropy (PMA).

This sample was evaporated by molecular beam epitaxy. PMA is induced in the Co layer with an anisotropy field of 1.2 T. The behavior of  $v(H_x)$  dependencies at different positive  $H_z$  was studied using a magneto-optical Kerr microscope. Firstly, we measured the dependence of the DW motion velocities on the perpendicular field  $v(H_z)$  (Fig. 1a). Curve  $v(H_z)$  can be divided into 3 regimes according to the nature of the dependence of the DW velocity on  $H_z$ : creep, depinning, and flow.

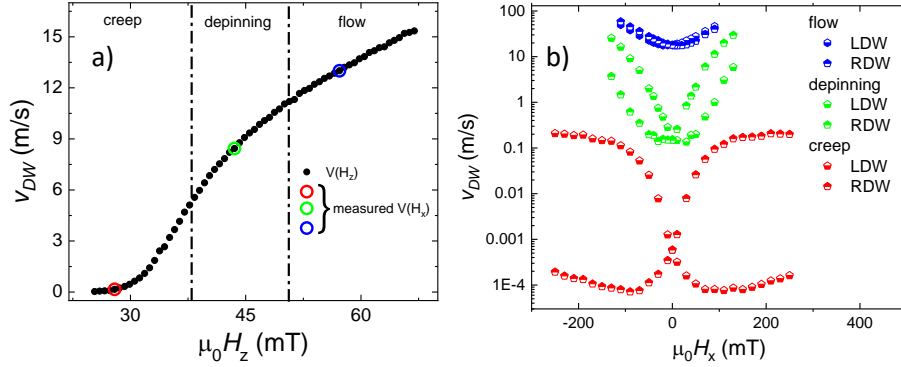


Fig. 1. a)  $v(H_z)$  dependence. The colored circles indicate the  $H_z$  values at which  $v(H_x)$  measurements were taken, shown in b)

Then, the dependencies of the velocities of the left and right DWs of a circular domain on the in-plane field  $v(H_x)$  were measured for different values of  $H_z$  (Fig. 1b). An asymmetry coefficient of the  $v(H_x)$  dependencies was defined as:

$$A = v_{right\ DW}(H_x)/v_{left\ DW}(H_x)$$

The maximal values of the asymmetry coefficient  $A_{max}(H_x > 0)$  were observed in the creep regime, and  $A_{max}$  decreased with an increase in the  $H_z$  magnetic field. In the flow regime, the dependencies  $v(H_x)$  have a parabolic shape with a minimum in a field equal to the Dzyaloshinskii-Moriya interaction (DMI) field taken with the opposite sign [1]. The direction of predominate growth of magnetic domains reversed during the transition from depinning to flow regime.

Such behavior of asymmetry of DWs motion could be explained by the effect of chiral damping; however, the chiral damping constant presents both in the equation describing the flow regime and in the creep law. Therefore, if the asymmetry of DWs motion was determined by chiral damping, then it would also be preserved in the flow regime and would not depend on  $H_z$ . This suggests that the reason for strong asymmetric DWs propagation in the creep regime in the investigated system is not chiral damping, but another unknown effect.

Acknowledgment: The authors thank for financial support of the Russian Ministry of Science and Higher Education (State Task № FZNS-2023-0012) and Endowment Fund of the Far Eastern Federal University in the form of Personal Grant named after the Nobel Prize in Physics, Academician I.E. Tamm (order No. 12-132133 dated 11.17.2022).

[1] Soong-Geun Je, Phys. Rev. B. 88, 214401 (2013)

# Biocompatible magnetoelectric core-shell nanoheterostructures for biomedical applications

R. Chernozem<sup>a,\*</sup>, A. Urakova<sup>a</sup>, P. Chernozem<sup>a</sup>, D. Koptsev<sup>a</sup>, A. Kholkin<sup>a,\*</sup>, M. Surmeneva<sup>a</sup>, R. Surmenev<sup>a,\*</sup>

<sup>a</sup> Tomsk Polytechnic University, 634050, Lenina 30, Tomsk, Russia

\*Corresponding author emails: r.chernozem@mail.ru, rsurmenev@mail.ru, holkin\_al@tpu.ru

**Introduction.** Magnetoelectric (ME) nanoparticles (NPs) attract great interest from the scientific community due to their unique properties for diverse biomedical applications. As compared to widely studied magnetic NPs, ME NPs are able to provide electrical stimulation due to the ME effect and their targeted locomotion [1, 4]. These properties of ME NPs are explained by their composition, which consist of magnetostrictive and piezoelectric phases. Despite the advantages of ME NPs, the attention should be addressed to several common challenges for clinical applications, such as biocompatibility, optimization of the size and morphology, determination of the bio-safety profile, and reproducibility. For instance, to date, mainly ME NPs were fabricated using toxic Co [1, 2], Ni [3], etc. Furthermore, since ME NPs are complex structures with many functions, their synthesis often can include a combination of several methods, leading to reducing reproducibility. Thus, the present study is aimed to design novel biocompatible ME nanoheterostructures by a cost-effective hydrothermal method. For this, biocompatible magnetic  $\text{MnFe}_2\text{O}_4$  (MFO) and ferroelectric  $\text{Ba}_{(1-x)}\text{Ca}_x\text{Zr}_y\text{Ti}_{(1-y)}\text{O}_3$  (BCZT) were studied for the first time.

**Materials and methods.** ME core-shell NPs were obtained by using two-steps hydrothermal approach. As the first step, magnetic MFO cores were formed using a mixture of  $\text{MnCl}_2 \cdot 4\text{H}_2\text{O}$ ,  $\text{FeCl}_3 \cdot 6\text{H}_2\text{O}$  and NaOH subjected to an autoclave at 180°C for 3 h with a subsequent surface functionalization using oleic acid (OA) and polyvinylpyrrolidone (PVP). As the second step, the BCZT shell on cores were obtained using a mixture of  $\text{CaCl}_2$ ,  $\text{BaCl}_2 \cdot 2\text{H}_2\text{O}$ ,  $\text{ZrOCl}_2 \cdot 8\text{H}_2\text{O}$ ,  $\text{TiCl}_4$  and NaOH subjected to an autoclave at 200°C for 24 h. All the obtained NPs were extensively characterized using scanning electron microscopy (SEM), X-ray diffraction (XRD), transmission electron microscopy (TEM), Raman spectroscopy and magnetometer. The catalytic activity of developed ME NPs under external magnetic field (ME effect) were studied using a model dye Rhodamine B and spectrophotometry.

**Results and Discussion.** The analysis of results revealed the successful formation of perovskite BCZT shell only on the surface of PVP- and OA-functionalized MFO cores as compared to pristine ones. However, slightly higher amount of the BCZT phase was detected in the case of PVP-functionalized MFO cores, likely, due to the hydrophilic nature of PVP as compared to hydrophobic OA. The formation of the BCZT shell obviously reduced the magnetization of both PVP- and OA-functionalized MFO cores from  $64.0 \pm 0.3$  to  $18.7 \pm 0.1$  emu/g and from  $67.4 \pm 1.3$  to  $20.7 \pm 0.2$  emu/g, respectively. Notably, both types of the developed ME NPs revealed a pronounced catalytic degradation of Rhodamine B up to 95% for 2.5 h under magnetic field (100 Hz, 150 mT).

**Acknowledgements.** The work was supported by the Ministry of Science and Higher Education (#075-15-2021-588 from 1.06.2021) and Russian Science Foundation (project #23-23-00511). Authors thank D.V. Wagner and E.Yu. Gerasimov for the magnetic and structural characterization, respectively. TEM was performed at “National centre of investigation of catalysts” at the Borekov Institute of Catalysis.

## References.

1. Chen X.Z., et al. *Mater. Horiz.*, 3(2), p. 113-118 (2016).
2. Betal S., et al. *Sci. rep.*, 8(1), p. 1-9. (2018).
3. Mushtaq F., et al., *Adv. Fun. Mater.*, 29(12), p. 1808135 (2019).

# Core-Shell Exchange Interaction Effect in the Approach to Magnetic Saturation of a Magnetite-like Nanoparticle

S. Komogortsev<sup>a,\*</sup>, S. Stolyar<sup>a</sup>, R. Iskhakov<sup>b</sup>, A. Mohov<sup>a</sup>

<sup>a</sup>FRC KSC SB RAS, 660036, Akademgorodok, 50, Krasnoyarsk, Russia

<sup>b</sup>Kirensky Institute of Physics, FRC KSC SB RAS, 660036, Akademgorodok 50/38, Krasnoyarsk, Russia

\*komogor@iph.krasn.ru

The core-shell model of the magnetic structure of iron oxide nanoparticles assumes a single-domain magnetically ordered core surrounded by a layer with frozen spin disorder. Owing to the exchange interaction between the shell and the core, spin disorder should lead to inhomogeneous magnetization in the core. The suppression of this inhomogeneity by an external magnetic field leads to a nonlinear behavior of the magnetization with respect to the field in the region approaching saturation. The expression proposed to describe this effect is tested using micromagnetic simulation. An analysis of the approach to magnetic saturation of iron oxide nanoparticles at different temperatures using this expression makes it possible to separate the contributions of the surface anisotropy related to the core-shell interface and the effective random anisotropy stabilizing the spin-glass state of the shell. A number of examples of the use of the proposed expression to describe the approximation of magnetization to saturation in magnetite-like particles indicate its universality and internal relationships of fitting parameters. In addition, this approach makes it possible to estimate the magnetic correlation length of the particle core. It is shown that this length can change with a change in the particle temperature.

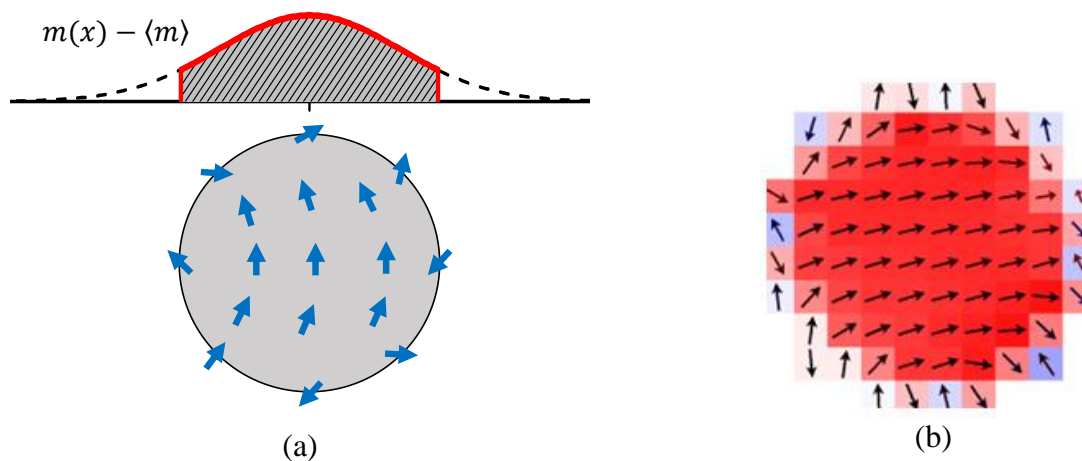


Fig.1. No uniform magnetization in the core of a particle caused by frozen spin disorder on its surface (a), the result of micromagnetic simulation of a 10 nm particle (b).



## Diode Effects in $\text{Y}_3\text{Fe}_5\text{O}_{12}$ -Nb and $\text{Y}_3\text{Fe}_5\text{O}_{12}$ -Al heterostructure

L. Uspenskaya\*, S.Egorov

Osipyan Institute of Solid State Physics RAS, 142432, Academician Osipyan 2, Chernogolovka, Russia

\*uspenska@issp.ac.ru

In recent years, large attention has been paid to the development of superconducting electronics [1]. In particular, spin valves are implemented on the basis of superconductor-magneto-soft and magneto-hard ferromagnet structures [2], and magnetoresistive switches are implemented on ferromagnet-superconductor structures [3], i.e. switching the resistance of a superconductor by a magnetic field.

Currently, the possibilities of field-free switching of hybrid structures are intensively investigated [4,5]. Recently we have shown [6,7] that in  $\text{Y}_3\text{Fe}_5\text{O}_{12}/\text{Al}$  structures in the temperature region of a superconducting transition, it is possible to switch the resistance of structures both by turning the magnetic field and by current inversion. The effect was as large as 1000% change of the resistance. It was well described by the influence of the Zeeman field on the superconducting transition of aluminum.

In this report, we suggest to use the magnetostrictive effect in  $\text{Y}_3\text{Fe}_5\text{O}_{12}$  to create structures in which the resistance is switched by current inversion, and experimentally show the possibility of implementing this idea using the example of the  $\text{Gd}_3\text{Ga}_5\text{O}_{12}/\text{Y}_3\text{Fe}_5\text{O}_{12}/\text{Nb}$  structure, where the magnetic domain structure of the garnet film is specifically modified due to deformation with a certain choice of orientation of the niobium strip.

Experiments were carried out on microstructures, but it is possible to reduce them to submicron sizes. The effect can be used to create a new type of low-temperature memory elements, low-temperature switches, and magnetic field sensors.

- [1] A. Sidorenko (Ed.). Functional Nanostructures and Metamaterials for Superconducting Spintronics. NanoScience and Technology, Springer, Cham. – 2018. [https://doi.org/10.1007/978-3-319-90481-8\\_1](https://doi.org/10.1007/978-3-319-90481-8_1).
- [2] R.G. Deminov, L.R. Tagirov., R.R. Gaifullin, et al., J. Magn. Magn. Mater. 373,16,(2015)
- [3] L.N. Karelina, R.A. Hovhannisyan, I.A. Golovchanskiy, V.I. Chichkov, A. Ben Hamida, V.S. Stolyarov, L.S. Uspenskaya, Sh.A. Erkenov, V.V. Bolginov, V.V. Ryazanov, Journ. Appl. Phys. 130, 173901 (2021).
- [4] Ja. Santamaria., Nature Materials, 21, 993 (2022).
- [5] S.S. Ustavshchikov, M.Yu. Levichev, I.Yu. Pashenkin, N.S. Gusev, S.A. Gusev, D.Yu. Vodolazov, JETP 135, 226 (2022)
- [6] O.A. Tikhomirov, O.V. Skryabina, L.S. Uspenskaya, Journ. Magn. Magn. Mat. 535, 168071 (2021)
- [7] O.V. Scriabina, L.S. Uspenskaya, Physics of the Solid State 64, 1356 (2022)

# Domain wall dynamics in cylindrical wires with non-uniform anisotropy

K. Chichay <sup>a,\*</sup>, I. Lobanov <sup>a</sup>, V. Uzdin <sup>a</sup>

<sup>a</sup>Faculty of Physics, ITMO University, 197101 St. Petersburg, Russia

\*ksenia.chichay@metalab.ifmo.ru

Low-dimensional magnetic systems with cylindrical symmetry (such as nano- and microwires) are of particular interest from the point of view of studying their magnetization reversal and domain wall dynamics [1]. Their shape determines a number of interesting properties and advantages comparing to planar structures. For example, the presence of strong shape anisotropy and cylindrical symmetry makes it possible to stabilize axisymmetric states; moreover, due to cylindrical geometry, the so-called Walker breakdown is suppressed [2] allowing to expect ultrafast domain wall velocities [3, 4]. The small spatial size of the system increases the role of surface and interface effects, and also makes it possible to significantly change the magnetic characteristics under the action of mechanical stresses or induced anisotropy, which turns out to be a very energy-efficient approach [5].

In this work, we discuss the micromagnetic structure and domain wall dynamics in cylindrical micro- and nanowires. We consider the effect of anisotropy of various origins, magnitudes, and distribution along the radius on such parameters as the DW velocity and values of the fields required for the DW nucleation and collapse. The evolution of the domain wall size and its structure as it moves under the action of an electric current and an external magnetic field is also examined.

To describe magnetic configurations in cylindrical systems, we used the micromagnetic model, the dynamics is modeled based on the Landau-Lifshitz-Gilbert equation. Given the symmetry of the problem, all the numerical calculations are made in the cylindrical coordinates.

This work was supported by RFS grant 22-22-00632

1. J. Alam, et.al., Cylindrical micro and nanowires: Fabrication, properties and applications, *JMMM* 513 (2020)
2. M. Yan, Beating the Walker Limit with Massless Domain Walls in Cylindrical Nanowires, *PRL* 104 (2010)
3. R. Hertel, Ultrafast domain wall dynamics in magnetic nanotubes and nanowires, *J. Phys.: Condens. Matter* 28 483002 (2016)
4. K. Chichay, et. al., Tunable domain wall dynamics in amorphous ferromagnetic microwires. *Journal of Alloys and Compounds*, 835, 154843 (2020)
5. A. A. Bukharaev, et al. Straintronics: a new trend in micro- and nanoelectronics and materials science, *Physics-Uspekhi* 61 (12): 1175 (2018)

# Dynamic susceptibility and magnetic hyperthermia in ensembles of ferromagnetic nanoparticles

L. Iskakova, A. Zubarev\*

Ural Federal University, 620083, Lenina 51, Ekaterinburg, Russia

\*A.J.Zubarev@urfu.ru

Magnetic hyperthermia (MH) is a progressive method of cancer diseases therapy. The key idea of this method is in injection of ferromagnetic nanoparticles, covered with special bioactive layers, into an area with diagnosed tumor. Due to these layers, the particles are captured by the tumor cells. Then an alternating magnetic field is applied to this area. This field heats the particles, consequently, the tumor cells, anchoring them. If the cell temperature exceeds 42-43°C, the protein in it denatures and the cell dies. At the same time the healthy cells are not injured till, approximately, 52-55°C.

Obviously, the clinical application of the MH therapy requires accurate prediction and control the heat generation and temperature in the tumor area. The classical Rosenzweig model of magnetic hyperthermia deals with the systems of non-interacting magnetic nanoparticles. However, experiments show that the particles, being embedded into a cell or another biological tissue, very often accumulate and form dense structures where the interparticle interaction can be very significant and must be taken into account. Solution of multiparticle problems like that is one of fundamental difficulties of statistical physics, physics of composite materials and other related topics. Some results can be obtained as semi-empirical ones, based on reliable experimental investigations. On the other hand, it is important to develop, for some model systems, mathematically robust approaches, which could be a basis for understanding of the studied phenomena and to give a key to study more realistic situations.

In the talk we present results of theoretical study of dynamic response and magnetic hyperthermia in two kind of systems of single-domain ferromagnetic nanoparticles. The first one is spatially homogeneous (gas-like) distribution, in a host medium, of the magnetically interacting particles with chaotical orientation of their axes of easy magnetization. The second one is the simplest kind of heterogeneous clusters, namely – dimer, consisting of two particles. The particles were considered under the action of a linearly polarized ac magnetic field. We restricted our analysis by consideration of the particles with strong magnetic anisotropy. For example, for magnetite particles it corresponds to the particle diameter about 15nm and more. The relatively large diameter of the particle provides its good coupling with the applied field, and, therefore, efficiency of the magnetically induced effects.

In the case of the homogeneous particles disposition, their interaction has been considered in the frame of the regular pair approximation. For the both types of the particles morphology (gas-like and clustered ones), our analysis has been carried out based on the Fokker-Planck equation for the distribution function over orientations of the particles magnetic moments by using the ideas of the classical Kramer's approach.

Analysis shows that for the homogenous systems the interparticle interaction increases characteristic time of magnetization relaxation when the field is weak and speeds up the relaxation if the Langevin parameter of the particle is comparable with 1 or more. In the case of the particles in the dimer, the interparticle interaction significantly, up to orders of magnitude, increases the time of their moments relaxation. Effect of these factors on intensity of the heat production, provoked by the field, is discussed.

# Effect of $\text{Pr}^{3+}$ singlet ground state on magnetoelectric properties of paramagnetic $\text{Pr}_3\text{Ga}_5\text{SiO}_{14}$ langasite

A. Tikhanovskii<sup>a,\*</sup>, V. Ivanov<sup>a</sup>, A. Kuzmenko<sup>a</sup>, A. Mukhin<sup>a</sup>

<sup>a</sup> Prokhorov General Physics institute of the Russian Academy of Sciences, 119991, Vavilova 38, Moscow, Russia

\*tikhanovskii@phystech.edu

In our work, we report for the first time on a field-induced magneto-electric effect in the  $\text{Pr}_3\text{Ga}_5\text{SiO}_{14}$  langasite (Figure 1). Previously, this compound attracted attention due to its interesting magnetic properties [1],[2]. It has a non-centrosymmetric space group  $P321$  in which rare earth magnetic ions occupy three low-symmetry  $C_2$  positions, with a local axis coinciding with one of the three second-order crystal axes ( $a$ ,  $b$ ,  $-a-b$ ). The magnetic ions remain in a paramagnetic state down to low temperatures and form a triangular lattice topologically equivalent to Kagome. We propose a model according to which the magnetic properties of the compound are determined by two lower singlet levels. The random distribution of Ga/Si in the  $2d$  positions leads to a local violation of  $C_2$  symmetry, distortion of the crystal field, and distribution of the splitting magnitude in the crystal field, which determines their unusual behavior in a magnetic field. Using this model of local magnetic structure and a phenomenological approach, we have shown that the electric polarization induced by a magnetic field is determined only by the sum of magnetic ions local susceptibilities and an additional Van Vleck contribution, which manifests itself at high temperatures (Figure 1b).

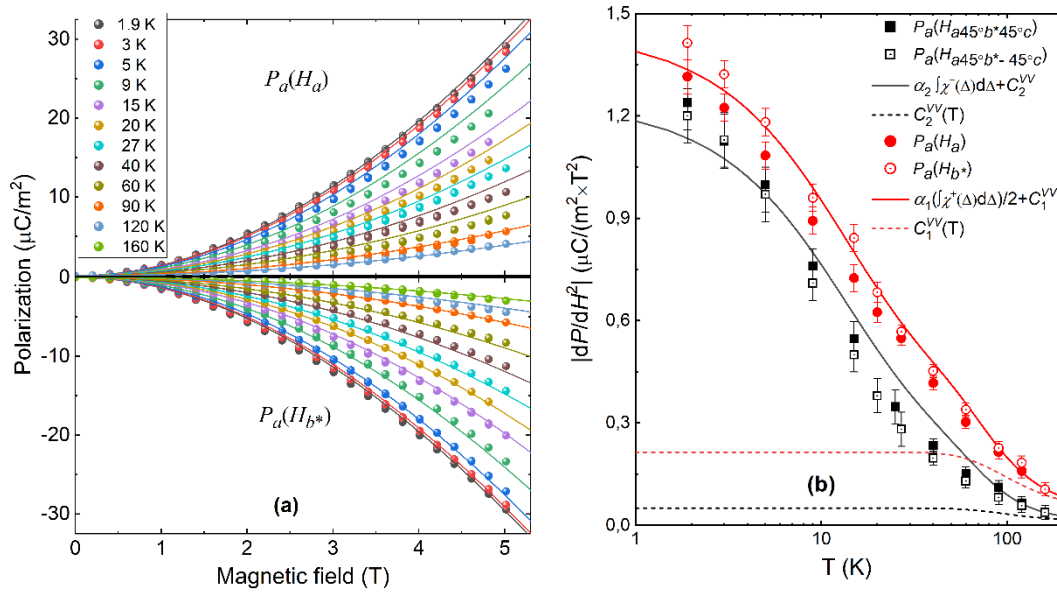


**Fig. 1** (a) Field dependencies of the electric polarization  $P_a$  induced by a magnetic field  $H \parallel a, b^*$  and (b) temperature dependencies of the magnetoelectric susceptibility in fields  $H \parallel a, b^*, a45^\circ b^* \pm 45^\circ c$ , which indicates that the field deviates from the  $ab^*$  plane at an angle  $\pm 45^\circ$  towards the  $c$  axis in the vertical plane crossing the  $ab^*$  plane at an angle of  $45^\circ$  to the  $a$  axis. Symbols represent experimental data, lines – theory.

This work was supported by the Russian Science Foundation (Project No. 22-42-05004).

[1] P. Bordet, J. Phys.: Condens. Matter, 18, 5147 (2006)

[2] A. Zorko, PRL, 104, 057202 (2010)

# Enhancing magneto-optical effects by controlling the radiative losses of surface plasmons

A. Frolov\*, M. Kiryanov, I. Novikov, V. Popov, T. Dolgova, A. Fedyanin

Lomonosov Moscow State University, 119991, Leninskie gory 1, Moscow, Russia

\*frolovay@my.msu.ru

Magneto-optics plays a significant role in modern nanophotonics as it gives a feasibility to control the intensity, polarization, and phase of the light under external magnetic field. The values of well-known Faraday and Kerr magneto-optical effect should be significantly increased for practical applications. Surface plasmons (SPs) have been actively employed to enhance magneto-optical effects [1]. A lot of works have been devoted to optimization of the SP absorption losses to increase magneto-optical effects [2,3]. However, the tailoring SPs radiation losses has not been considered in terms of control and enhancement of magneto-optical effects.

In this work, we firstly show that dark SPs can significantly increase the transverse magneto-optical Kerr effect (TMOKE) in the magnetoplasmonic crystals (MPCs) consisting of 1D array of Au/Ni/Au nanoantennas (Figure 1(a)) [4]. Dark SPs possess the symmetric field distribution and, therefore, can not be excited by a plane wave source at normal incidence. Therefore, it has lower radiative losses than that of bright modes with antisymmetric field distribution. Such a difference of radiative losses leads to a higher quality factor of dark SPs and consequently to the greater magneto-optical response.

In the second part of the work, we consider the influence of SP radiation losses on the TMOKE in the all-nickel one-dimensional periodically corrugated gratings with quasi-sinusoidal profiles (Figure 1(b)). Radiative losses in this MPC are tailored by a change of the grating height ( $h$ ). At the certain height, radiative losses become equal to absorption ones that manifests the critical coupling between SPs and incident light. Such critical coupling implements higher field localization in the MPC that leads to the significant enhancement of the TMOKE in comparison with other grating heights [5].

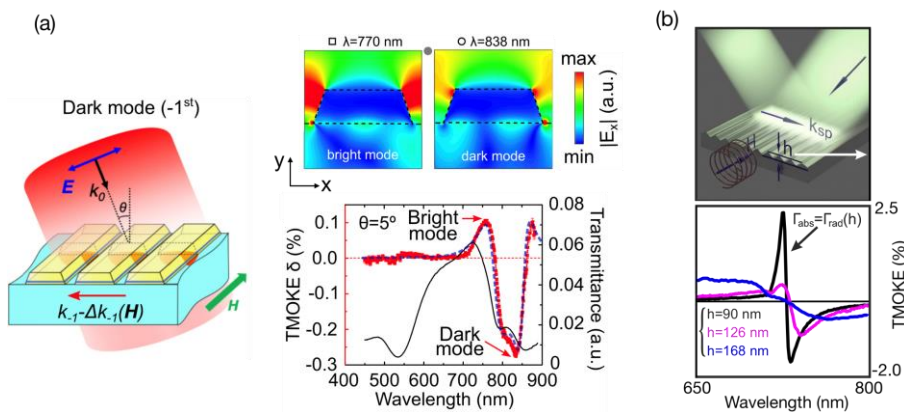


Figure 1. (a) Schematic of the TMOKE enhancement by dark SPs in the MPC consisting of 1D array of Au/Ni/Au nanoantennas. (b) Tailoring TMOKE enhancement by a change of the radiative losses of SPs through variation of corrugation depth ( $h$ ) of the all-nickel MPC.

- [1] R. S. Singh et al., Mater. Today 4, 100033 (2023)
- [2] V. I. Belotelov et al., Nat. Nanotechnol. 6, 6 (2011)
- [3] A.I. Musorin et al., Appl. Phys. Lett. 115, 151102 (2019)
- [4] A.Yu. Frolov et al., Phys. Rev. B 101, 045409 (2020)
- [5] M.A. Kiryanov et al., APL Photonics 7, 026104 (2022)

# Exchange enhancement of the magnetocaloric effect in ferromagnetic nanostructures

I. Pashenkin<sup>a,\*</sup>, N. Polushkin<sup>a</sup>, A. Fraerman<sup>a</sup>, M. Sapozhnikov<sup>a</sup>, E. Kravtsov<sup>c,d</sup>

<sup>a</sup>Institute for Physics of Microstructures RAS, 603950, Nizhny Novgorod, Russia

<sup>c</sup>M. N. Mikheev Institute of Metal Physics, Ural Branch, RAS, 620108, Yekaterinburg, Russia

<sup>d</sup>Ural Federal University after the first President of Russia B. N. Yeltsin, 620002, Yekaterinburg, Russia

\*pashenkin@ipmras.ru

Usually a sufficiently large (up to 10 degrees) magnetocaloric effect (MCE) is achieved in a magnetic field of several T near the Curie temperature ( $T_C$ ) of the magnetic material. The need to create such strong fields hinders the development and application of magnetic cooling systems. The authors of [1] proposed a new approach to increase the magnetocaloric efficiency based on the use of the magnetic proximity effect of a “weak” ferromagnet (PM) with “strong” ferromagnets (FM) in thin-film  $FM_1/PM/FM_2$  nanostructures. Due to the exchange interaction at the PM and FM interfaces, the average magnetization of the PM interlayer depends on the mutual orientation of the magnetizations of the  $FM_1$  and  $FM_2$ , which can be controlled by applying a relatively small external magnetic field of the order of  $10^{-2}$  T.

In this work, an experimental study of the MCE in Gd layers sandwiched between Fe layers in  $Cr(50)/CoSm(30)/Fe(1)/Gd(2.5 - 5)/Fe(1)CoFeB(2)/Ta(5)$  (thicknesses are given in nm) structures is carried out. Films are deposited by RT magnetron sputtering onto Si-substrates. The  $Fe(1)/CoFeB(2)$  is a free layer with relatively low magnetization reversal field, while the  $CoSm(30)/Fe(1)$  is a fixed layer. The magnetocaloric potentials  $\Delta S$  of the investigated samples are determined from the magnetization curves (Figure 1 (a,b)) obtained at different temperatures on a Lake Shore Cryotronics, Inc. vibro-magnetometer. To calculate  $\Delta S$ , the Maxwell thermodynamic relation is used:

$$\Delta S = \int_{H_1}^{H_2} \frac{\partial M(H,T)}{\partial T} dH \quad (1)$$

$\Delta H = H_2 - H_1$  is the free layer magnetization reversal field range.  $\Delta S(T)$  is determined approximately by calculating the values of  $[M(H, T_i) - M(H, T_{i+1})]/\Delta T$  and then integrating the calculation result over the interval of fields  $\Delta H(T_i)$ .

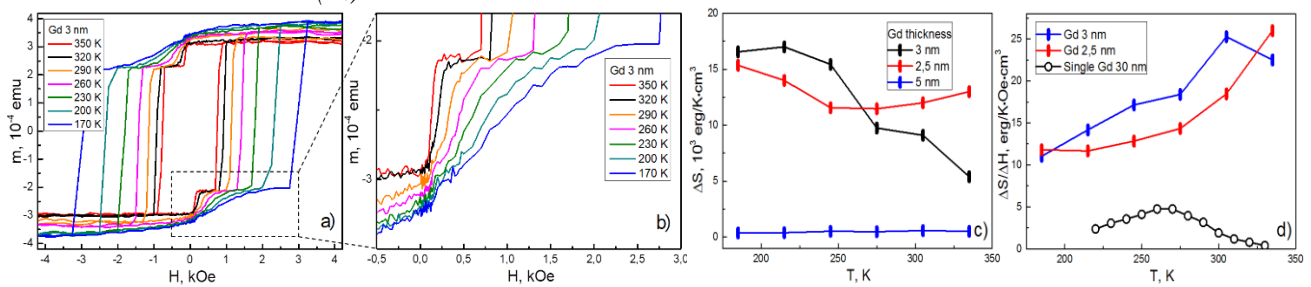


Figure 1. a),b) – magnetization curves of the  $FM_1/Gd(3nm)/FM_2$  sample in the 350 – 170 K temperature range. c),d) –  $\Delta S(T)$  and  $\Delta S/\Delta H(T)$  for samples with Gd thickness of 2.5,3 and 5 nm.

The measured magnetocaloric potential  $\Delta S$  decreases strongly with increasing Gd interlayer thickness up to 5 nm (Figure 1c)). The maximum obtained value of  $\Delta S$  in the investigated systems is about  $1.7 \cdot 10^4$  erg/K·cm<sup>3</sup> in 1 kOe magnetic field range. The magnetocaloric efficiency  $\Delta S/\Delta H$  in  $FM_1/Gd(2.5, 3\text{ nm})/FM_2$  samples is significantly higher than in a single Gd(30 nm) layer (Figure 1d)), which indicates the effectiveness of exchange enhancement of the magnetocaloric effect.

The work was supported by the Russian Science Foundation (project No. 23-22-00044).

[1] A. A. Fraerman, I. A. Shereshevskii, *Jetp Lett.* 101, 618–621 (2015).

# Exchange mechanism of ultrafast optical demagnetization in nanolayers of transition metals

V. Skidanov<sup>a,\*</sup>

<sup>a</sup>Institute for Design Problems in Microelectronics RAS, Moscow 124365, Sovetskaya str. 3, Russia

[\\*skidanov@ippm.ru](mailto:*skidanov@ippm.ru)

Universal and striking phenomenon of ultrafast demagnetization of ferromagnets by means of femtosecond optical pulse has been investigated widely during last decades. Nevertheless the nature of demagnetization was not understood clearly up to now [1, 2].

Demagnetization was considered as a consequence of spin relaxation of optically excited majority electrons. Few artificial models such as superdiffusion of excited electrons or enhanced spin-orbit coupling were suggested to describe demagnetization effect and its very high rate which is specific rather to exchange interaction. Thermal equilibration process between hot electrons, spins and lattice reservoirs was considered in many papers as well.

The main features of ultrafast demagnetization which should be explained are:

- demagnetization after femtosecond optical pulse irradiation itself and femtosecond rate of this process;
- universal character of the demagnetization effect which is inherent for all ferromagnetic transition metals;
- rapid process ( $\sim 1$  ps) of magnetization partial recovery after optical pulse termination;
- relatively long lifetime of partially demagnetized state ( $> 10$ ps).

The simple model is suggested in present report to explain the main features of the demagnetization effect in transition metals on the basis of intra-band exchange interaction between d-band electrons below Fermi level.

In accordance with Stoner model of d-band splitting in transition metals minority sub-band has always higher energy and more number of empty states than majority sub-band above Fermi level so that minorities dominate over majorities among excited electrons [3]. Therefore the number of minority empty states below Fermi level exceeds the number of majority empty states forming the inversion of majority/minority populations during optical pulse. The localized polarized electrons suffer varying exchange interaction with neighbours. As a consequence significant part of localized majorities changes their polarity transferring to released minority states with spin inversion thus reduce magnetization of medium.

The transfer rate corresponds to exchange interaction frequency. Spin inversion accompanies by broadband circularly polarized terahertz electromagnetic emission in the direction of magnetization to conserve angular momentum.

Reverse recombination of excited minorities is restricted since a significant part of minority states are occupied now by intra-band inversion of majorities so that partial demagnetization conserves during long spin-lattice relaxation time.

Partial recovery of magnetization occurs due to recombination with spin inversion of a small fraction of excited minorities near Fermi level (within  $\sim 100$  meV) with released majority states induced by internal terahertz emission when light pulse is terminated.

[1] A. Kirilyuk, A.V. Kimel, and T. Rasing, *Rev. Mod. Phys.*, 82, 2731 (July–September 2010).

[2] F. Hellman, A. Hoffmann, Y. Tserkovnyak *et al.*, *Rev. Mod. Phys.*, 89, No. 2, 025006-2 (2017).

[3] V. P. Zhukov, E. V. Chulkov, and P. M. Echenique, *Phys. Rev. B* 73, 125105 (2006).

# Experimental evidence of the sublattice ferrimagnetism in quasi-freestanding graphene on Au/Co(0001)

A. Tarasov<sup>a,\*</sup>, A. Eryzhenkov<sup>a</sup>, A. Rybkin<sup>a</sup>

<sup>a</sup> St. Petersburg State University, 7/9 Universitetskaya nab., St. Petersburg, 199034, Russia

\*artem.tarasov@spbu.ru

Today graphene remains one of the most intensively researched materials due to its high potential for application in 2D electronics and spintronics. Even though graphene in its quasi-freestanding state is a non-magnetic material with weak spin-orbit interaction (SOC), its electronic properties can be significantly modified upon contact with the atoms of the substrate. For example, the interaction of graphene with heavy atoms can lead to an increase in SOC in graphene, which in turn makes it possible to efficiently generate spin currents based on the spin Hall effect and its quantum version [1]. On the other hand, the combination of strong spin-orbit interaction and magnetism is a necessary condition for observing the quantum anomalous Hall effect [2]. Such a combination can be realized in the magneto-spin-orbit (MSO) graphene at the Au/Co(0001) interface, which not only provides conditions for the implementation of the magnetic proximity effect and the giant Rashba effect [3], but also allows to preserve the linear nature of the dispersion of electron bands near the Fermi level and the ultrahigh mobility of charge carriers.

In this work, calculations within the framework of density functional theory (DFT) have shown the presence of ferrimagnetic order in the A and B sublattices of graphene induced by the dislocation loops in Au/Co interface [4]. Such magnetic ordering of the system along with Rashba spin-orbit coupling induced by Au, as it turned out, leads to the appearance of a band gap in the K-point of the Brillouin zone of graphene and the asymmetry of its spin texture. At the same time our tight-binding calculations indicate that graphene in such a system can exhibit non-trivial topological properties that can be used to realize the Hall effect of circular dichroism and create an infrared detector of circularly polarized radiation based on graphene [4,5].

However, it is worth noting that the MSO graphene reveal one important problem of experimental study of such systems. Due to the very small magnetic moments of carbon atoms (the presence of which, however, significantly affects the electron and spin structures of the MSO graphene), the study of the magnetic order of graphene by standard methods represents an unsolvable task. In this work by modeling the spatial and energy distribution of the electron density, it was shown that the magnetism of carbon atoms manifest itself in the data of scanning tunneling spectroscopy (STS). Modeling of STS data and its comparison with the experimental results gives us strong confidence in the induction of the ferrimagnetic state in graphene on the Au/Co(0001) substrate and makes it possible to estimate the magnitude of the energy gap in its band structure.

This work was supported by the Russian Science Foundation (Grant No. 23-12-00016).

- [1] C. L. Kane, E. Mele, *J. Phys. Rev. Lett.* 95, 146802 (2005)
- [2] V. T. Phong, N. R. Walet and F. Guinea, *2D Mater.* 5, 014004 (2017)
- [3] D. Marchenko et al., *Nat. Commun.* 3, 1232 (2012)
- [4] A. G. Rybkin et al., *Phys. Rev. Lett.* 129, 226401 (2022)
- [5] A.V. Eryzhenkov et al., *Symmetry* 15, 516 (2023)



## Features of $(\text{Cr}_{1-x}\text{Mn}_x)_2\text{GeC}$ Thin Film Magnetron Deposition

S. Lyaschenko<sup>a,\*</sup>, T. Andryushchenko<sup>a</sup>, I. Yakovlev<sup>a</sup>, A. Lukyanenko<sup>a,b</sup>, D. Shevtsov<sup>a</sup>, S. Varnakov<sup>a</sup>  
and S. Ovchinnikov<sup>a,b</sup>

<sup>a</sup> Kirensky Institute of Physics, 660036, Akademgorodok 50/38 Krasnoyarsk, Russia

<sup>b</sup> Siberian Federal University, 660041, Svobodniy 79, Krasnoyarsk, Russia

\*isa@iph.krasn.ru

The structural features that distinguish epitaxial nanolayers from bulk isotropic systems impose significant difficulties in their synthesis. The requirements for high purity of the used reagents and the presence of an ultrahigh vacuum in the technological chamber are usual. There are also high requirements for the surface sensitivity of analytical methods for such systems. It is also advisable to analyze samples under ultrahigh vacuum conditions without exposing them to air, i.e. in situ mode. However, the problems of thin-film synthesis are compensated by the high structural perfection of the resulting samples due to the direct transition of the substrate crystal structure into the growing film during the epitaxy regime. The application of epitaxial controlled growth of thin films makes it possible to investigate such complex nanolayers as MAX phases in more detail [1].

In this work we show the details of synthesis of epitaxial thin films of pure and Mn-substituted MAX-phase  $\text{Cr}_2\text{GeC}$ , by magnetron co-deposition from elementary targets. The synthesis was performed on  $\text{MgO}(111)$  substrates heated to  $650^\circ\text{C}$ , followed by annealing of the samples in ultrahigh vacuum ( $10^{-9}$  Torr) for 30 minutes at  $850^\circ\text{C}$ . The synthesis process was monitored in situ by RHEED and Auger spectroscopy. It was found that samples with a pure MAX phase were formed at a high process carbon flux and an atomic ratio  $(\text{Cr}+\text{Mn})/\text{Ge}$  of about 2.8.

After comparing the synthesis technology and the results of comprehensive analysis of sample structure and morphology, optical and transport properties, the mechanism of  $(\text{Cr}_{1-x}\text{Mn}_x)_2\text{GeC}$  epitaxial growth through the formation of an additional chromium carbide nucleating phase [2], which stabilizes the Cr-Ge bond in excess of carbon atoms, was proposed [3].

### Acknowledgement

The research was performed at the Magnetic MAX Materials Laboratory of the Kirensky Institute of Physics with the financial support of the Russian Science Foundation #21-12-00226, <http://rscf.ru/project/21-12-00226/>.

[1] M. W. Barsoum et al., *Journal of the American Ceramic Society* 94 (12), 4123-4126 (2011)

[2] A. Ganguly et al., *Mater. Res. Express* 7, 056508 (2020)

[3] W. Zhou et al., *Journal of Applied Physics* 106, 033501 (2009)

## Features of phase composition and structure of rapidly quenched ferromagnetic Mn-Al-Ga alloy

A. Fortuna<sup>a,\*</sup>, T. Morozova<sup>a</sup>, M. Gorshenkov<sup>a</sup>

<sup>a</sup> National University of Science and Technology MISIS, 119049, Leninskiy Prospekt 4, NUST MISIS,

Moscow, Russia

\*fortuna.as@misis.ru

Mn(51-59% at.)-Al(49-41% at.) alloys exhibit ferromagnetic properties provided the formation of a metastable  $\tau$ -phase (L1<sub>0</sub>, P4/mmm). The theoretical value  $(BH)_{\max}$  for these alloys is  $\approx 100$  kJ/m<sup>3</sup>, however, experimentally only 56.5 kJ/m<sup>3</sup> was achieved [1]. To increase the stability of the ferromagnetic phase,  $\tau$ -MnAl is alloyed with Ga or C. The influence of the first element on the phase equilibrium of bulk samples was studied in [2–3]. However, Ga-doped rapidly quenched ribbons have not been investigated yet. The purpose of this work was to establish the influence of Ga on the phase equilibrium of a rapidly quenched ferromagnetic alloy of the Mn-Al system.

An alloy of composition (in % at.) Mn<sub>55</sub>Al<sub>36</sub>Ga<sub>9</sub> was obtained by induction melting of pure components in an inert gas atmosphere. Rapid quenching was carried out by spinning at a rotation linear speed of the copper wheel of 10 m/s. The structure was studied by X-ray diffraction (XRD), scanning (SEM) and transmission (TEM) electron microscopy on Vega 3 Tescan and Jeol JEM-1400 microscopes. The phase transformation temperatures (from 30 to 800 °C) were analyzed by differential scanning calorimetry (DSC) on a NETZSCH STA 449 F3 Jupiter setup (heating rate 10°C/min).

As XRD analysis showed, the structure of as-spun ribbons contained two phases:  $\gamma_2$  (57.6 % vol.) and  $\varepsilon$  (42.4 % vol.). The study of ribbons cross section on the SEM did not reveal significant inhomogeneities in the distribution of phases over the thickness. The phase composition of rapidly quenched ribbons differed from the phase composition of a massive sample of the same composition quenched into water: in its structure, more than 90% vol. was occupied by the  $\varepsilon$ -phase.

DSC analysis of rapidly quenched ribbons revealed the presence of two exothermic transformations: the first occurs at 250-400 °C, the second – at 500-620 °C. After annealing at 440 °C, which corresponded to the bottom between two peaks on the DSC curve, the presence of three phases was observed in the sample (in % vol.): 79.0 -  $\gamma_2$ , 15.3 -  $\varepsilon$  and 5.7 -  $\tau$ . Thus, the first exothermic peak on the DSC curve probably corresponds to the  $\varepsilon \rightarrow \gamma_2 + \tau$  transformation. The lattice parameters of the  $\tau$ -phase were  $a = 2.786$  Å,  $c = 3.524$  Å, and the parameter ratio  $c/a = 1.265$ . Annealing at a temperature of 720 °C, chosen as the end of the second transformation, led to the formation of a large amount (77.9 % vol.) of the ferromagnetic phase. In addition to the  $\tau$ -phase,  $\gamma_2$  (13.6%) and ( $\beta$ -Mn) (8.5%) were present in the sample. The lattice parameters of the  $\tau$  phase after such annealing differed significantly:  $a = 2.761$  Å,  $c = 3.621$  Å, and the parameter ratio  $c/a = 1.311$ . The increase in lattice tetragonality was due to the redistribution of elements during annealing. Apparently, after the first annealing, the  $\tau$  - phase is formed from the  $\varepsilon$ -phase, which is depleted in gallium; therefore, the degree of lattice tetragonality is low. During the second annealing, the transformation  $\gamma_2 \rightarrow \tau$  occurs, and the resulting phase is enriched in gallium, which leads to an increase in  $c/a$ . The ribbon annealed at 720°C was also studied by TEM. The grains of the  $\tau$ -phase showed the presence of a banded contrast, and on the electron diffraction patterns in the reflections of the  $\tau$ -phase relrods were observed in the direction perpendicular to these bands. The formation of relrods is caused by the presence of internal stresses, which in the case under consideration can be due to concentration inhomogeneity. Such a structure was not observed in bulk samples of the same composition after the same heat treatment.

[1] H. Fang et al., J Solid State Chem., 237 (2016)

[2] T. Mix et al. Acta Mater., 128 (2017)

[3] T. Mix et al. Results Mater., 5 (2020)

# Ferromagnetic resonance: a new method for the implementation of magnetic hyperthermia

S. Stolyar<sup>a,b,\*</sup>, O. Li<sup>a,b</sup>, E. Nikolaeva<sup>a,b</sup>, A. Vorotynov<sup>c</sup>, D. Velikanov<sup>c</sup>, R. Iskhakov<sup>c</sup>, O. Kryukova<sup>a</sup>,  
V. Pyankov<sup>a</sup>, V. Ladygina<sup>a</sup>, N. Boev<sup>c</sup>

<sup>a</sup>FRC KSC SB RAS, 660036, Akademgorodok, 50, Krasnoyarsk, Russia

<sup>b</sup>Siberian Federal University, 660041, Svobodny pr., 79, Krasnoyarsk, Russia

<sup>c</sup>Kirensky Institute of Physics, FRC KSC SB RAS, 660036, Akademgorodok 50/38, Krasnoyarsk, Russia

\*oali@sfu-kras.ru

In biomedicine, there are already proven approaches to the practical applications of magnetic nanoparticles. For example, in magnetic hyperthermia, heating of biological tissues by an alternating magnetic field in the processes of magnetization reversal of particles. Usually, particles of the magnetite-maghemite series or ferrites based on them are chosen as objects of study for this direction. In this work, we demonstrate the possibility of heating magnetic powders in the ferromagnetic resonance (FMR) mode.

The magnetization vector  $\mathbf{M}$  in the magnetic field  $\mathbf{H}_{eff}$  is determined by the Landau-Lifshitz equation:

$$\dot{\mathbf{M}} = -\gamma \mathbf{M} \times \mathbf{H}_{eff} - \frac{\gamma \alpha}{M} \mathbf{M} \times (\mathbf{M} \times \mathbf{H}_{eff})$$

where  $\gamma$  is the gyromagnetic ratio and  $\alpha$  is the damping parameter.

If the magnetization  $M$ , in addition to the constant field  $H$ , is affected by a high-frequency microwave field with frequency  $\omega$  and amplitude  $h$  orthogonal to the external field  $H$ , resonant absorption of microwave energy by a ferromagnet (FMR) is possible. In the FMR mode for a spherical ferromagnet, the imaginary component of the magnetic susceptibility is  $\chi''_{res} \approx \frac{1}{2} \frac{\gamma' M_s}{\alpha f}$ , where  $\gamma' = \gamma/2\pi \approx 2.8$  MHz/Oe. The absorption of energy by a spherical particle with volume  $V$  per unit time is determined by the expression  $P = \omega \frac{V}{2} \chi'' h^2$ . Assuming that all the absorbed microwave energy goes to nanoparticles heating, we get:  $dT/dt = h^2 \gamma' M_s / 4C\rho\alpha$ , where  $\rho$  is the density,  $C$  is the specific heat capacity.

In this work, the frequency-field dependences of FMR for particles of nickel  $\text{NiFe}_2\text{O}_4$  and cobalt  $\text{CoFe}_2\text{O}_4$  ferrites, ferrihydrite  $5\text{Fe}_2\text{O}_3 \cdot 9\text{H}_2\text{O}$ , hematite  $\alpha\text{-Fe}_2\text{O}_3$ , and maghemite  $\gamma\text{-Fe}_2\text{O}_3$  were studied. The kinetic dependences of nanoparticle temperature in the FMR mode at a frequency of 8.9 GHz are measured (Fig. 1).

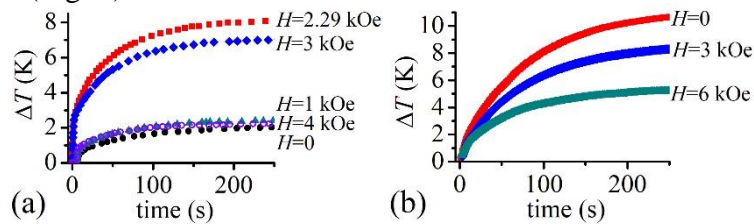


Fig. 1. Time dependence of the temperature increment of nickel (a) and cobalt (b) ferrite powders at various magnetic fields  $H$ .

To assess the effectiveness of the hyperthermic effect of magnetite nanoparticles functionalized with aptamers, we performed a cytometric analysis of the viability of Ehrlich ascitic carcinoma cells. The percentage of viable cells in Ehrlich ascitic carcinoma suspension decreased after FMR hyperthermia from  $(92.1 \pm 0.7)\%$  in the control to  $(78.5 \pm 1.4)\%$  in the group with magnetic nanoparticles under 10 min FMR exposure in vitro.

# FeZrN films with nanocomposite structure for soft magnetic applications

E. Sheftel\*, V. Tedzhetov, E. Harin, G. Usmanova

Baikov Institute of Metallurgy and Materials Science RAS, 119334, Leninsky prospect 49, Moscow, Russia

\*titan000@mail.ru

Films characterized by nanocomposite structure  $\alpha\text{Fe} + \text{Me}_{\text{IV}}\text{X}$  ( $\text{Me}_{\text{IV}} = \text{Ti, Zr, Hf; X} = \text{C, N, O, B}$ ) are considered as promising materials capable to provide a combination of high saturation magnetization  $B_S$  and low coercive field  $H_C$  for soft magnetic application [1]. The above nanocomposite structure can be formed in the films of the alloying system Fe-Zr-N containing equilibrium concentration region with two-phase structure  $\alpha\text{Fe} + \text{ZrN}$  and eutectic crystallization (quasi-binary system Fe-ZrN). The report presents the results of Fe-Zr-N alloying system film investigations aimed at finding the composition range and the magnetron deposition conditions followed by annealing providing the nanocomposite structure  $\alpha\text{Fe} + \text{ZrN}$ . The report presents the results of investigations of static magnetic properties of the films in different structural states as well.

The  $\text{Fe}_{92-78}\text{Zr}_{3-11}\text{N}_{5-12}$  films (near the eutectic composition of quasi-binary system Fe-ZrN) were prepared by dc and rf magnetron deposition on glass substrates and subsequent 1-hour annealing at temperatures of 300-600°C [2,3]. The film phase composition and structure were studied by XRD, TEM methods. Static magnetic properties were measured by VSM method. Metastable phase composition is formed in the deposited films. It is presented by one or few following phases: supersaturated solid solution  $\alpha\text{Fe}(\text{Zr,N})$ ,  $\text{Fe}_4\text{N}/\text{Fe}_3\text{N}$  or ZrN and amorphous phases. As Zr and N content in the films increases the supersaturation of  $\alpha\text{Fe}(\text{Zr,N})$  phase by these elements increases and the phase grain size decreases from 14 nm to 5 nm depending on the film composition. The volume fraction of an amorphous phase increases when Zr and N content in the film increases and when the rate of the film cooling during its growth on the substrate increases. Complete amorphization of the studied films is not achieved. The XRD amorphous structure formed in the films contains highly dispersed grains or clusters of  $\alpha\text{Fe}$ -based phase (1-2 nm). The annealing of the films leads to the crystallization of the amorphous phase providing a formation of new grains of the phases  $\alpha\text{Fe}(\text{Zr,N})$ ,  $\text{Fe}_3\text{N}/\text{Fe}_4\text{N}$ , ZrN in addition to the ones formed during deposition and to a decrease in supersaturation of the solid solution  $\alpha\text{Fe}(\text{Zr,N})$ . The  $\alpha\text{Fe}(\text{Zr,N})$  grain size doesn't change during annealing up to 500°. The high compressive macrostresses  $\sigma$  (up to 1.5 GPa) are formed in all deposited films. As the annealing temperature increases, macrostresses  $\sigma$  decrease reaching zero at 300-500°C depending on the composition. Further increase in the annealing temperature leads to a transformation of the compressive macrostresses to tensile ones. High microstrain in  $\alpha\text{Fe}(\text{Zr,N})$  phase grain  $\varepsilon_{\alpha\text{Fe}(\text{Zr,N})}$  (2,6 %) formed in deposited films decreases after annealing (1,7 %).

The  $B_S$  and  $H_C$  values of the films as-deposited depending on the composition are 1.3-2.1 T and 0.08-1.0 kA/m respectively. The annealing leads to small decrease of  $B_S$  (up to 1.2-1.9 T) due to additional nonferromagnetic phase formation and to the decrease of  $H_C$  to the level of super softness (25-26 A/m) after annealing at 400-500°C. The decrease of  $H_C$  after annealing is explained by the decreasing of  $\sigma$  in the films and  $\varepsilon_{\alpha\text{Fe}(\text{Zr,N})}$  in  $\alpha\text{Fe}(\text{Zr,N})$  grains. The physicochemical concept of a purposeful choice of compositions and producing conditions of super soft magnetic FeZrN films with a nanocomposite structure ( $\alpha\text{Fe} + \text{ZrN}$ ) and high  $B_S$  is formulated.

The study was supported by the Russian Science Foundation (project no. 23-23-00434).

[1] E.N. Sheftel, Inorganic Materials: Applied Research 1(1) 17(2010)

[2] E.N. Sheftel, V.A. Tedzhetov, E.V. Harin et al., Materials 15, 137(2022)

[3] E.N. Sheftel, V.A. Tedzhetov, E.V. Harin et al., Thin Solid Films 748, 139146(2022)

## Fluorescent quantum dots for analytical test methods

O. Goryacheva, I. Goryacheva

Saratov State University 410012, Astrakhaskaya 83, Saratov, Russia

olga.goryacheva.93@mail.ru

Quantum dots are semiconductor nanocrystals with great potential to replace classical fluorescent labels in analytical spectroscopy. The fluorescence wavelength variation, wide excitation spectrum, and surface modification capability allow their use in various analytical methods. Quantum dots of CdSe/CdS composition are obtained by high-temperature synthesis in organic solvent. Hydrophilization by reverse microemulsion yields surfaces with different functional groups [1]. Such quantum dots can be conjugated to antibodies and other proteins for use in immunoassays. By using quantum dots with different fluorescence colours it is possible to obtain on a single flow immunoassay strip the results for several analytes [2]. By using the antibody as a receptor, the matrix effect of the samples is minimized and the sample preparation time for the analytes is considerably reduced. Strip tests based on quantum dots can be used for both low molecular weight substances and protein structures. With this method it is possible to detect NT- proBNT which elevated levels are indicative of a heart failure [3].

By using a thinner coating of polymer quantum dots cover, interaction with gold nanoparticles applies for detection low molecular weight structures. A decrease in fluorescence due to Förster Resonance Energy Transfer (FRET) during interaction of the antibody with the antigen can be used to obtain a signal. FRET allows the transition to homogeneous formats for immunoassays, and thus to 96 or 384-well plate format. The method is suitable for the simultaneous screening of a large number of samples [4].

The coating of the quantum dot surface with thioglycolic xylene makes the quantum dots sensitive to certain types of molecules. The adsorption of molecules on the surface of the quantum dot leads to a quenching of the fluorescence, which has great potential for the use of quantum dot fluorescence for extrusion tests.

This research was funded by the Russian Science Foundation, grant number 21-73-10046

[1] O. Goryacheva, ABC 414, 15 (2022)

[2] O. Goryacheva, ACS Appl. Mat & int. 12, 22(2020)

[3] O. Goryacheva, Tal. Op. 7(2023)

[4] O. Goryacheva Tal. 225(2021)

# From 2D to 3D topological solitons: stability, lifetime, interactions

V. Uzdin<sup>a\*</sup>, I. Lobanov<sup>a</sup>

<sup>a</sup>Faculty of Physics, ITMO University, 197101, St.Petersburg, Russia

\*v\_uzdin@mail.ru

Topological solitons are considered as promising candidates for the role of information bits in magnetic racetrack memory devices. Their advantages relate to small size, stability, and the possibility of fast movement under the action of weak electric current and small external influences. The stability of such systems with respect to thermal fluctuations is usually associated with the existence of topological numbers, that are discrete quantities that do not change with a continuous variation of the magnetization. Examples of 2D topological solitons are quasi-two-dimensional chiral magnetic skyrmions and antiskyrmions in thin magnetic films deposited on the surface of a heavy metal with strong spin-orbit interaction. In the continuous model, they have a topological charge  $|q| = 1$ , in contrast to the zero charge for a homogeneous magnetic state. For a discrete system with magnetic moments localized at the sites of the crystal lattice, stability should manifest itself through energy barriers separating different magnetic states and the shape of the energy surface in the vicinity of initial state and the state near the top of barriers. The rate of spontaneous thermal magnetic transitions and the lifetimes of magnetic states can be evaluated within the framework of transition state theory for magnetic degrees of freedom [1].

The same methods can be used to calculate the rate of transitions induced by thermal fluctuations and lifetimes of three-dimensional topological solitons, such as hopfions [2], skyrmion tubes, torons, heliknotons [3] and localized magnetic topological structures in synthetic antiferromagnets [4]. In present work the minimum energy paths between topologically different states on the multidimensional energy surface of 3D systems will be presented. Various scenarios of collapse and nucleation of 3D topological solitons will be shown.

Three-dimensional topological solitons in chiral films demonstrate a wide variety of forms and interactions associated with the perturbation of the medium in which they are embedded. Some of the interactions turn out to be attraction at long distances and strong repulsion at short ones. This makes it possible to build new complex superstructures from topological solitons. This will be illustrated by the example of pairwise interactions of three-dimensional thorons, skyrmion tubes, and leeches in thin chiral films.

The study was supported by the Russian Science Foundation grant No. 22-22-00632, <https://rscf.ru/project/22-22-00632/>

[1] I. S. Lobanov, M.N. Potkina, V. M. Uzdin, JETP Letters, **113**, 801 (2021).

[2] I. S. Lobanov, V. M. Uzdin, PRB, **107**, 104405 (2023).

[3] V. M. Kuchkin, N. S. Kiselev, F. N. Rybakov, I. S. Lobanov, S. Blügel, V. M. Uzdin, Frontier in physics. Condensed Matter Physics, in press (2023); arXiv:2304.10181v1

[4] K.V. Voronin, I. S. Lobanov, V. M. Uzdin, JETP Letters, 116, 242 (2022).

## Functionalization of MXenes with magnetic nanoparticles

Shilov R.<sup>1\*</sup>, Sobolev V.<sup>1</sup>, Omelyanchik S.<sup>1</sup>, Magomedov E.<sup>1</sup>, Rodionova V.<sup>1</sup>

*1-Immanuel Kant Baltic Federal University, Kaliningrad, Russia*

*\*E-mail: [nikolayshilov2002@gmail.com](mailto:nikolayshilov2002@gmail.com)*

MXenes are a new class of two-dimensional nanomaterials with the general formula  $M_{n+1}X_nT_x$ , where M is an early transition metal, X is either C or N and  $T_x$  is a surface functional group, typically -OH, -O or -F; n is an integer index that usually takes values from 1 to 3. [1] Due to their unique properties, such as metallic conductivity, hydrophilicity, and large surface area, MXenes are highly applicable for various fields, ranging from energy to medicine. [2]

One important feature of MXenes is that they can be combined with other materials, likewise nanoparticles, carbon nanotubes, graphene, polymers, etc. to form functional composites. Up to date, MXenes have been functionalized with nanoparticles of different composition, shape, and size, which is helpful not only to strengthen their existing properties, but also to induce the new ones. [3]-[5]

This work considers a new, cheap and environmentally friendly method to functionalize MXenes with various nanoparticles. This method is schematically described in Figure 1, taking  $Fe_3O_4$  nanoparticles as an example. It allows growing different types of nanoparticles directly on the surface of MXenes of different composition, providing novel functionality to such MXene-bases composites. It was also observed that multilayer precursor MXenes tend to delaminate as an effect of the nanoparticle growth. This phenomenon provides a second life to multilayer MXenes, as it is commonly complicated to obtain enough single-layer MXenes for functionalization.

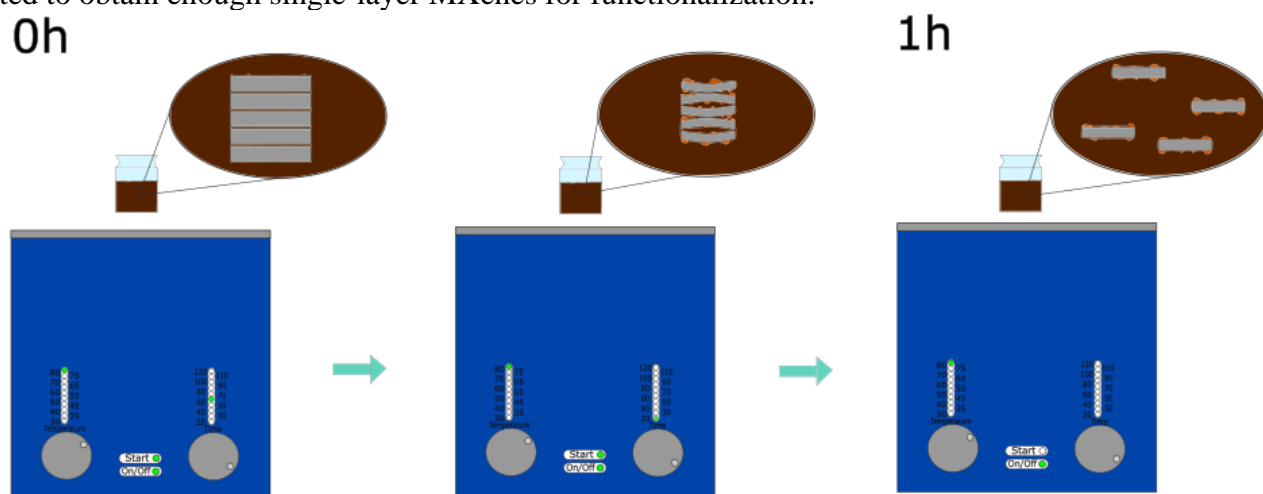


Figure 1. Functionalization of  $Ti_3C_2T_x$  MXenes with  $Fe_3O_4$  nanoparticles (scheme).

**Acknowledgment:** This work was supported by the Russian Science Foundation, grant №22-12-20036, regional part no. 12-C/2023.

[1] M. Naguib, V.N. Mochalin, M.W. Barsoum, Y. Gogotsi, *Adv. Mater.* 2014, 26, 992.

[2] M. Khazaei, A. Mishra, N.S. Venkataramanan, A.K. Singh, S. Yunoki, *Curr. Opin. Solid State Mater. Sci.* 2019, 23, 164.

[3] X. Hu, C. Chen, D. Zhang, Y. Xue, *Chemosphere* 2021, 278, 130206.

[4] L. Wang, H. Song, L. Yuan, Z. Li, Y. Zhang, J.K. Gibson, L. Zheng, Z. Chai, W. Shi, *Environ. Sci. Technol.* 2018, 52, 10748.

[5] V. Thirumal, R. Yuvakkumar, P.S. Kumar, S.P. Keerthana, G. Ravi, D. Velauthapillai, B. Saravanakumar, *Chemosphere* 2021, 281, 130984.

# Gasogyrochromic Effect in Oxidized Permalloy

D. Kulikova<sup>a,b</sup>, K. Afanasyev<sup>a,c</sup>, A. Baryshev<sup>1,\*</sup>

<sup>a</sup> Dukhov Automatics Research Institute (VNIIA), 127030, ul. Sushevskaya 22, Moscow, Russia

<sup>b</sup> Lomonosov Moscow State University, 119991, Leninskie gory 1, Moscow, Russia

<sup>c</sup> Institute for Theoretical and Applied Electromagnetics of RAS, ul. Izhorskaya 13, 125412, Moscow, Russia

\*baryshev@vniia.ru

Gasochromic materials that change their optical properties in a target gas have found application for gas sensing [1]. Usually, a gas-sensitive system is based on a gasochromic metal oxide coupling with a catalyst (Pd, Pt)—for example, the WO<sub>3</sub>/Pt bilayer [2]. The typical response to a target gas of such systems is a relative change in the amplitude of transmitted/reflected light. In terms of the tensor of the dielectric permittivity, gasochromism is a change in the diagonal elements. The question rises as to whether there is any effect on the non-diagonal elements. The magneto-optical (MO) response on a gas is of great interest for gas sensing technologies since one can monitor the change of polarization rotation of light instead of its amplitude. In work [3] the MO response on hydrogen of alloys and multilayers combining catalyst and magnetic metals is demonstrated. To the best of our knowledge, there are no works discussing the change of MO properties of magnetic oxides in a hydrogen-containing atmosphere except for a recently published one [5].

In our work, we investigate the applicability of oxidized 30 nm-thick permalloy nanofilms to hydrogen sensing. It was found that their structural, magnetic, optical and magneto-optical properties significantly change during annealing depending on the oxidation temperature [4]. Unexpectedly, the angle of Faraday rotation (AFR or  $\theta$ ) rose by an order of magnitude in the near IR wavelength range. For gas-sensing experiments, the as-deposited and oxidized nanofilm with the largest MO response (NiFeO<sub>x</sub>) were covered with 5 nm-thick Pt catalyst layer. Figure 1(a) demonstrates that 0.5 vol.% H<sub>2</sub> in N<sub>2</sub> did not affect the AFR values of the as-deposited permalloy/Pt and NiFeO<sub>x</sub>, and the NiFeO<sub>x</sub>/Pt and same NiFeO<sub>x</sub>/Pt annealed after hydrogenation at 300 °C irreversibly changed their AFR response that stabilized after twenty minutes of exposure. The non-reciprocal nature of observed effect was confirmed by measurement of MO response of the studied samples in a multipass-regime—a triple transmission of light through the sample lead to the tripling of its magneto-optical response on hydrogen (Fig. 1(b)).

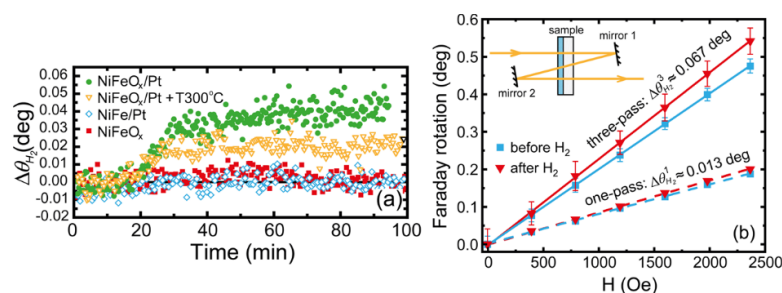


Fig. 1. (a) MO response on 0.5 vol.% H<sub>2</sub> of NiFeO<sub>x</sub>, Pt-covered permalloy, NiFeO<sub>x</sub>/Pt and same NiFeO<sub>x</sub>/Pt annealed after hydrogenation at 300 °C. (b) Faraday rotation dependence of NiFeO<sub>x</sub>/Pt before and after interaction with 0.5 vol.% H<sub>2</sub> on value of applied magnetic field measured in 1-pass and 3-pass regimes.

The accumulation of the polarization rotation of NiFeO<sub>x</sub>/Pt in different states pointed out that MO response on hydrogen was due to “gasogyrochromism” of magnetic oxide film NiFeO<sub>x</sub> being a complex mixture of oxides of metals that compose permalloy alloy.

[1] A. Mirzaei, et al., Appl. Sci. 9, 1775 (2019)

[2] S. Okazaki and S. Johjima, Thin Solid Films 558, 411-415 (2014)

[3] P.C. Chang, et al., Communications Chemistry, 2:89 (2019)

[4] D. P. Kulikova, et al., Opt. Mater. 107, 110067 (2020)

[5] D. P. Kulikova, et al., Applied Surface Science 613, 155937 (2023)



## Giant anisotropy of magnetic properties of hydrated iron fluoridotitanate molecular single crystal.

A. Dubrovskiy<sup>a</sup>, Y. Knyazev<sup>a</sup>, D. Velikanov<sup>a</sup>, A. Vorotynov<sup>a</sup>, N. Laptash<sup>b</sup>, Yu. Gerasimova<sup>a</sup>.

<sup>a</sup>*Kirensky Institute of Physics, Siberian Branch of RAS, 660036 Krasnoyarsk, Russia*

<sup>b</sup>*Institute of Chemistry, Far Eastern Branch of RAS, 690022 Vladivostok, Russia*

Study of the magnetic properties of the  $\text{FeTiF}_6 \cdot 6\text{H}_2\text{O}$  molecular single crystal [1,2] has shown that this compound is a two-dimensional antiferromagnet with a Néel temperature of  $T_N = 8$  K and its magnetic moment anisotropy attains 7000 % at a temperature of  $T = 4.2$  K [3]. The Mössbauer spectroscopy data unambiguously indicate the paramagnetic state of iron cations in the temperature range of 4.2–300 K. However, a sharp change in the difference between the quadrupole doublet line widths at 10 K has been observed, which is consistent with the temperature of magnetic ordering. It has been suggested that the long-range magnetic order is established in the crystal through the formation of the exchange coupling revealed by the electron spin resonance measurements on the oriented single crystals. Also it was found that the presence of spin-orbit interaction of the transition metal ion has a significant effect on anisotropy of magnetic properties of these compounds [4].

This work was supported by the Russian Science Foundation, Government of Krasnoyarsk Territory and Krasnoyarsk Regional Fund of Science according to the research project "Synthesis, spectral and magnetic properties of  $\text{ABF}_6 \cdot 6\text{H}_2\text{O}$  systems, new materials for photonics." No. 23-22-10037.

1. Yu.V. Gerasimova, A.S. Aleksandrovsky, N.M. Laptash, M.A. Gerasimov, A.S. Krylov, A.N. Vtyurin, A.A. Dubrovskiy // *Spectrochimica Acta Part A: Molecular and Biomolecular Spectroscopy* **264**, 2022, p. 120244
2. Yu.V. Gerasimova, A.S. Krylov, A.N. Vtyurin, N.M. Laptash, E.I. Pogoreltsev, A.A. Dubrovskiy, M.A. Gerasimov // *Journal of Raman spectroscopy*, 2022, **53**, 1704-1709.
3. A.A. Dubrovskiy, Yu.V. Knyazev, D.A. Velikanov, A.M. Vorotynov, N.M. Laptash, Yu.V. Gerasimova // *Journal of Alloys and Compounds*, Volume **898**, 25 March 2022, 162748.
4. A. A. Dubrovskiy, Y. V. Knyazev, Yu V. Gerasimova, A. A. Udovenko, N. M. Laptash // *Physics of the Solid State*, 2022, **64** (11), pages 1709-1712.

# Giant Photo-Induced Magnetic Polarons in Europium Chalcogenides

P. Usachev

Ioffe Institute, 194021, St. Petersburg, Russia

usachev@mail.ioffe.ru

Europium chalcogenides EuX (X = O, S, Se, Te) are intrinsic magnetic semiconductors with unique electronic, magnetic, optical and magneto-optical properties. The top of the valence band of the Eu<sup>2+</sup> atom in these compounds is formed by 4f states, which contain 7 strongly localized electrons with a total spin of 7/2. The first empty 5d state forms the conduction band. When the light excites 4f electrons into the 5d band, a strong d-f exchange interaction appears. Acting on the lattice spins, it leads to the formation of giant magnetic polarons with a large magnetic moment. An ensemble of such polarons will exhibit super-paramagnetic behavior. We report on an experimental study of photo-induced magnetization in europium chalcogenides, which occurs when the sample is illuminated by light with photon energy exceeding the band gap.

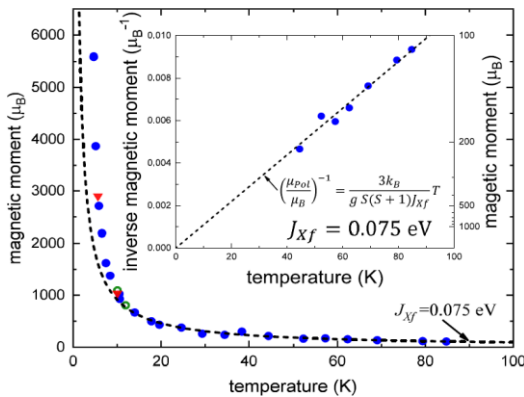


Fig. 1. Magnetic moment of a photo-induced polaron in EuSe as a function of the temperature.

the magnetic polarons is determined. In ferromagnetic EuS [3, 4] and EuO giant magnetic polarons are detected even with a larger magnetic moment than in EuTe and EuSe. The first observation of photo-induced magnetic polarons in EuO with a magnetic moment of about 100 000 Bohr magnetons is extremely important not only from the fundamental point of view but also for practical applications.

The support from the Russian Foundation for Basic Research – the Deutsche Forschungsgemeinschaft (grant no. 19-52-12063) is acknowledged.

- [1] A.B. Henriques, A.R. Naupa, P.A. Usachev, V.V. Pavlov, P.H.O. Rappl, E. Abramof. Phys. Rev. B, 95, 045205 (2017).
- [2] A.B. Henriques, X. Gratens, P.A. Usachev, V.A. Chitta, G. Springholz. Phys. Rev. Lett., 120, 217203 (2018).
- [3] X. Gratens, Y. Ou, J.S. Moodera, P.H.O. Rappl, A.B. Henriques, Appl. Phys. Lett. 116, 152402 (2020).
- [4] P. A. Usachev, V. N. Katz, V. V. Pavlov, Phys. Sol. State 62, 1619 (2020).

# Growth, magnetic and transport properties of highly ordered Mn<sub>5</sub>Ge<sub>3</sub> thin film on Si(111)

A. Lukyanenko<sup>a,b\*</sup>, A. Tarasov<sup>a,b</sup>, I. Yakovlev<sup>a</sup>, M. Rautskii<sup>a</sup>, A. Sukhachev<sup>a</sup>, R. Rudenko<sup>b</sup>, M. Volochaev<sup>a</sup> and S. Varnakov<sup>a</sup> and N. Volkov<sup>a,b</sup>

<sup>a</sup> Kirensky Institute of Physics, FRC KSC SB RAS, 660036, Akademgorodok 50/38, Krasnoyarsk, Russia

<sup>b</sup> Siberian Federal University, 660041, Svobodny 82A, Krasnoyarsk, Russia

\*lav@iph.krasn.ru

The search for suitable ferromagnetic (FM) materials for spin devices is a complex and urgent task. An example of such a material is Mn<sub>5</sub>Ge<sub>3</sub>. It is an FM metal with  $T_C = 296$  K that can be increased by doping. Moreover, Mn<sub>5</sub>Ge<sub>3</sub> has significant spin polarization, and the effects of spin injection from Mn<sub>5</sub>Ge<sub>3</sub> and detection into a semiconductor have already been demonstrated. [1]. Another attractive aspect of Mn<sub>5</sub>Ge<sub>3</sub> is its significant magnetocaloric effect (MCE) near room temperature, which makes Mn<sub>5</sub>Ge<sub>3</sub> a promising candidate to replace expensive rare earth MC materials [2]. Recently we demonstrated the growth of Mn<sub>5</sub>Ge<sub>3</sub> on a Si(111) substrate [3], which is important for silicon spintronics. Despite the lattice mismatch of 8%, the growth of Mn<sub>5</sub>Ge<sub>3</sub> remains epitaxial for a high thickness (~ 200 nm). This is made possible by the use of a buffer layer with different orientation between the substrate and the film (Fig.1(a)).

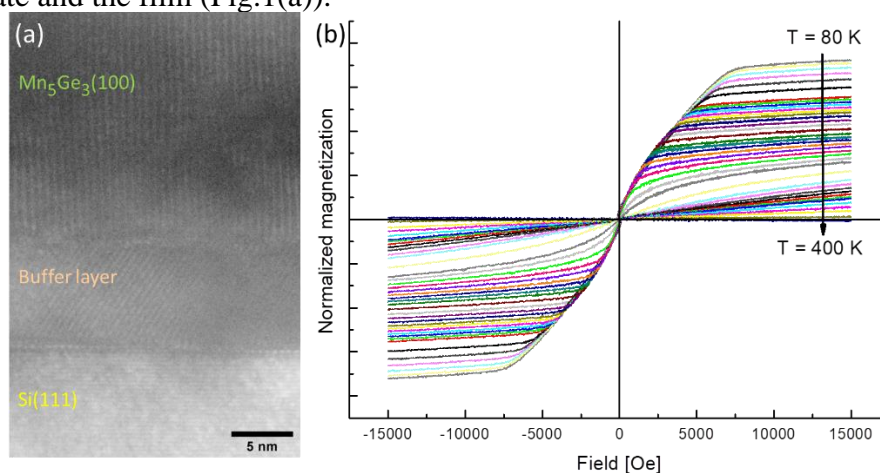


Fig.1 (a) TEM image of Mn<sub>5</sub>Ge<sub>3</sub>/Si(111) interface. (b) M(H) curves at different T.

Here we present the most recent results on magnetic properties and calculated MC effect of Mn<sub>5</sub>Ge<sub>3</sub> thin films grown on Si(111). The films exhibit complex magnetic anisotropy with easy magnetic axis parallel to the crystallographic direction of Mn<sub>5</sub>Ge<sub>3</sub> hexagonal cell. To analyze the MCE, integration of M(H) curves (Fig.1(b)) was used for numerical calculation of the entropy change  $\Delta S$  during magnetic ordering. The maximum  $\Delta S$  is slightly more than  $3 \text{ J kg}^{-1} \text{ K}^{-1}$  observed at 300 K, i.e. at  $T_C$ . The MCE reaches as high as bulk values reported for Mn<sub>5</sub>Ge<sub>3</sub> [4]. More interesting, MCE is anisotropic that can be connected with film anisotropy and/or magnetostriction due to mechanical stress in epitaxial film.

Supported by the Russian Science Foundation Grant of the № 23-22-10033, Krasnoyarsk Regional Fund of Science

[1] A. Spiesser, PRB 90, 205213 (2014)

[2] N. Maraytta, J. Appl. Phys. 128, 103903 (2020)

[3] I. Yakovlev, Nanomaterials. 12, 4365 (2022)

[4] N. Maraytta, J. Appl. Phys. 128, 103903 (2020)

## Gyrotropic oscillations of magnetic vortices in two interacting ferromagnetic disks

E. Skorokhodov<sup>a,\*</sup>, D. Tatarskiy<sup>a,b</sup>, R. Gorev<sup>a</sup>, V. Mironov<sup>a</sup>, A. Fraerman<sup>a</sup>

<sup>a</sup> Institute for Physics of Microstructures RAS, 603087, Akademicheskaya str., 7, Afonino, Nizhny Novgorod region, Russia

<sup>b</sup> Lobachevsky State University, 603095, Gagarin ave., 23, Nizhny Novgorod

\*evgeny@ipmras.ru

Gyrotropic oscillations in magnetic vortices are of interest for use in vortex spin-transfer nanoscillators (STNO) [1]. At the same time, one of the problems of STNO application is a small output microwave power. The main way to solve this problem is implementation of phase synchronization between nanoscillators. Synchronization is achieved due to various interactions – magnetostatic, exchange *etc.* The exchange interaction between magnetic vortices can be organized by the overlap of ferromagnetic disks or by the nanowires connecting ferromagnetic disks. The exchange interaction in this case has a strong influence on the distribution of magnetization and on the resonant properties in such systems. In this report we investigate systems of overlapping ferromagnetic disks and disks-nanowire manufactured by electron-beam lithography. The methods of Lorentz transmission electron microscopy (LTEM) (figure 1) and magnetic force microscopy (MFM) were used to investigate magnetic states.

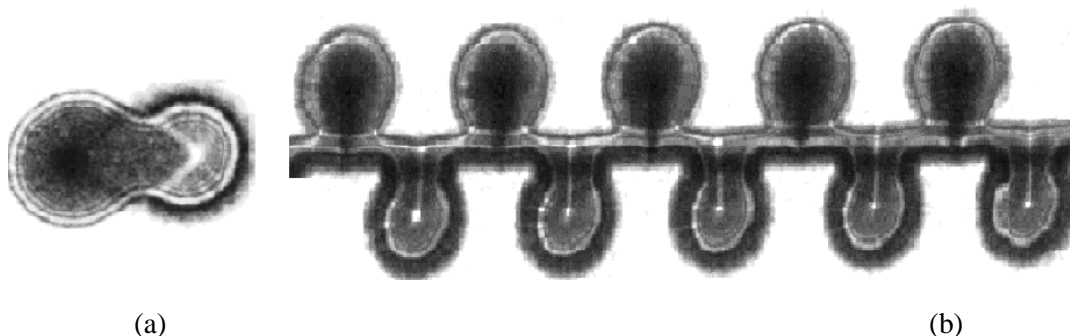


Figure 1. LTEM image of overlapping Permalloy disks (a) and system of disks-nanowire (b). The lateral dimensions of the disks are 1 micron.

The study of the exchange interaction effect on the frequency characteristics of ferromagnetic resonance was carried out using the magnetic resonance force microscopy (MRFM) method [2]. The energy of interaction between magnetic vortices was estimated using the model of linear interacting oscillators, the results of numerical simulation and the MRFM data. Calculations show that the exchange interaction between disks significantly increases the interaction energy of vortices, which can be used for phase synchronization of vortex STNOs.

The work is supported by the Russian Science Foundation (project No. 21-12-00271).

[1] V. S. Pribiag, I. N. Krivorotov, G. D. Fuchs, et al., *Nat. Phys.* 3, 498 (2007).

[2] E. В. Скороходов, М. В. Сапожников, и др., *Приборы и техника эксперимента*, 5, 140 (2018).

[3] E. В. Скороходов, и др., *Письма в ЖЭТФ*, т. 117, вып. 2, с. 165 (2023).

## Magnetic hybrid materials based on natural spider silk

A. Kryuchkova, P. Krivoshapkin

ITMO University, Saint-Petersburg, Russia

Artificial polymers properties do not always meet the requirements of strong functional materials. In this work we develop methods for obtaining magnetic bioactive hybrid materials based on natural spider silk for use in medicine and soft robotic applications. [1]. One of the most effective ways to modify spider silk is to include various nanoparticles in its structure, which leads to a change in thermal, magnetic and mechanical properties. [2]. The uniform silk fibers from the silk gland of *Linothele Fallax* (LF) and *Holothele incei* spiders that belong to the *Mygalomorphae* lineage were used in this work to create functional hybrid materials with magnetic properties based on natural spider silk by two approaches: influencing the biosynthetic processes of a spider with magnetite sol and impregnation of the fibers with ferromagnetic nanoparticles.

Firstly, the magnetite nanoparticles in sol with an average hydrodynamic radius 30 nm and above 30 mV  $\zeta$ -potential were injected with a syringe into the adult spiders. Computed tomography images show that magnetite nanoparticles are concentrated in the lower part of the abdominal cavity, presumably in the area where the spider's silk glands are located. The iron content of the silk produced by the injected spiders was 1.6%, and no iron was found in the control group. The magnetic controllability of the obtained materials was studied in a rotating magnetic field of Helmholtz coils with a frequency of 200 Hz and an amplitude of 15 mT. The introduction of inorganic nanoparticles into the structure of spider silk fiber significantly affects its properties. First, this increase the strength of the fiber, which correspond to the dependence of the Young's modulus, which is  $71.00 \pm 4$  GPa for magnetic fibers, compared with  $39.43 \pm 4$  GPa for native spider silk threads. We assume that mechanical properties improved because of new bonds formation between  $\beta$ -sheets and chains in the amorphous phase. Thus, magnetite nanoparticles contribute to the transformation of the silk protein conformation from random sequences into  $\beta$ -sheets by interacting with the side chain of silk carboxylic acids and changing its orientation.

Secondly, multifunctional hybrid materials based on native spider silk fibers modified with ferromagnetic nanoparticles and liposomes have been developed for enabling continuous thermally triggered drug release from liposomes for cartilage regeneration. Ferromagnetic NPs of the following composition  $Mn_{0.9}Zn_{0.1}Fe_2O_4$  were obtained by the hydrothermal synthesis from chlorides of zinc, manganese, and iron (III) at 180 °C. The Curie temperature of this material falls within the range 40–46 °C. TEM shows that the particles consist of nanocrystallites not exceeding in size of 10 nm. Liposomes loaded with a fluorescent dye were used as a model object. Under the influence of a magnetic field, local heating of the system occurs, because of which dye is released from liposomes that are attached to modified spider silk fibers. Hybrid spider silk fibers inure as strong support matrices for human postnatal fibroblasts cells, increase survival, and stimulate their aligned growth.

Acknowledgments: this work was financially supported by the Russian Science Foundation (project no. 22-23-00790).

1. Wen D. L. et al. Recent progress in silk fibroin-based flexible electronics //Microsystems & nanoengineering. – 2021. – T. 7. – №. 1. – C. 1-25.
2. Kiseleva A. P., Krivoshapkin P. V., Krivoshapkina E. F. Recent advances in development of functional spider silk-based hybrid materials //Frontiers in Chemistry. – 2020. – T. 8. – C. 554.

# **Magnetostrictive vs magnetostrainsome contributions of magnetic particles to the magnetoelectric response of piezopolymer-based composite films**

O. Stolbov<sup>a,b</sup>, Yu. Raikher<sup>a,b\*</sup>,

<sup>a</sup> Institute of Continuous Media Mechanics, Russian Academy of Sciences, Ural Branch,  
614018, Korolyova 1, Perm, Russia

<sup>b</sup> Immanuel Kant Baltic Federal University, 236004, Nevskogo 14, Kaliningrad, Russia

\*raikher@icmm.ru

The conventional way of inputting the energy of an alternating magnetic field into a magnetoelectric transducing element of composite structure employs the magnetostriction effect (MSE) in the ferromagnetic component of the composite. The ferromagnetic grains generate the MSE-induced stress that is transferred either to the electrically neutral matrix and, by it, further to the piezoelectric component of the composite, or directly to the matrix provided the latter is piezoelectric as itself. A well-known example of easily commercially accessible and widely available ferromagnetic material of that kind are nano- or micropowders of cobalt ferrite ( $\text{CoFe}_2\text{O}_4$ , CFO).

This ferrite has a sufficiently strong spin-orbit interaction that entails both a relatively high magnetic anisotropy and a substantial MSE. Therefore, each CFO grain under application of external magnetic field that is not parallel to the axis of its easy magnetization, strives not only to undergo MSE-induced deformation but is also subject to a torque that tends to establish the grain easy axis along the direction of the applied field. Due to that, the particle experiences a magnetic strain qualitatively different from that imposed by MSE, see [1]. In the magnetoelectric composite, each CFO grain dwells in the environment that responds by electric polarization as soon as the mechanical state of the system (that it had under zero field) is perturbed by some additional stresses brought in by the exerted magnetization.

Evidently, both stress-inducing effects produce the electric polarization of the composite sample, so that any measurement delivers just the overall result. It is instructive to analyze the relative proportion of those contributions. It is the more interesting that, as the MSE and strainsome stresses are to different extent coupled to different components of the piezoelectric tensor, their actions might either enhance the total response or diminish it in comparison with partial contributions. Because of that, a number of situations would occur, especially when the CFO particles are anisometric.

The numerical modelling is performed for a test cell comprising several CFO particles embedded in the matrix possessing mechanical and electric properties of an archetypal polyvinylidene difluoride (PVDF) that is a conventional polymer with piezoelectric properties. The dependencies of the net polarization on the orientations of the magnetizing field, particle magnetic moment and electric anisotropy axis of the matrix are presented and analyzed.

Partial support by RSF grant # 21-72-30032 is gratefully acknowledged.

[1] O. Stolbov, A. Ignatov, V. Rodionova, Yu. Raikher, *Soft Matter* 19, 4029 (2023)

## **Hydrodynamics of composite magnetic fluid systems in microfluidic chips of various configurations under the influence of a magnetic field**

P. Ryapolov<sup>a,\*</sup>, E. Sokolov<sup>a</sup>, D. Kaluzhnaya<sup>a</sup>

<sup>a</sup>Southwest State University, 305048, 50 let Otyabrya 94, Kursk, Russia

\*r-piter@yandex.ru

We propose a new technique for creating active bubbles and drops with a nonmagnetic core and a coating formed by a magnetic fluid [1, 2]. The hydrodynamics of these systems is considered in various channels under the influence of an inhomogeneous magnetic field. Magnetic fluids are a colloidal solution of magnetic nanoparticles coated with a surfactant, dispersed in a carrier fluid.

The process of formation of active bubbles and drops consists in the introduction of a non-magnetic phase into the magnetic one, which is held by the inhomogeneous magnetic field of a combined source that combines a ring magnet and an electromagnet. We have investigated various regimes leading to various active bubbles and drops, and the influence of the magnetic field on the size, speed and acceleration of active droplets formed has also been investigated. It is shown that active bubbles change their trajectory under the action of a constant magnetic field, and also decay under the action of a pulsed one. This provides a new mechanism for controlling drops and bubbles using a magnetic field. Unlike the flow focusing method, which is one of the main methods in drip microfluidics, non-magnetic drops and bubbles detach from a levitating non-magnetic volume rather than from a capillary. In this case, the levitating gas cavity acts as a receiver, making it possible to stabilize the size of the detached bubbles and increase the range of adjustment, in contrast to the data of [3], in which the detachment of bubbles in a magnetic fluid occurred in a uniform magnetic field.

This creates the prerequisites for the development of liquid multilayer capsules controlled by a magnetic field, which can be concentrated in a certain place and destroyed under impulse action. The results obtained can be applied to create drop-based microfluidics systems in which a non-uniform magnetic field can be used to focus drop and bubble flows in a ferrofluid.

The work was supported by the Russian Science Foundation grant No. 22-22-003113 <https://rscf.ru/project/22-22-00311/>

1. Sokolov, E.; Kaluzhnaya, D.; Shel'deshova, E.; Ryapolov, P. Formation and Behaviour of Active Droplets and Bubbles in a Magnetic Fluid in an Inhomogeneous Magnetic Field // *Fluids* – 2023 V8, №2.
2. Ryapolov P. A., Sokolov E. A., Postnikov E. B. Behavior of a gas bubble separating from a cavity formed in magnetic fluid in an inhomogeneous magnetic field // *Journal of Magnetism and Magnetic Materials*. – 2022. – T. 549. – C. 169067.
3. Yamasaki H. et al. Dynamic behavior of gas bubble detached from single orifice in magnetic fluid // *Journal of Magnetism and Magnetic Materials*. – 2020. – T. 501. – C. 166446.

# Impact of the mutual direction of Polarizer and Free Layer on the auto-oscillation mode of magnetic tunnel junctions (MTJs) of different geometry

V. Kikteva<sup>a,b,\*</sup>, K. Kiseleva<sup>a,c,§</sup>, G. Kichin<sup>a</sup>, P. Skirdkov<sup>a,d</sup>, K. Zvezdin<sup>a,d</sup>

<sup>a</sup> New spintronic technologies, Bolshoy Boulevard 30/1, Moscow, Russia, 121205

<sup>b</sup> Bauman Moscow State University, 2<sup>nd</sup> Baumanskaya 5/1, Moscow, Russia, 105005

<sup>c</sup> Skolkovo Institute of Science and Technology, Bolshoy Boulevard 30/1, Moscow, Russia, 121205

<sup>d</sup> Prokhorov General Physics Institute, st. Vavilov 38, Moscow, Russia, 119991

\*[v.kikteva@nst.tech](mailto:v.kikteva@nst.tech)

Spin transfer nano-oscillators based on magnetic tunnel junctions (MTJ) are one of the most promising candidates to become a key element in electronic devices [1] for variety of spheres, including wireless communication, radar, and microwave electronics. The study of STNOs and their properties is an active area of research in science and engineering [2] because of the possibility of tuning the oscillation frequency in a broad range. In view of potential for a compact and tunable nanogenerator, it is important to explore more flexible designs [3] and their key properties to find a specific position with a narrow peak and high-power output.

We use source measurement units (SMU) to pass the dc current through the elliptical samples. Characteristic values of the current vary from -2 mA to +1 mA. Spectrum analyzer records the average signal power distribution over frequencies (PSD). The signal is investigated in the frequency range from 100 MHz to 4 GHz. The external magnetic field is created by an electromagnet that can be rotated and the field range is  $\pm 300$  Oe. Schematic of the experiment and the sample's structure are shown on Fig. 1.

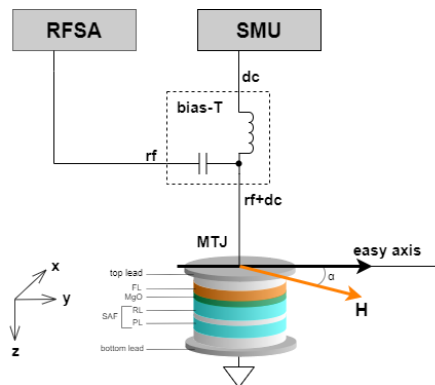


Fig.1. Schematic of the experiment

Among tested samples we highlight ones where the auto-oscillation mode is more stable and have a higher value of PSD. We show the complex behavior of the auto-oscillation mode and its connection with the magnetoresistance graph. Maximum value of PSD is detected on bigger samples at -40 Oe and about 2.25 GHz while the width of peak seems to concentrate at lower fields and at ones sharply expands.

In this work we have found more optimal configuration of the orientation of the magnetic field and ellipse. We have showed that this orientation make system reach the auto-oscillation mode easier and effective.

[1] S. Ning et al. // Fund Research 2 535-538 (2022)

[2] T. Wasa et al. // Phys. Rev. B 81 104410 (2010)

[3] Wenlong Cai et al. // IEEE 44 5 (2023)



## Interface magnetic layer in almost compensated iron garnet film

Yu. Kudasov<sup>a,b</sup>, M. Logunov<sup>c</sup>, R. Kozabaranov<sup>a,b</sup>, I. Makarov<sup>a,b</sup>, V. Platonov<sup>a,b</sup>, O. Surdin<sup>a,b</sup>, D. Maslov<sup>a,b</sup>, A. Korshunov<sup>a,b</sup>, I. Strelkov<sup>a,b</sup>, A. Stognij<sup>d</sup>, V. Selemir<sup>a,b</sup>, S. Nikitov<sup>c</sup>

<sup>a</sup> Sarov Physics and Technology Institute NRNU “MEPhI,” 6, str. Dukhov, Sarov 607186, Russia

<sup>b</sup> Russian Federal Nuclear Center—VNIIEF, 37, pr. Mira, Sarov 607188, Russia

<sup>c</sup> Kotel’nikov Institute of Radio-Engineering and Electronics of RAS, 11-7 Mokhovaya Street, Moscow 125009, Russia

<sup>d</sup> Scientific-Practical Materials Research Centre NAS of Belarus, 19 P. Brovki Street, Minsk 220072, Belarus

Iron garnets are ferrimagnets which characteristics can be varied in a wide range due to flexibility of their composition [1]. In particular, if non-magnetic rare-earth ions are in dodecahedral positions, a selective substitution by nonmagnetic ions in tetrahedral iron positions allows of fabricating an almost compensated ferrimagnet.

We performed a precise measurements of magneto-optical Faraday effect in almost compensated iron garnet  $(\text{Lu}_{3-x}\text{Bi}_x)(\text{Fe}_{5-y-z}\text{Ga}_y\text{Al}_z)\text{O}_{12}$  film grown on the  $\text{Gd}_3\text{Ga}_5\text{O}_{12}$  substrate [2]. An interface magnetic layer at the boundary between the film and substrate was observed. Its width grew drastically while approaching the compensation temperature.

A model of the giant widening of the interface magnetic layer was proposed. A very thin uncompensated layer in the film existed at the interface due to intermixing of the gadolinium ions. It induces the magnetic surface layer. The easy-plane magnetic anisotropy led to a complex behavior of the inhomogeneous surface magnetic structure.

Open questions and perspectives are discussed.

The work was supported by National Center for Physics and Mathematics (Project “Researches in high and ultrahigh magnetic fields”), the Russian Foundation for Basic Research (Project No. 18-29-27020) and Russian Federation State support (Project No. 075-15-2019-1874).

[1] A.K. Zvezdin, V.A. Kotov, *Modern Magneto-optics and Magneto-optical Materials*, IPP, Bristol, 1997

[2] Yu.D. Kudasov et al., *APL* 120, 122403 (2022)

# Investigation of $d^0$ - $d$ XMnY (X = K, Rb, Y = As, Bi, Ge, Si, P, Pb, Sb, Sn) half-Heusler alloys

M. Matyunina<sup>a,\*</sup>, D. Baigutlin<sup>a</sup>, M. Zagrebin<sup>a</sup>, V. Sokolovskiy<sup>a</sup>, V. Buchelnikov<sup>a</sup>

<sup>a</sup> Chelyabinsk State University, 454001, Bratiev Kashirinykh 129, Chelyabinsk, Russia

\*matunins.fam@mail.ru

Half-metallic (HM) ferromagnetic (FM) alloys are of interest as perspective materials for improving of spintronic devices [1–4]. An insulating channel for one spin direction and 100% spin-polarization at the Fermi level in the opposite spin direction are significant characteristics of these materials. In [3] the idea was proposed to replace the transition metal (TM) (e.g., Ni, Ti, Fe, Co, Mn) with an atom  $d^0$  of an alkali metal (K, Rb, Cs) in half Heusler (HH) alloys. Investigation of electronic band structure of new  $d^0$ - $d$  alloys produced all kinds of HM behavior.

The purpose of this work is to study the electronic structure at optimized lattice constants and atomic arrangement, structural stability and magnetic properties of XMnZ (X = K, Rb, Y = As, Bi, Ge, Si, P, Pb, Sb, Sn)  $d^0$ - $d$  HH compounds. Calculations were performed using the density functional theory with the plane-augmented wave method as implemented in the Vienna ab-initio simulation package [5,6]. The SCAN meta-GGA [7] was used for treating exchange correlation effects. The  $k$ -points grid density of  $\approx 5000$   $k$ -points per reciprocal lattice was considered for the calculations. In FM state of  $C1_b$  crystal structure (space group  $F4 -3m$ ) the three  $\alpha$ ,  $\beta$ , and  $\gamma$  possible phases which, respectively, correspond to placing the  $d^0$ -,  $sp$ -, and TM atoms at the unique (1/4, 1/4, 1/4) site were considered. Table 1 shows the most energetically stable phases and the corresponding calculated equilibrium lattice constants, magnetic moments, and shear constants.

Table 1. The calculated equilibrium lattice constant  $a_0$  (in Å), atomic and total spin magnetic moments  $\mu_X$ ,  $\mu_Y$ ,  $\mu_Z$ , and  $\mu_{tot}$  (all in  $\mu_B$ ), shear moduli  $C'=(C_{11}-C_{12})/2$ ,  $C_{44}$  (in GPa) and the Zener's anisotropy  $A_Z = C_{44} / C'$  for the energetically preferable  $d^0$ - $d$  XMnY (X = K, Rb, Y = As, Bi, Ge, Si, P, Pb, Sb, Sn) half-Heusler alloys

No.	XYZ	$a_0$	$\mu_X$	$\mu_Y$	$\mu_Z$	$\mu_{tot}$	$C'$	$C_{44}$	$A_Z$
1.	KMnSi ( $\beta$ )	6.87	-0.03	4.18	-0.29	3.86	13.12	-23.27	-1.77
2.	KMnBi ( $\gamma$ )	7.14	0.02	4.25	-0.06	4.21	24.09	19.29	0.80
3.	KMnSb ( $\gamma$ )	7.00	0.03	4.25	-0.07	4.21	29.62	0.22	0.01
4.	KMnPb ( $\gamma$ )	7.16	0.00	4.09	-0.26	3.83	14.71	9.58	0.65
5.	KMnP ( $\beta$ )	6.68	0.02	4.30	-0.03	4.21	34.60	-23.10	-0.67
6.	KMnAs ( $\beta$ )	6.83	0.01	4.31	-0.08	4.24	27.67	-6.56	-0.24
7.	KMnGe ( $\beta$ )	6.91	-0.03	4.19	-0.39	3.77	17.56	-15.12	-0.86
8.	KMnSn ( $\gamma$ )	7.08	0.0	4.09	-0.35	3.74	18.81	2.21	0.12
9.	RbMnPb ( $\gamma$ )	7.40	0.01	4.14	-0.26	3.89	16.52	-8.70	-0.53
10.	RbMnGe ( $\beta$ )	7.20	-0.03	4.25	-0.40	3.82	12.99	-21.74	-1.67
11.	RbMnSn ( $\gamma$ )	7.30	0.01	4.14	-0.35	3.80	20.66	-16.58	-0.80
12.	RbMnSi ( $\beta$ )	7.15	-0.03	4.25	-0.29	3.93	9.21	-167.95	-18.23

The research was supported by the Russian Science Foundation project No. 22-12-20032.

[1] S.A. Wolf, et al., Science 294 1488(2001).

[2] W.E. Pickett, J.S. Moodera, Phys. Today 54 39 (2001)

[3] A. Dehghan, S. Davatolhagh, Mater. Chem. Phys. 273, 125064 (2021)

[4] A. Dehghan, S. Davatolhagh, J. Alloys Compd. 772, 132 (2019)

[5] G. Kresse and J. Furthmuller, Phys. Rev. B 54, 11169 (1996)

[6] G. Kresse and D. Joubert, Phys. Rev. B 59, 1758 (1999)

[7] J. Sun, A. Ruzsinszky, and J. P. Perdew, Phys. Rev. Lett. 115, 036402 (2015)

# IR Magnetotransmission in Double Manganites $R\text{BaMn}_2\text{O}_6$

E. Mostovshchikova<sup>a,\*</sup>, S. Pryanichnikov<sup>b</sup>, E. Sterkhov<sup>b</sup>

<sup>a</sup> M.N. Mikheev Institute of Metal Physics of Ural Branch of Russian Academy of Sciences, 620108

Ekaterinburg, Russia

<sup>b</sup> Institute of Metallurgy of Ural Branch of Russian Academy of Sciences, 620016 Ekaterinburg, Russia

\*mostovsikova@imp.uran.ru

Double manganites of the  $R\text{BaMn}_2\text{O}_6$  type ( $R$  are rare-earth ions) are characterized by layer-by-layer ordering of  $R$  and Ba ions. The formation of such an ordering leads to a change in the properties of the initial disordered  $R_{0.5}\text{Ba}_{0.5}\text{MnO}_3$  manganites, in particular, the temperatures of magnetic phase transitions increase significantly (to room temperature), the ground state of the spin glass changes to an antiferromagnetic state, orbital ordering and related structural transitions appear [1]. In addition, a number of works have shown the possibility of detecting high values of magnetoresistance at room temperature, which additionally draws attention to these materials [2].

In this work, we consider double  $R\text{BaMn}_2\text{O}_6$  manganites with different rare-earth ions (Pr, Nd, Sm) and with different degrees of ordering. The degree of ordering was varied by annealing in oxygen at different temperatures and for different times, which do not change the oxygen stoichiometry and, accordingly, the ratio of  $\text{Mn}^{3+}/\text{Mn}^{4+}$  ions. To determine changes in the charge subsystem depending on the ordering of  $R$  and Ba, we measured the temperature dependences of transmission in the near-IR range, in the region where the contribution from the interaction of light with charge carriers dominates. It has been found that the application of an external magnetic field can lead to the appearance of the magnetotransmission (MT) effect. The relationship between the type of rare earth ion and the degree of ordering and the effect of magnetic transmission are analyzed. It is shown that the highest MT is found in manganites with partial ordering, when there is a transition to the ferromagnetic state (Figure).

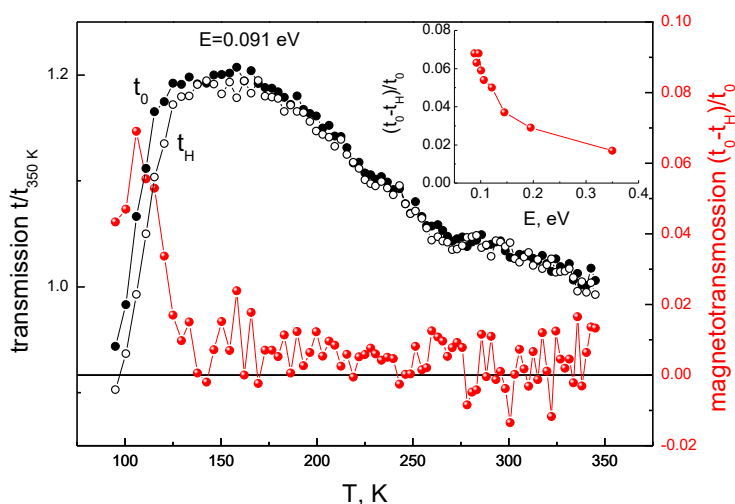


Figure. Manganite  $\text{NdBaMn}_2\text{O}_6$  annealed at 1250 C for 48 h: temperature dependence of the IR light transmission (black) measured in magnetic field of 8 kOe ( $t_H$ ) and without magnetic field ( $t_0$ ) and MT effect (red). Inset shows dependence of MT on the energy.

The research was supported by RSF (project No. 22-22-00507).

[1] T. Nakajima, J. Phys. Soc. Jpn. 75, 233(2013)

[2] S. Yamada, PRL 123, 126602 (2019)

# Laser control of pinning effect in ferromagnetic\antiferromagnetic nanofilms

I. Kolmychek<sup>a,\*</sup>, V. Novikov<sup>a</sup>, N. Gusev<sup>b,c</sup>, I. Pashenkin<sup>b</sup>, T. Murzina<sup>a</sup>

<sup>a</sup> Lomonosov Moscow State University, 119991, Leninskie gory 1, Moscow, Russia

<sup>b</sup> Institute for Physics of Microstructures RAS, GSP- 105, Nizhny Novgorod 603950, Russia

<sup>c</sup> Lobachevsky State University, Nizhny Novgorod 603950, Russia

\*irisha@shg.ru

Modern technology allows to create high quality metal magnetic nanofilms and thus opens up opportunities to introduce novel magnetic and transport effects in artificial nanomaterials. It is well known that if an antiferromagnetic film (material with antiparallel spin alignment) is adjacent to a ferromagnetic one, exchange coupling between spins of both magnetic materials leads to the appearance of a preferential direction of the ferromagnetic magnetization, i.e., pinning. Thus, the unidirectional magnetic anisotropy of the structure can be formed that manifests itself as a shift and widening of the magnetic hysteresis loop [1]. The exchange bias effect in the ferromagnetic\antiferromagnetic nanofilms breaks down at the temperature exceeding the so-called blocking temperature of the antiferromagnet [2]. In this work we propose switching of the pinning direction by means of intense laser beam pumping the magnetic structure. The experiments are performed for three-layer NiCu(4 nm)/CoFe (4 nm)/IrMn (10 nm) films obtained by magnetron sputtering in an argon atmosphere at a pressure of  $2 \times 10^{-3}$  Torr, with a static magnetic field of about 130 Oe applied in the film plane during the deposition of the antiferromagnetic IrMn layer.

Magnetic properties of the structures were investigated by means of transversal magneto-optical Kerr effect (MOKE) and magnetization-induced second harmonic generation (SHG). The SHG measurements were performed using a Ti:Sa laser radiation (with pulse duration of 50 fs, mean power of 10-12 mW) focused by 5 cm lens on the nanofilm. The MOKE and SHG measurements in the reflected light direction were carried out in the same point of the film after it was irradiated with the focused laser beam of about 50 mW power, causing the local heating of the film above the blocking temperature, and subsequent cooling of the sample in a static saturating magnetic field (about 800 Oe).

It was shown that after laser beam-induced film heating and cooling in the positive magnetic field the hysteresis loop shifts towards the negative field by 240 Oe in the MOKE and by 80 Oe in the SHG (Fig. 1). The widths of loops are about 220 and 160 Oe, respectively. We note that the linear MOKE characterizes the magnetic properties of the "bulk" of the structure at the penetration depth of light, while the SHG sources are localized exclusively at the surface and interfaces of the nanofilm, resulting in the observed difference of the hysteresis loop parameters in the linear and nonlinear response. Importantly, after the similar procedure in the negative magnetic field, the same shifts to the

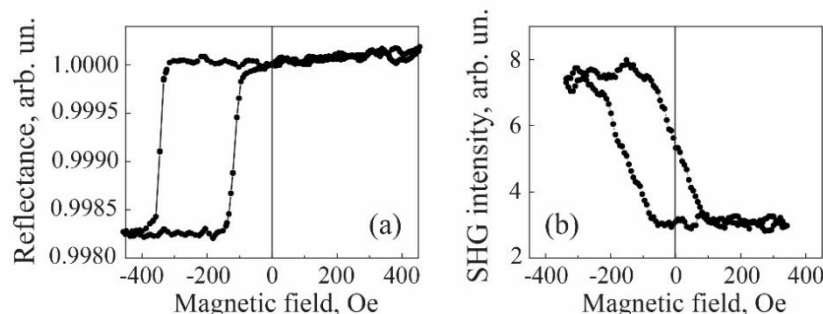
opposite direction were observed, indicating the laser-beam-induced switching of the pinning.

This research was funded by RSF, Grant 19-72-20103.

[1] J. Nogues et al., *Physics Reports* 422, 65 (2005).

[2] A. J. Devasahayam et al., *J. Appl. Phys.* 85, 5519 (1999).

Fig. 1. (a) MOKE hysteresis and (b) SHG intensity hysteresis obtained for NiCu/CoFe/IrMn nanofilm after laser beam irradiation and cooling applying the positive saturating magnetic field.



## Machine-learning interatomic potentials for magnetic materials

I. Novikov<sup>a,b\*</sup>, A. Kotykhov<sup>a,b</sup>, M. Hodapp<sup>c</sup>, C. Tantardini<sup>d,e</sup>, and A. Shapeev<sup>a</sup>

<sup>a</sup>Skolkovo Institute of Science and Technology, Skolkovo Innovation Center,  
Bolshoy boulevard 30, Moscow, 143026, Russian Federation

<sup>b</sup>Moscow Institute of Physics and Technology, Russian Federation

<sup>c</sup>Materials Center Leoben Forschung GmbH (MCL), Leoben, Austria

<sup>d</sup>Hylleraas center, Department of Chemistry, UiT The Arctic University of Norway,  
PO Box 6050 Langnes, N-9037 Tromsø, Norway

<sup>e</sup>Department of Materials Science, Rice University,  
Houston, Texas 77005, United States of America

\*i.novikov@skoltech.ru

Magnetism is important and should be explicitly taken into account for successful prediction of many properties of single-component metals and magnetic alloys in theoretical models. Magnetism can be responsible for the unusual properties like negative thermal expansion [1] or anomalous volume-composition dependence [2].

One of the most widely used methods for simulations of magnetic materials is density functional theory (DFT). However, DFT calculations are computationally expensive even when used them on modern supercomputers. Machine-learning interatomic potentials (MLIPs) can be considered as an alternative approach to expensive DFT calculations. The main idea behind MLIPs is their ability to avoid running the full DFT simulation by interpolating between a relatively small training set of carefully selected single-point DFT calculations. The accuracy of MLIPs is close to the accuracy of DFT calculations, but MLIPs require much less computing resources than DFT. MLIPs have recommended themselves as a reliable tool for predicting the properties of different alloys [3].

In this talk we present magnetic MLIPs including magnetic moments in their functional form. We fit (train) magnetic MLIPs on the data of DFT calculations. We demonstrate the predictive power of magnetic MLIPs for the systems of pure Fe and bcc Fe-Al with different concentrations of Al and Fe. For pure Fe we show that phonon spectra, vacancy formation energy, and energy/volume curves predicted with MLIPs are close to the ones obtained with DFT [4]. We also show that magnetic MLIPs are capable to reproduce energies and local magnetic of Fe at finite temperature. For the system of bcc Fe-Al we show that the formation energies, the equilibrium lattice parameters, and the total magnetic moments of the unit cell for different Fe-Al structures calculated with MLIPs are in good correspondence with the ones obtained with DFT. We also show that magnetic MLIPs reproduce the experimentally observed anomalous volume-composition dependence in the Fe-Al system.

This work was supported by Russian Science Foundation (grant number 22-73-10206, <https://rscf.ru/project/22-73-10206/>).

[1] Y. Song, N. Shi, S. Deng, X. Xing, and J. Chen, *Progress in Materials Science* 121, 100835 (2021).

[2] M. Friak and J. Neugebauer, *Intermetallics* 18, 1316 (2010).

[3] I. Novikov, O. Kovalyova, A. Shapeev, and M. Hodapp, *Journal of Materials Research* 37, 3491 (2022).

[4] I. Novikov, B. Grabowski, F. Kormann, and A. Shapeev, *npj Computational Materials* 8, 13 (2022).

## Machine-learning models in on-lattice modelling

T. Kostiuchenko<sup>a,b\*</sup>, A. Shapeev, I. Novikov<sup>a,b</sup>

<sup>a</sup> Skolkovo Institute of Science and Technology, 121205, Bolshoy Boulevard 30, bld. 1, Moscow, Russia

<sup>b</sup> Moscow Institute of Physics and Technology, 141701, Institutskiy Pereulok 9, Dolgoprudny, Moscow region, Russia

\*Tatiana.Kostiuchenko@skoltech.ru

For the last decades, atomistic modelling became an important complementary part in the problem of materials properties investigation. New multicomponent materials and especially materials with designed properties are of high interest, but it takes a long time and resources to consider large configurational space within only experiment. Thus, efficient methods of numerical investigation and properties prediction are in demand at least for choosing directions in experimental investigations.

In this work, we present methodology based on “on-lattice” interatomic potential (Low-rank potential, LRP) implemented as interatomic interaction model in Monte-Carlo method. The potential is based on quantum mechanical calculations and its form is close to cluster expansion approach. We applied this methodology in order to investigate chemical short-range order and stability in such equiatomic systems as bcc NbMoTaW [1], bcc AlNbTiV [2] and fcc VCoNi [3]. It is important to notice that in the latter case it is crucial to account for atomic spin interactions in order to get a physical prediction of the phase transition temperature. Although the form of LRP does not include explicit account for magnetic interactions, we found that our results are in agreement with experiment [4-5]. Thus, we decided to develop special form of LRP explicit account for spin interaction so to use it in the problem of magnetic order investigation. For the first attempt, we included collinear spin directions explicitly in the LRP form, but it turned out that in spite of the increase in the accuracy it does not reproduce transition temperatures in bcc Fe and FeCo systems. Thus, we decided to expand the number of "spin directions" in LRPs form in polyhedral spherical approximation. Successful realization of this new form can make it possible to investigate the process of magnetic order formation more precisely and efficiently.

This work was supported by Russian Science Foundation (grant number 22-52473-10206, <https://rscf.ru/project/22-73-10206/>).

[1] Kostiuchenko, T., Körmann, F., Neugebauer, J., & Shapeev, A. (2019). Impact of lattice relaxations on phase transitions in a high-entropy alloy studied by machine-learning potentials. *npj Computational Materials*, 5(1), 55.

[2] Körmann, F., Kostiuchenko, T., Shapeev, A., & Neugebauer, J. (2021). B2 ordering in body-centered-cubic AlNbTiV refractory high-entropy alloys. *Physical Review Materials*, 5(5), 053803.

[3] Kostiuchenko, T., Ruban, A. V., Neugebauer, J., Shapeev, A., & Körmann, F. (2020). Short-range order in face-centered cubic VCoNi alloys. *Physical Review Materials*, 4(11), 113802.

[4] Kim, Y. M., Lee, S., Kim, K. J., Jang, T. J., Do, H. S., Jang, K., ... & Sohn, S. S. (2022). Effects of aging time on the microstructural evolution and strengthening behavior of a VCoNiMo medium-entropy alloy. *Materials Science and Engineering: A*, 857, 144112.

[5] Chen, X., Wang, Q., Cheng, Z., Zhu, M., Zhou, H., Jiang, P., ... & Ma, E. (2021). Direct observation of chemical short-range order in a medium-entropy alloy. *Nature*, 592(7856), 712-716.

## Magnetic nanowires of different types- features of obtaining by matrix synthesis, properties and applications

D.Zagorskiy<sup>1\*</sup>, I.Doludenko<sup>1</sup>, O.Zhigalina<sup>1</sup>, L.Panina<sup>2</sup>, D.Biziaev<sup>3</sup>, D.Chairetdinova<sup>1,2</sup>,  
S.Chigarev<sup>4</sup>, L.Fomin<sup>5</sup>

<sup>1</sup>FSRC “Crystallography and Photonics” of RAS, Russia, Moscow, Leninski pr.,59

<sup>2</sup>Moscow Institute of Steel and Alloys, Moscow, Leninski pr.,4

<sup>3</sup>Zavoisky Physical-Technical Institute, FRC Kazan Scientific Center of RAS

<sup>4</sup>Institute of microelectronics technology and high purity materials of RAS, Chernogolovka

<sup>5</sup>Kotel'nikov Institute of Radio Engineering and Electronics of RAS, Fryazino

\*corresponding author email [dzagorskiy@gmail.com](mailto:dzagorskiy@gmail.com)

Matrix synthesis - filling the pores of a special matrix with the required material - provides unique opportunities for obtaining arrays of nanosized filaments - nanowires (NWs) from various materials. Nanowires from iron group metals were obtained by galvanic filling of pores in track membranes.

**Synthesis.** The features of obtaining three main types of NWs are studied: from one metal, binary with a homogeneous distribution of metals and heterogeneous, consisting of alternating layers of different metals. For the first type, the possibilities of changing the crystallographic structure or controlling the grain size were studied. For the second type, the difference between NWs from FeNi and FeCo alloys is shown: in the first case, there is a higher difference in the composition of NWs from the composition of the electrolyte, as well as a change in the composition along the length of the NW. The difference can be explained by the anomalous co-deposition of iron and the lower mobility of nickel ions. For layered NWs, methods for obtaining NWs with layers with the same (along the length of the NW) thickness with a controlled composition and flat interlayer boundaries (interfaces) are shown. Best results were obtained by the precise control of the passed charge and the deceleration of the deposition rate by the dilution or cooling of the electrolyte.

**Structure and magnetic properties.** SEM confirmed the correspondence of NWs' quantity and diameter to the same parameters of matrix. XRD data showed the change of the structure (fcc to bcc) with Fe content increase (in alloyed NWs) and fcc to hcp for Co NWs (with an increase of solution's pH). Integral magnetic properties (hysteresis loops) were investigated via VSM method: it was demonstrated that the orientation of an easy magnetization axes changed accordingly to the change of aspect ratio of magnetic (Ni or Co) and diamagnetic Cu layers. Magnetic force microscopy (MFM) was used to test local magnetization of single NW. The domain structure was visualized; the coercive force ( $H_c$ ) was estimated by changing the external magnetic field.  $H_c$  of the single NW appeared to be much lower than integral  $H_c$  due to interaction between close-packed NWs in matrix.

**THz generation.** Samples consisting of two different magnetic parts (FeCo/FeNi, for example) demonstrate the possibility of THz irradiation generation (during the current passing through inter-layer contacts). The space distribution of irradiation was investigated and optimal construction of emitter (with conductive stripes at the surface) was developed. Thermal ( $\lambda=10-12 \mu\text{m}$ ) and dynamic peaks ( $\lambda=15-17 \mu\text{m}$ , due to spin-flip transition) were detected in irradiation spectra, and the “competition” between these types of irradiation was supposed. The threshold nature of the appearance of the last maximum confirmed the nonthermal, dynamic nature of emerging radiation. These investigations demonstrate the possibility of developing THz radiation emitters and detectors. Some other possibilities of NWs applications - radiation absorption (screens), medicine (drug delivery and local heating) and magneto-optics are also discussed.

**Acknowledgements.** This work was done within the Russian Science Foundation Project №22-22-00983

## Magnetic phase transitions in (R'R'')Ni (R — Gd, Tb, and Dy) compounds and their hydrides: transition order elaboration

A. Kurganskaya<sup>a,\*</sup>, I. Tereshina<sup>a</sup>, A. Karpenkov<sup>a,b</sup>, S. Lushnikov<sup>a</sup>, and V. Verbetsky<sup>a</sup>

<sup>a</sup> Lomonosov Moscow State University, 119991, Leninskie gory 1, Moscow, Russia

<sup>b</sup> Tver State University, 170100, Zhelyabova street, 33, Tver, Russia

\*kurganskaia.aa17@physics.msu.ru

Rare earth metal compounds with nickel of the RNi type are appealing for their manifestation of a significant magnetocaloric effect (MCE) around the liquid nitrogen boiling temperature. Moreover, compounds of the RNi type easily absorb hydrogen, forming stable hydrides. At the same time, hydrogenation reduces the Curie temperature of these compounds, which expands the possibilities for using these materials in science and technology in the low temperatures field [1, 2]. An important criterion for the practical applicability of a compound demonstrating a large MCE in the area of magnetic phase transition (MPhT) is the order of this transition, namely the first or second. Preference is given to the compounds with the MPhTs of the latter type, since there is no magnetic hysteresis in that case. The purpose of this study was to clarify the type of MPhTs in R'R''Ni compounds and their hydrides, where R' = Gd, R'' = Tb or Dy.

Gd<sub>x</sub>(Dy,Tb)<sub>1-x</sub>Ni ( $x = 0.1, 0.9$ ) compounds were prepared in an arc furnace under an Ar protective atmosphere, and their hydrides Gd<sub>x</sub>(Dy,Tb)<sub>1-x</sub>NiH<sub>y</sub> ( $x = 0.1, 0.9; y = 3, 4$ ) were synthesised in a Sievert-type setup with a hydrogen pressure operating range to 100 MPa. An XRD-analysis of the crystal structure of the compounds was obtained. It has been determined that compounds with a high gadolinium content crystallize in a CrB-type orthorhombic structure (spatial group 63), whereas the Gd<sub>0.1</sub>Dy<sub>0.9</sub>Ni and Gd<sub>0.1</sub>Tb<sub>0.9</sub>Ni compounds crystallize in FeB-type (spatial group 62) and TbNi-type (spatial group 11) structures respectively. At the same time, all the hydrides studied had a CrB-type spatial structure.

The magnetocaloric effect in the area of the phase transition from the magnetically ordered to the magnetically disordered state (around Curie temperature) was determined by an indirect method using the Maxwell's equation. Temperature and field dependences of magnetization were measured on standard PPMS – 9 equipment.

To clarify the type of magnetic phase transition, not only the Belov-Arrot curves were used, but also the recently proposed [3] quantitative criterion, namely, the analysis of the value of the parameter  $n$ , which was determined by the following formula:

$$n(T, H) = \frac{d \ln |\Delta S_M|}{d \ln H}$$

It has been found that all the initial Gd<sub>x</sub>Dy<sub>1-x</sub>Ni and Gd<sub>x</sub>Tb<sub>1-x</sub>Ni ( $x = 0.1, 0.9$ ) compounds exhibit MPhTs of the second order, whereas the addition of hydrogen can change the type of the magnetic transition from the second to the first order.

The research was carried out with the support of the Russian Science Foundation grant № 22-29-00773, <https://rscf.ru/project/22-29-00773/>.

[1] V.B. Chzhan *et al*, Materials Chemistry and Physics, 264 (2021), <https://doi.org/10.1016/j.matchemphys.2021.124455>.

[2] I.S. Tereshina *et al*, Journal of Magnetism and Magnetic Materials, 574 (2023), <https://doi.org/10.1016/j.jmmm.2023.170693>.

[3] Law, J.Y. *et al*, Nat Commun 9, 2680 (2018). <https://doi.org/10.1038/s41467-018-05111-w>



## Magnetic phase transitions in the GdFe<sub>2</sub>-H system

I. Tereshina<sup>a,\*</sup>, A. Karpenkov<sup>b</sup>, A. Aleroev<sup>c</sup>

<sup>a</sup> Lomonosov Moscow State University, 119991, Leninskie gory 1, Moscow, Russia

<sup>b</sup> Tver State University, 170100, st. Zhelyabova 33, Tver, Russia

<sup>c</sup> Grozny State Oil Technical University, 364024, Isaeva av. 100, Grozny, Russia

\*irina\_tereshina@mail.ru

Compounds of rare earth metals (R) with iron form a fairly large class of materials widely known not only in science but also in practice. Compositions of the RFe<sub>2</sub> type with the structure of Laves phases are of particular interest to scientists due to their simple crystal and magnetic structure, as well as due to unique magnetic properties, such as giant magnetostriction, a large magnetocaloric effect, etc., which are observed in the region of spontaneous and induced by an external magnetic field spin-reorientation phase transitions. Moreover, RFe<sub>2</sub> compounds easily absorb hydrogen, forming both stable and unstable hydrides. The purpose of this work was to study the effect of hydrogenation on magnetic phase transitions in the GdFe<sub>2</sub> compound, as well as to control the stability of the resulting hydrides over time.

We obtained the following GdFe<sub>2</sub>H<sub>x</sub> samples with both low and high hydrogen content, namely, with  $x = 0, 1, 1.8, 3, 3.7, 5.2, 5.4$ . The atomic crystal structure and phase composition were determined using X-ray methods of analysis. The temperature and field dependences of the magnetization were studied in static and pulsed magnetic fields up to 60 T.

It has been established that upon hydrogenation of the GdFe<sub>2</sub> compound, the type of the crystal structure of MgCu<sub>2</sub> does not change. At the same time, hydrogenation can lead to a significant increase in the volume of the unit cell up to approximately ~ 30% at the maximum hydrogen content  $x = 5.4$  at.H/f.u.

The Curie temperature of the GdFe<sub>2</sub>H<sub>x</sub> samples was determined using thermomagnetic analysis (TMA). It has been established that the transition temperature of ferrimagnetic to paramagnetic state (which is determined by the contributions from exchange interactions inside the Fe-Fe iron sublattice, the Gd-Fe intersublattice exchange interaction, and interactions inside the rare-earth R-R sublattice) decreases from 790 K for the parent GdFe<sub>2</sub> compound to 65 K for the hydride GdFe<sub>2</sub>H<sub>5.4</sub> with the maximum hydrogen content. Thus, hydrogenation significantly weakens interactions, including intersublattice Gd-Fe exchange interactions, which allows us to observe and analyze magnetic phase transitions in the GdFe<sub>2</sub>H<sub>x</sub> system induced by external magnetic fields.

It has been found that hydrides with a high hydrogen content ( $x > 5$ ) are not stable. The stability of hydrides is directly related to the fact that hydrogen atoms occupy different interstitials in the cubic structure of the MgCu<sub>2</sub> type [1]. Different interstitials have different sizes. Hydrogen atoms, located in interstitials, have in their environment a different number of nearest neighbors, both gadolinium atoms and iron atoms.

Using the molecular field theory, the parameters of the intersublattice exchange interaction for hydrides GdFe<sub>2</sub>H<sub>x</sub> are determined.

The study was supported by a grant from the Russian Science Foundation № 22-29-00773, <https://rscf.ru/project/22-29-00773/>.

[1] N. Mushnikov, et. al. Phys. Metals Metallogr. 100, 338 (2005).

# Magnetic Properties and Exchange Bias of a Compensated Ferrimagnet Mn<sub>2</sub>PtAl

A. Lukoyanov<sup>a,b</sup>, S. Shanmukharao Samatham<sup>c</sup>, A. Patel<sup>d</sup>, P. Babu<sup>e</sup>, K. Suresh<sup>f</sup>

<sup>a</sup>M.N. Mikheev Institute of Metal Physics of Ural Branch of Russian Academy of Sciences, 620108, S. Kovalevskaya 18, Ekaterinburg, Russia

<sup>b</sup>Institute of Physics and Technology, Ural Federal University, 620002, Mira 19, Ekaterinburg, Russia

<sup>c</sup>Department of Physics, Chaitanya Bharathi Institute of Technology, Gandipet, Hyderabad 500 075, India

<sup>d</sup>Research Centre for Magnetic and Spintronic Materials, National Institute for Materials Science, Tsukuba, Ibaraki 305 0047, Japan

<sup>e</sup>UGC-DAE Consortium for Scientific Research, Mumbai Center, BARC Campus, Mumbai 400085, India

<sup>f</sup>Magnetic Materials Laboratory, Department of Physics, Indian Institute of Technology Bombay, Mumbai 400 076, India

\*lukoyanov@imp.uran.ru

In this work, the structural, magnetic and electronic structure properties of the full Heusler alloy Mn<sub>2</sub>PtAl have been investigated. It was found to crystallize in hexagonal structure with lattice constants of  $a = b = 4.34 \text{ \AA}$ , and  $c = 5.47 \text{ \AA}$  at room temperature [1]. Magnetization revealed a weak martensitic transition at 307 K followed by a nearly compensated ferrimagnetic state below 90 K. Griffiths phase-like signature, positive Weiss temperature and a frequency independent peak confirm a nearly compensated ferrimagnetic order of Mn<sub>2</sub>PtAl. Magnetization isothermal curves in the ambient of a cooling field  $H_{\text{cool}}$  equal to 70 kOe show asymmetric hysteresis with a negative shift along  $H$ -direction. The estimated exchange bias in  $H_{\text{cool}}$  equal to 70 kOe is giant (2.73 kOe) at a temperature 3 K which is attributed to the unidirectional anisotropy associated with ferromagnetic clusters. Theoretical first-principles calculations reveal a ferrimagnetic arrangement of the magnetic moments of Mn with a small value of total magnetic moment in good agreement with the experimental magnetization measurements. Theoretical electronic structure calculations also revealed the nearly compensated ferrimagnetic arrangement of the Mn ions (at different sites) preferable in total energy with a total magnetic moment of 0.15 Bohr magneton in good agreement with the experimental magnetization measurements. Giant exchange bias and coercivity are attributed to the creation of ferromagnetic clusters in the nearly compensated ferrimagnetic matrix under field cooling. Finally, this study shows that there are many differences between the structural, magnetic and exchange bias properties of Mn<sub>2</sub>PtGa and Mn<sub>2</sub>PtAl, arising mainly due to the difference in the strength of the ferrimagnetic anisotropy between the two alloys. To throw more light on the underlying exchange bias effect in Mn<sub>2</sub>PtAl, magnetic hysteresis measurements under the application of high magnetic fields of the order 300-500 kOe are desired. For more details, see our paper [1].

The theoretical calculations were supported by Russian Science Foundation (pr. no. 22-42-02021). AKP thanks the University Grants Commission, Govt. of India, for the financial support through senior research fellowship (ref. no: 21/06/2015(i)EU-V). SSS was supported by the Science and Engineering Research Board through the TARE Project (TAR/2018/000454).

[1] A.K. Patel, S. Shanmukharao Samatham, A.V. Lukoyanov, P.D. Babu, K.G. Suresh, PCCP 24, 29539 (2022)

# Magnetic Properties and Modeling Hysteresis Parameters of Foraminifera Shells from the Mid-Atlantic Ridge

E. Sergienko<sup>a</sup>, S. Janson<sup>a</sup>, K. Gareev<sup>b,\*</sup>, P. Kharitonskii<sup>b</sup>, A. Ralin<sup>c</sup>, T. Sheydaev<sup>b</sup>, E. Setrov<sup>b</sup>

<sup>a</sup> Saint Petersburg University, 199034, 7–9 Universitetskaya Emb., Saint Petersburg, Russia

<sup>b</sup> Saint Petersburg Electrotechnical University “LETI”, 197022, 5 Prof. Popov Str., Saint Petersburg, Russia

<sup>c</sup> Far Eastern Federal University, 690922, 10 Ajax Bay, Russky Island, Vladivostok, Russia

\*kkgareev@yandex.ru

An experimental and theoretical study of the magnetic properties, as well as the phase- and elemental composition, of iron-containing inclusions in foraminifera [1],[2] shells of the Mid-Atlantic Ridge (MAR) was provided. Samples of Holocene and Upper Pleistocene sediments containing microbiota (mainly benthic and planktonic foraminifera and coccoliths) were collected during studies carried out by the Polar Marine Geosurvey Expedition on the research vessel Professor Logachev in the Russian exploration region of MAR. The scanning electron microscopy (SEM) image and the magnetic characteristics of one of the samples are shown in the Figure 1.

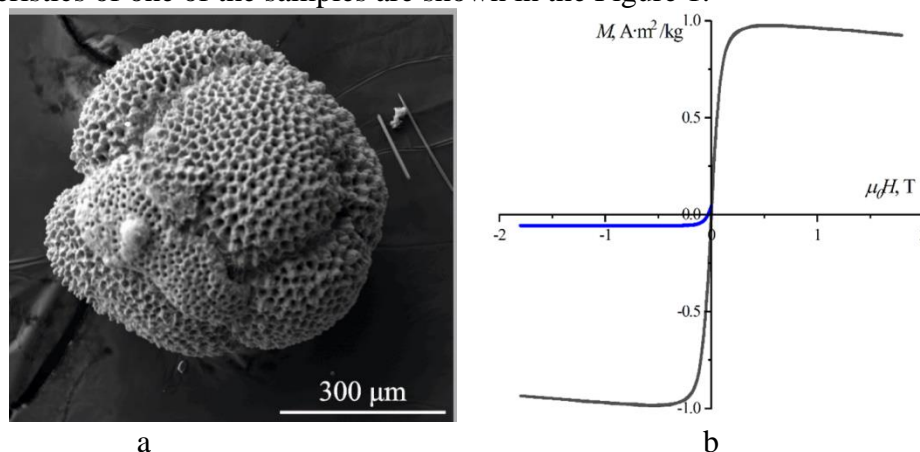


Figure 1. SEM image (a) and hysteresis loop with backfield curve (b) of foraminifera shells with iron-containing inclusions

Magnetic granulometry of the samples was simulated on the basis of two models. The first one is the model of an ensemble of single-domain magnetostatically interacting ferrimagnetic particles with effective spontaneous magnetization [3]. This parameter allowed us to phenomenologically take into consideration the magnetic and chemical inhomogeneity of the particles. The advantage of the model is a more strict consideration of magnetostatic interaction at any concentration of ferrimagnetic particles, as well as less complicated calculations if the expansion of the random interaction field distribution function is limited to the first few terms (Gram-Charlier or Edgeworth series) [4]. The second model is the model of an ensemble of interacting chemically inhomogeneous two-phase particles [5]. The advantage of the two-phase model is the explicit consideration of chemical inhomogeneity and magnetostatic interaction between phases using the method of magnetic rectangles, which allows calculating the number of particles in different magnetic states and remagnetization fields.

- [1] J. Pawlowski, M. Holzmann. *Eur. J. Protistol.* 38, 1 (2002)
- [2] J. Pawlowski, W. Majewski. *J. Foraminifer. Res.* 41, 3 (2011)
- [3] P. Kharitonskii et al. *J. Magn. Magn. Mater.* 553, 169279 (2022)
- [4] A. Al'miev et al. *Phys. Met. Metallogr.* 78, 28 (1994)
- [5] P. Kharitonskii et al. *Chinese J. Phys.* 78, 271 (2022)

# Magnetic Properties of $\text{GdFe}_3(\text{BO}_3)_4$ Multiferroic Grown From Various Melt Solutions

E. Eremin\*, I. Gudim, V. Titova

Kirensky Institute of Physics, Krasnoyarsk Scientific Center, Siberian Branch, Russian Academy of Sciences, Krasnoyarsk 660036, Russia

\*[eev@iph.krasn.ru](mailto:eev@iph.krasn.ru)

Recently, rare-earth ferrobates with the huntite structure  $\text{RFe}_3(\text{BO}_3)_4$  ( $\text{R} = \text{Y}, \text{La-Lu}$ ) have attracted increased attention due to the discovery of their multiferroic properties.

Initially, for isostructural nonlinear optical crystals of trigonal aluminoborates  $\text{RAl}_3(\text{BO}_3)_4$ , a method was developed for growing from melt solutions based on potassium trimolybdate  $\text{K}_2\text{Mo}_3\text{O}_{10} - \text{B}_2\text{O}_3$ . Later, new melt solutions based on bismuth trimolybdate  $\text{Bi}_2\text{Mo}_3\text{O}_{12} - \text{B}_2\text{O}_3$  were proposed for growing  $\text{RAl}_3(\text{BO}_3)_4$  and  $\text{RFe}_3(\text{BO}_3)_4$  single crystals. Unfortunately, in both cases, during the growth process, rare-earth ions are replaced by uncontrolled impurities from the solvent [1]. Therefore, solutions-melts based on lithium tungstate were proposed. In the latter case, it is assumed that the crystal matrix does not contain impurities from the solvent.

The paper presents a comparative analysis of the influence of impurities K, Mo and Bi on the phase diagram (T-H) of magnetic transitions of the  $\text{GdFe}_3(\text{BO}_3)_4$  multiferroic.

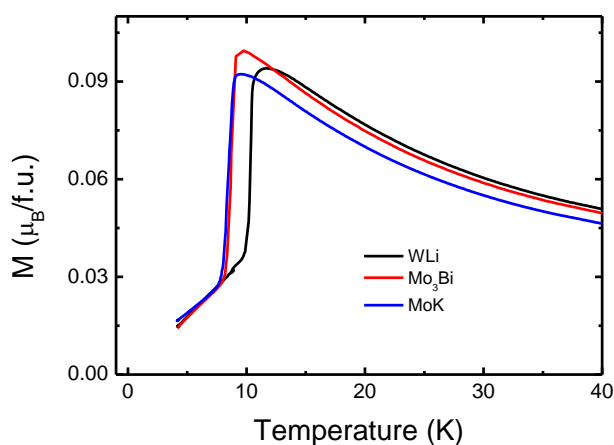


**Fig 1.** Temperature dependence of the magnetization of  $\text{GdFe}_3(\text{BO}_3)_4$  in a field  $H = 1$  kOe, in the direction  $H||c$ , for crystals grown in various solvents.

It was shown in the work that the phase diagram (T-H) of the spin-flop transition  $T_S$  and the Neel temperature  $T_N$  shift to lower fields and temperatures for  $\text{GdFe}_3(\text{BO}_3)_4$  grown using bismuth trimolybdate and potassium molybdate solvents compared to  $\text{GdFe}_3(\text{BO}_3)_4$  grown from lithium solvent tungstate. Figure 1 shows an example that clearly shows the shift of the spin flop to smaller fields.

All this pointed to the fact that impurities from the solvent do not enter the crystal matrix from the lithium tungstate solvent.

Support by RSF and KRFS № 22-12-20019 are acknowledged.

1. Boldyrev K.N., Popova M.N., Bettinelli M., at all // Optical Materials, (2012), V. 34, Is. 11, P. 1885-1889

# Magnetic properties of $Mn_2YSn$ ( $Y = Sc, Ti, V$ ) Heusler alloy: Insights from *Ab initio* and Monte Carlo investigations

M. Zagrebin<sup>a,\*</sup>, V. Sokolovskiy<sup>a</sup>, D. Baigutlin<sup>a</sup>, V. Buchelnikov<sup>a</sup>

<sup>a</sup> Chelyabinsk State University, 454077, Brat'ev Kashirinykh Str. 129, Chelyabinsk, Russia

\*miczag@csu.ru

At present, the study of new solid-state compounds and alloys with multifunctional properties is becoming increasingly popular in the scientific community around the world. This interest is due to the potential application as material for spintronics, where the spin degree of freedom of an electron plays a significant role in encoding, faster transfer and processing of data as compared to a charged based equivalent transistor [1]. The spintronic devices mostly consist of a non-magnetic layer sandwiched between two ferromagnetic electrodes like giant-magnetoresistance [2], tunneling magnetoresistance [3] and magnetic tunnel junction [4] devices. One of such compounds are Heusler alloys which having multifunctional properties such as exchange bias, magnetocaloric effect and magnetic shape memory alloys. Among the Heusler alloys,  $Mn_2YZ$  based members ( $Y$  being a  $3d$  or  $4d$  transition element and  $Z$  a  $sp$  element) are of significant interest due to high electron-spin polarization with high  $T_C$  and efficient spin-transfer torque are responsible a promising material in future spintronic devices [5]. So, this work is devoted to the *ab initio* and Monte Carlo investigations of the magnetic properties of the  $Mn_2YSn$  ( $Y = Sc, Ti, V$ ) alloys depending on the applied external pressure.

To perform *ab initio* calculations, the projected augmented wave method implemented in the VASP code [6, 7] was employed. For the exchange-correlation functional, the generalized gradient approximation in the scheme of Perdew, Burke, and Ernzerhof [8] was applied. To investigate the pressure dependencies, the Pulay stress on the equilibrium cell shape was calculated. To calculate the magnetic exchange constants  $J_{ij}$ , the Green's function method with the local rigid spin rotation treated as a perturbation [9] was used. To do this, the maximally-localised Wannier functions were firstly calculated by the Wannier90 code [10]. Magnetic exchange parameters have been used for thermomagnetic curves calculations via classical Heisenberg model and Monte Carlo simulations. From this curves Curie temperature were estimated. Using classical Heisenberg model and Monte Carlo simulations allowed also to obtain the adiabatic temperature change ( $\Delta T_{ad}$ ) for considered compounds.

As a result, dependencies on external pressure of magnetic moments (total and partial), magnetic exchange parameters, Curie temperatures and magnetocaloric effect for  $Mn_2YSn$  ( $Y = Sc, Ti, V$ ) alloys were obtained.

Support by Russian Science Foundation (Project No. 22-12-20032) is acknowledged.

- [1] S. A. Wolf et al., Science 294, 1488 (2001).
- [2] K. Nikolaev et al., Appl. Phys. Lett. 94, 222501 (2009).
- [3] S. Tsunegi et al., Appl. Phys. Lett. 93, 112506 (2008).
- [4] T. Ishikawa et al., Appl. Phys. Lett. 89, 192505 (2006).
- [5] M. Ram et al., RSC Adv. 10, 7661 (2020).
- [6] G. Kresse and J. Furthmüller, Phys. Rev. B 54, 11169-11186 (1996).
- [7] G. Kresse and D. Joubert, Phys. Rev. B 59, 1758-1775 (1999).
- [8] J.P. Perdew et al., Phys. Rev. Lett. 77, 3865 (1996).
- [9] A.I. Liechtenstein et al., J. Magn. Magn. Mater. 67, 65 (1987).
- [10] G. Pizzi et al., J. Phys. Condens. Matter 32, 165902 (2020).

# Magnetic, electron and lattice dynamics of CoTiO<sub>3</sub> in high magnetic fields

M. Prosnikov <sup>a,\*</sup>, R. Pisarev <sup>a</sup>, P. C. M. Christianen <sup>b</sup>, A. Kalashnikova <sup>a</sup>

<sup>a</sup> Ioffe Institute, Russian Academy of Sciences, 194021 St. Petersburg, Russia

<sup>b</sup> High Field Magnet Laboratory (HFML–FELIX), Radboud University, 6525 ED Nijmegen, The Netherlands

\*yotungh@gmail.com

The experimental observation of the Dirac magnons in CoTiO<sub>3</sub> [1], trigonal honeycomb antiferromagnet with  $T_N = 38$  K and a part of a broad family of ilmenite materials, opened up an opportunity to study bosonic analogue of the widely known massless Dirac electrons in graphene [2].

In this work we present the results of the comprehensive polarized and azimuthally-resolved Raman scattering study of the spin, electron and lattice dynamics of the high-quality single crystals of the CoTiO<sub>3</sub> in wide temperature (4–300 K) and applied DC magnetic field (0–30 T).

Pronounced spin-phonon effect was observed at temperatures below  $T_N$  as was before predicted by the means of DFT calculations, where it was shown that only part of the phonons should be affected based on modulation of the superexchange path by dynamical variation of the Co-O-Co angles [3]. Measurements at high fields up to 30 T point to the competition between spin-phonon and magnetoelastic interactions [4], observed through both shift and splitting particular phonon modes.

Multiple electronic (magnetic exciton or crystal field) excitations were also observed at low temperatures, with a much superior energy resolution than in neutron scattering measurements [1]. These excitations are strongly affected by both temperature and field and thus could be directly used for phase diagram construction and determination of the microscopic parameters of the exchange model of CoTiO<sub>3</sub> such as anisotropy and exchange constants.

As for magnetic dynamics, both acoustic and optical magnon branches were observed in the AFM phase. The former one (AFMR) directly provides the value of the spin gap (~1 meV), and together with all other excitations used to further reexamine the exchange structure of the CoTiO<sub>3</sub>. Extremely dampened, but clearly observed modes at temperatures higher  $T_N$  hint for strong short-ordering effects.

The support from Russian Science Foundation grant #22-72-00039 is acknowledged.

[1] B. Yuan, I. Khait, G.-J. Shu, F. C. Chou, M. B. Stone, J. P. Clancy, A. Paramakanti, Y.-J. Kim, *Phys. Rev. X* 10, 011062 (2020)

[2] X. Du, I. Skachko, F. Duerr, A. Luican, E.Y. Andrei, *Nature*, 462, 192 (2009)

[3] R. M. Dubrovin, N. V. Siverin, M. A. Prosnikov, V. A. Chernyshev, N. N. Novikova, P. C. M. Christianen, A. M. Balbashov, R. V. Pisarev, *J. Alloy Compd.* 858, 157633 (2021)

[4] M. Hoffmann, K. Dey, J. Werner, R. Bag, J. Kaiser, H. Wadepohl, Y. Skourski, M. Abdel-Hafiez, S. Singh, R. Klingeler, *Phys. Rev. B* 104, 014429 (2021)

## **Magneto-optical Kerr spectroscopy of ferromagnetic metal-dielectric nanocomposites**

E. Gan'shina<sup>a\*</sup>, I. Pripechenkov<sup>a</sup>, N. Perova<sup>a</sup>, A. Yurasov<sup>b</sup>, M. Yashin<sup>b</sup>,  
A. Granovsky<sup>a</sup>.

<sup>a</sup> Lomonosov Moscow State University, 119991, Leninskie gory 1, Moscow, Russia

<sup>b</sup> MIREA-Russian Technological University, 119454 Moscow, Russia

<sup>\*</sup>eagan@mail.ru

Magneto-optical spectroscopy is an effective method for studying the magnetic microstructure of homogeneous and inhomogeneous magnets. The review is devoted to the analysis of the factors affecting the magnitude and spectral dependence of the magneto-optical signal of the transversal Kerr effect of ferromagnetic metal-dielectric nanocomposites in the visible and near-IR spectral regions. It is shown that the magneto-optical spectrum of nanocomposites depends on the metal concentration, size and shape of nanoparticles, dielectric material, deposition method, etc. Magneto-optical spectroscopy makes it possible to reveal the superferromagnetic behavior and the magnetically inhomogeneous state of two or more magnetic phases with different field dependences of magnetization. In the presence of a state with a magnetically soft and magnetically hard fraction, the magneto-optical signal is nonlinear in magnetization. In the near infrared region of the spectrum, a sign reversal and an increase in the transversal Kerr effect are observed. The interpretation of the magneto-optical spectra in terms of the effective medium methods makes it possible to explain the obtained regularities at a qualitative or semi-quantitative level.

Thus, MO Kerr spectroscopy makes it possible to obtain additional information on the magnetic microstructure of nanocomposites in addition to other magnetic and structural methods and can serve to control the processes of self-organization of nanocomposites during their production

# Magnetolectric effect in ring heterostructures with inner and outer magnetic layers

F. Fedulov<sup>a,\*</sup>, D. Savelev<sup>a,\*</sup>, V. Musatov<sup>a</sup>, L. Fetisov<sup>a</sup>

<sup>a</sup> MIREA – Russian technological university, 119454, Pr. Vernadskogo 78, Moscow, Russia

\*ostsilograf@ya.ru

Magnetolectric (ME) effect in ferromagnetic-piezoelectric (FM-PE) composite heterostructures manifests itself the generation of voltage across PE layer when the structure is placed in a magnetic field [1]. The study of ME effect in ring heterostructures is promising for creation of highly sensitive current sensors and tunable inductors due to the significant reduction of the demagnetizing factor compared to planar ones.

In this work, the resonant ME effect was investigated in ring heterostructures with a FM layer attached to the outer or inner surface of the PE ring. The FM layer of amorphous magnetic alloy Metglas 2605SA1 was 5 mm wide and 27  $\mu\text{m}$  thick. The PE rings made of piezoceramics PZT-19 had an inner diameter of 16 mm, a thickness of 1 mm, and a height of 5 mm. The structures were placed in plastic case on which two toroidal coils were wound with a number of turns  $N = 90$  for creating circular magnetic fields. The first coil created a constant magnetic field up to  $H = 100$  Oe, while the second coil generated an alternating magnetic field  $h\cos(2\pi ft)$  with an amplitude up to  $h = 1.7$  Oe in the frequency range from 1 to 100 kHz.

Figure 1 shows the measured dependencies of ME voltage generated by the heterostructures on the constant magnetic field at its resonance frequencies. The maximum measured ME voltage generated by the structure PZT-Metglas with an outer FM layer is approximately twice that of by the structure PZT-Metglas with an inner layer. The maximum ME coefficients were  $\alpha_m^{\text{out}} \approx 6$  V/(Oe·cm) and  $\alpha_m^{\text{in}} \approx 3$  V/(Oe·cm) at the optimal fields  $H_m^{\text{out}} = 1.7$  Oe and  $H_m^{\text{in}} = 2$  Oe, resonance frequencies  $f_0^{\text{out}} \approx 56$  kHz and  $f_0^{\text{in}} \approx 54$  kHz when the FM layer was on the outer and inner surface, respectively. The values of the optimal magnetic fields  $H_m$  are several times smaller than those obtained for similar composite planar FM-PE structures [2].

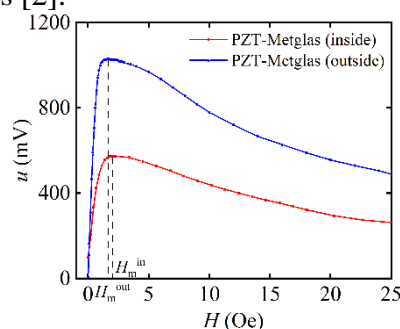


Figure 2. The dependence of ME voltage  $u$  on the constant magnetic field  $H$  for Metglas-PZT ring heterostructures.

The research was supported by the Russian Science Foundation, project № 19-79-10128-P. The samples were made with the support of the grant «For young scientists RTU MIREA 2022-2023» (НИЧ-57). Part of the measurements was performed on the equipment of the Joint scientific and educational center for collective use of RTU MIREA.

[1] D. Viehland, J. Phys. D.: Appl. Phys, 51, 26 (2018)

[2] D. T. H. Giang, Sensors and Actuators A: Physical. 179 (2012)



## Magnetotransport properties of transition metal silicides

M. Dorokhin, P. Demina, A. Zdoroveyshchev, V. Lesnikov, Yu. Kuznetsov, M. Ved', D. Zdoroveyshchev

Lobachevsky University, 603950, Gagarin Avenue 23/3, Nizhny Novgorod, Russia

\*dorokhin@nifti.unn.ru

The transition metal silicides such as FeSi<sub>2</sub>, NiSi<sub>2</sub> or higher manganese silicide can be used in a number of practical applications, such as thermoelectricity [1], optics [2] or spintronics [3]. Considering the spintronics area such materials are of interest due to possibility of revealing ferromagnetic properties upon proper technological parameters selection. These systems are capable of efficient integration with silicon-based devices and thus can act as sources of spin-polarized carriers in a silicon spintronics [3]. The present paper is devoted to studying the fabrication techniques and magnetic properties of a number of thin films based on transition metal silicides.

Two basic techniques were used for the fabrication of MeSi<sub>x</sub> thin films (Me=transition metal). The first one was pulsed laser deposition in vacuum. The MeSi<sub>x</sub> layers were grown on semi-insulating GaAs (100) substrates by sputtering of semiconducting Si and metal (Fe, Ni, Co, Mn) targets in a vacuum chamber with a background gas pressure of about  $2 \times 10^{-5}$  Pa. The growth temperature ( $T_g$ ) in these experiments was 250 °C. The metal content was first set by the technological parameter  $Y_{Me} = t_{Me} / (t_{Me} + t_{Si})$ , where  $t_{Me}$  and  $t_{Si}$  are the ablation times of the metal and Si targets, respectively. In some cases, the film was obtained by sputtering pre-fabricated target of metal silicide compound. The elemental composition corresponded of the composition in target to be sputtered.

The second technique used was implantation of Me<sup>n+</sup> ion in the ILU-3 accelerator with a fluence of  $10^{13} - 10^{15}$  cm<sup>-2</sup> and an energy of 20-80 keV. The choice of the ion fluence was made taking into account the calculations of the distribution of metal over the depth of structures, carried out using the SRIM program. To form a silicide phase the structures were subjected to rapid (30 sec) annealing at the temperature of 1000 °C in the atmosphere of argon. In both cases the composition was determined by energy dispersive X-ray spectroscopy (EDX) using a JSM-IT300LV (JEOL) scanning electron microscope with X-Max<sup>N</sup> 20 (Oxford Instruments) detector. Additional tool for investigating crystalline structure and phase composition was X-Ray diffraction spectroscopy which was carried out using a Shimadzu 7000 X-ray powder diffractometer (CuK $\alpha$  radiation was used).

The magnetic properties of the fabricated films were studied at room temperature by measuring the magnetic field dependencies of magnetization and Hall resistance. The Hall effect measurements were carried out in a van der Pauw geometry in the temperature range of (10-300 K). The Hall resistance in ferromagnetic films is a sum of two components: a linear one and anomalous component which is proportional to the perpendicular magnetization [4]. Thus, the Hall effect measurements allowed us to draw the conclusions on the magnetic hysteresis loops of the investigated films. In the present paper the Hall resistance value was normalized to unit to take into account different total film thicknesses of the samples. The magnetic properties were found to be strongly dependent on the exact material composition. In the most of the cases the samples revealed ferromagnetic Hall effect behavior at low temperatures (30 K). In some cases, the Curie temperature can be increased even to 300 K.

This study was supported by the Ministry of Science and Higher Education of the Russian Federation within a State assignment (project no. FSWR-2023-0037) and the federal academic leadership program "Priority 2030" of the Ministry of Science and Higher Education of the Russian Federation.

[1] S. Perumal, Mater. Science in semicond. Processing. 104, 104649 (2019)

[2] B. Schuller, J. Appl. Phys. 94, 207 (2003)

[3] R. Jansen, Nature mat. 11, 400 (2012)

[4] N. Nagaosa, Rev. Mod. Phys. **82**, 1539 (2010)

## Mechanism of sensitivity of CdTe crystals to pulsed magnetic action

I. Volchkov<sup>a,\*</sup>, M. Pavlyuk<sup>a</sup>, P. Podkur<sup>a</sup>, V. Kvartalov<sup>a</sup>, R. Morgunov<sup>b</sup>, V. Kanevskii<sup>a</sup>

<sup>a</sup> FSRC «Crystallography and Photonics» RAS, Leninskiy Prospekt 59, 119333, Moscow, Russia.

<sup>b</sup> Institute of Problems of Chemical Physics, Russian Academy of Sciences, Chernogolovka, Moscow oblast,  
142432 Russia

\*volch2862@gmail.com

Cadmium telluride CdTe belongs to the class of wide-gap semiconductors and stands out among analogues by a number of properties: the high density (5.85 g/cm<sup>3</sup>) and atomic numbers of the CdTe components (48 and 52, respectively) lead to a high photoelectric absorption coefficient [1]; the high absorption capacity of CdTe makes it a promising material for detectors operating in a wide energy range (from 0.005 to 10 MeV) [2]. As a result, semiconductor materials based on CdTe are of considerable practical interest for the fields of microelectronics, power engineering, and as materials for X-ray detectors. All these application places demand on the production technology of high-quality semiconductor crystals. Obtaining large volumes of perfect crystals is possible either by modernizing the processes of crystal growth, or by various processes of post-growth improvement of the properties. One of these methods is the impact of "weak" ( $\mu_B B \ll kT$ ) static and pulsed magnetic fields (PMF). This impact can lead to changes in the properties of semiconductor crystals [3], including irreversible ones, however, the mechanism of the described changes is not fully understood and does not have an unambiguous description. It seems logical to assume that the magnetic defects present in the crystals should be responsible for the sensitivity of diamagnetic semiconductor crystals to influence of magnetic fields. This work is devoted to the confirmation of this assumption.

CdTe samples grown by the modified Obreimov-Shubnikov method at the FSRC "Crystallography and Photonics" RAS were used as the object of study. The impurity composition and structure of the samples were controlled by mass spectrometry by an iCAP Q ICP-MS (Thermo Scientific), EDX analysis by a JCM 6000 Plus (Jeol), and X-ray phase analysis by a X'PERT Pro MRD (Panalytical). Magnetic hysteresis was recorded by a SQUID MPMS XL (Quantum Design) magnetometer. Changes in the properties of the studied samples were recorded by changing the electrical, thermoelectrical and mechanical characteristics. The electrical and thermoelectrical properties of the samples were studied by two-contact and four-contact methods by a Cresbox (Napson) and by a CTN 300.600.3Omega ("NPK "Spetstechnauka") before exposure to a PMF and, repeatedly in time, after. The samples were subjected for  $t_{\text{exp}}=10$  min to the PMF (amplitude of  $B=1$  T, frequency of  $\nu=12$  Hz).

It was found that the sensitivity of CdTe samples to the action of a PMF directly depends on the magnetic properties, but not of the entire sample, which remains diamagnetic, but of the impurity sublattice. Thus, the magnetic properties of a series of samples CdTe with different impurity compositions were studied. Some of the samples showed ferromagnetic ordering of the impurity sublattice, which is observed not only at 2 K, but also at 300 K. These samples turned out to be the most sensitive to pulsed magnetic action. Possible mechanisms of the observed changes in properties are discussed.

This work was performed within the State assignment of Federal Scientific Research Center "Crystallography and Photonics" of Russian Academy of Sciences.

[1] A. Owens, et al., Nucl. Instrum. Methods Phys. Res. A 531, 18 (2004).

[2] S. Takeda, Ph. D. Thesis, University of Tokyo, Tokyo (2009).

[3] I. Volchkov, et al. JETP Letters, 107, 269 (2018).

## Mechanism of sensitivity of CdTe crystals to pulsed magnetic action

I. Volchkov<sup>a,\*</sup>, M. Pavlyuk<sup>a</sup>, P. Podkur<sup>a</sup>, V. Kvartalov<sup>a</sup>, R. Morgunov<sup>b</sup>, V. Kanevskii<sup>a</sup>

<sup>a</sup> FSRC «Crystallography and Photonics» RAS, Leninskiy Prospekt 59, 119333, Moscow, Russia.

<sup>b</sup> Institute of Problems of Chemical Physics, Russian Academy of Sciences, Chernogolovka, Moscow oblast,  
142432 Russia

\*volch2862@gmail.com

Cadmium telluride CdTe belongs to the class of wide-gap semiconductors and stands out among analogues by a number of properties: the high density (5.85 g/cm<sup>3</sup>) and atomic numbers of the CdTe components (48 and 52, respectively) lead to a high photoelectric absorption coefficient [1]; the high absorption capacity of CdTe makes it a promising material for detectors operating in a wide energy range (from 0.005 to 10 MeV) [2]. As a result, semiconductor materials based on CdTe are of considerable practical interest for the fields of microelectronics, power engineering, and as materials for X-ray detectors. All these application places demand on the production technology of high-quality semiconductor crystals. Obtaining large volumes of perfect crystals is possible either by modernizing the processes of crystal growth, or by various processes of post-growth improvement of the properties. One of these methods is the impact of "weak" ( $\mu_B B \ll kT$ ) static and pulsed magnetic fields (PMF). This impact can lead to changes in the properties of semiconductor crystals [3], including irreversible ones, however, the mechanism of the described changes is not fully understood and does not have an unambiguous description. It seems logical to assume that the magnetic defects present in the crystals should be responsible for the sensitivity of diamagnetic semiconductor crystals to influence of magnetic fields. This work is devoted to the confirmation of this assumption.

CdTe samples grown by the modified Obreimov-Shubnikov method at the FSRC "Crystallography and Photonics" RAS were used as the object of study. The impurity composition and structure of the samples were controlled by mass spectrometry by an iCAP Q ICP-MS (Thermo Scientific), EDX analysis by a JCM 6000 Plus (Jeol), and X-ray phase analysis by a X'PERT Pro MRD (Panalytical). Magnetic hysteresis was recorded by a SQUID MPMS XL (Quantum Design) magnetometer. Changes in the properties of the studied samples were recorded by changing the electrical, thermoelectrical and mechanical characteristics. The electrical and thermoelectrical properties of the samples were studied by two-contact and four-contact methods by a Cresbox (Napson) and by a CTN 300.600.3Omega ("NPK "Spetstechnauka") before exposure to a PMF and, repeatedly in time, after. The samples were subjected for  $t_{\text{exp}}=10$  min to the PMF (amplitude of  $B=1$  T, frequency of  $\nu=12$  Hz).

It was found that the sensitivity of CdTe samples to the action of a PMF directly depends on the magnetic properties, but not of the entire sample, which remains diamagnetic, but of the impurity sublattice. Thus, the magnetic properties of a series of samples CdTe with different impurity compositions were studied. Some of the samples showed ferromagnetic ordering of the impurity sublattice, which is observed not only at 2 K, but also at 300 K. These samples turned out to be the most sensitive to pulsed magnetic action. Possible mechanisms of the observed changes in properties are discussed.

This work was performed within the State assignment of Federal Scientific Research Center "Crystallography and Photonics" of Russian Academy of Sciences.

[1] A. Owens, et al., Nucl. Instrum. Methods Phys. Res. A 531, 18 (2004).

[2] S. Takeda, Ph. D. Thesis, University of Tokyo, Tokyo (2009).

[3] I. Volchkov, et al. JETP Letters, 107, 269 (2018).

# Micromagnetic Approach to Modeling the Output Signal of Thin-Film GMI Sensors of Arbitrary Design

G. Demin<sup>a,\*</sup>, A. Fedina<sup>a</sup>, N. Djuzhev<sup>a</sup>

<sup>a</sup> National Research University of Electronic Technology (MIET), 124498, Shokina sq. 1, Moscow, Russia

\*gddemin@edu.miet.ru

The development of miniature highly sensitive sensors capable of detecting ultra-low magnetic fields (at a level from hundreds of pT to several nT) is an urgent task of modern telemedicine (diagnosis of brain activity, heart rhythms, building neurocomputer interfaces), geology (discovery of new iron ore deposits) and geomagnetic navigation. The giant magneto-impedance (GMI) effect in amorphous ferromagnetic (FM) structures (wires, ribbons, thin films and multilayers), associated with a noticeable (hundreds of percent) change in their complex impedance  $Z = Z(H_{DC}, H_{AC})$  in a constant magnetic field ( $H_{DC}$ ) in the presence of a high-frequency one ( $H_{AC} = H_{AC}(f, t)$ ), provides parameters of GMI sensors suitable for this purpose [1]. Compared to well-studied sensors based on amorphous FM wires and ribbons, the film technology of GMI sensor devices demonstrates record field sensitivity (up to 304%/Oe) and GMI effect (up to 700% and higher), is reproducible and perfectly combined with silicon CMOS technology [2, 3]. Nevertheless, for its further commercialization, it is still necessary to search for the optimal composition of materials and promising design of the thin-film GMI structure, which requires the use of new theoretical approaches that go beyond simple approximations and take into account the specific features of spin dynamics in an inhomogeneous magnetic field for a given technological spread of parameters (shape and thickness) of the layers. To evaluate the characteristics of a thin-film GMI sensor (Figure 1a), we have built a complex theoretical model that combines 3D simulation of time maps of the distribution of the magnetic field  $H_{AC}$  generated by an alternating current in the metal core, micromagnetic calculation of the spin behavior in a FM shell under the total field  $H_{\Sigma} = H_{DC} + H_{AC}$  and the Fourier analysis of the prevailing harmonics of the output pick-up coil signal. On the basis of our model, it is shown that upon transition from parallel to perpendicular orientation of the anisotropy field  $H_{AN}$  (relative to the long side of the FM shell), the amplitude of the main (second) harmonic of the output signal  $V_{C2}$  increases by more than 10 times (Figure 1b).

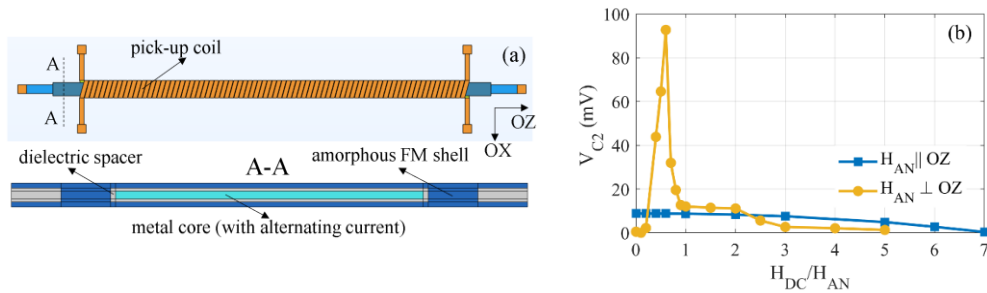


Figure 3. (a) Design of the thin-film GMI sensor. (b) Second harmonic ( $V_{C2}$ ) of the output signal as a function of the magnetic field  $H_{DC}$ .

The maximum  $V_{C2}^{max} \approx 92mV$  in this configuration is achieved at relatively low field  $H_{DC} = 0.6H_{AN}$ , which is consistent with experiment and seems promising for increasing the sensitivity of thin-film GMI sensors at low harmonics. The results obtained can be useful in the development of a new technology of GMI sensor with arbitrary geometry of functional layers. This work was financially supported by the RF Ministry of Science and Higher Education (project No. 075-15-2021-1350).

[1] V.O. Jimenez et al., Biosensors 12(7), 517 (2022)

[2] T. Morikawa et al., IEEE Trans. Magn. 32(5), 4965 (1996)

[3] A. Garcia-Arribas et al., J. Magn. Magn. Mater. 400, 321 (2016)

# Multi-sublattice magnetic structures in charge ordered perovskite manganites with high doping level

L. Gonchar<sup>a,b,\*</sup>

<sup>a</sup> Ural State University of Railway Transport, 620034, Kolmogorova St. 66, Yekaterinburg, Russia

<sup>b</sup> Ural Federal University, 620002, Mira St. 19, Yekaterinburg, Russia

\*l.e.gonchar@yandex.ru

The manganese crystals  $R_{1-x}A_xMnO_3$  (where  $R^{3+}$  is a rare earth ion or  $Bi^{3+}$ ,  $A^{2+}$  is an alkaline earth ion, and  $x$  is a doping level) are investigated as strongly-correlated magnet with  $Mn^{3+}$  Jahn-Teller ions' sublattice. The interrelation between crystal lattice, charge, orbital and magnetic subsystems leads to low-dimensional, incommensurate and frustrated magnetic structures.

The current investigation is devoted to overdoped manganites with  $x=2/3, 3/4, 4/5$  doping levels. The  $Mn^{3+}$  orbital state is described by an angle  $\Theta_i$  of  $^5E$  multielectronic wave functions mixing [5]. The model of Wigner crystal [1–4] describing the crystalline structure considers that charge-orbital ordering consists of  $Mn^{3+}$  ions in  $bc$ -planes (in  $Pnma$  notation) with the same orbital state, that alternate with corresponding amount of  $Mn^{4+}$  (2, 3 or 4) planes in  $a$ -axis direction. Orbital ordering in adjacent  $Mn^{3+}$  planes along  $a$ -direction is described by relation:

$$\Theta_1 \approx 2\pi - \Theta_2 \approx 5\pi/3, \quad (1)$$

where  $\Theta_1$  characterizes one  $bc$ -plane, and  $\Theta_2$  complies with next  $bc$ -plane of  $Mn^{3+}$  ions. The approximate equality in Eq. (1) is used to point the fine difference between certain compounds and their space symmetry ( $Pnma$  [1–3] or  $P2_1/m$  [4]).

The superexchange interaction between nearest-neighboring (nn) manganese ions is dependent upon orbital state of each interacting ion in exchange pair.

$$J_{ij}(\Theta_i, \Theta_j) = \frac{J_{0,k} \cos^2 \varphi_{ij}}{r_{ij}^{10}} F_{ij}(\Theta_i, \Theta_j), \quad (2)$$

where  $\varphi_{ij}$  and  $r_{ij}$  are Mn–O–Mn bond configuration characteristics. The orbitally-dependent functions  $F_{ij}(\Theta_i, \Theta_j)$  can not only scale the value of superexchange interaction, but cause different signs of parameters in some crystallographic directions. The Eq. (2) includes  $Mn^{3+}$ – $Mn^{3+}$ ,  $Mn^{3+}$ – $Mn^{4+}$  and  $Mn^{4+}$ – $Mn^{4+}$  interacting pairs in all directions and with different number of  $\Theta$  variables. It is a numerical model of Goodenough-Kanamory -Andersen rules [5].

Dependences (2) cause non-geometric magnetic frustration in the crystals. The structural elements of magnetic orderings are nn  $Mn^{4+}$ – $Mn^{3+}$ – $Mn^{4+}$  ferromagnetic trimers [5, 7] with magnetic moments, approximately ordered along pseudoperovskite axes  $x_p$  and  $y_p$  or collinear along  $a$  or  $c$  orthorhombic directions. The interjacent  $Mn^{4+}$  layers have competing superexchange interaction with trimers within  $ac$  plane.

The dependences of magnetic structure upon orbital mixing angle  $\Theta$ , upon the amount of intermediate  $Mn^{4+}$  layers and upon ratio of planar AFM parameters are discussed. The possible magnetic structures for  $x=2/3, 3/4, 4/5$  are supposed.

- [1] P.G. Radaell, et al., Phys. Rev. B 59, 14440 (1999)
- [2] D.P. Kozlenko, et al., Phys. Rev. B 82, 014401 (2010)
- [3] S. Grenier et al., Phys. Rev. B 75, 085101 (2007)
- [4] M. Pissas et al., Phys. Rev. B 72, 064426 (2005)
- [5] L.E. Gonchar, J. Magn. Magn. Mater., 513, 167248 (2020)
- [6] J. B. Goodenough, Phys. Rev., 100, 564 (1955)
- [7] L. E. Gonchar, Low Temp. Phys. 48, 37 (2022)

# Multispin interaction Spin Boltzmann machine

I. Lobanov<sup>a,\*</sup>

<sup>a</sup> ITMO University, 191002, Lomonosova St. 9, St. Petersburg, Russia

\*corresponding author email

For decades, spintronics have been considered as the next step in evolution of digital electronics devices, promising the appearance of faster, more compact and energy-efficient devices than existing ones. There are a number of approaches to replacing the standard computer hardware with spintronic devices. For example, logical gates and memory units can be implemented using topological solitons, such as skyrmions, as an information carrier, whose creation and movement are controlled by spin-polarized currents and magnetic fields. On the other hand, the software revolution associated with the rapid progress in artificial intelligence taking place right now, draws the attention of the researchers to neuromorphic devices that mimic organic brain functionality using different physical principles. Several implementations of synapses in the magnetic system have been proposed, including those based on memristors and skyrmions. Such devices are analogs of artificial neural networks, which are the most widely used approach to machine learning (ML) nowadays. Other approaches to ML are possible and may be better suited for hardware other than electric circuits. One of the alternatives is the Boltzmann machine (BM), which is capable of solving classification problems, can be used as an associative memory and so on [1]. However training of large scale BM using electric computers is problematic. On the other hand BM is an information theory abstraction of the Ising model, hence it can be naturally implemented as a magnetic system, e.g. as a spin ice.

In [2] Spin Boltzmann Machine (SBM) was proposed, which is based on the Heisenberg model and hence reproduces magnetic systems more accurately than classic BM. The main feature of SBM is the ability to learn the demonstrated samples internally, without additional electronic devices. For that purpose SBM is augmented with macrospins, which are used to store weights of the ML model. The training is happening naturally due to relaxation, providing an efficient way to minimize the Kullback-Leibler divergence. The approach of [2] allows to optimize biases of BM, but to solve general problems it is necessary to take into account correlations between variables. In the presented work we show that the correlations can be learned by relaxation of SBM, if three or four spin interactions are present. The search for suitable materials is an open problem, however as demonstrated in [3] the multispin interactions can be comparable to conventional Heisenberg exchange in real materials.

We numerically simulated various magnetic systems implementing SBM where individual spins represent units of BM. The interaction between two units is controlled by macrospins via multispin interaction. The SBM dynamics were simulated using the Landau-Lifschitz-Gilbert equation with training samples encoded in the external magnetic field. Simulation is done using a custom code based on a stable semi-implicit integrator taking into account temperature. The performance of the SBM is benchmarked on image classification and reconstruction problems using multiple datasets including MNIST handwritten digits recognition.

The work is supported by the Russian Science Foundation, Project 22-22-00565, <https://rscf.ru/en/project/22-22-00565/>.

[1] G. Li, et al. Scientific Reports 6, 19133 (2016).

[2] I. Lobanov, Nanosystems 13(6), 593 (2022).

[3] M. Hoffmann, S. Blügel, Phys. Rev. B 101, 024418 (2020).

## Non-uniform (heterogeneous) magnetic media

N. Perov

Lomonosov Moscow State University, 119991, Leninskie gory 1-2, Moscow, Russia

\*ya.alekhina@physics.msu.ru

Already at the very first stages of the formation of magnetic materials science, it became obvious that the properties of homogeneous magnetic materials and alloys could not meet the full range of needs for magnetic materials. In accordance with this, in order to explain the behavior of magnetic systems, researchers had to gradually move from the scale of infinite homogeneous magnets (containing more than  $10^{23}$  atoms), first to separate domains ( $10^{12}$  -  $10^{18}$  atoms), then to clusters ( $10^2$  -  $10^3$  atoms). Further studies have shown that critical phenomena are associated with the behavior of local sites, sometimes containing only dozens of atoms. At the same time, it is very significant that the properties of ensembles of such particles are not a simple arithmetic sum of their components: the system has new very interesting behavior features. Various types of heterogeneous materials have been intensively developed especially in recent decades, which was a consequence of the needs primarily of information and computing systems. After composite magnetic materials based on powders, thin films and multi-film structures appeared first, then granular metal-metal and metal-dielectric alloys, amorphous and nanocrystalline magnetic alloys.

A huge role in understanding the properties of inhomogeneous materials was played by the theory of small magnetic particles (MMPs), the foundations of which were laid by Frenkel and Dorfman [1]. This theory predicted at one time such a fundamental phenomenon as the transition to single-domain (Kondorsky [2,3,4], Stoner and Wolfarth [5]). The main role in the theory was played by the processes associated with a decrease in the volume of the particle, without taking into account the influence of its surface. But with a volume of MMH of the order of  $10^{-10}$  cm<sup>3</sup>, one should expect a strong influence of the surface on their magnetic properties (Neel [6]) and the dependence of this influence on the immediate environment of magnetic particles, which is important both in the technologies of preparation of magnetic carriers and ferrofluids, and in understanding the behavior of granular systems and thin films. Questions about inhomogeneities of magnetic structures in small particles, about the influence of the external environment, magnetic field, and temperature on them remain essential. The influence of the asymmetry of the environment of magnetic atoms on the behavior of the magnet is also decisive in the case of thin and multilayer films.

The importance of the tasks associated with the development of new functional magnetic materials, various magnetic nanostructures, semiconductor magnetic materials for spintronics and photonics led to the need for significant development of magnetostatic measurement techniques. Most of the new materials are either ultrathin films, or small volumes of powders, or simply have low magnetization. The purpose of this work is to study the magnetostatic properties of a wide class of new magnetic materials with micro- and nano-scale inhomogeneities.

1. Френкель Я.И., Дорфман Я.Г. Spontaneous and induced magnetization in ferromagnetic bodies// Nature.- 1930.- V.126.- №3173.- P.274-275.
2. Кондорский Е.И. О гистерезисе ферромагнетиков// ЖЭТФ.- 1940.-Т.10.-В.4.-С.420-422.
3. Кондорский Е.И. Однодоменная структура в ферромагнетиках и магнитные свойства мелкодисперсных веществ// ДАН СССР.-1950.-Т.74.- №2.-С.213-216.
4. Кондорский Е.И. Природа высокой коэрцитивной силы мелкодисперсных ферромагнетиков и теория однодоменной структуры// Изв. АН СССР.-1952.-Т16.-С.398-411.
5. Stoner E.G., Wohlfarth E.C. A mechanism of magnetic hysteresis in heterogeneous alloys// Phil.Trans.Royal Soc.-1948.- V.A240.- №26.-P.599-642.
6. Neel L. Les surstructures d'orientation// Compt.Rend.-1953.-V.2J1.- №25.- P.1613-1616.

# Nonlinear Magnetolectric Effect in Flexible Structure Based on PVDF and Magnetostrictive Fiber Composite

D. Savelev<sup>a,\*</sup>, L. Fetisov<sup>a</sup>, D. Chashin<sup>a</sup>, V. Musatov<sup>a</sup>, Y. Fetisov<sup>a</sup>

<sup>a</sup> MIREA – Russian Technological University, 119454, Pr. Vernadskogo 78, Moscow, Russia

\*dimsav94@gmail.com

Magnetolectric (ME) effect manifests itself as a change of polarization in external magnetic field. The effect in composite structures consisting of mechanically bonded piezoelectric (PE) and ferromagnetic (FM) layers arises due to combination of magnetostriction of FM layer and piezoelectricity in PE layer. The highest ME coefficients were obtained in flexible composite structures [1]. One of the most promising magnetostrictive material for flexible composites are magnetostrictive fiber composites (MFC). Such a materials have magnetostriction comparable to that of a plate made of the same material, but they are flexible and biologically inert [2]. In this paper we propose flexible ME structure containing piezoelectric PVDF and magnetostrictive MFC layers. The latter consisted of parallel amorphous microwires immersed in a polymer matrix.

In this work nonlinear ME effect of higher voltage harmonics generation in a flexible composite structure PVDF-MFC was investigated. Piezoelectric and magnetostrictive layers with dimensions  $25 \times 13 \times 0.1 \text{ mm}^3$  and  $20 \times 13 \times 0.1 \text{ mm}^3$ , respectively, were bonded together using cyanoacrylate adhesive. The MFC consisted of amorphous magnetic alloy wires (FeCoSiB, Eliri<sup>®</sup>) arranged parallel and close to each other, coated with glass and immersed in a polymer matrix. Wires had a diameter of  $71 \text{ }\mu\text{m}$ . The structure was fixed at one end and placed in a Helmholtz coils, which generated a magnetic field  $H = 0\text{-}100 \text{ Oe}$ , and excitation coil, creating AC magnetic field  $h \cos(2\pi ft)$  with amplitudes up to  $3 \text{ Oe}$  in frequency range from  $0$  to  $100 \text{ kHz}$ . The frequency spectra of the ME voltage were measured at various values of  $H$  and  $h$ . Based on them, ME voltage dependences of the  $n$  harmonic on the constant and amplitude of the alternating magnetic field were obtained.

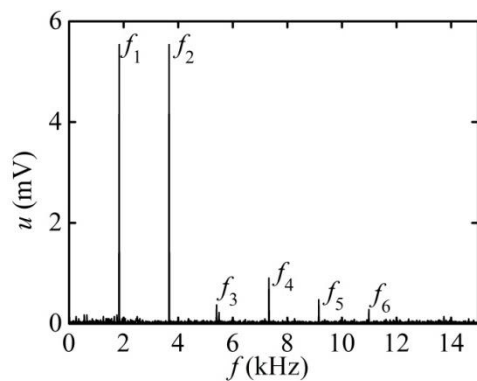


Figure 1 shows the frequency spectrum of the ME voltage generated by the structure upon excitation by a magnetic field with a frequency of  $f_1 = 1.8 \text{ kHz}$  and amplitude  $h = 1.5 \text{ Oe}$  and bias magnetic field  $H = 1 \text{ Oe}$ . The spectrum shows the generation of 6 harmonics. Harmonics were observed at frequencies  $f_n = f_1 \cdot n \text{ kHz}$ ,  $n$  – harmonic number. ME harmonics voltage dependences on amplitudes of the constant and alternating magnetic fields were obtained. The shape of the dependence of the ME voltage of the  $n$  harmonic was determined by the  $n$  derivative of the magnetostriction with respect to the magnetic field.

Figure 1. ME voltage frequency spectrum of the sample in magnetic fields  $H = 1 \text{ Oe}$  and  $h = 1.5 \text{ Oe}$  with frequency  $1.8 \text{ kHz}$ .

University #FSFZ-2023-005).

The research is supported by Ministry of Science and High Education of Russian Federation (State task for the

[1] X. Liang, et al. IEEE. Trans. Mag. 57, 8, 400157 (2021)

[2] L. Fetisov, et al. APL, 119, 25, 252904 (2021)



# Nonlinear Optical Effects Due to Magnetization Dynamics In a Uniform Ferromagnet

E. Karashtin<sup>a,b\*</sup>

<sup>a</sup> Institute for Physics of Microstructures RAS, GSP-105, 603950, Nizhny Novgorod, Russia

<sup>b</sup> University of Nizhny Novgorod, 23 Prospekt Gagarina, 603950, Nizhny Novgorod, Russia

\*eugenk@ipmras.ru

Nonlinear optical effects such as second harmonic generation or rectification attract a lot of attention. On one hand, this is governed by the fact that these effects may exist only in non-centrosymmetric systems. If the medium itself is centrosymmetric the effects appear at the surface which provides a powerful method of studying surface properties. On the other hand, the rectification effects provide mechanisms of generation of THz electromagnetic waves by a femtosecond laser pulse. A particular research direction in this field is devoted to magnetization-induced phenomena in solid state systems containing magnetic materials. For instance, THz sources based on ferromagnet / heavy metal multilayer systems are widely studied [1]. The magnetization vector brings new symmetry properties into such systems [2]. It is known that if a surface of a ferromagnet is irradiated by a p-polarized wave the magnetization-induced double-frequency reflected wave would be s-polarized. However, recently the forbidden p-polarized double-frequency wave was observed in ferromagnet / heavy metal systems such as Co/Pt or Co/Ta multilayers [3-5]. Note that all mentioned nonlinear effects are quite small with the efficiency of the order of  $10^{-6}$  or smaller.

The symmetry consideration [2] does not take into account possible magnetization dynamics due to the electromagnetic wave. Usually it is supposed that the magnitude of such magnetization change is small because the frequency of optical wave is much greater than eigenfrequency of magnetization oscillations. However if a strong femtosecond optical pulse is considered (the electric field of the order of 100kV/cm is realistic) the frequency ratio is of the order of  $10^{-4}$ . Therefore the effects that appear due to magnetization dynamics may be comparable to that provided by static magnetization due non-linearity at the ferromagnet surface. In this work we study such effects. The magnetization dynamics caused by the magnetic field of the wave is investigated in the framework of the Landau-Lifshitz-Gilbert equation solved with the use of the Kapitza pendulum approach (the electromagnetic wave frequency is much greater than the magnetization oscillation eigenfrequency). The Maxwell equations are solved with the assumptions of small gyrotropic term in the dielectric constant and small oscillating magnetization component. We obtain both double frequency electric field and constant electric polarization or electric current (depending on the conductive properties of the ferromagnet) induced by the electromagnetic wave. Finally, a boundary problem is solved. We suppose that the electromagnetic wave is incident at the surface of a ferromagnet magnetized in the meridional geometry. We show that p-polarized incident wave leads to both p- and s-polarized reflected waves at double frequency. The estimations show that the investigated mechanism may explain recent experiments [3-5]. Big effect in a cobalt / heavy metal system may be explained by enhanced dissipation due to spin current from the ferromagnet to the heavy metal. Static polarization and photocurrent are also found. If the system is irradiated by a femtosecond laser pulse this current should follow the pulse envelope and hence lead to the emission of a THz electromagnetic wave.

This work was supported by the Russian Science Foundation (Grant #23-22-00295).

[1] C. Bull, S. M. Hewett, R. Ji et al., *APL Mater.* 9, 090701 (2021).

[2] R. P. Pan, H. D. Wei, and Y. R. Shen, *Phys. Rev. B* 39, 1229 (1989).

[3] T. V. Murzina, I. A. Kolmychek, N. S. Gusev et al., *Optics Express* 29, 2, 2106 (2021).

[4] I. A. Kolmychek, V. V. Radovskaya, K. A. Lazareva et al., *JETP* 130, 4, 555-561 (2020).

[5] T. V. Murzina, V. V. Radovskaya, I. Yu. Pashen'kin et al., *JETP Letters* 111, 6, 333-337 (2020).

# Peculiarities of crystal structure and antiferromagnetic order of ferromagnetic spin-1/2 ladders in $\text{MoOBr}_3$

O.Volkova<sup>a,b\*</sup><sup>b</sup> Lomonosov Moscow State University, 119991, Leninskie gory 1, Moscow, Russia<sup>a</sup> National University of Science and Technology “MISiS”, Moscow 119049, Russia

\*os.volkova@yahoo.com

Molybdenum compounds are often non-magnetic. Its 4d orbitals are more extended in space and better overlapped with ligands than in 3d metals due to a larger principal quantum number [1]. Hereby we present a rare case of magnetism of localized magnetic moments on  $\text{Mo}^{5+}(4d^1)$  ions. The magnetic subsystem of molybdenum oxybromide,  $\text{MoOBr}_3$ , is constituted by orthogonal spin  $S = 1/2$  two-leg ladders running along the  $c$  – axis shown in left panel of Fig. 1. The ladder itself is organized by edge-sharing  $\text{MoBr}_4\text{O}_2$  octahedra on the rung and corner-sharing on the leg. In any given ladder, the Mo atoms are shifted either above ( $+z$ ) or below ( $-z$ ) the basal plane of the Br atoms. In measurements of magnetic susceptibility  $\chi$ , shown in right panel of Fig. 1, and specific heat  $C_p$  the formation of an antiferromagnetic order at  $T_N = 33$  K has been established, while both GGA+ $U$  calculations and Curie-Weiss fitting of the experimental data at elevated temperatures point to the predominance of ferromagnetic exchange interaction. The latter can be attributed to the spin exchange between  $\text{Mo}^{5+}$  ions on the rungs through orthogonal  $p$ -orbitals of the ligand. Reduced effective magnetic moment evidences the unquenched orbital moments anti-aligned with the spins. The work is supported by the megagrant project 075-15-2021-604.

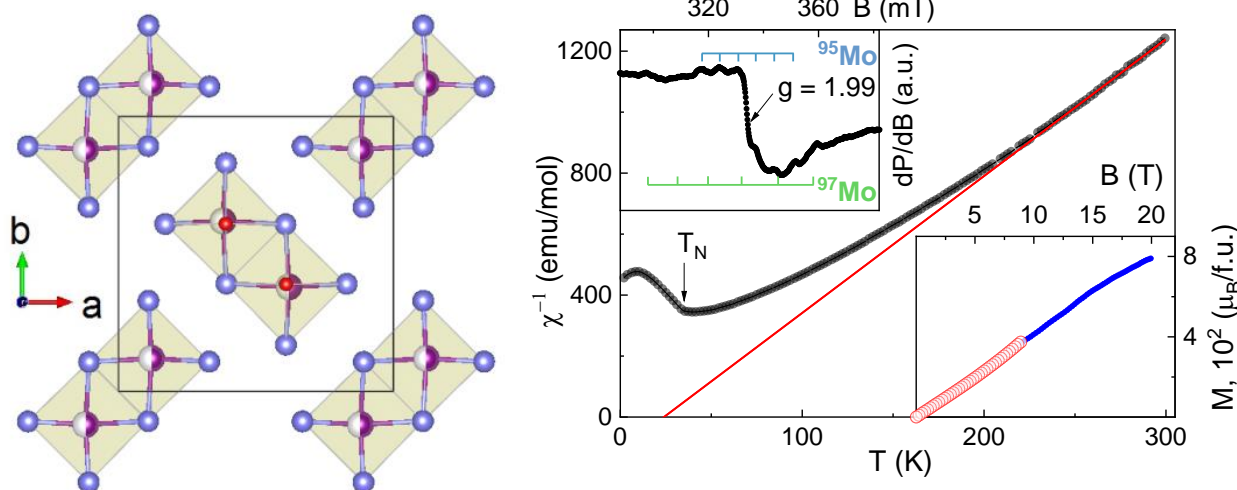


Fig. 1. Left panel: the fragment of crystal structure of  $\text{MoOBr}_3$ . Large spheres are  $\text{Mo}^{5+}$  ions coordinated by four spheres of  $\text{Br}^-$  in the  $ab$  plane and two spheres  $\text{O}^{2-}$  along  $c$  – axis. Right panel: Temperature dependence of inverse magnetic susceptibility  $\chi^{-1}(T)$  of  $\text{MoOBr}_3$  taken in the field cooled regime at  $B = 1$  T. Solid line is the Curie - Weiss fit. Upper inset represents the ESR spectrum taken at 77 K. Lower inset demonstrates the magnetization curves obtained with VSM setup (open circles) and in pulsed magnetic fields (closed circles) at  $T = 2$  K.

[1] Goodenough J B Magnetism and the Chemical Bond (New York: Interscience Publ., 1963).

## Photothermal properties of magnetic nanoparticles

A. Anikin<sup>a,\*</sup>, V. Salnikov<sup>a,b</sup>, V. Khanadeev<sup>c</sup>, C. Sangregorio<sup>d,e</sup>, L. Panina<sup>a,f</sup>, V. Belyaev<sup>a</sup>  
and V. Rodionova<sup>a</sup>

<sup>a</sup> *Immanuel Kant Baltic Federal University, Kaliningrad, Russia*

<sup>b</sup> *Dagestan State University, Makhachkala, Russia*

<sup>c</sup> *Institute of Biochemistry and Physiology of Plants and Microorganisms, Saratov Scientific Centre of the Russian Academy of Sciences, Saratov, Russia*

<sup>d</sup> *Institute of Chemistry of Organometallic Compounds – C.N.R., Sesto Fiorentino, Italy*

<sup>e</sup> *Department of Chemistry ‘Ugo Schiff’ & INSTM, University of Florence, Sesto Fiorentino, Italy*

<sup>f</sup> *National University of Science and Technology «MISIS», Moscow, Russia*

\*anikinanton93@gmail.com

Magnetic nanoparticles (MNPs) are frequently studying materials in the scope of their prospective use in cancer treatments. Small (5÷20 nm) spherical MNPs found their application in local magnetic hyperthermia [1], while larger MNPs of various shapes could be used in magnetomechanical therapy [2]. Gold can be incorporated with MNPs in the form of composite consisting either of magnetic core with gold coating or gold core with magnetic coating. Gold coating provides better biocompatibility and chemical stability. With gold inclusion, nanoparticles have significant optical absorption, which also makes composites suitable for use in photothermal therapy [3]. Photothermal therapy is another local hyperthermia treatment; it involves the heating of nanoparticles by absorbing the light, which results in irreversible changes in cells, leading to their death. The material, size and shape of nanoparticles determine their absorption spectra and the photothermal performance. Photothermal therapy typically uses an optical range around 800 nm, at which pure MNPs do not have descent absorption. The combination of several treatments with a single composite made of gold and magnetic material will increase the therapy effectiveness without the use of high nanoparticles concentrations and high exposures intensities, that should reduce the side effects.

This work is devoted to discussion of prospects for use of the MNPs with and without gold inclusion in treatments combined with photothermal therapy. Optical absorption and photothermal study of aqueous solutions nanoparticles having various shapes and sizes were performed. Photothermal studies were carried out with a setup consisting of a laser with a wavelength of 815 nm, an infrared camera, and a photodiode. In addition, an AC magnetic field was used for unstable aqueous solutions of larger-sized MNPs to prevent them from sedimentation during the experiments. The following samples were used: spherical Fe<sub>3</sub>O<sub>4</sub> nanoparticles (diameter 8 nm); spherical CoFe<sub>2</sub>O<sub>4</sub> nanoparticles (diameters 15 and 20-25 nm); iron microdiscs (thickness up to 150 nm, diameter up to 1 µm) with gold coating; nickel microtubes (outer diameter 500 nm, length up to 10 µm) with/without gold coating. Gold nanostars (synthesized in Nanobiotechnology laboratory of IBPPM RAS; core diameter 50 nm, cones length 19 nm) were used for comparison.

The results show a strong spread in photothermal performance depending on the MNPs morphology. Pure MNPs solutions exhibit moderate heating limited by several degrees depending on the system. However, as expected the gold incorporated nanoparticles show 3-5 times higher degree of heating at the same concentrations. Gold nanostars have the highest measured values of photothermal efficiency and optical absorption. The comparison study and analysis of the different systems would be given.

This work has been supported by the Russian Science Foundation grant, RSF 21-72-20158.

[1] Xiaoli Liu et al., *Theranostics*, **10**(8), 3793 (2020)

[2] Cécile Naud et al., *Nanoscale Adv.*, **2**, 3632 (2020)

[3] Moustafa R. K. Ali et al., *J. Phys. Chem. C*, **123**, 15375 (2019)

## Potential agent for photothermal therapy based on Gold/Cobalt Ferrite Nanocomposite

S. Pshenichnikov<sup>a</sup>, A. Motorzhina<sup>a</sup>, A. Anikin<sup>a</sup>, V. Belyaev<sup>a</sup>, L. Litvinova<sup>b</sup>, S. Jovanović<sup>c,d</sup>, L. Panina<sup>a,e</sup>, V. Rodionova<sup>a</sup>, K. Levada<sup>a,\*</sup>

<sup>a</sup> Research & Education Center "Smart Materials & Biomedical Applications", Immanuel Kant Baltic Federal University, Kaliningrad, Russia.

<sup>b</sup> Center for Immunology and Cellular Biotechnology, Immanuel Kant Baltic Federal University, Kaliningrad, Russia.

<sup>c</sup> Department of Physics, Vinča Institute of Nuclear Sciences – National Institute of the Republic of Serbia, University of Belgrade, Belgrade, Serbia.

<sup>d</sup> Advanced Materials Department, Jožef Stefan Institute, Ljubljana, Slovenia.

<sup>e</sup> National University of Science and Technology «MISIS», Moscow, Russia

\* corresponding author email: kateryna.levada@gmail.com

Nanocomposites are prospective instruments for biomedical applications, due to opportunity to combine wide range of physical and structural characteristics. In current research we propose the nanocomposite (CNP, Fig. 1 A) based on gold nanoparticles (AuNP) surrounded by cobalt ferrite nanoparticles (CFO), as potential tool for the photothermal therapy (PTT). AuNP and CFO were covered with arginine and DHCA, respectively, to increase the biocompatibility. CNP synthesis techniques represented in publications [1,2]. CNP structure was characterized using TEM (Fig. 1 B). Dark spherical AuNP demonstrate size distribution between 10 and 20 nm. Average size of CFO is 5 nm. CNP potential for PTT was analyzed using laser heating setup. Suspensions of CNP were affected by 815 nm laser at 0.6 W output optical power for 15 min. Solutions containing CNP of different concentrations demonstrated overheating in comparison with controls solutions without CNP (data not shown). On the next step PTT was performed on human hepatocarcinoma cell line (Huh7). Cell viability were analyzed using WST-1 viability assay. After 15 min cell viability was greatly decreased in comparison with control cells and cells, treated only with CNP. The results demonstrate the high potential of CNP as an instrument for induction cytotoxic effects during PTT. Further optimization of CNP characteristics and modification of PTT techniques will provide opportunities to develop novel PTT methods of cell death induction in tumor cells.

This research was funded by RSF, grant number 21-72-20158.

[1] A. Motorzhina, et al., Processes 9, 1 (2021).

[2] A. V. Motorzhina, et al., Nanobiotechnology Reports 17, 436 (2022).

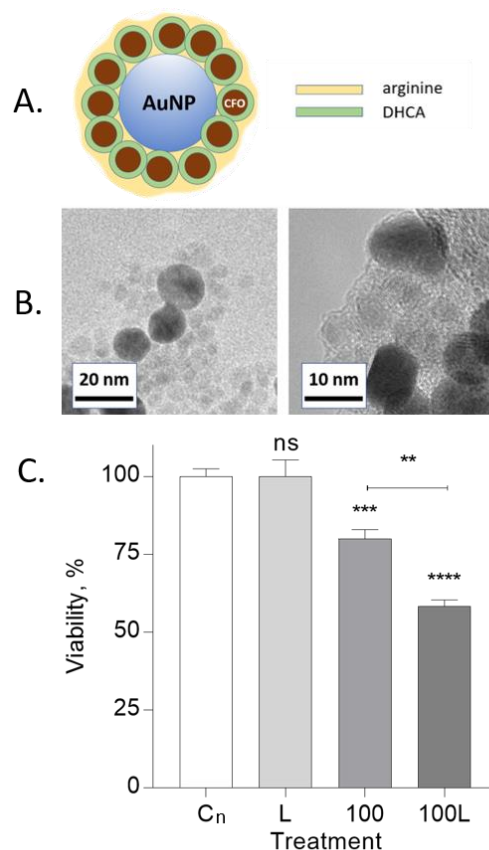


Fig. 1. CNP for photothermal therapy. A – CNP structure, B – TEM images of CNP, C – viability of Huh7 cells after application of infrared irradiation (L), 100 µg/ml CNP treatment (100) and PTT treatment (100L). C<sub>n</sub> – control cells.

## Relaxation in the Jahn-Teller Subsystem in Magnetic Field

V. Gudkov<sup>a,\*</sup>, N. Averkiev<sup>b</sup>, M. Sarychev<sup>a</sup>, I. Zhevstovskikh<sup>c</sup>, Yu. Korostelin<sup>d</sup>

<sup>a</sup> Ural Federal University, 620002, Mira st. 19, Ekaterinburg, Russia

<sup>b</sup> Ioffe Institute, RAS, 194021, Politekhnikeskaya st. 26, St. Petersburg, Russia

<sup>c</sup> M.N. Mikheev Institute of Metal Physics, UB RAS, 620137, S. Kovalevskaya st. 18, Ekaterinburg, Russia

<sup>d</sup> P.N. Lebedev Physical Institute, RAS, 119991, Leninsky Avenue 53, Moscow, Russia

\*v.v.gudkov@urfu.ru

Ultrasonic methods of investigation are very informative when physical properties of solids are studied. With regard to the diluted magnetic crystals, they proved their efficiency in investigation of the Jahn-Teller (JT) effect (JTE) manifestation. The first specificity of this manifestation is relaxation origin of the temperature anomalies in attenuation and phase velocity of ultrasonic waves [1] in contrast to optical or magnetic resonance experiments. The second one follows from the first: the physical acoustics methods deliver information about the lowest energy ground state of the JT complex provided that the experiments are carried out at low temperatures. Ultrasonic techniques make it possible to determine the static [adiabatic potential energy surface (APES)] and dynamic (relaxation mechanisms) properties of the JT complex which consists of the ion with the orbital degenerate ground states and the nearest neighbors. Such complexes form the JT subsystem of a crystal which macroscopic properties, the elastic moduli and relaxation time can be investigated as function of an external parameter (temperature  $T$ , magnetic induction  $\mathbf{B}$ ). The zinc selenide crystal (sphalerite structure) doped with  $\text{Cr}^{2+}$  ions is one of the most well studied examples in this field. First experiments are dated with 2006 [2] and the latest with 2023 [3]. The  $\text{Cr}^{2+}$  ion in tetrahedral coordination has  ${}^5T_2(e^2t^2)$  high-spin ground term and subject to the  $T \otimes e + t_2$  JTE problem with the tetragonal global minima of the APES. First attempt to determine the magnetic field relaxation time was made with the assumption of two relaxation mechanisms at low temperatures: thermal and magnetic relaxations with two relaxation velocities,  $\tau_T^{-1}$  and  $\tau_B^{-1}$ , respectively[4]. Such approach does not indicate the magnetic field dependence of the relaxed modulus which is required for unambiguous determination of the relaxation time magnetic-field dependence from the experimental data. In [3], the explicit expressions for the relaxed moduli were obtained. The expressions were derived with account of the spin Hamiltonian which was used for interpretation the results of optical [5] and ESR [6] experiments. In  $\text{ZnSe:Cr}^{2+}$  crystal, the JTE manifests itself in the tetragonal mode associated with the modulus  $c_E = (c_{11} - c_{12})/2$ . This mode propagates along the [110] crystallographic axis and is polarized in the [-110] direction. Two cases were considered:  $\mathbf{B} \parallel [110]$  and  $\mathbf{B} \parallel [001]$ . The explicit form of the relaxed moduli which in the discussed case are the moduli defined at constant  $T$  and  $\mathbf{B}$  made it possible to construct the expression which was used for unambiguous determination of the relaxation time dependence on the magnetic induction from the experimental data on ultrasonic attenuation and phase velocity. The experiments that provided these data were done at the High Magnetic Field Laboratory (Dresden-Rossendorf, Germany) in magnetic fields up to 17 T at 1.3 – 100 K. The frequency used was in the range of 29 – 57 MHz.

Support by the Russian Science Foundation (project № 22-22-00735) is acknowledged.

- [1] M.D. Sturge, J.T. Krause, E.M. Gyorgy, *et al.*, Phys. Rev. 155, 218 (1967)
- [2] V.V. Gudkov, A.T. Lonchakov, V.I. Sokolov, *et al.*, Phys. Rev. B 73, 035213 (2006)
- [3] M.N. Sarychev, I.V. Zhevstovskikh, Yu.V. Korostelin, *et al.*, JETP 136, 803 (2023)
- [4] V.V. Gudkov, I.B. Bersuker, I.V. Zhevstovskikh, *et al.*, Phys. Status Solidi A 73, 1800586 (2018)
- [5] J.T. Vallin, G.A. Slack, S. Roberts, *et al.*, Phys. Rev. B 2, 4313 (1970)
- [6] J.T. Vallin, G.D. Watkins, Phys. Rev. B 9, 2051 (1974)

# Simulation of Magnetic Properties of Different Types of Spin-Valve Nanostructures

E. Drovorub<sup>a,\*</sup>, P. Prudnikov<sup>b</sup>, V. Prudnikov<sup>a</sup>

<sup>a</sup> Dostoevsky Omsk State University, 644077, Mira 55a, Omsk, Russia

<sup>b</sup> Centre of New Chemical Technologies of IC SibBr RAN, 644040, Neftezhavodskaya 54, Omsk, Russia

\*drovorub.egor@gmail.com

The creation of spin-valve systems, which consist of magnetic layers divided by nonmagnetic metal layers, is a great improvement in structures that experience the GMR effect. However, the direction of magnetization in one ferromagnetic layer is pinned by its interaction with an additional antiferromagnetic layer. To reduce exchange coupling between magnetic layers, a nonmagnetic intermediate conductor made thick enough for the orientation of magnetization in a layer not coupled with an antiferromagnetic layer to change freely under the influence of a weak external magnetic field. An advantage of the spin-valve structures are fields of saturation ( $H_s = 5\text{--}50$  Oe) much smaller than in multilayered magnetic structures. This property of spin valves makes their technical use quite promising and, at present time, these structures have found wide application in, e.g., read heads of HDDs with data densities of more than 100 gigabytes per square inch. A variety of more complicated spin-valve structures have been designed [1] that contain a three-layered antiferromagnetic system Co/Ru/Co in addition to the usual valve presented in [2]. This system magnifies the effect antiferromagnetic layer has on a freely magnetizing ferromagnetic layer. Another spin-valve structure, which has a practical interest, is classified as dual symmetrical one [3]. The aim of this study is to Monte Carlo simulate behavior and magnetic properties of these three types of spin-valve structures and identify the effect magnetic anisotropy and intra- and interlayer exchange interaction on hysteresis phenomena in a spin valve upon varying the thickness of nanosized ferromagnetic films.

An anisotropic Heisenberg model [4] described by the Hamiltonian

$$H = - \sum_{\langle i,j \rangle} J_{ij} \{ S_i^x S_j^x + 0.8 S_i^y S_j^y + (1 - \Delta(N)) S_i^z S_j^z \} - h \sum_i S_i^x \quad (1)$$

is used for Monte Carlo methods description of magnetic properties of thin films comprising these structures. In (1),  $S_i = (S_i^x, S_i^y, S_i^z)$  is the classical three-dimensional unit vector of a spin fixed in the  $i$ -th center of the FCC lattice of a ferromagnetic cobalt films, and  $\Delta(N)$  are parameters of the effect anisotropy caused by the crystalline field of the substrate has on the magnetic properties of a film consisting of  $N$  monolayers. Parameter  $\Delta(N)$  describes easy-plane anisotropy [4], which allowed us to consider magnetization in the film plane. The dependence of the magnetic characteristics of the films on temperature and external magnetic field was obtained. The effect the magnetic film thickness, temperature, and intra- and interlayer exchange interaction had on the hysteresis effects was investigated. Factors were revealed that facilitated the stable giant magnetoresistance effect in the structures. Our dependences of the magnetic characteristics of the films and spin-valve structures are in good agreement with results from experimental studies.

Present study is supported by Russian Science Foundation, project no. 23-22-00093.

- [1] C.H. Marrows, F.F. Stanley, B.J. Hickey, J. Appl. Phys. 87, 5058 (2000)
- [2] B. Dieny, V.S. Speriosu, S.S.P. Parkin, et al. Phys. Rev. B, 1991, 43, 1297 (1991)
- [3] K. Shimazawa, Y. Tsuchiya, K. Inage, et.al. IEEE Trans. Magn. 42, 120 (2006)
- [4] P. Prudnikov, V. Prudnikov, M. Mamonova, N. Piskunova. JMMM. 482, 201 (2019)

# Skyrmion lattices phase driven by interfacial-engineered Dzyaloshinskii-Moriya interaction in frustrated antiferromagnetic/ferroelectric bilayers

S. Ildus, Y. Alina, A. Danil and B. Aliya

Ufa University of Science and Technology

Russia, Republic of Bashkortostan, Ufa, Zaki Validy,32

Sharafullinif@yandex.ru

In the last few decades, nonuniform spin structures, such as skyrmions in nanofilms with magnetic or ferroelectric long-range ordering or systems with both types of ordering has become a central focus of condensed matter physics [1-3]. Magnetic skyrmion is a topologically nontrivial local spin texture that forms at low temperature (in special cases at zero temperature) from competition among exchange interactions, exchange frustrations and external fields. On the one hand, skyrmions can be used to store, transmit, and manipulate information with high efficiency in terms of energy consumption due to their topologically protected textures [2]. On the other hand, magnetic skyrmions form lattices in antiferromagnetic, synthetic antiferromagnetic and compensated ferrimagnetic materials – it represents an exciting state of matter[3,4]

We study properties of a skyrmion lattices, phase diagrams and conditions of their stability in a multiferroic bilayer with Heisenberg spin model by using Monte Carlo simulation and steepest descent method. Ground state spin configuration in an interface between overfrustrated antiferromagnetic layer and ferroelectric layer is calculated by minimizing the spin interaction energy. It is shown that the angles between spins near the surface are strongly modified with respect to the bulk configuration. Taking into account magnetoelectric interface interaction between ferroelectric and antiferromagnetic layer and weak in-plane Dzyaloshinskii – Moriya interaction in this frustrated magnetic layer, we calculate the energy and the order parameters and layer magnetizations as functions of temperature up to the two different disordered phases.

The dependence of order parameters versus temperature shows the existence of stable skyrmion lattice branch which causes a low surface magnetization. We show that magnetoelectric interaction give rise to a stable phase of skyrmion lattices at zero temperatures and can stabilize skyrmions in antiferromagnetic layer at zero external field ant spin-polarisation current at low temperatures. We calculate the transition temperature and show that it depends strongly on the magnetoelectric coupling. Results are in agreement with existing experimental observations on the stability of skyrmion structure in thin films and on the insensitivity of the transition temperature with the film thickness. We also study effects of various parameters such as surface exchange and anisotropy interactions.

## References

1. Diep, Hung T. Theory of magnetism. World Scientific, Singapore, 2014
2. Shaikhulov, T.A., Safin, A.R., Stankevich, K.L., Matasov, A.V., Temiryazeva, M.P., Vinnik, D.A., Zhivulin, V.E. and Nikitov, S.A., Magnetic Properties of SrMnO<sub>3</sub>/La<sub>0.7</sub>Sr<sub>0.3</sub>MnO<sub>3</sub> Heterostructure on NdGaO<sub>3</sub> Substrate. JETP Letters, (2023)pp.1-6.
3. El Hog, S., Sharafullin, I.F., Diep, H.T., Garbouj, H., Debbichi, M. and Said, M., 2022. Frustrated antiferromagnetic triangular lattice with Dzyaloshinskii–Moriya interaction: Ground states, spin waves, skyrmion crystal, phase transition. Journal of Magnetism and Magnetic Materials, (2023), 563, p.169920.
4. Zhang, X., J. Xia, Tretiakov OA, G. Zhao, J. Yang, Y. Zhou, M. Ezawa, and X. Liu. "Current-Induced Helicity Switching of Frustrated Skyrmions on a Square-Grid Obstacle Pattern." Journal of the Magnetism Society of Japan 47, no. 1 (2023): 20-27.

## **Spin accumulation, anomalous Hall and spin-Hall effects in two-layer magnetic system**

M. Zhuravlev<sup>a</sup>, A. Vedyayev<sup>b</sup>, A. Alexandrov<sup>c</sup>

<sup>a</sup>*Saint Petersburg State University, Saint Petersburg, 199034, Russia*

<sup>b</sup>*Lomonosov Moscow State University, Moscow 119991, Russia*

<sup>c</sup>*Moscow Institute of Physics and Technology, Dolgoprudny, 141700, Russia*

Spin accumulation, anomalous Hall and spin-Hall effects are the phenomena which take place in magnetic tunnel junctions. Usually, the main current flows perpendicularly to the interfaces in such systems. We demonstrate that similar effects occur in two-layer system when the current flows parallelly to the interface. The system consists of a semi-infinite ferroelectric barrier and a thin ferromagnetic layer. We assume that Dresselhaus and Rashba spin-orbit coupling is linear in electron wave number in ferroelectric barrier. Such spin-orbit coupling can be found in ferroelectric materials of the  $C_{2v}$  point group. E.g.,  $HfO_2$  is one of such compounds. We demonstrate that planar Hall effect takes place in this two-layer system. We discuss the origin of this planar Hall effect and demonstrate that this is a size effect. Also, we describe spin accumulation (a kind of Edelstein effect) and spin-Hall effect in this two-layer system. The charge and spin Hall currents in such system can be manipulated in several ways. In particular, it is shown that spin accumulation and spin current can be reversed by changing the direction of the magnetization of the FM layer with respect to the crystallographic axes of the ferroelectric barrier. We estimate the current and magnetization for reasonable parameters.

Besides, we analyze the possibility of the appearance not only of spin accumulation, but also the appearance of Hall current in a non-magnetic system with spin-orbit coupling.



# Spin wave beam formation and focusing in magnonic 2d stripe lattice

A. Khutieva<sup>a,\*</sup>, A. Sadovnikov<sup>a</sup>

<sup>a</sup> Saratov State University, 410012, Astrakhanskaya 83, Saratov, Russia

\*abkhutieva@gmail.com

The study of wave processes in magnetic materials has been one of the most important areas of condensed matter physics and spin-wave electronics since the prediction of the existence of magnons and their collective excitation – magnetostatic spin waves (MSWs) [1]. Along with the development of the theory of ferrites, progress in the technological processes of manufacturing thin magnetic films has made it possible to design and create micro- and nanostructured surfaces [2]. Of great interest is the study of the characteristics and methods of controlling linear and nonlinear spin-wave transport in various micro- and nanoscale magnetic waveguide systems, since magnetic oscillations in such structures can be excited at frequencies from the megahertz to terahertz range with a length spin wave from units of millimeters to tens of nanometers.

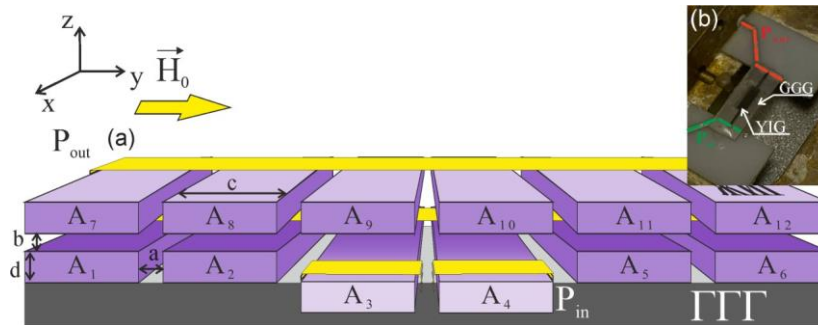


**Figure 1** Scheme of the examined system of the coupled magnetic microwaveguides

In this work, we have demonstrated the features of MSW propagation in a three-dimensional structure consisting of magnetic films of yttrium iron garnet (YIG). One of the key problems in the creation of spin-wave devices is associated with the decay of MSWs. The magnetic dielectric, YIG, has the lowest dynamic attenuation, which makes it possible to have an MSW propagation length sufficient to create various magnonic devices. Figure 1a shows a schematic representation of the structure magnetic microwaveguides. Figure 1b shows an experimental layout. A study was carried out using the method of Mandelstam-Brillouin spectroscopy of light of linear and nonlinear spin-wave transport in the waveguide structure. To determine the range of parameters in the experimental study (the geometric dimensions of the microwave guides, the magnitude and direction of the magnetic field), micromagnetic modeling was carried out based on the solution of the equation of magnetization dynamics in the case of a small signal (linear mode) and with an increase in the input signal level (nonlinear mode). The results of the study showed the possibility of transmission of the spin-wave mode in the region of translational symmetry breaking both in the lateral and vertical directions. The proposed structure of a three-dimensional magnetic micro-waveguide can serve as a functional unit in multilayer integrated magnon networks. Improvement in technologies for the formation of ferromagnetic thin films suggests the possibility of integrating ferrite devices into standard devices based on CMOS technologies, as unique flat versions of compact microwave guides with low losses and low cost.

The work is supported by Russian Science Foundation (Project No. 23-79-30027).

[1] S.A. Nikitov, Phys. Usp. 63, 945 (2020)

[2] A.V. Sadovnikov, Phys. Rev. B 99, 054424 (2019)

## Spin waves dispersion in amorphous ferromagnets: small-angle polarized neutron scattering study

S. Grigoriev<sup>1,2</sup>, L. Azarova<sup>1,2</sup>, K. Pshenichniy<sup>2</sup> and O. Utesov<sup>1,2</sup>

<sup>1</sup> Saint Petersburg State University, Ulyanovskaya str. 1, Saint Petersburg, 198504, Russian Federation

<sup>2</sup> Petersburg Nuclear Physics Institute, NRC «Kurchatov Institute», Gatchina, 188300, Russian Federation

We show that the spin wave dispersion of amorphous ferromagnets in the magnetic field is described by the expression:  $\varepsilon(q) = Aq^2 + g\mu_B H + \delta\omega(q)$ , where  $\delta\omega(q)$  is an linear on  $|q|$  additive coming from the random anisotropy [1]. We use the method of small-angle polarized neutron scattering to determine the value of the spin-wave stiffness  $A$  at the quadratic term and to prove the significance of the  $\delta\omega(q)$  - term in dispersion. The measurements were performed with amorphous ferromagnetic compound 40Fe40Ni14P6B at different values of an external magnetic field  $H$  and neutron wavelength  $\lambda$ . The neutron scattering image displays a circle with a certain radius centred at  $q = 0$ . The spin-wave stiffness  $A$  is directly extracted from the  $\lambda$ -dependence of the radius of this circle. The field dependence of the radius reveals presence of the additive  $\delta\omega(q)$  as an energy "gap" with a very characteristic field dependence. We show that the spin-wave stiffness  $A$  of the amorphous alloy increases upon lowering temperature. The additive coming from the random anisotropy increases as well with temperature in the range from 50 to 300 K.

[1] V. A. Ignatchenko and R. S. Iskhakov, Zh. Eksp. Teor. Fiz. 72, 1005 (1977) [Sov. Phys. JETP 45, 526 (1977)].

# Star-shaped Au@Fe<sub>3</sub>O<sub>4</sub> nanoparticles for photothermal therapy

S. Pshenichnikov<sup>a,\*</sup>, A. Motorzhina<sup>a</sup>, A. Anikin<sup>a</sup>, V. Belyaev<sup>a</sup>, M. Albino<sup>b,c</sup>, L. Panina<sup>a,d</sup>, V. Rodionova<sup>a</sup>, C. Sangregorio<sup>b,c</sup>, K. Levada<sup>a</sup>

<sup>a</sup> Research & Education Center "Smart Materials & Biomedical Applications", Immanuel Kant Baltic Federal University, Kaliningrad, Russia.

<sup>b</sup> Institute of Chemistry of Organometallic Compounds – C.N.R, Sesto Fiorentino, Italy

<sup>c</sup> Department of Chemistry 'Ugo Schiff' & INSTM, University of Florence, Sesto Fiorentino, Italy

<sup>d</sup> National University of Science and Technology «MISIS», Moscow, Russia

\* corresponding author email: spshnikov@gmail.com

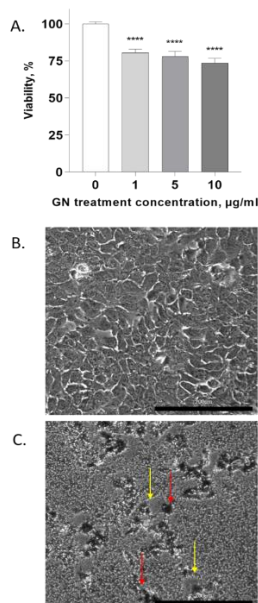


Fig. 1. GN induce cytotoxic effects in Huh7 cells. A. – viability of tumor cells after 24 h treatment with GN, B. – controls cells, C. – morphology of Huh7 was dramatically changed after 24 h treatment with 100 µg/ml GN. Red and yellow lines – show GN agglomerates and cells, accordingly.

Multifunctional nanomaterials offer promising prospects for the development of innovative cancer therapies. Photothermal therapies utilizing nanoparticles can be enhanced by employing nanosized hybrid materials, that exhibit plasmonic effects and high magnetic susceptibility. Here we propose star-shaped Au@Fe<sub>3</sub>O<sub>4</sub> nanoparticles (GN) as an instrument for anticancer photothermal therapy (PTT). GN synthesis and physical characterization were previously reported [1]. GN used in current research demonstrate highly uniform star-like morphology. GN biocompatibility was analyzed using WST-1 cytotoxicity assay. GN decreased viability of human hepatocarcinoma cell line (Huh7) after 24h treatment (Fig 1. A). Additionally, Huh7 cell morphology was analyzed using the Cell-IQ® v2 MLF integrated platform. Morphology of Huh7 cells was changed after 24h 100 µg/ml GN (Fig 1. C) in comparison with control cells (Fig 1. B). On next step, GN efficiency for PTT treatment was evaluated using laser heating setup, based on ThorLabs L808P500MM laser diode. Infrared laser irradiation (at 0.6 W output optical power and 815 nm wavelength) was applied to GN suspensions. After 15 min suspensions of GN with concentrations 25, 10 and 5 µg/ml were overheated up to 34, 30 and 27 °C (data not shown) in comparison with 25.5 °C in control solutions of nutrient medium. The results demonstrate the high potential of GN as the instrument for PTT. In further experiments biocompatibility of GN should be optimized to decrease the potential side effects during the PTT.

This research was funded by RSF, grant number 21-72-20158.

[1] B. Muzzi, et al., ACS Applied Materials and Interfaces 14, 29087 (2022).

# Stripe-induced Anisotropy of the Hall Effect in the Paramagnetic Phase of $\text{Ho}_{0.8}\text{Lu}_{0.2}\text{B}_{12}$

A. Khoroshilov<sup>a</sup>, K. Krasikov<sup>a</sup>, A. Azarevich<sup>a</sup>, A. Bogach<sup>a</sup>, V. Glushkov<sup>a</sup>,  
N. Shitsevalova<sup>b</sup>, V. Filipov<sup>b</sup>, S. Gabáni<sup>c</sup>, K. Flachbart<sup>c</sup>, N. Sluchanko<sup>a,\*</sup>

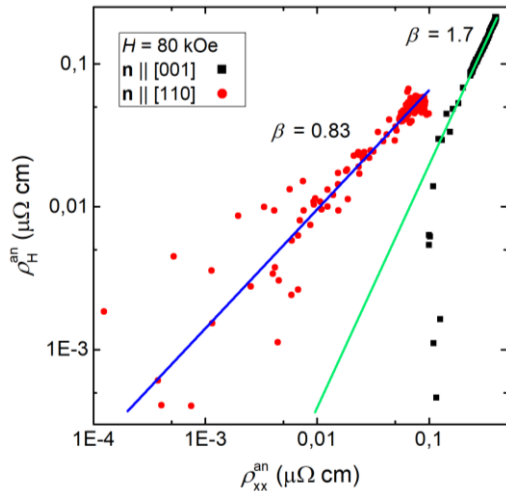
<sup>a</sup> Prokhorov General Physics Institute of RAS, 119991, Vavilova 38, Moscow, Russia

<sup>b</sup> Frantsevich Institute for Problems of Materials Science, NASU, 3142, Krzhizhanovskogo 3, Kyiv, Ukraine

<sup>c</sup> Institute of Experimental Physics SAS, 04001, Watsosnova 47, Košice, Slovakia  
\*nes@lt.gpi.ru

A detailed study of charge transport in the paramagnetic phase of the antiferromagnet  $\text{Ho}_{0.8}\text{Lu}_{0.2}\text{B}_{12}$  with an instability both of the *fcc* lattice (cooperative Jahn-Teller effect) and the electronic structure (dynamic charge stripes) was carried out at temperatures 1.9–300 K in magnetic fields up to 80 kOe [1]. Four mono-domain single crystals of  $\text{Ho}_{0.8}\text{Lu}_{0.2}\text{B}_{12}$  samples with different crystal axis orientation were investigated in order to establish the singularities of anomalous Hall effect (AHE), which develop due to (i) the electronic phase separation (stripes) and (ii) formation of the disordered cage-glass state below  $T^* \sim 60$  K. It was demonstrated that a considerable intrinsic anisotropic positive component  $\rho_{xy}^{\text{an}}$  appears at low temperatures in addition to the ordinary negative Hall resistivity contribution in magnetic fields above 40 kOe applied along the [001] and [110] axes.

A relation between anomalous components of the resistivity tensor  $\rho_{xy}^{\text{an}} \sim \rho_{xx}^{\text{an} 1.7}$  was found for  $\mathbf{H} \parallel [001]$  below  $T^* \sim 60$  K, and a power law  $\rho_{xy}^{\text{an}} \sim \rho_{xx}^{\text{an} 0.83}$  for the orientation  $\mathbf{H} \parallel [110]$  at temperatures  $T < T_S \sim 15$  K (Figure 1). It is argued that below characteristic temperature  $T_S \sim 15$  K the anomalous odd  $\rho_{xy}^{\text{an}}(T)$  and even  $\rho_{xx}^{\text{an}}(T)$  parts of the resistivity tensor may be interpreted in terms of



formation of long chains in the filamentary structure of fluctuating charges (stripes). We assume that these  $\rho_{xy}^{\text{an}}(\mathbf{H} \parallel [001])$  and  $\rho_{xy}^{\text{an}}(\mathbf{H} \parallel [110])$  components represent the intrinsic (Berry phase contribution) and extrinsic (skew scattering) mechanism, respectively. Apart from them, an additional ferromagnetic contribution to both isotropic and anisotropic components in Hall signal was registered and attributed to the effect of magnetic polarization of *5d* states (ferromagnetic nano-domains) in the conduction band of  $\text{Ho}_{0.8}\text{Lu}_{0.2}\text{B}_{12}$ .

The study was supported by RSF Project No. 22-22-00243.

Figure 1. Anisotropic AHE components for  $\mathbf{H} \parallel [001]$  and  $\mathbf{H} \parallel [110]$  in magnetic field  $H = 80$  kOe scaled in double logarithmic plot. Solid lines display the linear approximations and  $\beta$  denotes exponent

[1] A.L. Khoroshilov et al., *Molecules* 28, 676 (2023)

## Study of the magnetoelectric response of PVDF-based composite films

A. Ignatov<sup>a\*</sup>, Yu. Raikher<sup>b,a</sup>, O. Stolbov<sup>b,a</sup> and V. Rodionova<sup>a</sup>

<sup>a</sup> Immanuel Kant Baltic Federal University, Kaliningrad 236004, Russia

<sup>b</sup> Institute of Continuous Media Mechanics, Russian Academy of Sciences, Ural Branch, Perm 614018, Russia

\*artem.ignatov98@gmail.com

Magnetoelectric composites are capable of producing a direct magnetoelectric effect (electric polarization under the influence of a magnetic field) as well as the inverse one (to change the magnetization in response to an applied electric field). In composites, this effect is a consequence of the mechanical interaction of the ferromagnetic and piezoelectric phases. Such materials have advantages over single-phase magnetoelectrics: an order of magnitude greater magnitude of the magnetoelectric effect [1] and the ability to vary the composition of the phases, and, consequently, to select the properties of the composite in accordance with the conditions of use of the material. The large magnitude of the magnetoelectric effect makes it possible to use such composites as sensitive elements of magnetic or electric field sensors [2, 3], energy harvesting devices [3], and the possibility of varying the phases makes it possible to select, for example, biocompatible components for designing smart supports for tissue engineering [4] etc.

A "smart scaffold" capable of inducing surface charges in response to an applied magnetic field allows not only to increase the rate of precipitation of osteogenic stem cells from the environment, but also to create more favorable conditions for cell differentiation and then proliferation. Polymers intended to create "smart scaffolds", for example, for the regeneration of animal/human bones, must comply with the requirement of biocompatibility. Such requirements are met by polyvinylidene fluoride (PVDF).

These "smart scaffolds" place special demands on manufacturing methods. When choosing a manufacturing method, it is reasonable to use the method of a computer experiment. In turn, to achieve the correct result of a computer experiment, it is necessary to know the properties of the composite [5] - the concentration and distribution of the piezoelectric phase (the so-called  $\beta$ -phase of PVDF) and the magnetic phase, the mechanical properties of all phases, possible material defects and their distribution. The topic of this report is the study of the magnetoelectric response of a composite film based on PVDF with magnetic nanoparticles and a comparison of the obtained results with the results of a computer experiment.

The support from the RSF project No. 21-72-30032 is gratefully accepted.

- [1] N. Pereira, A.C. Lima, S. Lanceros-Mendez, P. Martins, *Materials* 13, Art. no. 4033 (2020).
- [2] J. V. Vidal, A. V. Turutin, I. V. Kubasov, A. M. Kislyuk, D. A. Kiselev, M. D. Malinkovich, Y.N. Parkhomenko, S.P. Kobeleva, N. A. Sobolev, A. L. Kholkin, *IEEE Trans. Ultrason. Ferroelectr. Freq. Control* 67, 1219 (2020).
- [3] N. Pereira, A. C. Lima, V. Correia, N. Perinka, S. Lanceros-Mendez, P. Martins, *Materials* 13, Art. no. 1729 (2020).
- [4] A. Omelyanchik, V. Antipova, C. Gritsenko, V. Kolesnikova, D. Murzin, Y. Han, A. V. Turutin, I. V. Kubasov, A. M. Kislyuk, T. S. Ilina, et al. *Nanomaterials* 11, Art. no. 1154 (2021).
- [5] O. Stolbov, A. Ignatov, V. Rodionova, Yu. Raikher, *Soft Matter* 19, 4029 (2023)

# Studying of characteristics of rectified microwave signal in magnetic tunnel junctions with perpendicular magnetic anisotropy in perpendicular and planar magnetic field

K. Kiseleva<sup>1,2,\*</sup>, G. Kichin<sup>1</sup>, P. Skirdkov<sup>1,3</sup>, K. Zvezdin<sup>1,3</sup>

<sup>1</sup>New spintronic technologies, Russian quantum center, Innovation center Skolkovo

<sup>2</sup>Skolkovo Institute of Science and Technology

<sup>3</sup>Prokhorov General Physics Institute of the Russian Academy of Sciences

\*[kseiiiia.kiseleva@skoltech.ru](mailto:kseiiiia.kiseleva@skoltech.ru)

The growing of interest in process of automation and monitoring systems requires many sensors and control systems. With a decrease in the size of sensors, the efficiency of the energy supply of such systems becomes a problem. To solve this problem, an importance task is to find new approaches to make new sensor that would be autonomous, low-power, and wirelessly powered.

A promising solution to this problem is structures based on a magnetic tunnel junction (MTJ) [1]. MTJ is a nanoscale multilayer structure in which the key elements are ferromagnetic layers separated by an insulator layer.

MTJs with perpendicular magnetic anisotropy (PMA) demonstrate outstanding microwave signal rectification characteristics [2], that makes such structure interesting for potential applications for harvesting electrical energy and converting it into a form suitable for powering various sensors. The high coefficient of microwave-to-dc conversion in such structures is associated with the appearance of a cone magnetic state, in which the magnetization of the free layer is inclined from the normal to the film plane [3].

In this work we experimentally study MTJs with PMA and the possibility of appearance of cone magnetic state in these samples. Theoretically, cone magnetic state in MTJ with PMA can lead to high sensitivity. With using spin-torque ferromagnetic resonance (ST-FMR) method we studied the effect of rectification of microwave signal. The experiment was taken in perpendicular and planar magnetic fields on round and elliptical MTJs.

The experiment showed that the same sample shows different characteristics and values of rectification in planar and perpendicular external magnetic field. The maximal rectified voltage was observed on elliptical sample with the size 100x150 nm and on round sample with the diameter 125 nm. Both samples showed a big TMR ratio.

We also observed the appearance of modes in the low frequency range (from 500 MHz to 1.5 GHz) for both round and elliptical samples in planar magnetic external field. Such behavior of MTJs PMA is different to the traditional resonance regime in samples with planar magnetic anisotropy [4].

The work is done with financial support by the Russian Science Foundation, Project № 22-12-00367.

[1] O. V. Prokopenko et al // Journal of App. Phys. 111 123904 (2012).

[2] B. Fang et al // Nature Communications. No 1 (7) (2016).

[3] A.G. Buzdakov, P.N. Skirdkov, K.A. Zvezdin. // Phys. Rev. App. No 5 (15) (2021).

[4] M. Tarequzzaman et al // Appl. Phys. Lett. 112 252401 (2018)

## Substitution effect of magnetic MAX-phases

### $(\text{Cr}_{4-x}\text{Fe}_x)_{0.5}\text{AC}$ (A = Ge, Si, Al)

S. Ovchinnikov<sup>a,b\*</sup>, V. Kozak<sup>b</sup>, N. Fedorova<sup>b</sup>, J. Olshevskaya<sup>b</sup>, A. Kovaleva<sup>b</sup>, A. Shubin<sup>b</sup>, A. Tarasov<sup>a,b</sup>, T. Ovchinnikova<sup>c</sup>, S. Varnakov<sup>a</sup>, F. Tomilin<sup>a,b</sup>

<sup>a</sup> Kirensky Institute of Physics, FRC KSC SB RAS, 660036, Akademgorodok 50/38 Krasnoyarsk, Russia

<sup>b</sup> Siberian Federal University, 660041, Svobodny 79, Krasnoyarsk, Russia

<sup>c</sup> Sukhachev Institute of Forest, FRC KSC SB RAS, 660036, Akademgorodok 50/28 Krasnoyarsk, Russia

\* sgo@iph.krasn.ru

MAX phases form a family of layered ternary compounds with the formal stoichiometry  $\text{M}_{n+1}\text{AX}_n$  ( $n = 1, 2, 3\dots$ ), where M is a transition metal, A is a p-element (Si, Ge, Al, S, Sn, etc.) and X is carbon or nitrogen. MAX phases exhibit the unique physical properties typical of both metals and ceramics. The search for MAX phases with desired magnetic and electronic properties is very promising in order to widen the range of their applications in spintronics, magnetocalorics, computer and space technology, etc. Currently, there is a great interest in the study of magnetic MAX phases. The few magnetic MAX compounds that have been synthesized so far exhibit outstanding properties that are attractive for both fundamental research and advanced applications.

In this study, the atomic and electronic structure and spin states of a series of  $(\text{Cr}_{4-x}\text{Fe}_x)_{0.5}\text{AC}$  MAX phases with  $\text{M}=\text{Cr}$ ,  $\text{A}=\text{Al}$ ,  $\text{Si}$  and  $\text{Ge}$ , and  $\text{X}=\text{C}$  have been comprehensively investigated using Density Functional Theory (DFT) calculations. The chromium centers in the lattices have been continuously and consistently replaced by iron ions, since they have close atomic and ionic radii and exhibit similar ferromagnetic spin ordering in most compounds. Particular attention has been paid to the systematic search for iron-doped  $\text{Cr}_2\text{GeC}$ ,  $\text{Cr}_2\text{SiC}$  and  $\text{Cr}_2\text{AlC}$  MAX phases, which are promising for advanced spin-related applications. Based on extensive electronic structure calculations, it was shown that the substitution of even a small amount of chromium ions by iron ions can drastically change the magnetic properties of the parent MAX phases. For the electronic structure calculations of the crystalline structure and electronic properties of MAX, the B3LYP functional implemented in the CRYSTAL 17 code ([www.crystal.unito.it](http://www.crystal.unito.it)) was used. In order to simulate the magnetic properties, spin-polarized electronic structure calculations were carried out for unit cells consisting of four M (either Cr or Fe) ions, two A (Ge, Si or Al) and two carbon atoms, with alternating directions along the c-axis of magnetic moments localized at d-elements. All possible spin states have been considered in the study, with the ferrimagnetic and antiferromagnetic states specified by the alternation of the magnetic moments at the ions. Band structure and DOS diagrams show that all MAX phases exhibit metallic conductivity with high electronic density at the Fermi level.  $(\text{Cr}_{4-x}\text{Fe}_x)_{0.5}\text{GeC}$  MAX phases show the gradual appearance of the van Hove singularity with increasing Fe content. The  $\text{Cr}_2\text{AlC}$  MAX phase clearly shows the Dirac cone in the band structure, in contrast to germanium and silicon-based compounds, which can lead to the formation of topological phases and significantly affect their transport properties. The ferromagnetic and ferrimagnetic spin ordering in partially substituted MAX phases is energetically favorable. Structural transformations from  $\text{Cr}_2\text{SiC}$  to  $\text{Fe}_2\text{SiC}$  and from  $\text{Cr}_2\text{GeC}$  to  $\text{Fe}_2\text{GeC}$  lead to the change in magnetic states, while in  $\text{Cr}_2\text{AlC}$ - $\text{Fe}_2\text{AlC}$  the FiM spin order is preserved. In the latter case, the difference between the spin states is small, which may open up the prospect of using these structures in spintronic devices. It has been shown that single substituted  $(\text{Cr}_3\text{Fe})_{0.5}\text{AC}$  (A = Ge, Si, Al) MAX phases could be very useful for several spin related applications.

The authors are grateful to JCSS Joint Super Computer Center of the Russian Academy of Sciences for providing supercomputers for the simulation. This study was supported by the Russian Science Foundation, project no. 21-12-00226.

# Temperature dependence of spin pumping in Py/W and Py/Pt bilayers

A. Pakhomov<sup>a,b\*</sup>, V. Yurlov<sup>a</sup>, P. Skirdkov<sup>a,c</sup>, A. Chernov<sup>b</sup>, K. Zvezdin<sup>a,c</sup>

<sup>a</sup> “New Spintronic Technologies” LLC, 121205, Skolkovo Inno Center territory, Bolshoy Bulvar 30 bld. 1  
Moscow, Russia

<sup>b</sup> Center for Photonics and 2D Materials, Moscow Institute of Physics and Technology, 141701, Dolgoprudny,  
Russia

<sup>c</sup> Prokhorov General Physics Institute of the Russian Academy of Sciences, 119991, Vavilova 38, Moscow,  
Russia

\*a.pakhomov@nst.tech

Nowadays microelectronics and data storage devices rely mainly on transport and handling of charge currents. However, the ever-increasing miniaturization process has reached a point in which power consumption and heat dissipation make extremely difficult further technological improvements. A way to overcome this dead end is to change the control variable from charge to electronic spin.

The temperature dependence of the spin pumping process in Py/Pt and Py/W bilayers is analyzed for different Pt capping layer thickness.

Samples have been grown by means of dc magnetron sputtering, at room temperature, on top of Al<sub>2</sub>O<sub>3</sub> substrates. In order to get an optimized interface between the Py and the Pt layers, the Pt capping layers were deposited *In situ*. The values of the damping constant,  $\alpha$ , obtained for the Py/Pt and Py/W in a wide temperature range (5 – 290 K). Also, inverse spin hall voltage was measured for these samples. The increase of  $\alpha$  due to spin pumping into the Pt/W layer is clearly appreciated;  $\alpha$  values in Py/Pt and Py/W bilayers are investigated. Spin pumping is confirmed by direct measurements of the inverse spin Hall effect (ISHE) voltage signal ( $V_{\text{ISHE}}$ ) measured across the samples.

To separate ISHE and spin rectification contributions to  $V_{\text{ISHE}}$  the line shape analysis method has been used and the conditions for its applicability thoroughly discussed.  $V_{\text{ISHE}}$  increases almost linearly from 290 to 150 K. Than  $V_{\text{ISHE}}$  decreases until 50 K, and after 50 K voltage increasing until temperature reach 5 K. Py/Pt and Py/W both demonstrate such behavior. For Py/Pt bilayers such results observed earlier [1]. An explanation of this effect in temperature range 5-290 K is given.

Support by RSF №22-12-00367 is acknowledged.

[1] S. Martín-Rio et al, Journal of Magnetism and Magnetic Materials, Volume 500, (2020)



# Thermoelectric properties of $\text{Ti}_2\text{MnNiSi}_2$ double half-Heusler alloy

V. Buchelnikov<sup>a,\*</sup>, M. Matyunina<sup>a</sup>, V. Sokolovskiy<sup>a,b</sup>, D. Baigutlin<sup>a</sup>, N. Korneva<sup>a</sup>

<sup>a</sup> Chelyabinsk State University, 454001, Br. Kashirinykh Str., 129, Chelyabinsk, Russia

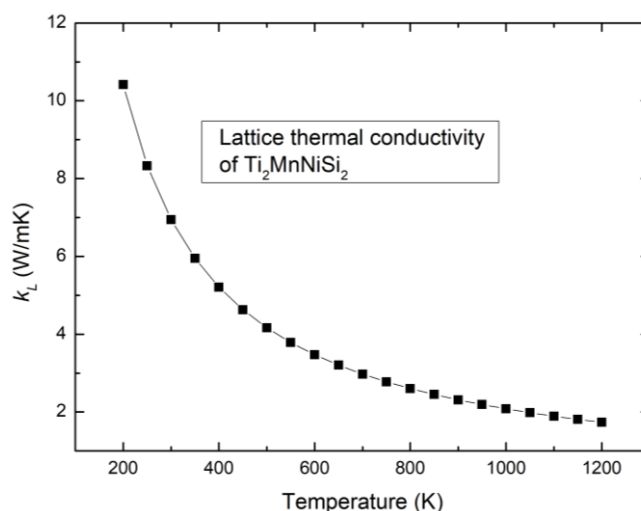
<sup>b</sup> National University of Science and Technology “MISiS,” Moscow 119049, Russia

\*buche@csu.ru

Half-Heusler compounds have attracted significant research attention for their thermoelectric properties in the last time [1]. Multi-functional half-Heusler semiconductors have been studied extensively as three-component systems (nominal formula XYZ) with valence balanced compositions. The high performance in half-Heusler compounds is primarily associated with their exceptional electrical transport properties. However, in comparison to some of the best thermoelectric materials based on IV-VI groups compounds, ternary half-Heusler compounds are at a disadvantage due to their intrinsically large lattice thermal conductivity ( $k_L$ ). ZrCoBi, for example, has one of the lowest reported  $k_L$  of 10 W/(m.K) among the high-performing half-Heusler compounds ( $T = 300$  K), whereas the state-of-the-art thermoelectric material PbTe has intrinsic  $k_L$  of 2 W/(m.K). Thus, it is desirable to find a new semiconductors with the electronic properties of half-Heusler compounds but with inherently lower  $k_L$ .

Recently it was shown that so-called double half-Heusler alloys may have significantly lower lattice thermal conductivity than ternary half-Heusler alloys [2]. The main reason of such behaviour of double half-Heusler alloys is a large number of atoms in their unit cell.

In this work we investigate the lattice thermal conductivity of  $\text{Ti}_2\text{MnNiSi}_2$  double half-Heusler alloy by density functional theory. It is shown that the lattice thermal conductivity of this alloy at 300 K is about 6 W/mK (see Figure). This value is lower than in above mentioned ZrCoBi alloy.



Based on the obtained lattice thermal conductivity the thermoelectric properties of  $\text{Ti}_2\text{MnNiSi}_2$  alloy were also calculated in this work.

The work was supported by the RSF - Russian Science Foundation, project No.~22-12-20032.

[1] W.G. Zeier, et al, Nat. Rev. Mater. 1, 16032 (2016).

[2] S. Anand, et al, Joule 3, 1226 (2019)

# Ti<sub>3</sub>C<sub>2</sub>T<sub>x</sub> MXenes as a potential agent for water remediation and photothermal treatment

Motorzhina A.V.\* , Shilov N.R., Davkina A.V., Anikin A.A., Murzin D.V., Levada K.V.,  
Sobolev K.V.

Immanuel Kant Baltic Federal University, 236004, Nevskogo 14, Kaliningrad, Russia

\*AMotorzhina1@kantiana.ru

Ti<sub>3</sub>C<sub>2</sub>T<sub>x</sub> MXene is a new two-dimensional material with promising photothermal effects and biocompatibility [1]. Therefore, there is an urgent need to explore the applicability of MXene Ti<sub>3</sub>C<sub>2</sub>T<sub>x</sub> for multimodal tumor therapy. Here, for the first time to our knowledge, MXene is shown as a promising agent for the photothermal treatment of human melanoma SK-MEL 28. In this work, we synthesize a two-dimensional MXene Ti<sub>3</sub>C<sub>2</sub>T<sub>x</sub> by etching a Ti<sub>3</sub>AlC<sub>2</sub> MAX phase precursor with LiF and HCl for 24 hours at 35 °C. The synthesized samples were dried and characterized by XRD and SEM-EDX. The analysis showed the presence of the 2D Ti<sub>3</sub>C<sub>2</sub> phase in our samples.

First, a Ti<sub>3</sub>C<sub>2</sub>T<sub>x</sub>+Fe<sub>3</sub>O<sub>4</sub> composite material was created and characterised using VSM and TEM. A detailed description of the synthesis of the composite is described in the appendix to the report. The growth of magnetite was found to favour additional delamination of multilayer MXene, resulting in the formation of single or low-layer flakes completely covered by MXene. The synthesis of this composite is a cheaper and environmentally friendly method to produce MXene-based magnetic composites for wastewater treatment.

In addition, it was observed that increasing the concentration of MXenes during the coprecipitation process leads to an increase in the size of Fe<sub>3</sub>O<sub>4</sub> from 14 nm to 52 nm. The magnetic properties of the obtained composites were investigated using VSM. The saturation magnetisation of the composites was shown to vary from 16 A m<sup>2</sup> kg<sup>-1</sup> to 38 A m<sup>2</sup> kg<sup>-1</sup> in proportion to the mass content of magnetic particles in the composite. The absorption properties of the composites towards Cu(II) ions from aqueous media were then investigated. It was proved that the MXen nanosheets still have high adsorption capacity, but at the same time, they possess ferrimagnetic properties, allowing the adsorbent to be completely removed from water. Ti<sub>3</sub>C<sub>2</sub>T<sub>x</sub> MXene powder was diluted in sterile distilled water at concentrations of 500 and 1000 µg/ml, and then dispersed using ultrasound. The obtained MXenes suspensions were studied by visible light spectroscopy in the wavelength range from 400 to 1000 nm. The results show an absorption peak at a wavelength of 810 nm (Fig. 1), which is typical for MXene composition Ti<sub>3</sub>C<sub>2</sub>T<sub>x</sub> x [1]. The absorption peak at a wavelength of 810 nm corresponds to the second tissue transparency window [2]. Thus, Ti<sub>3</sub>C<sub>2</sub>T<sub>x</sub> MXenes is a suitable material for photothermal therapy.

Biocompatibility analysis of Ti<sub>3</sub>C<sub>2</sub>T<sub>x</sub> MXenes was performed using the WST-1 viability test. The well-established and highly proliferative SK-MEL-28 cell culture was used for the experiments. Cell cultures were incubated according to standard protocols (at 37°C in a humid atmosphere with 5% CO<sub>2</sub>) in DMEM nutrient medium. Ti<sub>3</sub>C<sub>2</sub>T<sub>x</sub> MXenes was added to the nutrient medium to obtain treatment solutions at concentrations of 10, 50, and 100 µg/mL. After 24 hours of cultivation, the cells were stained with WST-1 (Roche Diagnostics GmbH) and the optical density was measured using a Multiskan FC microplate reader (Thermo Scientific). 100 µg/mL concentrated Ti<sub>3</sub>C<sub>2</sub>T<sub>x</sub> MXenes show 14% cytotoxic effect.

Acknowledgement: This work was supported by the Russian Science Foundation, grant 22-12-20036, region grant 12-C/23.

[1] G. Liu et al., ACS Appl. Mater. Interfaces 9, 40077 (2017)

[2] Zh. Zhou et al., Chem. Eng. 399, 125688 (2020)

## **Ti<sub>3</sub>C<sub>2</sub>T<sub>x</sub> MXenes with various surface terminations for environmental remediation technologies**

Sobolev K.<sup>1\*</sup>, Shilov N.<sup>1</sup>, Magomedov K.<sup>1</sup>, Omelyanchik A.<sup>1</sup>, Anikin A.<sup>1</sup>,

Murzin D.<sup>1</sup>, Belyaev V.<sup>1</sup>, Davkina A.<sup>1</sup>, Rodionova V.<sup>1</sup>

*1-Immanuel Kant Baltic Federal University, Kaliningrad, Russia*

*\*E-mail: [ksobolev1@kantiana.ru](mailto:ksobolev1@kantiana.ru)*

MXenes are a novel skyrocketing class of two-dimensional nanomaterials, sharing the common formula  $M_{n+1}X_nT_x$ , where M is a transition metal, X is C or/and N, and  $T_x$  is a surface termination group, which is typically -OH, -O or -F. [1] MXenes possess a unique set of properties, including functionalization-dependent conductivity (mostly metallic), hydrophilicity, large specific surface area, and outstanding tunability. This makes them promising for a huge amount of practical applications, such as energy harvesting, electronics, sensors, biomedicine, ecology, etc. [2]

Two-dimensional materials are widely used in environmental remediation technologies: adsorption of toxic heavy metal ions, sensing of hazardous gases, and many more. [3],[4] MXenes are not an exception, their exploration as both nanoadsorbents and gas-sensitive materials has become one of the clear trends in today's materials society. [5]-[7] Handling environmental pollution is one of the most urgent problems, facing humanity nowadays, as water contamination (with heavy metals and other pollutants) possesses long-term harmful effects on human health and natural ecosystems, while exhaustive CO<sub>2</sub> emission leads to the greenhouse effect and global temperature upraise, which will inevitably cause severe damage to civilization.

This work revises main directions of applying Ti<sub>3</sub>C<sub>2</sub>T<sub>x</sub> MXenes and MXene-based materials as environmental remediation agents, being developed in REC "SM&BA", IKBFU. One direction is the use of controllably functionalized MXenes as heavy metal ion nanoadsorbents. Surface termination plays the crucial role in adsorptive behavior of MXenes, enabling them with selectivity towards specified types of pollutants. The review focuses on the preparation of MXenes with different predominant functional groups (-O, -OH and -F are being considered), and their adsorptive performance in liquid media. Another direction is the use of MXenes, combined with magnetic nanoparticles (MNPs) in a synergistic MXene-MNPs composite, for the same purposes. MNPs in such composites allow performing magnetic decantation to evacuate the adsorbent from the purified media, while preserving high adsorption capacity of MXenes. The third direction focuses on using Ti<sub>3</sub>C<sub>2</sub>T<sub>x</sub> MXenes for CO<sub>2</sub> sensing and capture. We explore the ability to additionally functionalize MXene surface with various organic molecules to enhance the material's specificity and affinity towards CO<sub>2</sub> molecules, and assemble such functional 2D flakes into the custom device, allowing both optical and transport detection of CO<sub>2</sub>.

Acknowledgment: This work was supported by the Russian Science Foundation, grant №22-12-20036, regional part no. 07-C/2022.

- [1] M. Naguib, V.N. Mochalin, M.W. Barsoum, Y. Gogotsi, *Adv. Mater.* 2014, 26, 992.
- [2] M. Khazaei, A. Mishra, N.S. Venkataramanan, A.K. Singh, S. Yunoki, *Curr. Opin. Solid State Mater. Sci.* 2019, 23, 164.
- [3] K. V. Wong, B. Bachelier, J. *Energy Resour. Technol.* 2014, 136.
- [4] S. Wang, H. Sun, H.M. Ang, M.O. Tadé, *Chem. Eng. J.* 2013, 226, 336–347.
- [5] Y. Zhang, L. Wang, N. Zhang, Z. Zhou, *RSC Adv.* 2018, 8, 19895–19905.
- [6] Y. Sun, Y. Li, *Chemosphere* 2021, 271, 129578.
- [7] S. Yu, H. Tang, D. Zhang, S. Wang, M. Qiu, G. Song, D. Fu, B. Hu, X. Wang, *Sci. Total Environ.* 2022, 811, 152280.

# Transverse magneto-optical Kerr effect enhancement by Mie resonances in silicon-nickel nanogratings

K. Mamian\*, A. Frolov, I. Bozhev, V. Popov, A. Fedyanin

Lomonosov Moscow State University, 119991, Leninskie gory 1, Moscow, Russia

\*mamian.ka19@physics.msu.ru

The transverse magneto-optical Kerr effect (TMOKE) allows one to control the intensity of light for applications in nanophotonics. However, the effect is too weak in the common magneto-optically active materials for practical purposes. Earlier works proposed to use magnetoplasmonic crystals in order to enhance these effects by excitation of surface plasmon-polaritons at the metal/dielectric interface. This method leads to large losses due to high absorption in the metal. The alternative and more efficient way to enhance TMOKE is the use of Mie resonances in hybrid metal-dielectric nanostructures [1].

We study a nanograting consisting of rectangular silicon nanowires periodically placed on a nickel substrate. Preliminary calculations with the use of Ansys Lumerical FDTD software helped in determining the optimal geometrical parameters of the gratings, after which four samples were fabricated by electron beam lithography technique. The angular-wavelength dependencies of the reflectance and TMOKE were experimentally measured in the range of the angles of incidence from  $5^\circ$  to  $55^\circ$ .

The largest absolute TMOKE value of 4.3% (which is 40 times larger than in plain nickel film) was observed for the sample with a period of 720 nm, height of 180 nm and a width of 215 nm at the angle of incidence of  $50^\circ$ . The map of the TMOKE is shown on Figure 1 (A). The experimental and simulated reflectance and TMOKE spectra for  $50^\circ$  angle of incidence are shown on Figure 1 (B) and (C), respectively. The excitation of magnetic dipole resonance with the direction along the axis (z) of the nanowire, as demonstrated by the simulated magnetic field distribution (Figure 1 (E)), is the cause of the dip in the reflectance spectrum and the corresponding TMOKE peak at  $\lambda = 840$  nm. It's worth mentioning that the excitation of electric dipole resonance at  $\lambda = 725$  nm (Figure 1 (D)) leads to smaller values of TMOKE.

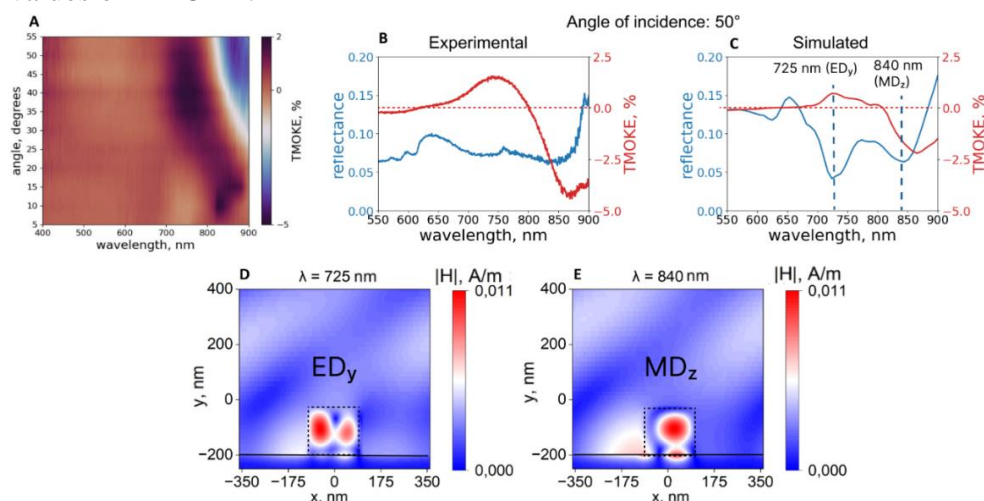


**Figure 1.** (A) – angular-wavelength dependence of TMOKE; (B) and (C) – experimental and simulated TMOKE and reflectance spectra at  $50^\circ$  angle of incidence; (D) and (E) – magnetic field distributions for ED and MD resonances.

[1] M. Barsukova, ACS Photonics, 4, 2390 – 2395 (2017)

## Understanding magnetic properties of natural hematite

S. Slimani<sup>\*a,b</sup>, E. Castagnotto<sup>a,c</sup>, A. Omelyanchik<sup>d</sup>, S. Laureti<sup>b</sup>, G. Barucca<sup>e</sup>,

Nader Yaacoub<sup>f</sup>, Federico Locardi<sup>a</sup>, Laura Gaggero<sup>c</sup>, Maurizio Ferretti<sup>a</sup> and Davide Peddis<sup>a,b</sup>

<sup>a</sup> Department of Chemistry and Industrial Chemistry, University of Genoa, Via Dodecaneso 31, I-16146, Italy.

<sup>b</sup> Istituto di Struttura Della Materia – CNR, Area Della Ricerca di Roma 1, Monterotondo Scalo, RM 00015, Italy.

<sup>c</sup> Department of Earth, Environment and Life Sciences, University of Genoa, Corso Europa 26, I-16132, Italy.

<sup>d</sup> Institute of Physics, Mathematics and Information Technology, Immanuel Kant Baltic Federal University,<sup>e</sup>

Dipartimento di Scienze e Ingegneria della Materia, dell'Ambiente ed Urbanistica-SIMAU, Università Politecnica delle Marche, Ancona, Italy

<sup>f</sup> Institut des Molécules et Matériaux du Mans CNRS UMR-6283, Le Mans Université, Avenue Messiaen, 72085 Le Mans, France.

\*[Sawssen.Slimani@edu.unige.it](mailto:Sawssen.Slimani@edu.unige.it)

Iron oxides are natural compounds that have been used since ancient times as pigments because of their stability in atmospheric conditions, along of course with their intense colour [1]. Hematite is particularly important in this context because of its great abundance in nature, and its variety of colors (e.g., deep red, brown and purple). Though several characterization techniques such as X-ray diffraction, transmission electron microscopy, thermoanalytical methods and Mössbauer spectroscopy enable to distinguish hematite from other materials found in paintings. However they have been unable to show differences and, consequently, to identify the origin of hematite, whether natural or synthetic [2], [3]. To address these issues, here we combine morpho-structural and magnetic investigations of natural, commercial, and synthesized by sol-gel chemical method, hematite samples. Thermal dependence of magnetization reveals the presence of Morin transition ( $T_M$ ) just for commercial hematite  $T_M = 230(3)$  K.  $M$  vs  $H$  curves have also been investigated at 5 and 300 K showing at low temperature for natural hematite a weak ferrimagnetic behaviour with saturation magnetization value  $M_S = 1(4)$  Am<sup>2</sup>Kg<sup>-1</sup>. Synthetic samples have shown the dominance of the antiferromagnetic (AFM)- like behavior with almost zero magnetization. Similar behaviors have been reported even after thermal treatment at 1100°C for 2 hours. Particularly, at 300 K a strong increase of the  $\mu_0 H_C \approx 450(3)$  mT in lab synthesized hematite sample was reported, suggesting an increase in the anisotropy that is strongly related to the presence of noncollinear spin structure. Complementary Mössbauer spectrometry measurements were carried out to investigate the magnetic structure, showing that for synthetic hematite samples the hyperfine parameters ( $B_{Hyp} = 54$  T) correspond to the stoichiometric hematite with a collinear AFM order below  $T_M$ . For natural hematite, the values of the quadrupole shift (QS) were distinctly changed (from  $-0.164$  mm s<sup>-1</sup> to  $0.377$  mm s<sup>-1</sup> and from  $0.347$  mm s<sup>-1</sup> to  $-0.08$  mm s<sup>-1</sup> at 300 K and 77 K respectively), indicating the coexistence of both magnetic phases: stoichiometric hematite with AFM structure below  $T_M$  and non-stoichiometric hematite with weak ferrimagnetic properties.

[1] E. Castagnotto, F. Locardi, S. Slimani, D. Peddis, L. Gaggero, and M. Ferretti. *Dye.Pigment*, 185, 108881 (2021).

[2] L. F. C. de Oliveira, H. G. M. Edwards, R. L. Frost, J. T. Kloprogge, and P. S. Middleton. *Analyst*, vol. 127, 4, 536–541 (2002)

[3] H. D. Ruan, R. L. Frost, J. T. Kloprogge, and L. Duong. *Spectrochim. Spectrosc. Acta - Part A*, 58, 5, 967–981 (2002).

## Uniaxial stresses in magnetic elastomers

A. Musikhin<sup>a,\*</sup>, A. Zubarev<sup>a</sup>, G. Stepanov<sup>b</sup>

<sup>a</sup> Ural Federal University, 620000, Lenin Ave., 51, Ekaterinburg, Russia

<sup>b</sup> State Scientific Research Institute of Chemistry and Technology of Organoelement

Compounds, 105118, Leninskie gory 1, Moscow, Russia

\*corresponding author email: Antoniusmagna@yandex.ru

A model is proposed that describes the experimentally observed nonlinear dependences of uniaxial stresses in an elastic magnetic polymer filled with magnetizable particles combined into linear chains on deformation in the presence of an external magnetic field.

Usually, these chains appear at the stage of polymerization of the composite, if it occurs under the action of an external magnetic field. Experiments show that the rheological properties of magnetic polymers with an internal anisotropic structure differ greatly from those of internally isotropic composites. Macroscopic magnetomechanical effects in these materials are determined by the morphology of the internal spatial arrangement of particles in the polymer. Chain morphology is shown in Fig.1.

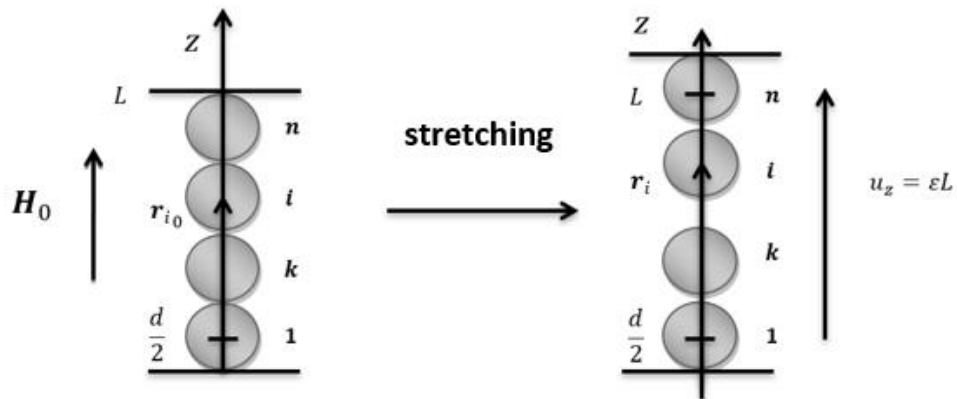


Figure 1 - Illustration of the simulated system.

The model is based on static equilibrium between the elastic forces of the polymer matrix and the magnetic forces of the dipole-dipole interaction between particles in a chain [1]:

$$\beta(\mathbf{u} - \mathbf{u}_i) + \mathbf{F}_i = 0, \quad i = 2, \dots, n - 1. \quad (1)$$

Here  $\mathbf{u}_i$  is the displacement of the  $i$ -th particle relative to the displacement  $\mathbf{u}$  of the matrix,  $\mathbf{F}_i$  is the magnetic forces acting on the  $i$ -th particle

This model will allow us to calculate the positions of each particle in a single chain after longitudinal deformation of the sample, as a result of which we plan to calculate the tensile stress in the composite and conduct a comparative analysis with experimental stress values.

The work was supported by the Ministry of Science and Education of the Russian Federation, project FEUZ-2023-0020.

[1] Zubarev A. Y., Iskakova L. Y. and Lopez-Lopez M. T., Physica A 455, 98 - 103 (2016)

## Unique magnetic properties of nanocrystalline Co-based glass-coated microwires

V. Kolesnikova<sup>a\*</sup>, N. Andreev<sup>a,b</sup>, A. Omelyanchik<sup>a</sup>, I. Baraban<sup>a</sup>, S. Shevyrtalov<sup>a</sup>, M. Gorshenkov<sup>b</sup>,  
M. Rivas<sup>c</sup>, M. Vazquez<sup>d</sup> and V. Rodionova<sup>a</sup>

<sup>a</sup> Immanuel Kant Baltic Federal University, Kaliningrad, Russia

<sup>b</sup> National University of Science and Technology «MISIS», Moscow, Russia

<sup>c</sup> Department of Physics, University of Oviedo, Gijón, Spain

<sup>d</sup> Instituto de Ciencia de Materiales de Madrid, CSIC, Spain

\*VGKolesnikoval@kantiana.ru

Metallic glasses can be considered as materials which are kinetically metastable and thermodynamically unstable. These materials could be transferred into a more stable state under appropriate circumstances, for example, thermal treatment leading to crystallization of amorphous phase into one or more metastable or stable crystalline phases. The development of complex nanocrystalline alloys from their metastable amorphous precursors became the state-of-art topic in creating new materials for high-temperature applications [1-2]. For constructional and magnetically soft nanocrystalline materials the optimum mechanical and magnetic properties, respectively, are obtained after partial crystallization of their amorphous precursors, which means that they are two-phase materials composed of nanocrystals and an amorphous matrix. Most of the methods offer two possibilities for the creation of nanocrystalline structure: directly in one process or indirectly through an amorphous precursor. Nanocrystallization of metallic glasses is an example of the second procedure. In this case, nanocrystalline material is produced in two steps: (1) formation of amorphous state by quenching of liquid alloy, and (2) partial or complete crystallization of the amorphous alloy by annealing.

The Co-based bulk magnetic glasses (BMGs) have excellent magnetic properties [3]. For instance, a large saturation magnetization makes the Co-based BMGs great for application in soft magnetic material design. These Co-based BMGs can be prepared in the form of microwires covering requirements for the micro-devices applications, such as high-temperature magnetic field sensors. The mastering of the knowledge—and control, whenever possible—of the thermodynamic conditions, is necessary for inducing the metastability of the structures. The metastability leads to uncommon physical effects and special properties of nanocrystalline materials treating a particular emphasis.

This work offers a novel and lightweight approach of creating nanocrystalline metallic glasses using the modified Taylor–Ulitsky method [4]. The traditional Taylor–Ulitsky method implies a water cooling during the quenching to form an amorphous metal nucleus coated with a glass shell. To process the nanocrystalline metallic nucleus it is enough to apply the air cooling during the quenching process. This modification allows us to provide the multiphase metallic glasses which consist of nanocrystallites embedded in an amorphous matrix without an additional step of annealing the amorphous precursor.

This research was supported by funds provided through the Russian Federal Academic Leadership Program “Priority 2030” at the Immanuel Kant Baltic Federal University, project number 123012700017-2.

[1] N. Zhou, T. Hu, J. Huang, and J. Luo, *Scr. Mater.* 124, 160 (2016).

[2] A. Zhukov, et al., *J. Alloys Compd.* 727, 887 (2017).

[3] A. Inoue, B. Shen, H. Koshida, H. Kato, and A.R. Yavari, *Nat. Mater.* 2, 661 (2003).

[4] J. Alam, et.al., *J. Magn. Magn. Mater.* 513 (2020) 167074.

## Yttrium-iron garnet film magnetometer for in vivo studies

I. Radchenko<sup>a,\*</sup>, N. Koshev<sup>b</sup>, P. Kapralov<sup>a</sup>, S. Evstigneeva<sup>a</sup>, O. Lutsenko<sup>a</sup>, M. Zharkov<sup>c</sup>, N. Pyataev<sup>c</sup>,  
A. Darwish<sup>d,e</sup>, A. Timin<sup>d,e</sup>, M. Ostras<sup>a</sup>, G. Sukhorukov<sup>b,f</sup> and P. Vetoshko<sup>a,g</sup>

<sup>a</sup> M-Granat, Russian Quantum Center, Moscow, Russia

<sup>b</sup> Skolkovo Institute of Science and Technology, Moscow, Russia

<sup>c</sup> National Research Ogarev Mordovia State University Saransk, Russia

<sup>d</sup> School of Physics and Engineering, ITMO University, St. Petersburg, Russia

<sup>e</sup> Peter The Great St. Petersburg Polytechnic University, St. Petersburg, Russia

<sup>f</sup> School of Engineering and Materials Science Queen Mary University of London, London, UK

<sup>g</sup> Kotelnikov Institute of Radioengineering and Electronics of RAS, Moscow, Russia

\*il.radchenko@gmail.com

The magnetic nanoparticles (MNPs) are subject to two main magnetic relaxation mechanisms: Neel and Brownian relaxations [1]. The first one depends mostly on the properties of MNPs, while the second is affected by the properties of the area, which contains MNPs [2]. Evaluation of the Magnetic Relaxometry (MRX) on the surface and inside the living organism allows reconstruction of the MNPs distribution in the organism, which reflects the accumulation in certain organs and tissues, as well as to evaluate the intensity of blood flow. The totality of the obtained data can allow to detect tumor nodes, as well as areas of tissue ischemia and present a strong tool to support medical diagnostics [3].

We present a new kind of magnetometer for quantitative determination of magnetic objects in biological fluids and tissues. The sensor is based on yttrium-iron garnet film with optical [4] and impedance signal registration systems. It works at a room-temperature, can operate in an unshielded environment. A small size of sensitive element (less than 10 mm) combined with a short recovery time after the excitation coils are off (less than 1 ms) provides high spatial and temporal resolution of magnetic signal measurements. We show the feasibility of the sensor by sensing both the magnetic relaxation and remanent magnetization of Magnetic Nanoparticles (MNPs) of different size and origin both in vitro (test tubes, dry MNPs, method sensitivity down to 25  $\mu\text{g}$  of magnetite) and in vivo (local injection of the MNPs into mice, method sensitivity down to 1mg of magnetite), Fig. 1.

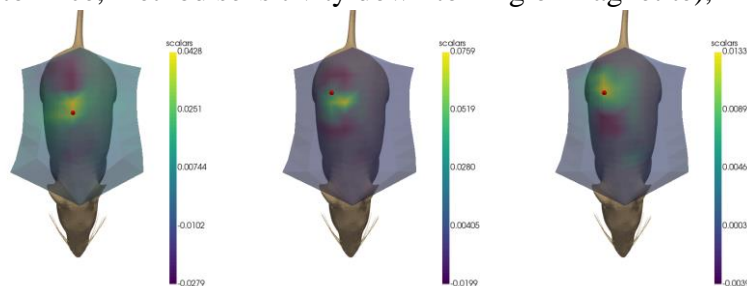


Figure 1: Measurements of the remanent magnetic field of different MNPs samples, injected in mice. The red sphere means the injection point. (a) - 10 mg of the 'nanosphere' sample; (b) - 5 mg of the 'rods' sample; (c) - 1 mg of the 'rods' sample.

- [1] R. M. Fratila, Nanomaterials for magnetic and optical hyperthermia applications. Elsevier, 2018.
- [2] R. Isshiki, Evaluation of the magnetization properties of magnetic nanoparticles in serum using hts-squid. IEEE Transactions on Applied Superconductivity, 28(4):1– 5, 2018.
- [3] A review on brain tumor diagnosis from mri images: Practical implications, key achievements, and lessons learned. Magnetic Resonance Imaging, 61:300–318, 2019.
- [4] N. Koshev, Evolution of meg: A first meg-feasible fluxgate magnetometer. Human Brain Mapping, 42(15):4844–4856, 2021.



# Poster presentations

## **"Substrate Effect" in the Microwave Magnetoelectric Effect in Layered Structures Based on Yttrium Iron Garnet**

S. Ivanov<sup>1</sup>, M. Bichurin<sup>1</sup>, O. Sokolov<sup>1</sup>

<sup>1</sup>Novgorod State University

In connection with the development of spintronics, interest in the magnetoelectric (ME) effect in nanostructures has increased. In [1], the ME effect was studied in multiferroics in the terahertz range based on various manganites. It is of interest to study the ME effect in the region of ferromagnetic resonance (FMR) in nanostructures based on yttrium iron garnet (YIG). In this work, the thickness of the YIG film was taken to be 20  $\mu\text{m}$ . In practice, such ferrite films are deposited by the epitaxial method on a gadolinium gallium garnet (GGG) substrate. The microwave ME effect is studied at an ac magnetic field frequency of 10 GHz for various orientations of the dc bias field. Orientations are considered when the bias field is perpendicular to the plane of the YIG film and is also directed in the plane of the YIG film along the [010] crystallographic axis. A comparison is made of two-layer ME composites, in which rectangular plates PZT, PMN-PT, PZN-PT, quartz and langatate with 0.5 mm thickness are used as piezoelectrics. When such ME composites are exposed to a constant electric field directed along the thickness of the plate, the FMR resonance line in the YIG film is shifted as a result of the microwave ME effect [2]. As a result of the calculation, it was found that the maximum shift of the FMR line in the YIG film in an electric field of 5 kV/cm was 75 Oe for the PZN-PT piezoelectric. A similar calculation was made for three-layer structures, taking into account the structure: YIG film - GGG substrate 0.5 mm thick. In this case, the influence of bending deformations on the result was also taken into account. As a result, the calculation showed that for the case with a GGG substrate, the shift of the FMR resonance line in the YIG film is approximately two times smaller than for the corresponding two-layer ME structure. The results obtained are discussed in [3] and can find practical application in the development of spintronic microwave devices.

### References

- [1] A.A. Mukhin et al. *Physics–Uspekhi* 52, 851 (2009).
- [2] M.I.Bichurin, V.M.Petrov, R.V.Petrov, A.S.Tatarenko. *Magnetoelectric Composites*, Pan Stanford Publ., 2019, 280p.
- [3] Mirza Bichurin, Oleg Sokolov, Sergey Ivanov, Elena Ivasheva, Viktor Leontiev, Vyacheslav Lobekin and Gennady Semenov, *Modeling the composites for magnetoelectric microwave devices*, *Sensors* 23(4), 1780 (2023).

## AC magnetic field sensor based on a magnetoplasmonic crystal

V. Belyaev\*, D. Murzin, V. Rodionova

Immanuel Kant Baltic Federal University, 236004, Nevskogo 14, Kaliningrad, Russia

\*vbelyaev@kantiana.ru

Magnetic field sensors require high sensitivity and resolution, low power consumption, inexpensive production and miniature dimensions. Thus, the magnetic field sensors market offers optimal sensors suitable for a large number of specified tasks [1]. One of the new approaches for magnetic field sensing is based on the use of magnetoplasmonic crystals (MPICs) – plasmonic crystals made of noble and ferromagnetic materials [2 - 4]. MPICs allow one to enhance the magneto-optical Kerr effect by the excitation of surface electromagnetic waves. The possibility to use the MPIC-based magnetic field sensor for DC magnetic field sensing with theoretically predicted achievable sensitivity of  $10^{-7}$  Oe was already shown in several works [5]. Additional advantage of such a magnetic field sensor is provided by high flexibility of magneto-optical measurements: one can easily change the area of a sample contributing the resulting signal by focusing an incident light beam and its position on the sample.

This work is devoted to the use of 1D MPIC for external AC magnetic field sensing. A set of MPICs was fabricated by magnetron sputtering of 100 nm silver and iron or permalloy layers on top of diffraction grating with the period of 320 nm and grooves height of 20 nm. Reflectivity and magneto-optical response in transversal Kerr effect geometry were recorded in UV-VIS spectral range. Magnetic properties were studied with the Kerr magnetometry technique. It is shown that the study of field dependent magneto-optical response in transversal Kerr effect geometry allows one to estimate the magnitude and frequency of external AC magnetic field with the sensitivity on par with demonstrated results for DC magnetic field measurements [5].

The study was financially supported by the Ministry of Science and Higher Education of the Russian Federation No. 13.2251.21.0143.

[1] Khan M.A., Eng. Res. Express., 3, 2 (2021).

[2] Grunin, A.A., Mukha, I.R., Chetvertukhin, A.V., Fedyanin, A.A.: Journal of Magnetism and Magnetic Materials, 415, 72-76 (2016).

[3] Knyazev, G.A., Belotelov, V.I.: ACS Photonics, 5(12), 4951-4959 (2018).

[4] Chandra, S., ACS Photonics, 8(5), 1316-1323 (2021).

[5] Belyaev, V.K., Sci. Rep., 10(1), 1-6 (2020).

# Analysis of the Josephson-like magnetic tunnel junction structure: from classical to quantum approach

V. Yurlov<sup>a,b,\*</sup>, A. Pakhomov<sup>a,b</sup>, K. Zvezdin<sup>a,b,c</sup>, A. Zvezdin<sup>a,b,c</sup>

<sup>a</sup> Moscow Institute of Physics and Technology, Institutskiy per. 9, 141700 Dolgoprudny, Russia

<sup>b</sup> New Spintronic Technologies, Bolshoy Bulvar 30, bld. 1, 121205 Moscow, Russia

<sup>c</sup> Prokhorov General Physics Institute of the Russian Academy of Sciences, Vavilova 38, 119991 Moscow, Russia

\*yurlov.vv@phystech.edu

The theoretical study of the easy plane based Josephson-like magnetic tunnel junction (MTJ) structure is proposed to find specific parameters for the transition to the quantum regime. For this purpose, we describe the classical spin dynamics induced by a short pulse of the electric current[1]. According to the fact that at low temperatures and damping parameters in the magnetic system may exist the quantum properties, we derive the effective Lagrangian and potential energy in the low dissipation case. The mathematical view of this Lagrangian is similar to Josephson transition theory.

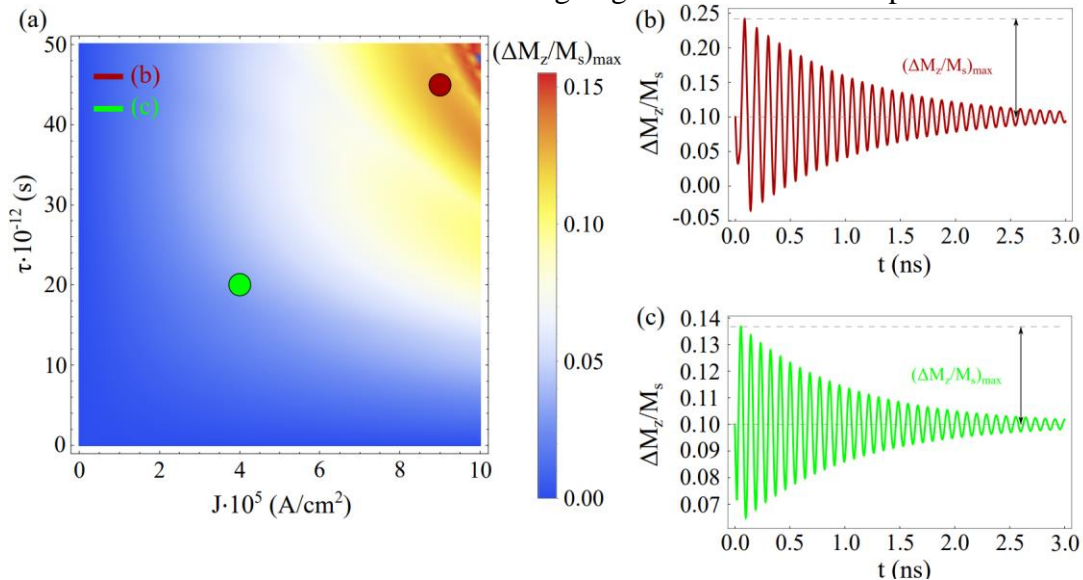


Figure 1. a) Diagram of the maximal value of the oscillations amplitude of the polar angle during the switching process in coordinates pulse duration ( $\tau$ ) - electric current ( $J$ ). b) and c) demonstrates the oscillations of the polar angle at fixed pulse duration and electric current.

Based on the isomorphism of these two problems we find the main MTJ parameters, pulse durations and spin current magnitudes (see in Fig. 1) for implementation of the quantum approach. Similar to superconducting theory a few different types of the qubit may be realized in the MTJ hypothetically: analogs of the charge, transmon and flux qubits[2],[3]. We derive the conditions for existence of these qubits and built the Hamiltonian formalism for detailed description of the two-level systems.

This research has been supported by RSF grant No. 22-12-00367.

[1] A. K. Zvezdin et al., Journal of Experimental and Theoretical Physics, V. 122, N. 4(2002).

[2] A. Kringhoj et al., Phys. Rev. B. V. 97, N. 6(2018).

[3] D. Riste et al., Nature Communications, V. 4, N 1(2013)

## Applications of magnetic structures in microelectronic sensor devices

N. Djuzhev<sup>a</sup>, M. Chinenkov<sup>a,\*</sup>, G. Oreshkin<sup>a</sup>, N. Filippov<sup>a</sup>

<sup>a</sup> National Research University of Electronic Technology (MIET), 124498, Bld. 1, Shokin Square, Zelenograd, Moscow, Russia

\*[chinenkov@inbox.ru](mailto:chinenkov@inbox.ru)

Microelectronic devices based on magnetic materials, in particular ferromagnetic structures, have been used in electrical engineering, microwave technology, sensors and actuators. One of the effects, which provides a promising use of magnetic structures is the electrical resistance change in the magnetic field, i.e. magnetoresistive effect. The improvement of sensitivity, thermal stability and miniaturization is the main objective of the development of magnetic sensitive devices and transducers based on the magnetoresistive microsystems. Magnetoresistor is the main element of magnetic sensor device. Magnetoresistive structure construction is the set of four magnetoresistors included in a bridge circuit [1]. When planar structure exposed to external magnetic field resistance change of all magnetoresistors bridge takes place. Since the strip of aluminum on one shoulder magnetoresistors bridge located at angles of  $45^\circ$  and  $135^\circ$ , resistance in one shoulder of the bridge change in opposite directions. This leads to an increase in the output signal by four times compared bridge to single resistor. The output signal of the bridge is registered from one diagonal of the bridge, while the other is energized. The sensitivity is determined as the ratio of the magnitude of the output signal (imbalance voltage of the bridge under the action of magnetic field) to the magnetic field magnitude on the linear range of transfer characteristic. The application of a planar field causes a corresponding change in the output signal, and this characteristic has a distinct linear region and it is odd.

In this work magnetoresistors are obtained by means of using magnetron sputtering at the temperature of the substrate about  $\sim 270^\circ\text{C}$  and a magnetic field of about  $\sim 50$  Oe. Films, which are obtained on the substrate  $\text{Si}_3\text{N}_4 / \text{SiO}_2$ , have pronounced anisotropy. Experimental samples were manufactured on the silicon wafer with an insulating layer of  $\text{Si}_3\text{N}_4$ , which were sprayed with the aid of a magnetron a layer of permalloy 80%Ni20%Fe, using photolithography operation (electric circuit was formed with a pattern corresponding to the combined magnetic and conducting layers). A new topology of anisotropic magnetoresistive structures is proposed.

In the course of this work it is shown that the sensor based on magnetoresistive structures can detect the magnetic field changes. It is shown that the variation of the shape and size ratio of magnetoresistive elements and barber-pole structures influence the characteristics of the magnetization and the dynamic range of the sensors, as well as their range of maximum magnetic field sensitivity. It is shown that the obtained structures sensitivity can be increased with decreasing bias field. It was proved that obtained magnetoresistive structures can be used in the harshest operating conditions. Successful testing of experimental samples of magnetoresistive structures in magnetic field sensors was carried out.

The work was supported by the Minobrnauki RF (contract No. 075-15-2021-1350, dated 5 October 2021, internal number 15.SIN.21.0004) and conducted using the equipment of Multi-access center «Microsystem technics and electronic component base» MIET.

[1] S. Tumanski, Thin Film Magnetoresistive Sensors, IOP Publishing Ltd., 2001.

## Charge ordering in RFe<sub>2</sub>O<sub>4</sub> compounds and multicomponent order parameter

D. Maslov, Yu. Kudasov  
*RFNC-VNIIEF, Sarov, Russian Federation*

At present, interest is high in the class of substances RFe<sub>2</sub>O<sub>4</sub> (R = Y, Dy, Ho, Er, Tm, Yb, Lu, Sc, In) [1] with a variable valence of iron ions. The most experimentally studied compound is LuFe<sub>2</sub>O<sub>4</sub>, a multiferroic [2] with special ferroelectric properties [3]. Ferroelectricity in this compound is associated not with the displacement of ions, as in conventional ferroelectrics, such as BaTiO<sub>3</sub>, but with the establishment of a special charge ordering (CO) of iron ions. At low temperatures, magnetic ordering develops in LuFe<sub>2</sub>O<sub>4</sub>, which is closely related to the charge order. Both the charge and magnetic systems on triangular iron bilayers turn out to be strongly frustrated [4]. Previously, approaches were developed to describe the charge ordering within the framework of the Ising model in the stoichiometric [5] and nonstoichiometric [6] compound LuFe<sub>2</sub>O<sub>4</sub>, the simulation of charge storage at elevated pressure was performed [7], and the complex permittivity was studied [8].

The charge ordering in RFe<sub>2</sub>O<sub>4</sub>, which develops in hexagonal iron bilayers, has a complex structure. In total, up to 6 sublattices can be distinguished, depending on the charge structure. Therefore, in this report, we propose a new approach to the description of charge storage in RFe<sub>2</sub>O<sub>4</sub> compounds in terms of a multicomponent order parameter. This method makes it possible to strictly determine the number and structure of equilibrium phases. Using the example of LuFe<sub>2</sub>O<sub>4</sub>, an analysis of possible charge structures is carried out, and its phase diagram is constructed. The results of pyroelectric measurements of the spontaneous polarization of LuFe<sub>2</sub>O<sub>4</sub> [3] and, in particular, its change recorded near the magnetic ordering temperature are discussed.

1. N. Ikeda, T. Nagata, J. Kano, S. Mori, Present status of the experimental aspect of RFe<sub>2</sub>O<sub>4</sub> study, *Journal of physics: Condensed matter*, 27 (2015) 053201.
2. van den Brink J., Khomskii D. Multiferroicity due to charge ordering, *Journal of physics: Condensed matter*, 20 (2008) 434217.
3. Ikeda N., Ohsumi H., Ohwada K. et al. Ferroelectricity from iron valence ordering in charge frustrated system LuFe<sub>2</sub>O<sub>4</sub>, *Nature*, 436 (2005) 1136.
4. Kudasov Yu.B., Korshunov A.S., Pavlov V.N., Maslov D.A., Frustrated lattices of Ising chains, *Phys. Usp.* 55 1169–1191 (2012).
5. Yu.B. Kudasov, D.A. Maslov, Frustration and charge order in LuFe<sub>2</sub>O<sub>4</sub>, *PRB* 86 (2012) 214427.
6. D.A. Maslov, Yu.B. Kudasov, Charge ordering of multiferroic LuFe<sub>2</sub>O<sub>4</sub>: influence of doping and electric field, *Solid State Phenomena*, 233 (2015) 375.
7. G. R. Hearne, E. Carleschi, W. N. Sibanda, P. Musyimi, G. Diguët, Yu. B. Kudasov, D. A. Maslov, A. S. Korshunov, Coexistence of site- and bond-centered electron localization in the high-pressure phase of LuFe<sub>2</sub>O<sub>4</sub>, *PRB* 93 (2016) 105101.
8. Yu.B. Kudasov, M. Markelova, D.A. Maslov, V.V. Platonov, O.M. Surdin, A. Kaul, Biased dielectric response in LuFe<sub>2</sub>O<sub>4</sub>, *Physics Letters A*, 380 (2016) 3932.

# Comparative study of magnetic properties of non-stoichiometric $TbNi_5Mn_x$ and quasi-binary $TbNi_{5-x}Mn_x$ alloys

P. Terentev<sup>a,b,\*</sup>, N. Mushnikov<sup>a,b</sup>, E. Gerasimov<sup>a,b</sup>, V. Gaviko<sup>a,b</sup>,

A. Gubkin<sup>a,b</sup>, A. Inishev<sup>a,b</sup>

<sup>a</sup> Institute of Metal Physics of UB RAS, 620108, Sofia Kovalevskaya 18, Ekaterinburg, Russia

<sup>b</sup> Institute of Natural Sciences and Mathematics, Ural Federal University, 620002, Mira 19, Ekaterinburg, Russia

\*terentev@imp.uran.ru

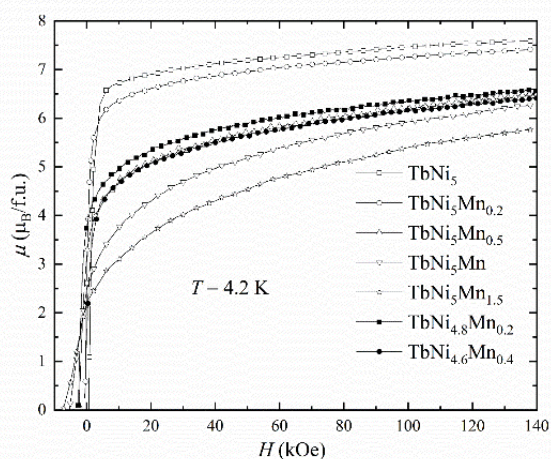


Fig. 3. Demagnetization curves of  $TbNi_5Mn_x$  and  $TbNi_{5-x}Mn_x$  compounds at  $T = 4.2$  K measured on powder samples.

We synthesized the non-stoichiometric  $TbNi_5Mn_x$  compounds and  $TbNi_{5-x}Mn_x$  quasi-binary solid solutions and studied their structure, magnetic and magnetothermal properties. The X-ray diffraction study allows to find that the single-phase hexagonal structure of the  $CaCu_5$  type is formed for the  $TbNi_5Mn_x$  non-stoichiometric compounds for  $x \leq 1.5$ , whereas the range of existence of the  $CaCu_5$  phase in the quasi-binary  $TbNi_{5-x}Mn_x$  alloys is limited to  $x \leq 0.4$ . The Mn alloying leads to an increase in the exchange interactions and Curie temperature of both compounds. Fig. 3 shows field dependencies of magnetization of  $TbNi_5Mn_x$  and  $TbNi_{5-x}Mn_x$  compounds. The magnetization decreases with increasing  $x$  as result of increasing magnetic moment of the  $3d$  sublattice which is oriented antiparallel to the magnetic moment of the Tb sublattice. The bulk magnetization data do not allow us to conclude

on whether the magnetic moment appears at the Ni sites. The magnetization curves of the compounds with manganese demonstrate lack of saturation in magnetic fields up to 140 kOe, which we attribute of the formation of non-collinear magnetic structure due to a competition of the exchange interactions and appearance of low-symmetry local crystal electric fields at the Tb positions. The coercive force increases with increase of the manganese concentration in  $TbNi_5Mn_x$  compounds due to the pinning of narrow domain walls on structural defects caused by local exchange/anisotropy variations.

The research was supported by RSF (project No. 23-22-00140).

## Composite of polymer ferromagnetic microwires for sensor applications.

A. Davkina<sup>1</sup>, A. Amirov<sup>2</sup>, V. Rodionova<sup>1</sup>

<sup>1</sup>Immanuel Kant Baltic Federal University, Kaliningrad, Russian Federation

<sup>2</sup>National Research Centre “Kurchatov Institute”, Moscow, Russian Federation

The development of magnetic/electric sensing materials with improved performance, microsize and wireless operation are increasingly critical for applications in structural health and environmental monitoring, security systems, biology, and medicine. Recently the concept of smart composites with magnetic sensing fibres has been extensively developing [1,2]. The present work devoted to the design and studies of smart composite materials with combined magnetic-electric effects based on Co-Fe ferromagnetic microwires (MW) embedded in polymer matrix of polyvinylidene fluoride (PVDF) polymer with piezoelectric response. These magnetoelectric smart composites (MESC) can be used as a sensitive element of sensory applications.

Magnetoelectric smart composite of MW/PVDF, consisted of Co-Fe based ferromagnetic microwires embedded in piezoelectric polymer PVDF matrix has been fabricated using solving casting method. For this procedure, PVDF granules (Alfa Aesar) were dissolved in dimethylformamide (DMF) (Sigma-Aldrich) with a weight ratio of 1:10. Complete dissolution of PVDF and obtaining a homogeneous solution was achieved using an ultrasonic bath for 45 minutes at a temperature of about 40 °C. Then ferromagnetic microwires were fixed, mounted parallel on template, coated by PVDF solution and dried at temperature 80 °C for 30 min. Coating by PVDF was repeated 4 times layer by layer to obtain the composite structure with fully embedded MWs in polymer matrix. The thickness of composite was about 0.5 mm with distance between microwires about 0.5 mm (Fig 1a). The harmonic spectrum of prepared samples has been studied by use of selective lock-in amplifier (SR830) with help of flat coil, which give an option of remote detection of voltage signal produced during remagnetizing of magnetic microwires.

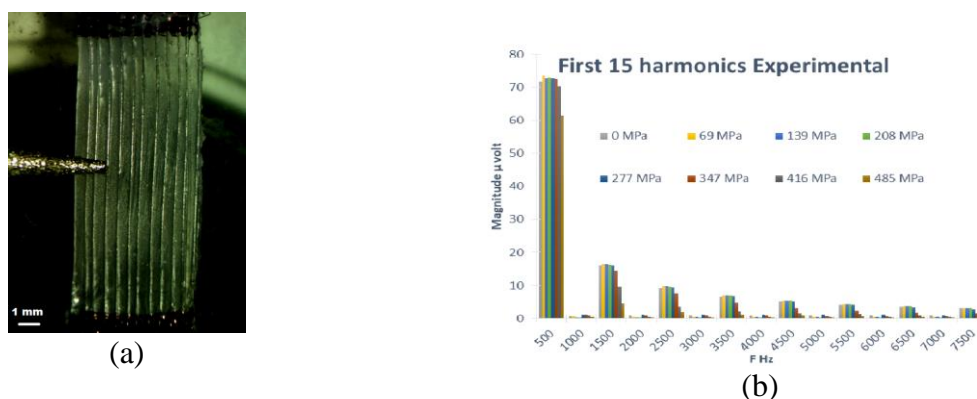


Fig. 1. Image (a) and harmonic spectrum (b) of MW/PVDF MESC (MW-glass-coated amorphous  $\text{Co}_{83}\text{Fe}_7\text{C}_1\text{Si}_7\text{B}_2$  microwires, PVDF- polyvinylidene fluoride).

We are presenting here a new method of monitoring internal stresses by using the stress-dependent harmonic spectra when the wire is remagnetized. The high harmonic spectrum of MESC of MW/PVDF are demonstrated in Fig.1 (b). The possibility of remote monitoring of effect of stress/strain, magnetic and electric field on properties of composite materials for sensory applications were demonstrated.

### Reference

[1] A.D.M. Charles, A.N. Rider, A.S. Brown, C.H. Wang / Progress in Materials Science 115 (2021) 100705.

[2] F.X. Qin, H-X. Peng / Progress in Materials Science 58 (2013) 183–259.



## Control of InGaAs/GaAs/Al<sub>2</sub>O<sub>3</sub>/CoPt spin light-emitting diodes characteristics by ion irradiation method

P. Demina, M. Dorokhin, A. Zdoroveyshchev, I. Kalentieva, Yu. Danilov, Yu. Dudin

Lobachevsky University, 603950, Gagarin Avenue 23/3, Nizhny Novgorod, Russia

\*demina@phys.unn.ru

The study of spin injection and relaxation processes in diodes based on semiconductor structures with ferromagnetic injectors is of interest from the point of view of introducing spintronic devices into modern microelectronics. The main principles of both the operation of spin LEDs based on InGaAs/GaAs nanostructures with a CoPt injector and the ways to increase their efficiency were discussed in [1]. In this paper, we report on the results of studying the modification of a CoPt film by irradiation with He<sup>+</sup> ions and its influence on the circular polarization of a spin light emitting diode (SLED). The irradiation doses were chosen so as to neither introduce visible changes into the micromagnetic structure of the CoPt film nor to quench the electroluminescence emission of the diode. At the same time the doses were high enough change the properties of the ferromagnetic film and its effect on the spin precession.

The semiconductor part of the diode structure was grown by MOCVD epitaxy on an AIX200RF setup (Aixtron). The ferromagnetic CoPt injector was deposited by electron beam evaporation in vacuum. The diode diameter was 500 μm, and the radiation was collected from the substrate side to prevent multiple reflections and the influence of the MCD effect. The resulting SSIDs were irradiated by He<sup>+</sup> ions at the ILU-3 accelerator with a fluence of  $1 \times 10^{12} \text{ cm}^{-2}$  ( $2 \times 10^{12} \text{ cm}^{-2}$ ) and an energy of 20 keV. The choice of the helium ion fluence was made taking into account the calculations of the distribution of arising defects over the depth of structures, carried out using the SRIM program.

The effect of ion irradiation on the I-V characteristics, electroluminescence intensity ( $I_{EL}$ ), and the degree of circular polarization of electroluminescence ( $P_{EL}$ ) of SLED was studied. It has been established that under ion irradiation with the indicated fluence, it is possible to preserve the emission properties of the InGaAs/GaAs quantum well, however, the  $I_{EL}$  of such diodes decreases by more than an order of magnitude due to the penetration of defects into the active region. Surprisingly near 4-fold increase in the degree of circular polarization of electroluminescence was revealed. The exact value was found to depend on the thickness of the GaAs cap layer. It has also been established that the reverse current of irradiated diodes decreases by an order of magnitude to values of  $1 \times 10^{-7} \text{ A}$  at a voltage of -2 V. We assume that the both the increase sign reversal of the circular polarization degree after exposure is associated with a change in the internal magnetic field of the inhomogeneously magnetized CoPt contact, which “twirls” the spin-polarized injected carriers with a different oscillation period. A change in such an “internal” magnetic field may be associated with an increase in the homogeneity of the alloy due to the mixing of the components under the influence of high-energy ions. Apparently, the change in the  $P_{EL}$  value is also influenced by the change in the recombination time  $\tau_R$ . Thus, when radiation defects are introduced, the value of  $\tau_R$  decreases at a constant spin relaxation time  $\tau_S$ , and the value of  $P_{EL} \sim 1/(1+\tau_R/\tau_S)$  increases [2].

Thus, the paper shows the possibility of controlling the degree of circular polarization of spin light-emitting diodes with a CoPt injector by exposing the finished diodes to low-energy and dose He<sup>+</sup> ion irradiation. The results obtained may be of interest for the technology of spin optoelectronic devices.

This work was supported by the Russian Science Foundation (grant no. 21-79-20186).

[1] M.V. Dorokhin, PSS. 59, 2155 (2017)

[2] G. Salis, APL. 87, 262503 (2005)

## Controlling the nucleation and collapse of magnetic skyrmions by an external magnetic field

M. Potkina<sup>a\*</sup>, I. Lobanov<sup>a</sup>, V. Uzdin<sup>a</sup>,

<sup>a</sup>Faculty of Physics, ITMO University, 197101, St.Petersburg, Russia

\* potkina.maria@yandex.ru

The fundamental problem of using topological solitons in the technology of magnetic racetrack memory is their stability with respect to thermal fluctuations and the possibility of writing and reading information contained in a sequence of moving magnetic structures. A quantitative measure of the stability of magnetic states is their lifetime, which can be estimated on the basis of the transition state theory (TST) for magnetic degrees of freedom [1].

A similar approach can be applied to estimate the probability of nucleation of topological solitons, such as skyrmions, from a homogeneous magnetic state. In this case, a topologically trivial ferromagnetic (FM) configuration should be chosen as the initial state, and a skyrmion should be considered as the final state. After finding the minimum energy path from the initial to the final state, the activation barrier is determined by the energy difference between the saddle point (SP) on the energy surface and the FM configuration. If a skyrmion is metastable, the activation barrier for nucleation is higher than for its collapse. The preexponential factor in the Arrhenius law for the nucleation of skyrmions can be computed in the harmonic approximation to TST if the energy surface near the initial FM state and near the SP is approximated by a quadratic expansion. The theory can be applied also for description of the nucleation of antiskyrmions [2] and antiferromagnetic skyrmions [3].

With increasing temperature, the rate of nucleation processes increases rapidly and can be comparable with the rate of collapse of the skyrmion and even exceed it. In which state it is more likely to detect a system at a fixed temperature depends on the magnitude of the external magnetic field. This explains the possibility of creating and deleting single magnetic skyrmions by applying current from the tip of a tunneling microscope [4].

Knowing the rate of collapse and nucleation of skyrmion states makes it possible to estimate the equilibrium concentration of skyrmions at arbitrary temperatures and magnetic fields. In equilibrium, the number of nucleated and decayed skyrmions per unit of time is the same. But it should be considered that a skyrmion can be nucleated at any node of the lattice, and collapse only where it was.

The study was supported by the Russian Science Foundation grant No. 22-72-00059, <https://rscf.ru/en/project/22-72-00059/>

[1] I. S. Lobanov, M.N. Potkina, V. M. Uzdin, JETP Letters, **113**, 801 (2021).

[2] M. N. Potkina, I. S. Lobanov, O. A. Tretiakov, H. Jónsson, V. M. Uzdin, PRB, **102**, 134430 (2020).

[3] M. N. Potkina, I. S. Lobanov, H. Jónsson, V. M. Uzdin, J. Appl. Phys., **127**, 213906 (2020)

[4] N. Romming, C. Hanneken, M. Menzel, J. E. Bickel, B. Wolter, K. von Bergmann, A. Kubetzka, R. Wiesendanger, Science, 2013, 341, 6146, P.636-639.

# Correlation Between FeCo Nanowire Growth Features and Their Structural and Magnetic Properties

D. Khairtdinova<sup>a,b,c,\*</sup>, I. Doludenko<sup>b</sup>, I. Volchkov<sup>b</sup>, L. Panina<sup>c,d</sup>

<sup>a</sup> Smart Sensors Laboratory, NUST MISIS, 119049, Moscow, Leninskiy avenue 4, Moscow, Russia

<sup>b</sup> FSRC “Crystallography and Photonics” RAS, 119333, Leninskiy avenue 59, Moscow, Russia

<sup>c</sup> NUST MISIS, 119049, Leninskiy avenue 4, Moscow, Russia

<sup>d</sup> Immanuel Kant Baltic Federal University, 236004, Nevskogo 14, Kaliningrad, Russia

\*khairtdr@gmail.com

Magnetic properties of nanowires (NWs) strongly depend on the combination of their crystal structure and shape anisotropy. One of the available methods for obtaining such structures is matrix synthesis, which makes it possible to obtain NWs with a given composition and aspect ratio. However, the electrodeposition of metals of the iron group has several features that affect the structural and magnetic properties of nanowires. Here, the properties of  $\text{Fe}_x\text{Co}_{1-x}$  NWs obtained with varying growth time were studied.

$\text{Fe}_x\text{Co}_{1-x}$  NWs were obtained by electrochemical deposition in the pores of industrial polymer track membranes (TM) (JINR, Dubna) with a pore diameter of 100 nm and a pore density of  $1.2 \cdot 10^9$  pore/cm<sup>2</sup>. Electrolytes containing  $\text{Fe}^{2+}$  and  $\text{Co}^{2+}$  ions in various proportions were used (% $\text{Fe}^{2+}$ : 6; 43; 92). For each composition, a series of samples with increasing growth times were obtained (maximum time corresponds to the time needed to completely fill TM). The obtained samples were studied using SEM, XRD, and VSM.

The SEM results showed that the length of the NWs of all compositions depends non-linearly on the growth time. A comparison of experimental data and theoretical analysis of NWs' lengths made it possible to estimate the percentage of charge involved in a deposition. On average, it was 45-60%, which can be explained by the specifics of NW growth, in particular, by the release of hydrogen bubbles during the electrodeposition.

The XRD method was used to determine the lattice parameters for each NWs' growth time and the element ratio based on the Vegard rule. It was shown that the ratio of elements in NWs differs from the ratio of  $\text{Fe}^{2+}$  and  $\text{Co}^{2+}$  ions in the electrolyte. The deviation has a complex nonlinear character along the entire length of NWs with a tendency to iron increase, which is due to anomalous co-deposition of iron.

The VSM results also reveal the change in the hysteresis loops (e. g. petal-like hysteresis loops in the magnetic field perpendicular to NW axis (IP)) depending on their growth time, which correlates with a change in the Fe content in NWs, magnetic shape anisotropy and the dipole-dipole interaction within the array. The change in coercive fields ( $H_c$ ) has a nonlinear dependency on NWs' lengths and tends to increase with increasing the length. However, there are some deviations, which can be explained by the change in NW composition. The values of  $H_c$  in all samples are higher in IP field configuration, which can be due to the prevailing dipole-dipole interactions between NWs in the array, as the distance between NWs is of the same order as their diameter.

The study of the growth features and structure of obtained NWs makes it possible to obtain nanoparticles with specified geometric parameters and controlled structural and magnetic properties for various applications.

Acknowledgments. NW synthesis was done within the State task of FSRC “Crystallography and Photonics” of RAS. The magnetic measurements were held and supported by NUST MISIS within the framework of the «Priority 2030» (project K6-2022-043). The authors are thankful to P. Apel for presenting polymer matrices.

# Creation and studying of a magnetoresistive spin light-emitting diode

M. Ved\*, M. Dorokhin, A. Zdoroveyshchev, P. Demina, D. Zdoroveyshchev

Research Institute for Physics and Technology of Lobachevsky State University, 603950, Gagarina ave., 23,

Nizhny Novgorod, Russia

\*mikhail28ved@gmail.com

The functional combination of the basic elements of spintronics (a magnetoresistive element and a spin light-emitting diode) is an urgent task, since the use of such an approach leads to an increase in the information capacity of semiconductor elements, which are memory cells in information storage, transmission, and processing circuits. In addition, such a device can be used as a detector of small magnetic fields.

This work reports on the creation of a laboratory model of a device with an independent change of two parameters (intensity and degree of circular polarization of radiation) carried out by applying external magnetic fields.

The device described in this paper is a magnetoresistive spin LED, which is a combination of an emitting heterostructure with an InGaAs/GaAs quantum well (QW) with a CoPd spin injector and a magnetoresistive element, which is a sequence of thin layers of Cr/Co<sub>90</sub>Fe<sub>10</sub>/Cu/Co<sub>90</sub>Fe<sub>10</sub>. The semiconductor light-emitting part of the studied structure was formed on an n-GaAs substrate by MOCVD in a hydrogen flow. The ferromagnetic CoPd injector and all layers of the magnetoresistive element were formed by electron beam evaporation in vacuum. At the final stage, using photolithography and chemical etching, contacts of a special shape were formed on the surface of the structures. For electrical isolation of the semiconductor structure around the mesa contacts, the parts of the structure not covered by the contacts were irradiated with He<sup>++</sup> ions before the deposition of the magnetoresistive element layers.

Two maxima are observed on the dependence of the relative intensity of electroluminescence (EL) on the magnetic field. The nature of the magnetic field dependence of the relative EL intensity is similar to the magnetic field dependence of the resistance of a magnetoresistive element. So observed EL intensity modulation is associated with a change in the resistance of the magnetoresistive contact layer. It should be noted that at a current of 36 mA the device operates in the key mode: in a magnetic field of  $\pm 50$  mT, the relative intensity takes on maximum values; in a zero magnetic field and in a field above 100 mT, it is equal to zero. An explanation of the most probable mechanism for increasing the EL intensity in a longitudinal magnetic field for a studied device is presented in [1].

When the magnetoresistive spin light-emitting diode is placed in a transverse magnetic field, the radiation becomes partially circularly polarized. The magnetic field dependence of the degree of circular polarization ( $P_{EL}$ ) is non-linear function with a hysteresis loop. The maximum value of  $P_{EL}$  was 0.4%. Such a dependence is due to the injection of spin-polarized charge carriers from the ferromagnetic contact CoPd.

Thus, in this work, a laboratory sample of the device was created and studied, which has four independently variable states (high-intensity radiation with right and left circular polarization and low-intensity radiation with right and left circular polarization).

By the support of the Russian Science Foundation (project № 21-79-20186).

[1] M. Ved, APL 118, 092402 (2021)

## Crystal structure investigation of Cr<sub>2</sub>GeC MAX-phase nanofilms by RHEED

S. Lyaschenko, T. Andryushchenko, I. Yakovlev\*, S. Varnakov  
Kirensky Institute of Physics, Federal Research Center KSC SB RAS, 660036,  
Akademgorodok 50/38, Krasnoyarsk, Russia

\*yia@iph.krasn.ru

MAX-phase materials (M<sub>n+1</sub>AX<sub>n</sub>, n = 1, 2, or 3) [1] are nano-layered hexagonal compounds. In these materials, M is an early transition metal, A is a main group element, and X is C or N. The atomic layers are stacked along the axis. MAX-phases combine both ceramic and metallic characteristics - resistance to high temperature oxidation, self-healing ability and susceptibility to thermal shock. Among the possible MAX-phase compounds, there are also materials with the strong magnetic ordering [2]. New properties combination of these materials originates new functionality for various sensors and actuators that are used in industry and high-tech technology.

To study the processes of Cr<sub>2</sub>GeC films synthesis, Cr, Ge, and C were co-deposited by magnetron sputtering in various atomic ratios on MgO(111) substrates at a temperature of 600 °C. After deposition, the films were annealed at a temperature of 850 °C for 30 minutes. The film thickness was about 10 nm. To clean the surface before experiment the substrates were annealed at T=850 °C in ultrahigh vacuum (UHV) and then it was etched with argon ions and removed 2–3 nm of the surface layer. The base pressure in the working chamber is not more than 10<sup>-8</sup> Pa, the pressure in the deposition process is not more than 10<sup>-1</sup> Pa. The crystal structure study was carried out by the reflection high energy electron diffraction method (RHEED) with 24.5 kV beam energy. The diffraction patterns were interpreted by visually combining the experimental and theoretically calculated patterns for a given crystal in a graphics editor. The theoretical picture was calculated based on the kinematic electron diffraction theory.

When the film was deposited in the stoichiometric Cr<sub>2</sub>GeC ratio (Cr(50 at.%) + Ge(25.2 at.%) + C(24.8 at.%)), two phases are formed according to the RHEED analysis (Figure 1): hexagonal Cr<sub>2</sub>GeC - gray dots and cubic Cr<sub>23</sub>C<sub>6</sub> - blue dots. The electron diffraction pattern for the first phase was calculated in the [100]<sub>Cr<sub>2</sub>GeC</sub> direction and for the second phase in the [210]<sub>Cr<sub>23</sub>C<sub>6</sub></sub> direction. But with an increase in chromium

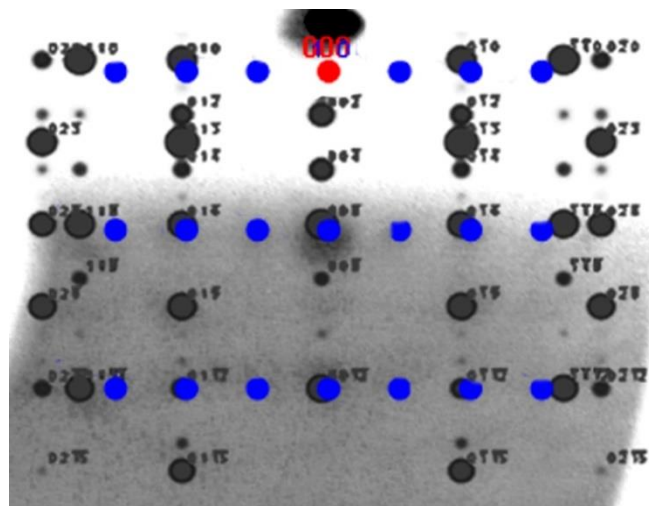


**Figure 4. RHEED pattern from the (Cr(50 at.%) + Ge(25.2 at.%) + C(24.8 at.%) film in**

and a decrease in germanium (Cr(55 at.%) + Ge(16.8 at.%) + C(28.2 at.%)), chromium germanide with a cubic crystal lattice (CrGe or

Cr<sub>3</sub>Ge) is formed in addition to Cr<sub>2</sub>GeC.

The research was performed at the Magnetic MAX Materials Laboratory of the Kirensky Institute of Physics with the financial support of the Russian Science Foundation #21-12-00226, <http://rscf.ru/project/21-12-00226/>.

[1] M. Sokol, et.al., Trends in Chemistry, 1(2), 210-223 (2019).

[2] F. M. Romer, M. Farle, et.al, RSC Advances 7(22), 13097-13103 (2017).

# Data Processing Algorithms for Magneto-optical Ellipsometry of Thin Films with Optical Uniaxial Anisotropy

O. Maximova <sup>a,b,\*</sup>, S. Lyaschenko <sup>a</sup>, I. Yakovlev <sup>a</sup>, D. Shevtsov <sup>a</sup>, T. Andryushchenko <sup>a</sup>,

S. Varnakov <sup>a</sup>, S. Ovchinnikov <sup>a,b</sup>

<sup>a</sup> Kirensky Institute of Physics, Federal Research Center KSC Siberian Branch Russian Academy of Sciences,  
660036, bld. 38, Akademgorodok 50, Krasnoyarsk, Russia

<sup>b</sup> Siberian Federal University, 660041, Svobodny 79, Krasnoyarsk, Russia

\* [maximo.a@mail.ru](mailto:maximo.a@mail.ru)

Despite the attractiveness of Mueller ellipsometry [1, 2], due to the development of its methodological side and the availability on sale of modern ellipsometers that measure all components of Mueller matrices for several angles of light incidence and immediately process this data set, it remains not widely available due to the high cost of the mentioned equipment, and also due to the difficulty of finding all 16 components of the Mueller matrices when working with an ellipsometer not sharpened for this specificity.

At the same time, taking into account all advantages of the ellipsometry method, especially its high sensitivity, one cannot deny the expediency of its use for determining the physical properties of thin films, which necessitates the development of the method with the aim of its popularization, especially by removing the key problematic issue that frightens many researchers, namely, how to process the obtained data.

In this regard, we have developed algorithms for processing data obtained by magneto-optical (MO) ellipsometry from ferromagnetic structures.

In previous papers, we reported on how to work with different isotropic structures, e.g. in [3] and [4], or with anisotropic [5] but being large enough to be described by a model of a semi-infinite medium. In this work, we have obtained all the necessary expressions for processing MO ellipsometry data from thin anisotropic ferromagnetic films on isotropic substrates. The resulting expressions can be applied to data collected in transverse geometry, at a certain angle of incident light, both in situ and ex situ, as well as for temperature studies of the optical and magneto-optical properties of samples.

This work was supported by the grant from the Russian Science Foundation No. 21-12-00226, <http://rscf.ru/project/21-12-00226/>

[1] K. Mok, Phys. Rev. B 84, 094413 (2011).

[2] K. Mok, Rev. Sci. Instrum. 82, 033112 (2011).

[3] O. Maximova JETP Letters, 110, No. 3, 166–172 (2019)

[4] O. Maximova, Physics of the Solid State, 63, 1485–1495 (2021).

[5] O. Maximova, JETP, 133, No. 5, 581–590 (2021)

# Effect of Synthesis Conditions on the Magnetic Properties of Chromium Borate Single Crystals

N. Mikhashenok<sup>a,\*</sup>, A. Pankrats<sup>b</sup>, I. Gudim<sup>b</sup>, S. Skorobogatov<sup>b</sup>, M. Molokeev<sup>b</sup>

<sup>a</sup> Federal Research Center KSC SB RAS, 660000, Akademgorodok 50, Krasnoyarsk, Russia

<sup>b</sup> Kirensky Institute of Physics, Federal Research Center KSC SB RAS, 66000, Akademgorodok 50/38, Krasnoyarsk, Russia

\*natali\_sapronova@mail.ru

The borate family with a general formula  $RM_3(BO_3)_4$  (R stands for Y or rare-earth (RE) elements,  $M = Al, Fe, Cr, Ga, Sc, Mn$ ) has wide variety of physical properties depending on chemical composition and growth conditions. Magnetic properties of RE borates with the magnetic ions  $Fe^{3+}$  and  $Cr^{3+}$  are of fundamental interest due to a coexistence and interaction of two magnetic subsystems (3d and 4f ions). Though there is a lot of research on the iron borates, the RE chromium borates are still understudied [1-3].

The RE chromium borates have polytypic nature and, depending on growth conditions, crystallize in two modifications, namely, a non-centrosymmetric rhombohedral one and a centrosymmetric monoclinic one [4, 5]. Rare-earth chromium borate  $TbCr_3(BO_3)_4$  single crystal with huntite-like structure were grown from fluxes based on two different solvents. When using  $Li_2WO_4$  as a solvent, the single crystals of trigonal symmetry with non-centrosymmetric sp. gr. R32 crystallized. Whereas, when  $Bi_2Mo_3O_{12}$  as a solvent was used, the single crystals grown in a series of syntheses predominantly belonged to the monoclinic sp. gr. C2/c.

Measurements of the magnetic properties were carried out for single crystals of both symmetries; the results are shown on Fig. 1.

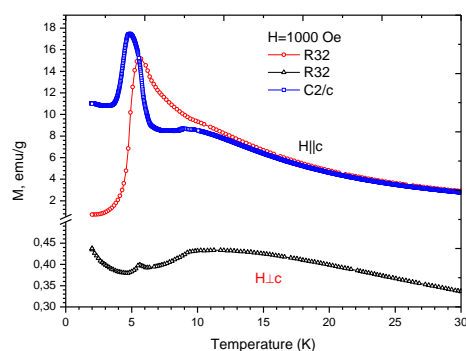


Fig. 1. The temperature dependences of magnetization of  $TbCr_3(BO_3)_4$  single crystals

The temperature dependences of magnetization show that most likely there are two critical temperatures:  $\sim 5.5K$  and  $\sim 9.5K$ . The upper temperature, apparently, is the Néel temperature corresponding to the magnetic ordering of the Cr subsystem, which polarizes the Tb subsystem due to the f-d exchange interaction. At the lower temperature, the spontaneous spin-reorientation transition from an “easy plane” antiferromagnetic state to an “easy axis” one occurs.

This work is supported by RSF and KRFS, grant no. 22-12-20019.

- [1] E.A. Popova et al., Phys. Rev. B 75, 054446 (2007)
- [2] K.N. Boldyrev, E.P. Chukalina, N.I. Leonyuk, Phys. Sol. St. 50, 1681 (2008)
- [3] L. Gondek et al., J. Sol. St. Chem. 210, 30 (2014)
- [4] V.S. Kurazhkovskaya et al., J. Struct. Chem. 52, 699 (2011)
- [5] E.Yu. Borovikova et al., Vibr. Spectr. 68, 82 (2013)

## Effect of Uncontrolled Impurities on Magnetic and Structural Transitions of the $\text{GdFe}_3(\text{BO}_3)_4$ Multiferroic

I. Gudim\*, E. Eremin, A. Krylov, V. Titova

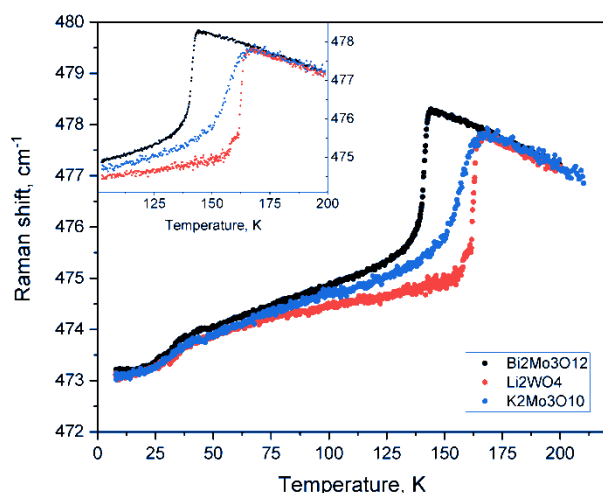
Kirensky Institute of Physics, Krasnoyarsk Scientific Center, Siberian Branch, Russian Academy of Sciences,  
Krasnoyarsk 660036, Russia

irinagudim@mail.ru

Rare-earth ferrobates with the huntite structure and with the general formula  $\text{RFe}_3(\text{BO}_3)_4$  ( $\text{R} = \text{Y}, \text{La-Lu}$ ) attract increased attention due to the discovery of their multiferroic properties. Initially, for isostructural nonlinear optical crystals of trigonal aluminoborates  $\text{RAl}_3(\text{BO}_3)_4$ , a method was developed for growing from melt solutions based on potassium trimolybdate  $\text{K}_2\text{Mo}_3\text{O}_{10} - \text{B}_2\text{O}_3$  [1].

Later, new melt solutions based on bismuth trimolybdate  $\text{Bi}_2\text{Mo}_3\text{O}_{12} - \text{B}_2\text{O}_3$  were proposed for growing  $\text{RAl}_3(\text{BO}_3)_4$  and  $\text{RFe}_3(\text{BO}_3)_4$  single crystals [2]. In these melt solutions,  $\text{Bi}_2\text{O}_3$  and  $\text{MoO}_3$  are bound more strongly than  $\text{K}_2\text{O}_3$  and  $\text{MoO}_3$ . Therefore, it was assumed that the replacement of the rare earth element by bismuth and molybdenum in the grown crystal is relatively small.

However, it was shown that  $\text{Bi}^{3+}$  ions replace the rare-earth ion in an amount of up to 5 at. %. Then, melt solutions based on lithium tungstate were proposed [3]. In the latter case, it is assumed that the crystal matrix does not contain impurities from the solvent. The paper presents a comparative analysis of the effect of K, Mo, and Bi impurities on the magnetic ( $T_N \sim 35 \text{ K}$ ) and structural ( $T_S \sim 160 \text{ K}$ ) transitions of the  $\text{GdFe}_3(\text{BO}_3)_4$  multiferroic.



The figure shows the temperature dependence of one of the vibration modes obtained using the Raman effect. One can clearly see a decrease in the temperature of both the magnetic and structural transitions for  $\text{GdFe}_3(\text{BO}_3)_4$  grown from potassium-molybdate and bismuth-molybdate solvents. This confirms the fact that the use of a lithium tungstate solvent makes it possible to obtain the purest crystals.

Support by RSF and KRFS № 22-12-20019 are acknowledged.

1. N. N. Kuzmina, V. V. Maltsev, E. A. Volkova, *Neorganicheskie Materialy*, (2020), Vol. 56, No. 8, pp. 873–881.
2. L.N. Bezmaternykh, S.A. Kharlamova, V.L. Temerov, *Krystallography Report* -2004. -v. 49, iss. 4, p. 1-3.
3. I.A. Gudim, E.V. Eremin, N.V. Mikhashenok, V.R. Titova *ФТТ*(2023), v. 65, iss. 2, p. 243.



## Electron Charge Accumulation by Island Surfaces of Cr-Mn Based MAX Phase Thin Films on MgO

T. Andryushchenko<sup>a,b,\*</sup>, S. Lyaschenko<sup>a</sup>, S. Varnakov<sup>a</sup>, S. Ovchinnikov<sup>a,c</sup>, D. Shevtsov<sup>a</sup>, I. Yakovlev<sup>a</sup>

<sup>a</sup>Kirensky Institute of Physics SB RAS, 660036, Akademgorodok 50/38, Krasnoyarsk, Russia

<sup>b</sup>Federal Research Center KSC SB RAS, 660036, Akademgorodok 50, Krasnoyarsk, Russia

<sup>c</sup>Siberian Federal University, 660041, Svobodny 79, Krasnoyarsk, Russia

\*ata12@iph.krasn.ru

The MAX phases  $M_{n+1}AX_n$  ( $n = 1-4$ ) are nanolayered hexagonal structures, with layers of transition metal  $M$  carbides or nitrides ( $X = C$  or  $N$ ) alternating with layers of the periodic table XIII–XV group elements ( $A = Al, Ge, Si, \text{etc.}$ ). The Cr- and Mn-containing MAX phases demonstrate ferromagnetic ordering [1], and their 2D derivatives, MXenes, are of particular interest as a potential materials with two-dimensional magnetism.

We have carried out the magnetron co-deposition synthesis of  $(Cr,Mn)_2GeC$  thin films at the Magnetic MAX materials laboratory in the Kirensky Institute of Physics SB RAS for the following transition to the Cr-Mn based MAX phases with gallium as an  $A$  element. The MAX phase  $Cr_2GeC$  and  $(Cr,Mn)_2GeC$  thin films with a thickness of 40–100 nm were synthesized on  $MgO(111)$  substrates at the temperature of  $850^\circ C$ . Thin films of pure MAX phases without secondary phase presence were obtained in the case of alteration of initial technological stoichiometry to carbon and  $(Cr, Mn)$  concentrations increasing.

The Auger electron spectroscopy were used as in-situ technique for determination of the thin film chemical composition, in particular to identify the carbon form – graphite or carbide. However, we have found the shift of thin film Auger peaks by  $+(7 \pm 1)$  eV for 40 nm  $Cr_2GeC$  sample. For other thin films there are distortions making the Auger spectra interpretation impracticable. It is the electron beam induced charging of sample surface that affect the spectra changes. The electron charge accumulation is caused by island surface of (metallic thin film)/ $MgO$  structure [2] and in our current research it was an indirect indication of sample morphology and substrate surface coverage.

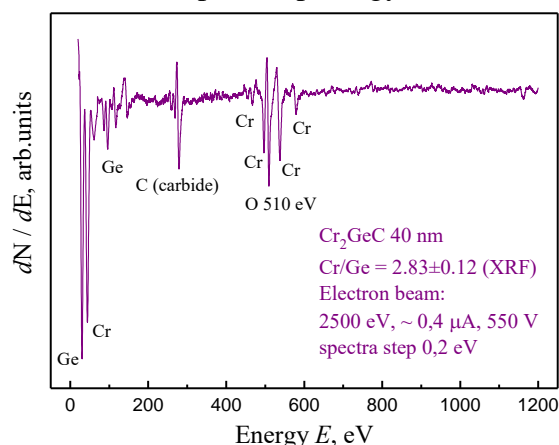


Figure 1. Auger electron spectra of  $Cr_2GeC$  MAX phase on  $MgO$  with a shift of peaks

The research was supported by the Russian Science Foundation (grant #21-12-00226, <http://rscf.ru/project/21-12-00226/>).

[1] R. Salikhov, Mater. Res. Lett. 3, 156 (2015).

[2] P.J. Møller, J. He, NIMB 17(2), 137 (1986).

# Electronic Transport in Cr<sub>2</sub>GeC and Cr<sub>2-x</sub>Mn<sub>x</sub>GeC Thin Films Grown by Magnetron Sputtering

A. Tarasov<sup>a,b\*</sup>, M. Rautskii<sup>a</sup>, A. Lukyanenko<sup>a,b</sup>, M. Bondarev<sup>a,b</sup>, S. Lyaschenko<sup>a</sup>,  
T. Andryushchenko<sup>a</sup>, and S. Varnakov<sup>a</sup>

<sup>a</sup> Kirensky Institute of Physics, Federal Research Center KSC SB RAS, 660036, Akademgorodok 50/38  
Krasnoyarsk, Russia

<sup>b</sup> Siberian Federal University, 660041, Svobodniy 79, Krasnoyarsk, Russia

\*taras@iph.krasn.ru

MAX phases are a family of layered hexagonal compounds with the general formula M<sub>n+1</sub>AX<sub>n</sub>, where M is early transition metal, A is A-group element, C is carbon or nitrogen. This material has unique properties, combining the lightness and strength of ceramics and metallic electrical and thermal conductivity [1]. In this work, we studied the transport and magnetotransport properties of thin films of pure and manganese-substituted MAX phase Cr<sub>2</sub>GeC synthesized by magnetron co-deposition from elementary targets focused on a heated sample. Synthesis was carried out on MgO(111) substrates heated to 750-800°C with post-annealing of the samples in UHV (10<sup>-9</sup> Torr) for 30 minutes at 850°C. The synthesis process was monitored in situ using RHEED and Auger spectroscopy. Using the analysis of in situ RHEED and ex situ XRD data, it was found that all samples contain the MAX phase of Cr<sub>2</sub>GeC, and some of them also contain chromium germanides CrGe and/or Cr<sub>3</sub>Ge. It was found that the samples with the presence of a pure MAX phase combine a high technological content of carbon (more than 28 at.%) and an 2.8 atomic ratio (Cr+Mn)/Ge, i.e. almost 50% more than the ideal stoichiometry. At the same time, the deposition rates and heating regimes practically do not affect the phase formation, in contrast to the Cr-Ge-C atomic ratios.

Resistivity ( $\rho$ ) for Cr<sub>2</sub>GeC samples 10 nm, 35 nm, 40 nm and 100 nm thick shows a metallic behavior regardless of the thickness, decreasing with decreasing temperature (300K – 4K). The value of  $\rho$  for a Cr<sub>2</sub>GeC film with a thickness of 100 nm at 300 K is 1.4  $\mu\Omega\cdot\text{m}$ , which is a typical value for MAX phases (0.5–4  $\mu\Omega\cdot\text{m}$ ), close to the values for the previously studied Mn<sub>2</sub>GaC (2.9  $\mu\Omega\cdot\text{m}$ ) and (Cr,Mn)<sub>2</sub>GaC (1.6  $\mu\Omega\cdot\text{m}$ ), and is consistent with the literature data on Cr<sub>2</sub>GeC bulk [2] and film [3]. An increase in  $\rho$  with decreasing thickness is directly related to the crystalline quality of the films and their microstructure, which agrees with the data of optical measurements and atomic force microscopy. The resistivity of the manganese-substituted (Cr,Mn)<sub>2</sub>GeC sample behaves radically differently: it increases with decreasing temperature and also exceeds  $\rho$  for Cr<sub>2</sub>GeC by 4 orders of magnitude. This behavior may be due to poor coalescence of crystallites, which was previously observed for Cr<sub>2</sub>AlC films [4]. For all samples, the Hall effect and magnetoresistance were measured in a wide temperature range (4K -300 K) and a magnetic field up to 9 T, the Hall constant, mobility and concentration of charge carriers were calculated. Carriers' mobility for all samples of Cr<sub>2</sub>GeC is about 1 cm<sup>2</sup>/V\*s, that is typical value for metals. It should be noted that the temperature dependence of the mobility is nonmonotonic, showing a maximum in the region of 40–50 K. A similar behavior was observed for bulk samples and, most likely, is associated with the electron–electron component of scattering [5].

The research was funded by RSF, project № 21-12-00226.

- [1] M. Sokol et al., Trends in Chemistry 1(2), 210-223 (2019)
- [2] M. W. Barsoum et al., Journal of the American Ceramic Society 94(12), 4123-4126 (2011)
- [3] P. Eklund et al., Physical Review B 84(7), 075424 (2011)
- [4] M. Stevens et al., Materials Research Letters 9(8), 343-349 (2021)
- [5] S. Lin et al., Journal of Alloys and Compounds 680, 452-461 (2016)

## Experimental study and modeling of nanostructured [Fe<sub>10</sub>Ni<sub>90</sub>/Cu]<sub>p</sub> thin films for using in composite multiferroics

E. Kudyukov<sup>a,\*</sup>, M. Kalinin<sup>a</sup>, K. Balymov<sup>a</sup>, V. Lepalovskij<sup>a</sup>, V. Vas'kovskiy<sup>a,b</sup>

<sup>a</sup> Ural Federal University, 620002, Mira 19, Yekaterinburg, Russia

<sup>b</sup> Institute of Metal Physics, UB RAS, 620137, S. Kovalevskaya 18, Yekaterinburg, Russia

\*e.v.kudyukov@urfu.ru

Composite multiferroics have been one of the most popular objects of researchers from all over the world for the past two decades [1]. These media acquired such interest due to the possibility of creating various technical devices and sensors that do not require an external power supply [2]. Among them, thin-film layered nanoscale systems and composites based on nanoparticles and nanowires have the greatest potential. As a rule, in such systems it is possible to achieve significantly lower values of the magnetoelectric effect in comparison with massive composites [3]. One of the ways to solve this problem can be the nanostructuring of the magnetic subsystem, by separating sufficiently thin layers of magnetostrictive material by non-magnetic interlayers, which will allow solving several problems at once, such as the damping effect of the substrate, the small volume of the magnetic subsystem and the occurrence of a “supercritical” state, characterized by the appearance of a perpendicular magnetic anisotropy. Thus, this work is devoted to the study of the magnetic properties of nanostructured composites of the [Fe<sub>10</sub>Ni<sub>90</sub>/Cu]<sub>p</sub>/Fe<sub>10</sub>Ni<sub>90</sub> type. The choice of the magnetic subsystem is due to good magnetic properties along with the presence of a magnetostriction constant of ~20 ppm.

Nanostructured films of the [Fe<sub>10</sub>Ni<sub>90</sub>/Cu]<sub>p</sub>/Fe<sub>10</sub>Ni<sub>90</sub> type were obtained by magnetron sputtering on an AJA ORION-8 device onto Corning cover glasses 0.2 mm thick with a magnetic field of 200 Oe applied in the substrate plane. To optimize the nanostructuring parameters, a computer model was built in the COMSOL Multiphysics software package. The magnetic properties were studied using a LakeShore VSM 7407 vibrating magnetometer and an Evico Magnetics Kerr magneto-optical microscope

Thus, in this work, the dependences of the magnetic properties and the magnetoelectric effect on the parameters of nanostructuring are obtained. Such parameters as the thickness of the ferromagnetic layer, the thickness of the Cu interlayer, and the number of nanostructuring periods were varied. The optimization of nanostructuring parameters was also carried out using a computer model built in the COMSOL Multiphysics package in order to achieve the best magnetoelectric properties. As a result, on the basis of experimental and calculated data, the optimal characteristics of nanostructured films were determined.

This work was financially supported by the RSF grant, project no. 23-22-00394.

[1] G. Srinivasan, *Annu. Rev. Mater. Res.* 40:153–78 (2010)

[2] J.M. Hu, L.Q. Chen, C.W. Nan, *Adv. Mater.*, 28, 15–39 (2016)

[3] H. Palneedi, V. Annapureddy, S. Priya, J. Ryu, *Actuators*, 5, 9 (2016)

# **Features of electrical conductivity and thermal expansion of amorphous ferromagnetic micro-wires under Joule heating below the Curie point**

A. Tkachenya, K. Shcherba, A. Pakhomova, M. Andreiko, N. Yudanov, A. Morchenko\*

MISIS University of Science and Technology, 119049, Leninsky Ave., 4, Moscow, Russia

\*dratm@mail.ru

Thermomagnetic treatment of ferromagnetic micro-wires makes it possible to change the characteristics of the material for use in a wide variety of technical applications, from microelectronics devices and microsystem technology to various biomedical purposes. At the same time, mechanical, magnetic, electrical and electromagnetic characteristics, including magnetic impedance, are affected. Near the axis of the wire, as a rule, an axial type of anisotropy is realized, and on its periphery, depending on the magnetostriction sign of the core material, on the conditions of preparation and on subsequent treatment, axial, circular or helical induced anisotropy of a magnetoelastic nature can be formed, and in the case of exceeding the crystallization temperature, the phase composition cardinally changes and a magnetocrystalline anisotropy appears.

And if the processes of exposure from external heat sources and the magnetic field can be controlled independently, then in the case of heating by passing current (current annealing), the strength of the transmitted current determines both the intensity of the magnetic field and the intensity of the heat influx. For purposeful control of the treatment mode, it is necessary to know the temperature reached in the wire. At the same time, the problem is that the heating temperature is determined not only by the power of the current source, but also by changes in the resistance of the wire during heating (including due to irreversible structural transformations at high temperature), as well as the conditions of outflow and dissipation of thermal energy, which can be completely different depending on the environment and the geometry of the wire. But direct measurement of the temperature of micro-wires in these conditions is an almost impossible task.

The study of the correlation of thermal expansion, electrical resistance and inductive characteristics of various types of micro-wires when heated from an external source and due to the thermal effect of current allows us to determine the regularities of the process of current heating and use these data to characterize the process of thermomagnetic treatment carried out in various environmental conditions and the geometry of the sample location. As a result of the experiments, the most significant factors affecting the heating process were identified, methods were proposed to minimize those that are difficult to control, and prerequisites were laid for constructing an adequate model of the current heating process.

## Features of temperature dependences of magnetic susceptibility of magnetic colloids in porous media

Yu. Dikansky<sup>a</sup>, D. Gladkikh<sup>a</sup>, D. Dorozhko<sup>a,\*</sup>

<sup>a</sup> North Caucasus Federal University, Stavropol, 355017, Russian Federation

\*[dsdorozhko@ncfu.ru](mailto:dsdorozhko@ncfu.ru)

The study of magnetization processes is an important issue in the area of magnetic fine particles research. Surface phenomena are one of the factors affecting the processes of magnetization of such media [1]. The need to take into account this factor arises during the magnetization of a magnetic colloid in the presence of a well-developed interfacial surface. For example, thin layers of a magnetic colloid, when filling porous matrices with it [2].

As a result of our investigations we found some differences on the dependencies of magnetic susceptibility on frequency of probing field and temperature of sample in saturated porous media and bulk ferrofluid. We established that the origin of the differences depends on the pore size: with average size of pores increase, the dependences of the magnetic susceptibility become similar to bulk ferrofluid. The experimental results corresponds with result of computation of temperature dependence of magnetic susceptibility performed on basis of model with relaxation time of magnetic moment of fine particle on pore size.

Fig. 1 shows that with a decrease in the size of the porous medium fraction, the position of the maximum of the  $\chi'(T)$  dependence shifts to higher temperatures. Fig. 2 shows the theoretical dependences of the real part of the magnetic susceptibility. One can see, indeed, with a decrease in the pore size, the maximum should shift to the region of higher temperatures, observed in the experiment.

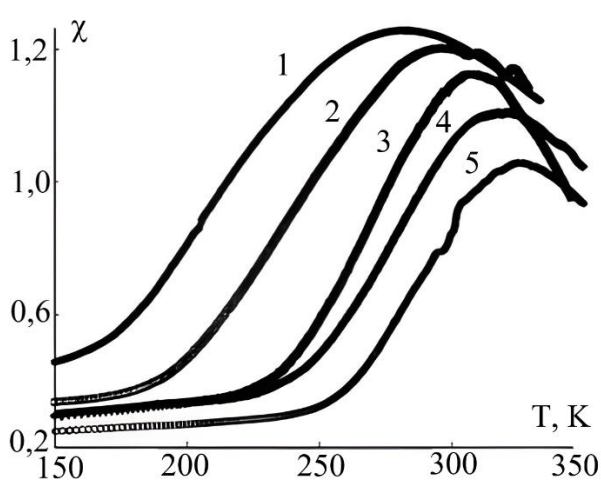


Fig. 1. Temperature dependences of the real part of the magnetic susceptibility of a magnetic colloid (1) and porous media of various fractions impregnated with this colloid: 1 - magnetic colloid, 2 - 250-300  $\mu\text{m}$ , 3 - 125-150  $\mu\text{m}$ , 4 - 90-105  $\mu\text{m}$ , 5 - 40 -50  $\mu\text{m}$ .

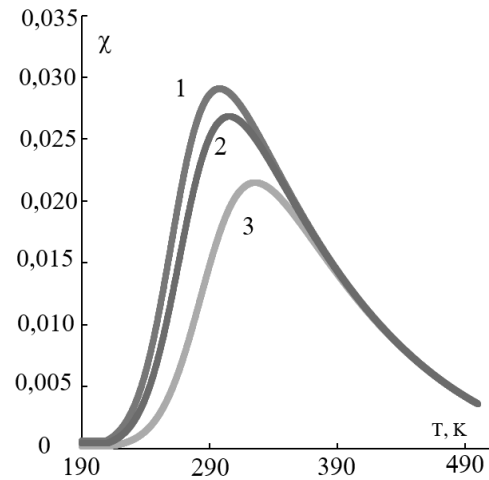


Fig 2. Theoretical dependences of the real part of the magnetic susceptibility on temperature for various pore sizes. 1 – 500  $\mu\text{m}$ , 2 – 50  $\mu\text{m}$ , 3 – 10  $\mu\text{m}$ .

[1] G. Viramontes-Gamboa, Phys.Rev. 75, 759 (1995)

[2] D. Gladkikh, Curr. Appl. Phys. 19, 1436 (2019)

## **Features of the magnetoelectric effect in layered composites nickel ferrite-CTS at various modes of mechanical vibrations**

V. Astakhov, V. Kostishyn, P. Tsepanin, A. Morchenko\*

MISIS University of Science and Technology, 119049, Leninsky Ave., 4, Moscow, Russia

\*dratm@mail.ru

The phenomenon of the occurrence of an electric voltage when a magnetic field is applied, called the magnetoelectric effect, continues to attract the attention of researchers due to a wide range of potential applications. At the same time, the results of experimental studies often differ from those predicted theoretically, which leaves a field for scientific research in this direction. Thus, it is usually assumed that when using materials with similar mechano-acoustic parameters, the maximum magnetoelectric effect for layered composites is achieved with an equal ratio of the thicknesses of the materials used, which (turns out to be true not) is not true for all types of vibrational modes. The influence of the  $\Delta E$ -effect on resonant frequencies and the magnitudes of the magnetoelectric effect achieved at these frequencies are also rarely considered.

The studied materials were layered composites consisting of layers of nickel-zinc ferrite of the M613SA brand and zirconate-titanate of lead of the CTS-42 brand, made in the form of disks with a thickness of 0.3 to 1.2 mm and 0.5 mm. The ferrite disks were covered with chromium on all sides to exclude the influence of the frequency dependence of the ferrite conductivity on the final results. The disks of magnetostrictive and piezoelectric ceramics were glued together with epoxy glue with a thickness of the adhesive seam of no more than 80 microns, which minimized the influence of the characteristics of the glue on the results obtained. Measurements of dielectric characteristics were carried out using an E7-20 impedance meter, magnetostriction of ferrite ceramics with an installation with BF-350AA strain gauges, magnetoelectric effect with an installation consisting of two pairs of Helmholtz coils, a shielded cell, a generator, an amplifier and an AC voltmeter.

The dependence of the magnetoelectric effect on the frequency of vibrational modes in the samples is analyzed.

# Ferromagnetic resonance and magnetic anisotropy of 3-d metal rods with gradients of composition

E. Denisova<sup>a, b, \*</sup>, L. Chekanova

<sup>a</sup>, S. Komogortsev<sup>a</sup>, I. Vashenina<sup>a, b</sup>, R. Iskhakov<sup>a</sup>, I. Nemtsev<sup>a</sup>

<sup>a</sup>Kirensky Institute of Physics, FRC KSC SB RAS, 660036, Akademgorodok 50/38, Krasnoyarsk, Russia

<sup>b</sup>Siberian Federal University, 660041, Svobodny 79, Krasnoyarsk, Russia

\*len-den@iph.krasn.ru

Our investigations concern a new class of advanced materials, known as structural and functional gradient materials, characterized by compositional gradation over macroscopic or microscopic distances. Coercivity, squareness, and magnetic anisotropy can be tailored by varying the structure, geometry and/or spatial distribution of the magnetic functional units. Elongated elements (nanowires and nanotubes) have been used in the number of technologies. The problems concerned with the complicated dipole-dipole interactions in arrays of such elements motivates in researching new designs for these elements. Two-phase nanowires with a coaxially combined or varied along axis phases could generate additional applied advances.

In this work, we describe experimental results concerning the multisegmented or coaxial Co/Ni and Fe/Co/Ni rods in porous of track etched polycarbonate membranes (PCTE) and focus on the comparison of their magnetic properties. The coaxial nanostructures investigated consist of a cylindrical cobalt core that is surrounded by a shell of nickel layer (CS). The multi-segmented (MS) rods contain coupled rods of nickel, iron, and cobalt. The rods arrays were prepared by electroless plating of ferromagnetic metals into pores of PCTE membrane. We report on the correlation between electroless growth and functional properties of individual rods characterized by FMR spectroscopy and magnetometry. The created composition gradient manifests in the features of the FMR spectrum and magnetization curves. A staggering difference is observed between the FMR spectra measured on arrays of Co/Ni MS rods, Co/Ni core-shell rods and Co-Ni gradient rods as well as the difference with the homogeneous Ni rods, Ni tubes without core and Co wires without Ni shell. The FMR spectra for rods with composition gradient exhibit a clear multi-peak character, which resonance field do not match to the peaks measured independently in the homogeneous rods. Assuming that the overall magnetic anisotropy of the magnetic nanowires array is mainly determined by the shape anisotropy of the individual wire and the anisotropy arising from magneto-dipole coupling among the wires, the Kittel equation would be:

$$\frac{\omega}{\gamma} = H_r + 2\pi M_s (1 - 3P \cdot f)$$

where  $\gamma = g\mu_B/h$  is the gyromagnetic ratio,  $g = 2$ ,  $P$  is the material porosity,  $f$  is the volumetric filling factor. By comparing the experimental and calculated values of  $H_r$  we estimated the values of additional anisotropy, which could appear due to interphase boundaries, segmented compositionally MS and CS Co/Ni rods. As expected, the value of  $H_{\text{eff}}$  for the Co segment determined by the additional anisotropy of the phase boundaries in the case of CS rod (2.5 kOe) is greater than for the MS rod (0.8 kOe). It was observed that main peak in the FMR spectrum weakly depend on the direction of the external field for MS rods with membrane porosity more than 20%. Thus, this composite membrane demonstrates isotropic microwave absorption, while the sample composite structure is characterized by shape anisotropy. So, we can conclude that the contribution from dipole-dipole interaction was comparable to those for shape anisotropy in this case. The local magnetic anisotropy field  $H_a$  of Co/Ni and Fe/Co/Ni rods was estimated to be in the range from 0.9 to 2 kOe.

So, it was demonstrated that the FMR properties may be controlled through a rods design, template characteristics and electroless deposition conditions.

# Formation of ferromagnetic semiconductors GaFeAs and GaMnAs by ion implantation and pulsed laser annealing

Yu. Danilov<sup>a,\*</sup>, I. Antonov<sup>a</sup>, V. Bachurin<sup>b</sup>, V. Bykov<sup>a</sup>, Yu. Dudin<sup>a</sup>, I. Kalentyeva<sup>a</sup>, R. Kriukov<sup>a</sup>,  
A. Kudrin<sup>a</sup>, A. Nezhdanov<sup>a</sup>, A. Parafin<sup>c</sup>, S. Simakin<sup>b</sup>, O. Vikhrova<sup>a</sup>, P. Yunin<sup>c</sup>, D. Zdoroveyshchev<sup>a</sup>

<sup>a</sup> Lobachevsky State University of Nizhny Novgorod, 603022, Gagarin Av. 23/3, Nizhny Novgorod, Russia

<sup>b</sup> Valiev Institute of Physics and Technology of RAS, Yaroslavl branch, 150007, Universitetskaya 21, Yaroslavl, Russia

<sup>c</sup> Institute for Physics of Microstructures of RAS, 603087, Academicheskaya 7, Nizhny Novgorod, Russia

\*danilov@nifti.unn.ru

Ferromagnetic semiconductors (FMS) are promising as a spin injectors in spintronics devices. An alternative to commonly used molecular beam epitaxy for creating structures with FMS is ion implantation, which is well integrated into the process of mass semiconductor production. This paper presents the results of a comparative study of the processes of ion-implantation production of FMS based on GaAs doped with Mn and Fe.

Layers of GaFeAs and GaMnAs magnetic semiconductors were obtained by implanting Fe or Mn ions into i-GaAs (100) wafers followed by pulsed laser annealing (PLA). Ion implantation was implemented in the Raduga-3M accelerator with an ion source based on a vacuum-arc discharge at an accelerating voltage of 80 or 30 kV. The ion dose varied from  $1 \times 10^{16}$  to  $5 \times 10^{16}$  cm<sup>-2</sup>. The implanted samples were annealed with a pulse of an LPX-200 excimer KrF laser ( $\lambda = 248$  nm, pulse duration = 30 ns). During PLA, the energy density varied from 100 to 400 mJ/cm<sup>2</sup>.

The impurity atomic profiles before and after annealing, obtained by ion mass spectrometry on a TOF.SIMS.5 setup with a time-of-flight mass analyzer, are compared with the simulated SRIM distributions. X-ray diffraction (XRD) studies revealed the deformation of the crystal lattice and an increase in the lattice parameter in the case of GaFeAs. Analysis of GaFeAs layers by X-ray photoelectron spectrometry (XPS) showed the presence of Fe-Ga and Fe-As chemical bonds and the absence of Fe-Fe bonds. The results of XRD and XPS indicate that the iron atoms replace sites approximately equally for both Ga and As. The absence of Fe atoms in interstitial or cluster form was noted. In GaMnAs, manganese atoms replace only Ga atoms at lattice sites. XRD studies showed the absence of inclusions of the second phase in the annealed GaMnAs and GaFeAs layers within the sensitivity of the method. After implantation of Mn and Fe ions, the annealed GaAs layers have a p-type conductivity. The Raman spectra, in addition to the LO and TO modes of GaAs, contained a coupled phonon-plasmon mode (CPPM) for the annealed layers. The GaMnAs Raman spectra indicate an enhancement of the phonon-plasmon interaction due to an increase in the concentration of holes up to  $\approx 10^{20}$  cm<sup>-2</sup> with an increase in the Mn ion fluence and energy density during PLA. For the GaFeAs layer, the behavior of the CPPM is different; its lower intensity and position are associated with a much lower hole concentration ( $\sim 10^{19}$  cm<sup>-2</sup>).

The low-temperature galvanomagnetic properties of the annealed GaFeAs and GaMnAs layers indicate their ferromagnetic properties. The dependence of the resistance of GaMnAs layers on temperature exhibits at  $\approx 100$  K a characteristic maximum coinciding with the Curie temperature. For GaMnAs, a nonlinear magnetic field dependence of the Hall resistance ( $R_H(H)$ ) with a hysteresis loop and a negative magnetoresistance (MR) with sections of anisotropic MR at temperatures below 100 – 110 K were recorded. GaFeAs layers exhibited nonlinear  $R_H(H)$  dependences up to room temperature (the hysteresis loop remained below 120 K) and negative magnetoresistance.

The work was supported by the Russian Science Foundation (project no. 23-29-00312).



## Formation of skyrmion states in thin ferromagnetic Co/Pd films

I. Kalentyeva<sup>a,\*</sup>, M. Dorokhin<sup>a</sup>, A. Zdoroveyshchev<sup>a</sup>, D. Zdoroveyshchev<sup>a</sup>, O. Vikhrova<sup>a</sup>, Yu. Kuznetsov<sup>a</sup>, D. Tatarskiy<sup>a,b</sup>, R. Gorev<sup>b</sup>, A. Orlova<sup>b</sup>

<sup>a</sup>Lobachevsky State University of Nizhny Novgorod, 603022, Gagarin av. 23, Nizhny Novgorod, Russia

<sup>b</sup>Institute for Physics of Microstructures RAS, 603950, Academic st. 7, Nizhny Novgorod, Russia

\*istery@rambler.ru

This work presents studies on the influence of technological parameters on the formation of various topological states in thin ferromagnetic Co/Pd films. Previously, we demonstrated the presence of Neel-type skyrmions in Co/Pt thin magnetic films, and found that their surface concentration strongly depends on the tuning coefficient ( $t$ ) of the bilayer thickness:  $([\text{Co}(0.3 \times t \text{ nm})/\text{Pt}(0.5 \times t \text{ nm})]_{10})$  [1].

The samples under study are Co/Pd(3/5) films, for which Pd ( $0.5 \times t \text{ nm}$ ) and Co ( $0.3 \times t \text{ nm}$ ) layers were successively deposited on GaAs substrates by electron beam evaporation at  $300^\circ\text{C}$  with a tenfold repetition [2]. The exact value of the thickness was set by the tuning coefficient  $t$ , which varied from 0.8 to 1.1. The Hall effect was studied at room temperature in the range of magnetic fields ( $\pm 2.5 \text{ T}$ ). Magnetic force microscopy (MFM) and Lorentz transmission electron microscopy (L-TEM) on a Carl Zeiss LIBRA 200 MC microscope were used to diagnose the magnetic properties of the provided samples.

All investigated films have orthogonal magnetic anisotropy. The dependences of the Hall resistance ( $R_H(H)$ ) contain a hysteresis loop, with the value of  $R_H$  in the zero field coinciding with the value in the saturation field for all structures. The curves are close to each other, the only exception is the sample with the largest bilayer thickness  $t = 1.1$ , for which the narrowing of the loop near  $H = 0$  is registered.

In the Lorentz images of structures with magnetic contrast, when the samples are tilted by  $30^\circ$  relative to the normal, the formation of skyrmions is observed. The sample with  $t = 0.8$  contains both skyrmions (cylindrical magnetic domains) and skyrmioniums (ring magnetic domains). Skyrmioniums are also present in the structure with  $t = 1$ , but the width of their ring is indistinguishable by L-TEM methods. And in the sample with  $t = 1.1$ , a dense lattice of skyrmions is formed.

The analysis of micrographs makes it possible to estimate the average size of coherent scattering regions (CSRs) in sample films. It has been established that the size of the CSR in Co/Pd films is directly proportional to the thickness tuning coefficient  $t$ , and the size of the skyrmions is inversely proportional to the

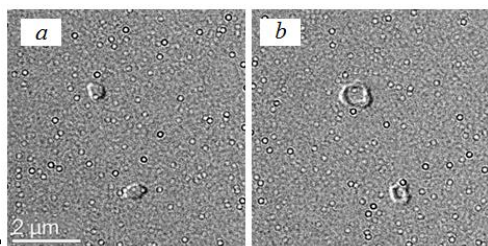


Figure structure surface with  $t = 0.8$ . Figure (a) identifies a skyrmion, figure (b) a skyrmionium. CSR size.

This work was supported by the Russian Scientific Foundation, project no. 21-79-20186.

[1] M.V. Dorokhin et al. Journal of Alloys and Compounds. 926, 166956 (2022).

[2] A. V. Zdoroveyshchev et al. Physics of the Solid State. 61, 1577 (2019).

# Frequency-Field Dependences of FMR in NiFe<sub>2</sub>O<sub>4</sub> Superparamagnetic Powders

S. Stolyar<sup>a,b,\*</sup>, O. Li<sup>a,b</sup>, E. Nikolaeva<sup>a,b</sup>, A. Vorotynov<sup>c</sup>, D. Velikanov<sup>c</sup>, R. Iskhakov<sup>c</sup>, V. Pyankov<sup>a</sup>, N.

Boev<sup>c</sup>, O. Kryukova<sup>a</sup>

<sup>a</sup>FRC KSC SB RAS, 660036, Akademgorodok, 50, Krasnoyarsk, Russia

<sup>b</sup>Siberian Federal University, 660041, Svobodny pr., 79, Krasnoyarsk, Russia

<sup>c</sup>Kirensky Institute of Physics, FRC KSC SB RAS, 660036, Akademgorodok 50/38, Krasnoyarsk, Russia

\*stol@iph.krasn.ru

Ferromagnetic resonance (FMR) in powder systems leads to their heating ( $\Delta T \sim 10$  K), which can be used in magnetic hyperthermia [1]. The resonance properties of superparamagnetic nanoparticles were studied in theoretical works [2–3]. In this work, the frequency-field dependences (Fig. 1) of the FMR of superparamagnetic powders of nickel ferrite NiFe<sub>2</sub>O<sub>4</sub> with a size of 4 nm, synthesized by chemical deposition, as well as NiFe<sub>2</sub>O<sub>4</sub> particles coated with polyvinyl alcohol (PVA) are studied at room temperature.

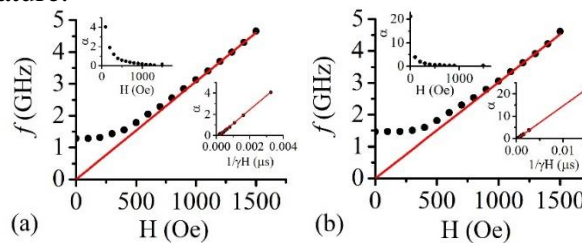


Figure 1. Dependence of the FMR resonant frequency on the external field  $H$  of the NiFe<sub>2</sub>O<sub>4</sub> nanoparticles (a) and particles coated with PVA (b).

Approximation of the dependence of the FMR resonant frequency on the external field  $H$  (Fig. 1) by a linear function  $\omega_0(H) = 2\pi f = \gamma H$  allowed us to estimate the value of the gyromagnetic ratio  $\gamma$ . The feature at low fields can be associated with an increase in the damping factor  $\alpha$ . The resonant frequency of the FMR, taking into account damping, is determined by the expression  $\omega^2 = \omega_0^2(1 + \alpha^2)$ , where  $\alpha$  is the damping factor[4]. The experimentally detected deviation of the resonant frequency from  $\omega_0$  allowed us to determine the damping factor  $\alpha$ . Using the relation  $\omega_r = \alpha\gamma H_{eff}$ , we found  $\omega_r$  – the frequency at which the absorption mode changes from relaxation to resonant. Using the data of [2], we estimated the values of the anisotropy constant  $K$  [2], particle anisotropy field  $H_a = 2\pi f(0)/\gamma$  from fig. 1, saturation magnetization  $M = 2K/H_a$ , which are given in the table 1.

Table 1.

	$d$ , nm	$\gamma$ , $\cdot 10^7$ Hz/Oe	$f(0)$ , GHz	$\omega_r$ , GHz	$M$ , G	$H_a$ , G	$K$ , $\cdot 10^4$ erg/cm <sup>3</sup>
NiFe <sub>2</sub> O <sub>4</sub>	4	1.9	1.3	1.3	360	430	7.8
NiFe <sub>2</sub> O <sub>4</sub> /PVA	4	1.9	1.5	1.5	320	490	7.8

- [1] С.В. Столяр и др., ФММ, 124, 182 (2023).
- [2] Y.L. Raikher et al. SOV. Phys. JETP, 40, 526 (1974).
- [3] R. S. Gekht et al. SOV. Phys. JETP 43, 677 (1976)
- [4] S. Krupička, Vieweg+Teubner Verlag, (1973)

# Galvanomagnetic and thermomagnetic phenomena in thin CoPt metal films

Yu Kuznetsov <sup>a,\*</sup>, M. Dorokhin <sup>a</sup>, A. Zdoroveyshchev <sup>a</sup>, A. Kudrin <sup>a</sup>, P. Demina <sup>a</sup>, D. Zdoroveyshchev <sup>a</sup>

<sup>a</sup> Lobachevsky State University, 603022, Gagarin av. 23, Nizhny Novgorod, Russia

\*corresponding author email: y.m.kuznetsov@unn.ru

The thermomagnetic Nernst-Ettingshausen effect is well known in the literature as a method for determining the electronic properties of semiconductor and metallic materials, which supplements measurements of the Hall effect [1]. An interesting variation of the Nernst-Ettingshausen effect is an anomalous effect, which consists in the distortion of the linear magnetic field dependence of the resulting transverse thermomagnetic voltage. This phenomenon is observed in ferromagnetic materials and is associated with the features of the spin-dependent scattering of free charge carriers on magnetic centers [2]. If the structure is in a ferromagnetic state, the magnetic field dependence of the Nernst-Ettingshausen voltage can take the form of a hysteresis loop.

From a practical point of view, it is important to note that the Nernst-Ettingshausen voltage can additively combine with the thermoelectric effect and thus increase the Seebeck coefficient. The physics of thermoelectric phenomena is a large scientific and practical area, the purpose of which is the creation of autonomous energy converters using waste heat from technological, industrial, or domestic processes [3].

The paper considers the physical and methodological foundations for measuring the anomalous Nernst-Ettingshausen effect on the example of CoPt ferromagnetic film structures. The main relationships between thermomagnetic and Hall coefficients with the parameters of the structures under study are discussed. The results of experimental studies of the magnetic field dependences of the Hall and Nernst-Ettingshausen voltages are presented (see Figures 1a and 1b), conclusions are drawn regarding the polarization of conduction electrons involved in kinetic processes, the nature of the dominant mechanism of spin-dependent scattering, and the temperature dependence of the position of the Fermi level [4].

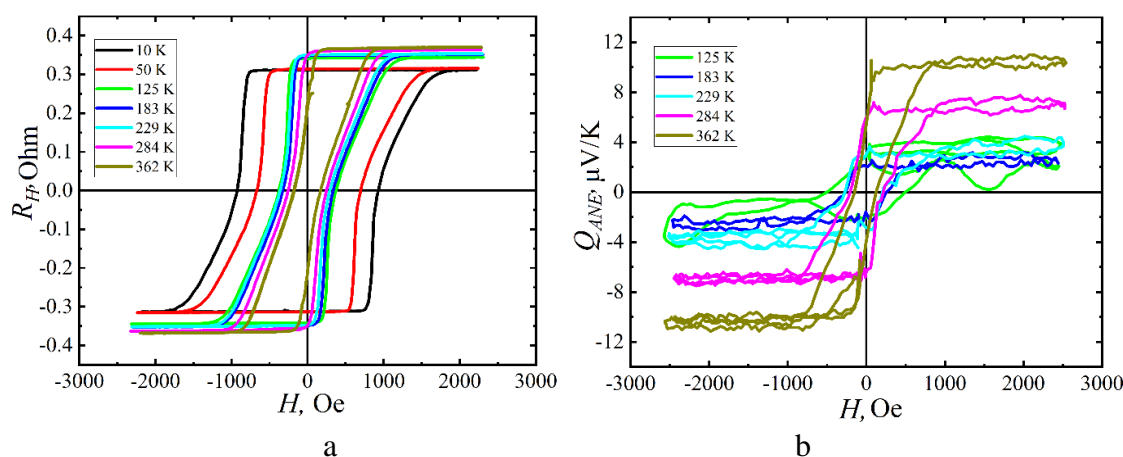


Figure 1. Magnetic field dependence: a – Hall resistance, b – anomalous component of the Nernst-Ettingshausen coefficient

By the support of the RSF grant 21-79-20186.

- [1] Z Alisultanov, JETP Letters, 99, 702 (2014)
- [2] H Wu, JMMM 441, 149 (2017)
- [3] B Ranjbar, Renew. Energy, 164, 194 (2021)
- [4] Yu Kuznetsov, Phys. Uspekhi, 3, 331 (2023)

# Growth and Characterization of CdTe Thin Films Grown by Molecular Beam Epitaxy

I. Koshelev<sup>a,\*</sup>, P. Reznikova<sup>a,b</sup>, I. Volchkov<sup>a</sup>, P. Podkur<sup>a</sup>, V. Kanevsky<sup>a</sup>

<sup>a</sup>FRC “Crystallography and Photonics” RAS, 119333, Leninskiy avenue 59, Moscow, Russia

<sup>b</sup>Russian Technological University MIREA, 119454, Vernadskogo avenue 78, Moscow, Russia

\*iliakoscheleff@yandex.ru

Cadmium telluride is one of the most promising semiconductor materials for thin-film solar cells. These applications are possible due to the properties of this material, such as the band gap (~1.45 eV) and a wide range of electrical properties (~1-1·10<sup>9</sup> Ohm·cm) [1]. Also of interest are the applications of bulk crystals and CdTe thin plates in various fields of semiconductor spintronics, since it is known that the impurity sublattice of bulk crystals may have weak ferromagnetic properties [2], because of possible ferromagnetic ordering in defective clusters. One of the most promising methods for obtaining perfect CdTe thin films is the method of molecular beam epitaxy (MBE) [3]. In the case of the growth of CdTe thin films by the MBE method, when sputtering from a single source, it is important to understand the kinetics of defects present in the source material. In particular, it is very important to understand the kinetics of magnetic impurities (Fe or Ni clusters) present in CdTe, in the general growth process and the degree of their entry into the structure of thin films.

The growth of CdTe thin films was carried out on a laboratory MBE installation at temperatures of 600-800 °C at the source and ≈200 °C on the substrate according to the procedure described in [3]. The vacuum during the growth process was maintained at least 10<sup>-8</sup> mbar. Growth time: 90-210 min. The obtained films were characterized by atomic force (AFM) and magnetic force microscopy (MSM) methods on Solver Pro-M AFM (NT-MDT, Russia) in semi-contact mode. X-ray studies were carried out on an XRD X'Pert Pro MRD (PANalytical, Netherlands). The elemental composition on the surface of the film was carried out by EDS on a scanning electron microscope JCM-6000Plus with an EDS spectrometer (Jeol, Japan). The impurity composition was determined by mass spectrometry.

The influence of temperature conditions and growth modes on the quality of cadmium telluride thin films obtained by the MBE method on C-orientation sapphire substrates was determined. It was found that at a growth temperature of 672 °C, a thin film of high quality with a homogeneous surface is observed in the result. According to the results of the X-ray analysis, there is one phase corresponding to the CdTe phase (111). At the same time, the EDS analysis showed almost complete stoichiometry of the sprayed films (± 0.1 at. %). With an increase in the growth rate, by increasing the temperature of the source, the quality of the film deteriorates, the surface becomes non-homogeneous, pronounced granularity is observed. In this case, the peak of CdTe (111) is shifted, in accordance with Vegard's rule, the stoichiometry of the films is violated. It was determined that the kinetics of defects significantly depends on the temperature conditions of the spraying process. Thus, in the case of an increase in the temperature of the source, not only an increase in the grain size of the film is observed, but also clusters of magnetic defects at the grain boundaries become noticeable. The concentration of magnetic impurities included in the structure of thin films was determined.

The work was carried out using the equipment of the Central Research Center of the FSRC “Crystallography and Photonics” RAS on the state assignment of the FSRC “Crystallography and Photonics” RAS.

[1]. A. Kondrick, *Functional microelectronics* 6 (2004)

[2]. P. Podkur, et al, *Crystallography Reports*, 68, 62 (2023).

[3]. I. Mikhailov, et al, *Surface. X-ray, synchrotron and neutron studies* 5, 595 (2011)

# Influence of particle size on the microstructure and magnetic properties of nickel-zinc ferrite powder

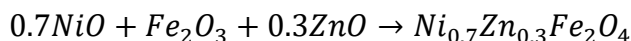
E. Nikolaev<sup>a,\*</sup>, E. Lysenko<sup>a</sup>, S. Bobuyok<sup>a</sup>

<sup>a</sup>National Research Tomsk Polytechnic University, 634050, Lenina Avenue 30, Tomsk, Russia

\*corresponding author nikolaev0712@tpu.ru

Currently, magnetic elements based on multicomponent ferrite materials are the key components to design and manufacture modern electronic, magnetic and radio engineering devices. A wide class of soft magnetic ferrite materials includes nickel-zinc ferrosinels with the chemical formula  $Ni_{0.7}Zn_{0.3}Fe_2O_4$  (Ni-Zn). Nickel–zinc ferrites are widely used in modern technology due to their electrical and magnetic properties [1, 2]. In addition, highly dispersed ferrite powders have been in focus of late due to their use in hyperthermia, drug transportation, magnetic storage, and electrochemical and gas sensors. Another promising application area for such powders is their use as a contrast agent in magnetic resonance imaging [3]. The scope of these ferrites application, in many respects, depends on specific electrical, magnetic and mechanical properties. These properties depend on chemical and phase composition and significantly depend on the particle size. Therefore, the aim of this study is to establish the influence of the dispersion of the synthesized powder of nickel-zinc ferrite on the structural and magnetic properties.

We studied nickel-zinc ferrite powder of  $Ni_{0.7}Zn_{0.3}Fe_2O_4$  composition (ferrite Ni-Zn). The ratio of the initial reagents in powder mixtures was calculated by the equation:



The mixture of the initial NiO-Fe<sub>2</sub>O<sub>3</sub>-ZnO reagents was mechanically activated in a high energy ball mill (Retsch E<sub>max</sub>) using steel grinding jars and balls at room temperature for 60 minutes. The drum rotational speed was 1000 rpm. Activated mixture was synthesized in a laboratory furnace with a heating rate 5 °C·min<sup>-1</sup>. The mixture was heated to 900 °C, and the isothermal exposure time was 240 minutes. After that, powder of Ni-Zn ferrite was divided into several batches in accordance with the number of modes of mechanical treatment. Part of the powder was not subjected to mechanical activation, other parts were mechanically activated for 15, 30 and 60 min in air. The rotation speeds of the grinding jars were 500, 1000, 1500 rpm. The phase composition and crystal lattice parameters of the studied samples were estimated by XRD analysis using an ARL X'TRA diffractometer (Switzerland). The particle size distribution was analyzed by laser diffraction using a Fritsch Analysette-22 NanoTec analyzer. The specific surface area (SSA) for ferrite samples was estimated by the Brunauer-Emmett-Teller (BET) analysis. In addition, the activated samples of Ni-Zn ferrite were analyzed by thermogravimetric analysis in magnetic field. Measurements were performed using a thermal analyzer STA 449C Jupiter (Netzsch, Germany). The results of the thermal analysis in the form of thermogravimetric (TG) and calorimetric (DSC) curves were processed using the Netzsch Proteus Analysis software.

According to XRD data, it was found that the intensity of reflections decreases with an increase in the rotation speed of the grinding jars. The Curie temperature of the study samples is observed in the range of 416-425 °C. Moreover, the magnetization of the samples increases with an increase in the rotation speed of jars and milling time.

This research was supported by the Russian Science Foundation (Grant no. 19-72-10078-P).

[1] N. Kavitha, P. Manohar. J. Supercond. Nov. Magn. 29, 2151 – 2157 (2016)

[2] Y. Gao, Z. Wang. J. Sol. Gel. Sci. Tech. 91, 111 – 116 (2011)

[3] U. Wongpratrat, S. Meansiri, E. Swatsitang. Microelectron. Eng. 126. 19 – 26 (2014)

# Investigation of the size of microdroplets of magnetic emulsions on magneto-optical effects

S. Belykh<sup>a,\*</sup>, C. Yerin<sup>a</sup>

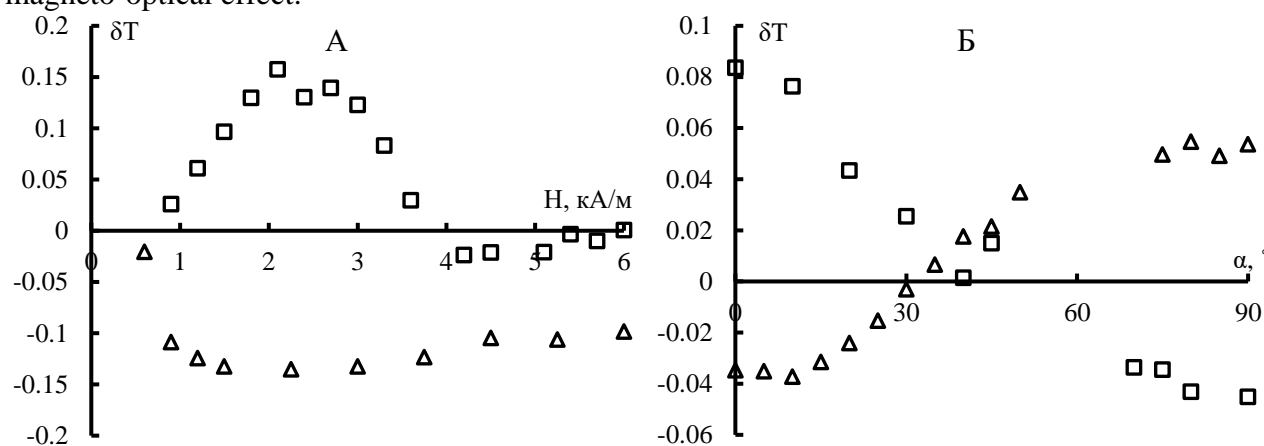
<sup>a</sup> North Caucasus Federal University, Stavropol, 355017, Russian Federation

\*sergeyb.stav@mail.ru

The study of the optical properties of functional magnetic nanostructures synthesized on the basis of magnetic fluids is a topical issue of the decade. Particular attention is drawn to magnetic emulsions with low interfacial tension, because their magneto-optical response to the action of the field is higher than that for magnetic fluids [1]. In a magnetic emulsion, the droplet size strongly depends on the synthesis conditions, which significantly affects the magnitude and sign of orientation effects that are sensitive to the shape and size of particles. [2].

In this work, the influence of a magnetic field of various strengths and orientations on the light transmission of magnetic emulsions synthesized on the basis of AMG-10 oil using two magnetic fluids of the «magnetite in kerosene» type from various manufacturers was studied. (NIPIGAS, Krasnodar and Applied Ferrohydrodynamics Lab, Ivanovo). A significant difference was found in the magnitude and sign of the magneto-optical effect in two magnetic emulsion samples. The characteristic times of relaxation processes are studied when the pulsed magnetic field is turned on and off.

Conclusions are drawn about the influence of droplet size on the difference in signs and magnitude of magneto-optical effects in two samples of magnetic emulsions. In the magnetic emulsion synthesized on the basis of the magnetic fluid produced by Applied Ferrohydrodynamics Lab, the average droplet size is 0.7-1  $\mu\text{m}$ , which is about 2-3 times smaller than the size of the microdroplets from the magnetic emulsion using the NIPIGAS magnetic fluid. The conclusions are confirmed by numerical calculations based on the anomalous diffraction approximation for optically soft scattering particles. A qualitative comparison of the experimental results with calculations allows us to propose a method for express estimation of particle sizes in magnetic disperse systems by the sign of the magneto-optical effect.



Curves of changes in transparency depending on the intensity (A) and orientation of the magnetic field (B) for a magnetic emulsion with larger (square marker) and smaller (triangular marker) drops

[1] A. Zakinyan, LAP (2011)

[2] S. Belykh, Opt.Spectrosc. 9, 129 (2021)

## Iron nanowires of various diameters: obtaining, characterization and NMR spectroscopy

I. Doludenko<sup>a,\*</sup>, D. Zagorsky<sup>a</sup>, I. Kalachikova<sup>a</sup>, A. Gippius<sup>b,c</sup>, S. Zhurenko<sup>c</sup>,  
L. Lupandin<sup>b</sup>, A. Tkachev<sup>c</sup>,

<sup>a</sup> FSRC “Crystallography and Photonics” RAS, 119333, Leninskiy avenue 59, Moscow, Russia

<sup>b</sup> Lomonosov Moscow State University, 119991, Leninskie gory 1/2, Moscow, Russia

<sup>c</sup> Lebedev Physics Institute, 119991, Leninskiy avenue 53, Moscow, Russia

\*[doludenko.i@yandex.ru](mailto:doludenko.i@yandex.ru)

At present, the magnetic properties of one-dimensional nanostructures, in particular, nanowires (NWs), are of great interest in view of the possibility of their further application in various fields. One of the ways to obtain such structures is matrix synthesis based on the galvanic filling of the pores of track membranes. This method is distinguished by the ability to vary various parameters of the obtained structures within wide limits. Depending on the geometric parameters of the matrix and the mode of obtaining of NWs, their physical properties can vary greatly. In this work, using pure iron NWs as an example, we studied the influence of the matrix pore diameter, and, consequently, the NWs diameter, on the nature of the NMR spectra.

In this work, NW arrays with diameters from 30 nm to 600 nm were obtained. Deposition was also carried out in the same mode on a flat surface. The deposition was carried out according to a two-electrode mode with an iron anode, at a potential of 1 V. The structure of the samples was investigated by SEM and X-ray diffraction analysis. According to preliminary studies, iron NWs undergo rapid oxidation, microscopy was carried out on a matrix cleavage. An analysis of the lengths of the obtained NW showed that an increase in the pore diameter leads to uneven filling of the pores of the entire array. X-ray diffraction analysis showed that the lattice parameter changes non-linearly as the diameter increases, and does not have a clearly expressed systematics.

The current efficiency was calculated based on the obtained structural studies and the known parameters of the matrices. It is shown that for all types of matrices, the current efficiency was about 50%.

Arrays of NWs of sufficient mass in the form of glued stacks were studied by NMR spectroscopy on <sup>57</sup>Fe nuclei in a zero magnetic field at T = 4.2 K. The dependences of the width and position of the center of mass of the spectrum, as well as the rates of nuclear spin-spin 1/T<sub>2</sub> and spin-lattice 1/T<sub>1</sub> relaxation on the NWs diameter, are studied. Results are compared with the spectrum and relaxation characteristics of bulk  $\alpha$ -iron, as well as of an iron microfilm deposited on a flat surface. It has been found that the transition from bulk iron to a film and, further, to nanowires leads to an increase in the local magnetic field on the iron. This effect may be due to an increase in the Fe-Fe exchange interaction in these objects due to a decrease in the lattice parameter, according to XRD data.

**Acknowledgment.** The work was supported by the RSF Grant 22-22-00983

## **Iron oxide nanorods as a potential tool for biofabrication of tissue structures by means of IR radiation and magnetic field**

D. Yakobson<sup>1\*</sup>, E. Brodovskaya<sup>1</sup>, I. Khutorskaya<sup>1</sup>, A. Al-khadj Aioub<sup>1</sup>, M. Zharkov<sup>1</sup>, V. Shlyapkina<sup>1</sup> and N. Pyataev.

<sup>1</sup>National Research Ogarev Mordovia State University, 430005, Republic of Mordovia, Saransk, Bolshevistskaya St., 68, Russian Federation

\* Correspondence: ykbsn@mail.ru

The use of magnetic nanorods under the action of a magnetic field or near-infrared laser radiation is a promising method for the formation of tissue structures. In particular, this is due to the high magnetisation of iron oxide-based nanorods and their low toxicity thanks to polymer coatings. The using of the thermal effect of laser exposure can solve the possibility of forming more complex tissue structures. The purpose of this study was the development of a method for the formation of tissue structures using nanorods under of magnetic fields and laser radiation in the near-infrared spectrum. Nanorods were prepared from Fe<sub>3</sub>O<sub>4</sub> and coated with polyacrylic acid (Fe<sub>3</sub>O<sub>4</sub>@PAA). By transmission electron microscopy, the nanorods were characterized by an average thickness of 30 nm and an average length of 700 nm. The zeta potential of the particles: - 79 mV. The MTT test for cytotoxicity of the fibroblast cell line L929 was carried out and showed that the nanorods were non-toxic at concentrations ranging from 5-60 µg(Fe)/mL. IC50 was 135.7 µg/mL. After laser exposure (808 nm, 10 min) with dose of 31.5 µg(Fe)/mL Fe<sub>3</sub>O<sub>4</sub>@PAA MTT test showed almost total cell death. The data of double stained acridine orange and ethidium iodide confirmed the data of MTT test and showed that necrosis was the main cause of cell death after laser exposure. The possibility of forming cell structures by exposing cells with nanorods to a magnetic field has been shown. Thus, our synthesized Fe<sub>3</sub>O<sub>4</sub>@PAA could be used to form different cell structures from fibroblasts using a magnetic field, as well as changing the structure with near-infrared spectrum laser.



## LaCoO<sub>3</sub> thin film growth and oxygen mobility investigation

A. Kozlov<sup>a,\*</sup>, P. Shvets<sup>a</sup>, A. Gohman<sup>a</sup>, K. Maksimova<sup>a</sup>

<sup>a</sup>REC «Functional nanomaterials», Immanuel Kant Baltic Federal University, 236004, Nevskogo 14,  
Kaliningrad, Russia

\*anatoly.kozlov2014@gmial.com

Lanthanum cobaltite LaCoO<sub>3</sub> (LCO) is a promising material for studying transitions in spin states and related phenomena. LCO has three spin states: low spin (LS), intermediate spin (IS), and high spin (HS) [1]. Various mechanisms, including the transformation of the electronic configuration caused by lattice deformation (rotation of Co–O octahedra), double exchange due to oxygen deficiency, and the effect of Co ions on the surface of thin films, explain the origin of ferromagnetic ordering [2–3].

Thus, the ability to analyze various magnetic properties implies the need to control the crystal structure of a thin LCO film. Oxygen defects arising during growth directly affect the magnetic properties of the material. Significant lack of oxygen can cause the crystal lattice rearrangement, as well as the formation of leakage currents through the film. However, the exact microscopic nature of the transition of the ferromagnetic state and the spin state and their behavior depending on the growth conditions remain unclear.

When thin films are deposited by the pulsed laser deposition method, it is necessary to consider many growth parameters. The process of laser ablation is important to consider the interaction of laser radiation with the target, which includes control over the main parameters, such as wavelength and laser beam power density. These parameters determine the energy of plasma particles condensed on the substrate surface and the interaction of laser beam with the target surface. The selection of the optimal laser parameters, sample quality, heating regime and growth chamber environment will make it possible to stabilize the growth of LCO in the desired phase and reduce the number of structural defects and large drops on the film surface. However, oxygen vacancies problem remains relevant and requires further study.

The exceptional ability of oxygen vacancies to exhibit high mobility can be considered not only as a material disadvantage; it also presents a unique opportunity for its use in catalytic processes. In our case, we are talking about the electrocatalysis of oxygen, which occurs during the interaction of an active gaseous medium with thin LCO films. To understand the dynamics of the formation of oxygen defects, as well as to determine the rate and limits of oxygen adsorption from the gas phase during growth, an experiment was carried out to grow an epitaxial LCO film in an atmosphere of the oxygen isotope <sup>18</sup>O. This experiment gives the percentage of <sup>16</sup>O from the target and <sup>18</sup>O from the growth chamber environment in the film during growth and during postgrowth annealing.

[1] Kwon, J. H., *Chemistry of Materials*, 26(8), 2496- 2501. (2104)

[2] Fuchs. D., *Physical Review B*, 75(14), 144402. (2007)

[3] Rondinelli, J. M., *Direct evidence for a half-metallic ferromagnet //Nature*. 392. 794-796. (1998)

# Large-scale automatic fabrication of superparamagnetic iron oxide microclusters for biomedical applications

E. Moiseeva, S. German, A. Yashchenok, D. Gorin\*

Center for Photonic Science and Engineering, Skolkovo Institute of Science and Technology, Skolkovo  
Innovation Center, Moscow 121205, Russia

\* D.Gorin@skoltech.ru

Superparamagnetic iron oxide nanoparticles (SPIONs) colloids have established themselves as an excellent material for wide commercial use in biotechnology and medicine. This is due to the combination of magnetic properties, low toxicity and high economic feasibility of production. In clinical practice, the magnetic separation technique is frequently employed for isolation and purification of immunoglobulins, antigens, DNA and RNA molecules from bacteria, viruses and cells [1]. However, superparamagnetic behavior characteristics only for iron oxide nanoparticles with a core size of 30 nm or less [2]. Due to their ferrimagnetic nature and remanence, larger particles are susceptible to aggregation after being exposed to external magnetic fields. In recent years, advances in colloidal synthesis have shown that SPIONs can be considered as "artificial atoms" capable of forming higher-ordered structures such as high-quality microclusters [3]. This secondary structure combines the ability to harness the size-dependent properties of individual nanoparticles with collective properties as result of interactions between the subunits. These superparamagnetic microclusters can provide a novel way of fabrication functional materials for bioassay applications.

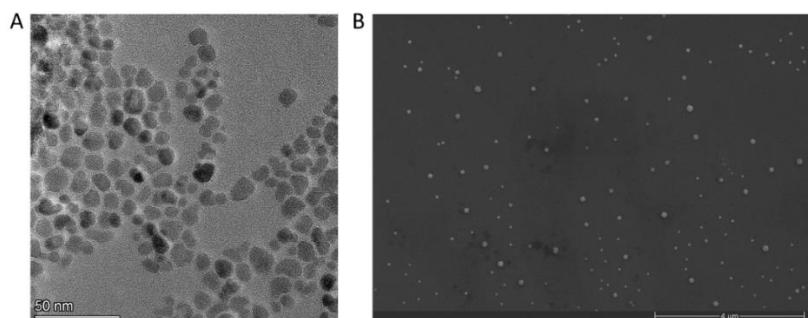


Figure 1. A. TEM image of initial hydrophobic iron oxide nanoparticles with average diameter of 14 nm. B. SEM image of clustered particles with an average diameter of 130 nm.

The iron oxide microclusters were synthesized in a two-stage procedure in a remotely controlled chemical reactor setup CR-1 fabricated by TetraQuant (Russia) [4]. At the first stage the oleic acid stabilized iron oxide nanoparticles were obtained by coprecipitation of iron (II) and (III) salts. At the second stage microclusters were formed under heat treatment in an inert atmosphere using the micelles of hydrophobic nanoparticles solution as precursor in presence of surfactant and polymeric stabilizer. Characterization of synthesized clusters was performed using transmission electron microscopy (TEM), scanning electron microscope (SEM) and dynamic light scattering (DLS) analysis and their magnetic properties were examined.

This work was supported by Russian Science Foundation (RSF) Grant № 23-74-00022 №

[1] Haukanes, *Biotechnology* 11,1 (1993): 60-63.

[2] Gubin, *Russ. Chem. Rev.* 74, 6 (2005): 489.

[3] Zhuang, *J. Am. Chem. Soc.* 129,46 (2007): 14166-14167.

[4] <https://www.tetraquant.com/products>

# **Li<sub>3</sub>V<sub>2</sub>(PO<sub>4</sub>)<sub>3</sub>-based Composites as Potential Cathode Materials for Lithium-Ion Batteries: ESR, Magnetization and Electrochemical Measurements**

T. Gavrilova<sup>a,\*</sup>, Yu. Deeva<sup>b</sup>, I. Yatsyk<sup>a</sup>, M. Cherosov<sup>c</sup>, R. Batulin<sup>c</sup>, N. Lyadov<sup>a</sup>, S. Khantimerov<sup>a</sup>

<sup>a</sup> Zavoisky Physical-Technical Institute, FRC Kazan Scientific Center of RAS, 420029, Sibirsky tract 10/7, Kazan, Russia

<sup>b</sup> Institute of Solid State Chemistry of RAS (UB), 620990, Pervomaiskaya St. 1, Ekaterinburg, Russia

<sup>c</sup> Institute of Physics, Kazan Federal University, 420008, Kremlevskaya st. 18, Kazan, Russia

\*tatyana.gavrilova@gmail.com

Compounds based on the lithium-vanadium phosphate Li<sub>3</sub>V<sub>2</sub>(PO<sub>4</sub>)<sub>3</sub> (LVPO) can be used as a cathode material in metal-ion batteries due to the stability of their crystal structure with respect to the change in the valence state of transition ion caused by the processes of intercalation/deintercalation of an alkaline element during the charge/discharge process of the electrochemical cell. In this context, the investigation of physical properties of Li<sub>3</sub>V<sub>2</sub>(PO<sub>4</sub>)<sub>3</sub>-based structures is of great interest. Here we present the magnetic and electrochemical properties investigations of Li<sub>3</sub>V<sub>2</sub>(PO<sub>4</sub>)<sub>3</sub>-based composites, including Li<sub>3</sub>V<sub>2</sub>(PO<sub>4</sub>)<sub>3</sub>/Li<sub>3</sub>PO<sub>4</sub> (LVPO/LPO) composite with the different Li<sub>3</sub>PO<sub>4</sub> salt concentration, Li<sub>3</sub>V<sub>2</sub>(PO<sub>4</sub>)<sub>3</sub>/C (LVPO/C) composite and three-component heterostructure Li<sub>3</sub>V<sub>2</sub>(PO<sub>4</sub>)<sub>3</sub>/C/Li<sub>3</sub>PO<sub>4</sub> (LVPO/C/LPO).

LVPO/LPO samples were obtained by the thermal hydrolysis method with the subsequent annealing in Ar atmosphere [1, 2]. In comparison, the LVPO/C composite was synthesized by the above-mentioned method and soft-template method [3]. The three-component heterostructure was obtained as a mechanical mixture of LVPO/C composite with Li<sub>3</sub>PO<sub>4</sub> salt. Magnetic properties of LVPO-based composites were investigated using magnetometry and electron spin resonance (ESR) methods. Electrochemical property investigations were performed by the galvanostatic method; the electrochemical voltage profiles and the discharge capacity depending on the number of charge–discharge cycles at different C-rates were obtained.

Based on magnetic properties measurements, it was shown that all as-prepared samples demonstrated the paramagnetic properties due to the presence of V<sup>4+</sup> ions (3d<sup>1</sup>, S=1/2). V<sup>4+</sup> ions appear due to the non-stoichiometry (lithium deficiency) of the sample and can be directly detected using the ESR method; the degree of non-stoichiometry depended on the chemical composition of the sample (including the amount of Li<sub>3</sub>PO<sub>4</sub> salt). Based on the electrochemical properties measurements, the increase in the discharge capacity for LVPO/LPO composite with increasing in lithium deficiency was observed.

As a result, the retention of the discharge capacity after hundred charge/discharge cycles was observed for LVPO-based composites and the almost complete reduction of vanadium ions to the valence state V<sup>3+</sup> after a few charge/discharge cycles was shown indicating the reversible intercalation of all lithium ions to the structure during the delithiation/lithiation process.

This work is supported by the Russian Science Foundation (grant #19-79-10216).

[1] T. Gavrilova, et al. Magnetochemistry 7, 64 (2021)

[2] T. Gavrilova, et al. Magnetochemistry 8, 105 (2022)

[3] T.P. Gavrilova, et al. Solid State Commun. 323, 114108 (2021)

# Low Temperature Phase Transitions in TbFeO<sub>3</sub> Orthoferrite: Magnetolectric Phase Diagrams

V. Ivanov\*, A. Kuzmenko, A. Tikhanovskii, A. Mukhin

Prokhorov General Physics Institute, RAS, 119991, Vavilov str. 38, Moscow, Russia

[ivanov@ran.gpi.ru](mailto:ivanov@ran.gpi.ru)

Terbium orthoferrite belongs to the class of multisublattice antiferromagnets with two magnetic subsystems: Fe<sup>3+</sup> ions, which are ordered at sufficiently high temperatures  $\approx 650$  K into the canted  $\Gamma_4(G_xF_z)$  configuration and undergo two spin-reorientation transitions into the  $\Gamma_2(G_zF_x)$  configuration at  $T_{sr} \approx 6 - 8$  K and back in  $\Gamma_4$  at the antiferromagnetic (AF) ordering of the Ising ions Tb<sup>3+</sup> into the configuration  $\Gamma_8(a_xg_y)$  at  $T_N \sim 3-3.5$  K. Based on the symmetry analysis of the magnetolectric interactions in rare-earth orthoferrites and orthochromites, the possibility of the existence of a magnetic field-induced electric polarization in TbFeO<sub>3</sub> was predicted in [1], and was found experimentally [2] in the  $P_a(H_b)$  geometry at  $T < T_N$ .

In this work, we study metamagnetic and orientational phase transitions in interacting rare-earth and iron subsystems in a magnetic field up to 5 T in the  $ab$ ,  $bc$ , and  $ac$  planes at  $T=1.85$  K. The transitions manifest themselves as anomalies (jumps) in the magnetization curves  $\sigma(H)$  for a fixed field orientation or anomalies on the angular dependences of the magnetization  $\sigma(\varphi)$ , as well as on the field dependences of the electric polarization  $P(H)$ . Phase diagrams are constructed (Fig. 1) and various magnetic structures are identified, two of which are magnetolectric. A theoretical model is proposed to describe the observed phase transitions and a quantitative description of the experimental phase diagrams is given. In addition to the  $P_a$  polarization component, a "hidden" (not manifested in the region of weak magnetic fields)  $P_c$  polarization component was also detected for some spatial orientations of the magnetic field. Specific features of the magnetolectricity manifestation are established, in particular, a linear increase of the polarization in an electric field up to 11 kV/cm, indicating a multidomain polar state in TbFeO<sub>3</sub> in these fields.

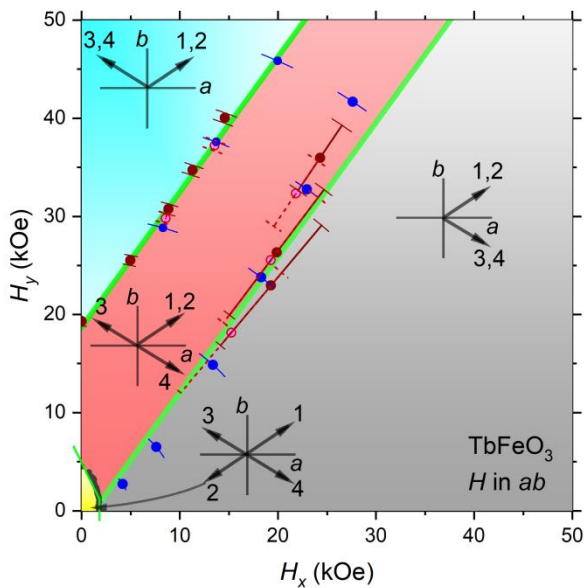


Fig. 1.  $H_x$ - $H_y$  phase diagram of the magnetic and magnetolectric states in TbFeO<sub>3</sub> at  $T=1.85$  K. The insets show the configurations of the magnetic moments of the terbium subsystem. The yellow low-field region corresponds to the AF configuration of Tb<sup>3+</sup> ions. In the gray and blue regions, all the Tb moments are reoriented along their Ising axes towards the  $a$ - or  $b$ - axes, respectively. The region of intermediate configurations with one reoriented Tb moment is highlighted in red. The black and maroon dots were obtained from the dependences  $\sigma(H)$ , and the blue dots, from  $\sigma(\varphi)$ . Green lines - calculated phase boundaries. The magnetolectric effect are observed in the yellow and red regions.

Support by RSF (Project No. 22-12-00375) is acknowledged.

[1] A.K. Zvezdin and A.A. Mukhin, JETP Letters **88**, 505 (2008).

[2] V.Yu. Ivanov, A.M. Kuz'menko, A.Yu. Tikhanovskii, A.A. Pronin, A.A. Mukhin, JETP Letters **117**, 38 (2023).

# Magnetic and Electronic Properties of $M_3B_2O_6$ (Me=Mn, Fe, Co, Ni) Kotoites: Representation Analysis and DFT Calculations

V. Zhandun<sup>a</sup>, O. Draganyuk<sup>a\*</sup>

<sup>a</sup> Kirensky Institute of Physics, Federal Research Center KSC SB RAS, Krasnoyarsk, Russia

\* [dron060694@mail.ru](mailto:dron060694@mail.ru)

In recent years, close attention has been focused on the compounds with geometric magnetic frustrations, because these materials can exhibit intriguing magnetic properties and magnetic states (spin glass, spin liquid, and spin ice). The magnetic structure of  $M_3B_2O_6$  ( $M = \text{Fe, Co, Ni, or Mn}$ ) oxyborates with a kotoite structure [1, 2] contain triangular groups connected into ribbons that can provide interesting magnetic peculiarities. In the present study the magnetic and electronic structures of  $M_3B_2O_6$  ( $M = \text{Fe, Co, Ni, or Mn}$ ) kotoites have been theoretically investigated at ambient and high pressures via a combination of representation analysis and density functional theory (DFT-GGA) calculations. A few spin configurations corresponding to the different irreducible representations have been considered. The total-energy calculations reveal that the magnetic ground state of  $M_3B_2O_6$  ( $M = \text{Fe, Ni, or Mn}$ ) corresponds to a collinear antiferromagnetic spin order along the  $z$  axis (Fig. 1a). In this case, in triangular structural elements, the magnetic moments are coupled ferromagnetically; and the coupling is antiferromagnetic between the triangles along the  $z$  axis. Cobalt kotoite has a magnetic structure with Co magnetic moments antiferromagnetic ordering along  $a$ -axis (Fig. 1b), while in triangular structural elements the magnetic moments are also coupled ferromagnetically. The exchanges constants obtained via DFT calculations showed that in Co- and Ni-based kotoites, interactions within triangles are much stronger than interactions between triangles. The evolution of the structural parameters, electronic structure and magnetic moments with pressure was investigated. The collapse of transition metal magnetic moments at the critical pressure about 50 GPa was found.

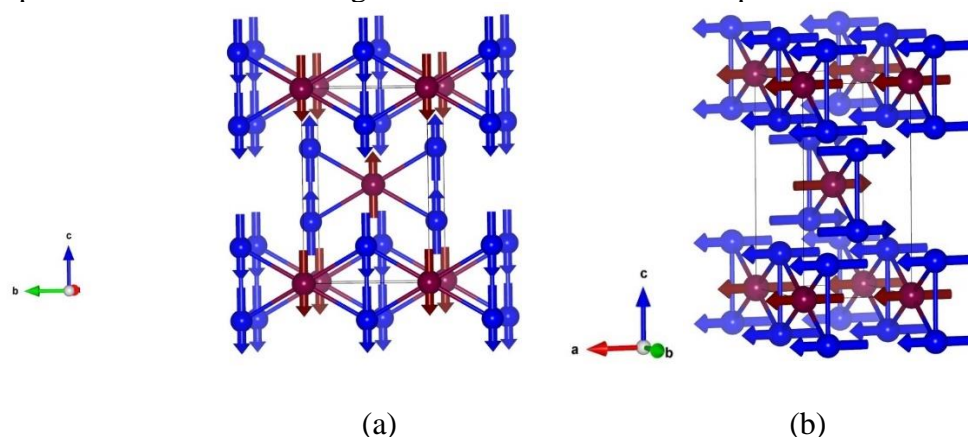


Figure 1. The magnetic structures of Mn-, Fe- Ni- (a) and Co- (b) based kotoites. The non-equivalent M1 and M2 sites are shown by garnet and blue color, correspondingly

Acknowledgements. The study was funded by a grant from the Russian Science Foundation # 22-22-20024 <https://rscf.ru/project/22-22-20024/>, Krasnoyarsk Regional Fund of Science.

[1] R. E. Newnham M. J. Redman, and P. Santoro, *Z. Kristallogr.* 121, 418 (1965).

[2] R. E. Newnham, R. P. Santoro, P. F. Seal, and G. R. Sallings, *Phys. Status Solidi* 16, K17 (1966).

# Magnetic and magneto-optical properties of lamellar magnetoplasmonic crystals based on $\text{Ni}_{80}\text{Fe}_{20}$

D. Murzin<sup>a,\*</sup>, V. Belyaev<sup>a</sup>, J. Kern<sup>b</sup>, C. Kaspar<sup>b</sup>, W. Pernice<sup>b,c</sup>, R. Bratschisch<sup>b</sup>,  
V. Rodionova<sup>a</sup>

<sup>a</sup> Research and Education Center “Smart Materials and Biomedical Applications” Immanuel Kant Baltic Federal University, 236041, Kaliningrad, Russia

<sup>b</sup> Institute of Physics and Center for Nanotechnology, University of Münster, 48149 Münster, Germany

<sup>b</sup> Kirchhoff-Institute of Physics, University of Heidelberg, 69120 Heidelberg, Germany

\*murzindmitri@gmail.com

Magnetoplasmonic crystals (MPICs) are periodically nanostructured multilayers of thin films made of combined noble and ferromagnetic materials [1]. MPICs exhibit enhanced transversal Kerr effect (TKE) if the phase-matching conditions for the surface plasmon polaritons excitation on their metal/dielectric interface are fulfilled making it possible to fabricate highly sensitive magnetic field probes based on them [2]. Optical, magnetic, and magneto-optical properties of MPIC, as well as the sensitivity of magnetic field probes based on them, strongly depend on their composition and morphological parameters making their complex characterization an important task for magnetic field sensors optimization.

This report demonstrates the results of reflectivity and TKE spectra as well as Kerr-magnetometry measurements for a series of lamellar MPICs with different diffraction stripes heights. Examples of obtained spectra and hysteresis loops for the MPIC sample with the diffraction stripes height of 67 nm are shown in Figure 1. According to the experimentally obtained spectra, the TKE modulation value had a linear dependence on the MPICs diffraction figure-of-merit for all studied samples and measured hysteresis loops showed that fabricated MPICs were in a state with rotatable magnetic anisotropy [3].

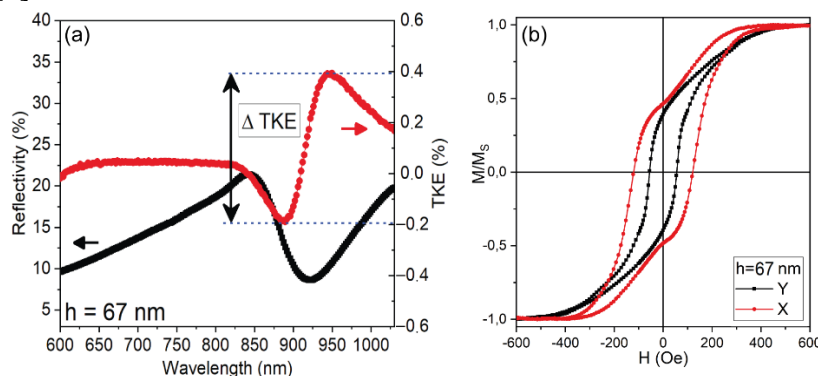


Figure 1. Results of spectroscopy and magnetometry measurements for the MPIC with the diffraction stripes height of 67 nm. Panel (a) shows the reflectivity (black) and TKE (red) spectra. Panel (b) shows hysteresis loops, measured in the in-plane magnetic field applied perpendicular (X direction, red) and parallel (Y direction, black) to the diffraction stripes of the MPIC.

This research was financially supported by the Ministry of Science and Higher Education of the Russian Federation, grant № 13.2251.21.0143. Authors appreciate the support of the M.V. Lomonosov Moscow State University Program of Development for the provided Kerr microscopy equipment.

[1] D. Murzin, *Photonics*, 9(12), 989 (2022)

[2] V.K. Belyaev, *Sci. Rep.* 10(1), 7133 (2020)

[3] A.V. Svalov, *IEEE Trans. Magn.*, 46(2), 333-336 (2010)

# Magnetic anisotropy and domain structure of epitaxial $\text{Mn}_5\text{Ge}_3$ thin film on Si(111) substrate

M. Rautskii<sup>a\*</sup>, I. Sobolev<sup>a,b</sup>, I. Yakovlev<sup>a</sup>, A. Lukyanenko<sup>a,b</sup>, A. Tarasov<sup>a,b</sup> and N. Volkov<sup>a,b</sup>

<sup>a</sup> Kirensky Institute of Physics, Federal Research Center KSC SB RAS, 660036, Akademgorodok 50/38,  
Krasnoyarsk, Russia

<sup>b</sup> Siberian Federal University, 660041, Svobodny 82A, Krasnoyarsk, Russia

\*[rmv@iph.krasn.ru](mailto:rmv@iph.krasn.ru)

Recently, much attention has been paid to magnetic materials based on Mn and Ge. One of such promising materials is  $\text{Mn}_5\text{Ge}_3$ , which is a ferromagnet with  $T_c = 296$  K, as well as high magnetization and polarization of about 42% [1]. Despite the fact that bulk  $\text{Mn}_5\text{Ge}_3$  was obtained quite a long time ago, high-quality  $\text{Mn}_5\text{Ge}_3$  epitaxial films have been grown relatively recently. At the same time, most of the  $\text{Mn}_5\text{Ge}_3$  films studied have been grown on Ge or GaAs substrates [2,3].

Nevertheless, in our opinion,  $\text{Mn}_5\text{Ge}_3/\text{Si}$  hybrid structures look more promising, since they make it possible to integrate a ferromagnetic element into the existing silicon semiconductor technology. However, the epitaxial growth of  $\text{Mn}_5\text{Ge}_3$  on silicon is a technologically more difficult task due to the mismatch of the crystal lattice parameters. Therefore, to implement the epitaxial growth of  $\text{Mn}_5\text{Ge}_3$  on Si, buffer layers were used. All samples were obtained using the Angara MBE [4] by molecular beam epitaxy on a p-Si(111) substrate at a temperature  $T = 390^\circ\text{C}$  and a pressure of  $6.5 \times 10^{-8}$  Pa.

In this work, we focused on studying the magnetic anisotropy of  $\text{Mn}_5\text{Ge}_3$  films. The investigations were carried out using measurements of the planar Hall effect and ferromagnetic resonance, which is very sensitive to magnetic anisotropy. All samples exhibit shape anisotropy typical of thin films. And the data obtained in the study of the planar Hall effect unambiguously indicate the formation of domains whose magnetic moment is noncollinear to the film plane. The presence of a complex magnetic anisotropy is also confirmed by the data obtained from the angular and temperature dependences of the FMR spectra. Such behavior of the domain structure, which is atypical for ferromagnetic films, can be associated with strong crystalline anisotropy or with the particular epitaxial relationship between the ferromagnet film and the substrate [5].

In addition, the temperature dependences of ferromagnetic resonance indicate a strong dependence of magnetic anisotropy on temperature, which increases significantly with decreasing temperature. The results obtained in this work indicate the high quality of the  $\text{Mn}_5\text{Ge}_3$  epitaxial films grown on Si substrates. We hope that these films will find application in silicon spintronic devices in the future.

Support by the Russian Science Foundation Grant of the № 23-22-10033, Krasnoyarsk Regional Fund of Science

- [1] A. Alvidrez-Lechuga et al. / *J. Alloys Compd.* 762, 363 (2018)
- [2] S. Olive-Mendez, et al. / *Thin Solid Films*, 517, 191 (2008)
- [3] R. Cardoso de Oliveira, et al. / *JMMM*, 539, 168325 (2021)
- [4] S. N. Varnakov, et al. / *Instrum. Exp. Tech.* 47, 839, (2004)
- [5] A. Truong, et al. / *Phys. Rev. B* 90, 224415 (2014)

# Magnetic Anisotropy of Nanostructured Cobalt Films

## Prepared by Oblique Spraying Method

L. Shendrikova<sup>a,\*</sup>, O. Trushin<sup>b</sup>, I. Fattakhov, A. Popov<sup>b</sup>, L. Mazaletsky<sup>b,c</sup>, A. Lomov<sup>d</sup>, D. Zakharov<sup>d</sup>

<sup>a</sup> Lomonosov Moscow State University, 119991, Leninskie gory 1, Moscow, Russia

<sup>b</sup> Valiev Institute of Physics and Technology, Yaroslavl Branch, Russian Academy of Sciences, 150007, Universitetskaya 21, Yaroslavl, Russia

<sup>c</sup> YARSU P. G. Demidov Yaroslavl State University, 150000, Sovetskaya 14, Yaroslavl, Russia

<sup>d</sup> Valiev Institute of Physics and Technology of Russian Academy of Sciences, 117218, Nakhimovskiy Prospekt 36, Moscow, Russia

\*corresponding author email

A promising method of forming films with special properties is to nanostructure them during growth. The formation of homogeneous structures and well-ordered arrays of nanostructures on the surface allows significantly change the electrophysical, magnetic and optical properties of films. One of the well-known techniques for growing nanostructures is angular spraying. This technique has attracted the interest of the community in recent years and many papers have been devoted to it. It is known that this method can produce nanostructures of different shapes and sizes, from inclined nanowires and nanospirals to vertical nanocolumns [1].

The aim of this work is to investigate the influence of the morphology of thin films on their magnetic properties. Previously, the conditions of nanostructuring of Co films on a silicon substrate under inclined deposition and the mechanisms of formation of arrays of nanocolumns with a high aspect ratio were investigated [2].

In this work, the samples obtained by electron beam evaporation on the Oratorio-9 were studied. The spraying conditions were as follows: base vacuum -  $4 \times 10^{-6}$  torr; electron beam voltage 8 kV; current 0.5 A. As a substrate, a piece of a standard monocrystalline silicon wafer with orientation (001) with a 300 nm thick thermal oxide layer of rectangular shape, size 20×15 mm, was used. The substrate was mounted on the holder at an angle to the flow of the sprayed material. The tilt angle was 85 degrees from normal. The distance between the target and the substrate was 1 m. Spraying was performed on both a stationary and a rotating substrate with rotating speed 0.6-30 rpm.

The magnetic properties of the films were measured using a LakeShore model 7407 vibrating sample magnetometer. Measurements were made at room temperature in fields up to 1.6 T. Hysteresis loops were measured at different orientations of the magnetic field relative to the plane of the samples.

It was found that spraying onto a stationary substrate result in the formation of an axis of light magnetization at an angle to the plane of the film. The samples obtained on rotating substrates formed an axis of light magnetization perpendicular to the substrate plane. The light magnetization axis is oriented along the axis of the nanofibers, thereby ensuring the inclination of the magnetization vector to the surface of the film.

[1] M.M. Hawkeye, M.T. Taschuk, M.J. Brett, London: John Wiley & Sons, 299 (2014).

[2] O. Trushin et al, Bull. Russ. Acad. Sci.: Phys., 85, 650 (2022)



# Magnetic machine-learning potential for magnetic alloys: a case study of Fe-Al

A. Kotykhov<sup>a,b\*</sup>, M. Hodapp<sup>c</sup>, C. Tantardini<sup>d,e</sup>, A. Shapeev<sup>a</sup>, and I. Novikov<sup>a,b</sup>

<sup>a</sup> Skolkovo Institute of Science and Technology, Skolkovo Innovation Center, Bolshoy boulevard 30, Moscow, 143026, Russian Federation

<sup>b</sup> Moscow Institute of Physics and Technology, Russian Federation

<sup>c</sup> Materials Center Leoben Forschung GmbH (MCL), Leoben, Austria

<sup>d</sup> Hylleraas center, Department of Chemistry, UiT The Arctic University of Norway, PO Box 6050 Langnes, N-9037 Tromsø, Norway

<sup>e</sup> Department of Materials Science, Rice University, Houston, Texas 77005, United States of America

\*kotykhov.as@phystech.edu

Magnetic properties of single-component metals or multi-component alloys are important to be taken into account for computer material modeling, because magnetism can affect phase stability or can be responsible, e.g., for negative thermal expansion, anomalous volume-composition dependence and other unusual properties. Density function theory calculations (DFT) can take magnetism into account, however they are computationally expensive. Therefore, we developed machine-learning interatomic potential for multi-component magnetic materials, which combines the accuracy of DFT calculations and the speed of semi-empirical potentials.

Our magnetic machine-learning potential (magnetic Moment Tensor Potential, mMTP) is based on the previously developed non-magnetic machine-learning MTP [1] and its magnetic single-component version [2]. Magnetism is taken into account through the explicit inclusion of the magnetic moments in the functional form of the potential.

To verify mMTP we created a training set with DFT calculations for the Fe-Al system with different concentration of Al atoms in supercell. We included configurations with both equilibrium and non-equilibrium magnetic moments to the training set. For DFT calculations we used the ABINIT package [3] including constrained DFT calculations [4] allows one calculating configurations with non-equilibrium magnetic moments. We next calculated formation energies, equilibrium lattice parameters and total magnetic moment of supercell for different Fe-Al structures. The results obtained with mMTPs are in good correspondence with the ones calculated with DFT. We also demonstrate that both mMTPs and DFT qualitatively reproduce the experimentally-observed anomalous volume-composition dependence in the Fe-Al system.

This work was supported by Russian Science Foundation (grant number 22-73-10206, <https://rscf.ru/project/22-73-10206/>).

[1] Novikov, Ivan S., et al. "The MLIP package: moment tensor potentials with MPI and active learning." *Machine Learning: Science and Technology* 2.2 (2020): 025002.

[2] Novikov, Ivan, et al. "Magnetic Moment Tensor Potentials for collinear spin-polarized materials reproduce different magnetic states of bcc Fe." *npj Computational Materials* 8.1 (2022): 13.

[3] Gonze, Xavier, et al. "The ABINIT project: Impact, environment and recent developments." *Computer Physics Communications* 248 (2020): 107042.

[4] Gonze X. et al. "Constrained Density Functional Theory: a potential-based self-consistency approach." *Journal of Chemical Theory and Computation* 18.10 (2022): 6099-6110.

# Magnetic nanoparticles produced via pulsed laser ablation of thin Co films in water

V. Nesterov<sup>a,\*</sup>, D. Shuleiko<sup>a</sup>, D. Presnov<sup>a,b</sup>, S. Zaboltnov<sup>a</sup>, E. Konstantinova<sup>a</sup>, N. Chechenin<sup>b</sup> and I. Dzhun<sup>b</sup>

<sup>a</sup> Skobeltsyn Institute of Nuclear Physics

<sup>b</sup> Faculty of Physics

Lomonosov Moscow State University, 1/2 Leninskie Gory, Moscow, 119991, Russia

\* n.slawa2011@yandex.ru

Pulsed laser ablation in liquids (PLAL) is a powerful, universal, and green method to produce nanoparticles (NPs) with desirable size and functional properties. In particular, this technique is a promising tool to synthesize magnetic NPs (MNPs) such as metal oxides or carbides which are important due to their high potential in applications: biomedicine, catalysis, data storage, environmental remediation and sensorics. This is because PLAL may readily provide fabrication of oxide or carbide NPs due to the interaction of species in the laser-induced plasma plume from a target material with chemical components from a buffer liquid (for example, water and acetone). Among the transient metal classes, cobalt and iron oxides are of interest due to their spinel structure, unique properties, and low costs.

Generally, to produce MNPs the PLAL of bulk materials is applied, while using thin films as targets is less studied. In our work, the generation of colloidal nanoparticles in water from thin Co films was explored for the film thicknesses in a range of 5–500 nm that covers both important for PLAL depths: the skin layer (typically about 30 nm) and the thermal diffusion length (about 500 nm).

The Co films were deposited on glass substrate via DC magnetron sputtering in Ar. These films were immersed in distilled water and illuminated by a 1064 nm wavelength of a picosecond pulsed Nd:YAG laser source to produce MNPs. These produced colloids were examined by placing the magnet to cuvette's surface and all of them demonstrated magnetic response.

The dependence of hydrodynamic radius (HDR) of NPs obtained from dynamic light scattering data on the film thickness is non monotonic. Thus, at decrease film's thickness from 500 to 50 nm MNPs size slightly increases from 80 to about 100 nm. At thicknesses of 25 and 15 nm HDR greatly increases up to 1  $\mu\text{m}$ , and then decreases to 150 nm at film thickness of 5 nm. Such dependence can be caused by the difference of PLAL mechanisms [1] and by peculiarities of thermal diffusion at the film-substrate interface and increased heating of the surrounding liquid medium [2]. All colloid size distributions are characterized with high standard deviation of 40% for 500–50 nm films and 20% for skin layer range films. The broad size distribution is confirmed by scanning electron microscopy that additionally showed coexistence of 100 nm sized MNPs among with few-tens nanometer MNPs. Besides the MNPs tended to form agglomerates.

Raman spectra for the obtained MNPs possess the same lines for all film thicknesses. That is, the typical spectrum for Guite ( $\text{Co}^{2+}\text{Co}_2^{3+}\text{O}_4$ ) was revealed.

Ferromagnetic resonance spectra for the MNPs are characterized with high resonance fields and broad lines due to dipole interaction of MNPs in agglomerates and dipole interaction of agglomerates. The low intensity of absorption peaks can be due to both relatively large size of the MNPs which leads to reduction of net magnetic moment arises from uncompensated spins of the MNPs surface and small MNPs concentrations.

[1] A. S. Scaramuzza, J. Phys. Chem C 120, 9453 (2016)

[2] D.M. Bubb Chem. Phys. Lett. 565 65 (2013)

# Magnetic properties of aerogels based on graphene decorated with iron oxide nanoparticles

I. Burmistrov<sup>a,b</sup>, V. Korovushkin<sup>a</sup>, A. Babkin<sup>c</sup>, E. Neskromnaya<sup>d,e</sup>, V. Kostishyn<sup>a</sup>, A. Morchenko<sup>a,\*</sup>

<sup>a</sup> MISIS University of Science and Technology, 119049, Leninsky Ave., 4, Moscow, Russia

<sup>b</sup> Plekhanov Russian University of Economics, 117997, Stremyanny lane 36, Moscow, Russia

<sup>c</sup> Lomonosov Moscow State University, 119991, Leninskie gory 1, Moscow, Russia

<sup>d</sup> Vernadsky Institute of Geochemistry and Analytical Chemistry,  
Russian Academy of Sciences, 119991, Kosygin str. 19, Moscow, Russia

<sup>e</sup> JSC "Giredmet", 111524, 2, p.1, Elektrodnyaya str., Moscow, Russia

\*dratm@mail.ru

Recently, reduced Graphene Oxide (rGO) has been used in the creation of materials for the adsorption storage and transportation of methane, sorbents for the purification of aqueous media from various types of pollutants. Composites based on it containing magnetic nanoparticles are used in the development of biosensors, microwave absorption materials and graphene aerogels. The latter have an increased efficiency of removing pollutants of organic and inorganic nature (petroleum products, pesticides, heavy metal salts, nitrates, nitrites, etc.), which is especially important in conditions when new substances with high chemical activity appear). In the review [1] devoted to this problem, among other aspects, absorbing materials are considered, which, after being used for their intended purpose, could be easily collected using magnetic systems. Among them, nanocomposite hydro- and aerogels based on low-layer packages of graphene sheets decorated with iron oxide nanoparticles  $\text{Fe}_3\text{O}_4$  and  $\gamma\text{-Fe}_2\text{O}_3$  (magnetite and maghemite) are distinguished, with specific surface area and sorption capacity up to  $750 \text{ m}^2/\text{g}$  and  $1400 \text{ mg/g}$ , respectively, surpassing such well-known absorbers as graphene oxide aerogel, graphene oxide/silk fibroin hybrid aerogel, agar/graphene oxide composite aerogel, chitosan cross-linked graphene oxide/lignosulfonate composite aerogel, partially reduced graphene oxide aerogels induced by proanthocyanidins, etc. At the same time, nanoparticles of iron and its compounds can act as a crosslinking agent, ensuring the formation of a stable gel structure [2]. However, in the very extensive bibliography of the mentioned review, there are practically no studies devoted to the actual magnetic properties of such absorbents. In this work, an attempt is made to fill this gap.

The objects of study were aerogels containing 10, 22, and 35.7 wt.% Fe. The number of carbon layers in them is  $\sim 5\text{--}7$ , and aggregates of iron oxide nanoparticles with a size of  $\sim 7\text{--}20 \text{ nm}$  are identified on the surface of randomly arranged graphene flakes. In the aerogel with the highest iron content, agglomerates with sizes of  $30\text{--}40 \text{ nm}$  are observed on the surface.

The data of aerogel research using methods of vibrational magnetometry and Mössbauer spectroscopy are presented. The ratio of the phases  $\text{Fe}_3\text{O}_4$  and  $\gamma\text{-Fe}_2\text{O}_3$  depending on the concentration of iron in the gels is determined. They were prepared the samples of composite materials based on aerogels with 22, and 35.7 wt.% Fe, polyethylene or polyvinylidene fluoride copolymers, and their magnetic and electrical characteristics were studied.

[1] A. Abidli, Y. Huang, Z.B. Rejeb, A. Zaoui, C.B. Park, *Chemosphere* 292, 133102 (2022)

[2] A.V. Melezhik, E.A. Neskromnaya, A.E. Burakov, A.V. Babkin, I.V. Burakova, A.G. Tkachev, The carbon nanomaterials with abnormally high specific surface area for liquid adsorption, Ch. 25 in: *Sustainable Nanotechnology for Environmental Remediation*. Elsevier (2022)

## Magnetic properties of Al-doped barium hexaferrite

### $\text{BaFe}_{12-x}\text{Al}_x\text{O}_{19}$

S. Gudkova<sup>a,b\*</sup>, V. Zhivulin<sup>b</sup>, G. Zirnik<sup>b</sup>, N. Cherkasova<sup>b</sup>, I. Solizoda<sup>b</sup>, D. Vinnik<sup>a,b</sup>

<sup>a</sup> Institute of Physics and Technology, 141701, Institutskiy per. 9, Dolgoprudny, Russia

<sup>b</sup> South Ural State University, 454000, pr. Lenina 76, Chelyabinsk, Russia

\*svetlanagudkova@yandex.ru

Interest in the study of barium hexaferrites (BaM) and their solid solutions is associated with the unique physical properties of these materials. Recently, interest in hexaferrites has been revived due to discovery of intrinsic multiferrocity in this class of compounds [1, 2].  $\text{Fe}^{3+}$  ions of barium hexaferrite crystal cell is located in five different crystallographic sites. It reveals the possibility of  $\text{Fe}^{3+}$  substitution by magnetic or nonmagnetic ions to improve BaM properties. Barium hexaferrite magnetic and electrical properties modification leads to discover new electronic applications.

There are many works in the literature devoted to the aluminum substitution of barium hexaferrite. It is known that substitution with aluminum leads to an increase in the frequency of ferromagnetic resonance, however, studies devoted to the study of modification of the magnetic sublattice in this solid solution have not been found. This work is devoted to the study of magnetic and structural parameters of barium hexaferrite substituted with aluminum in paramagnetic and ferromagnetic states.

$\text{BaAl}_x\text{Fe}_{12-x}\text{O}_{19}$  ( $x = 1$ ) samples were produced using solid state reaction method [3]. The composition of the samples was investigated using a scanning electron microscope (SEM) Jeol JSM7001F equipped with an energy dispersive X-ray fluorescence spectrometer (EDS) Oxford INCA X-max 80 for elemental analysis. X-ray powder diffraction (XRD) was performed on a diffractometer Rigaku Ultima IV in the angular range from  $15^\circ$  to  $65^\circ$  with filtered  $\text{CuK}\alpha$  radiation. The magnetic structure of Al-doped BaM have been studied by means of neutron diffraction at room temperature,  $500^\circ\text{C}$  and near Curie temperature. The distribution of substitutive Al ions in BaM crystal lattice was determined by means of Mossbauer spectroscopy. Macromagnetic properties was measured by SQUID magnetometer.

According to Mossbauer's data, aluminum ions occupy positions 2a and 12k in  $\text{BaAlFe}_{11}\text{O}_{19}$  crystal cell. According to neutron diffraction data, an increase in cell parameters is observed with an increase in temperature. Neutron diffraction fitting confirms the presence of Al ions in 2a and 12k positions. This nonmagnetic ions distribution leads to the magnetic moment decrease from  $20 \mu_B$  for undoped BaM to  $15 \mu_B$  for  $\text{BaAlFe}_{11}\text{O}_{19}$ , this is consistent with a 30 percent decrease in saturation magnetization of  $\text{BaAlFe}_{11}\text{O}_{19}$  in comparison with  $\text{BaFe}_{12}\text{O}_{19}$ .

Authors would like to acknowledge P. Borisova and E. Dujeva for neutron diffraction measurements, V.M. Kostishin for Mossbauer spectra, S.V. Taskaev for magnetic measurements.

[1] V. Turchenko [et al.], Adv. 931, 167433 (2023)

[2] S. Gupta [et al.], J. Magn. Vagn. Mat. 540, 168483 (2021)

[3] V. Zhivulin [et al.], J. Mat. Res. Tech. 11, 2235 (2021)

# Magnetic Properties of BaM- type Mn,Ti hexaferrites

K. Pavlova<sup>a,\*</sup>, V. Zhivulin<sup>a</sup>, S. Taskaev<sup>a</sup>, I. Solizoda<sup>a</sup>, D. Sherstyuk<sup>a</sup>, D. Vinnik<sup>a,b</sup>

<sup>a</sup>South Ural State University (National Research University), 454080, Leninn Ave. 76, Chelyabinsk, Russia.

<sup>b</sup>Moscow Institute of Physics and Technology (National Research University), 141701, Institutskiy per. 9,

Dolgoprudny, Moscow Region, Russia

\*pavlovakp@susu.ru

Ferritic materials with the structure of magnetoplumbite  $BaFe_{(11.9-x)}Mn_{0.1}Ti_xO_{19}$ , where  $x = 0.1; 0.5$ , obtained by solid-phase synthesis at a temperature of 1400 °C and an isothermal exposure of 5 hours. The phase composition and structure of the obtained samples were studied using a Rigaku powder diffractometer Optima IV model (Cu–K $\alpha$  radiation). The elemental composition was studied using an electron scanning microscope JEOL JSM 7001F. The areas of phase transitions were determined by the DSC curves recorded at a heating rate of 10 °C/min, Netzsch STA 449F1 Jupiter. Magnetic properties were measured using a Versa Lab Quantum Design vibration magnetometer in the range of magnetic fields 0 – 3 T at a temperature of 300 K.

Using the data of powder radiographs, the parameters of the unit cell of the studied samples were calculated (tabl. 1), the nonmonotonic nature of the change in the crystal's lattice parameters is associated with the irregular substitution of substituent elements at low concentrations.

Table 1. Parameters of the crystal structure of the obtained compounds

Brutto formula	Lattice parameters, Å		Magnetization (300K) Am <sup>2</sup> /kg
	<i>a</i>	<i>c</i>	
BaFe <sub>11.75</sub> Mn <sub>0.1</sub> Ti <sub>0.1</sub> O <sub>19</sub>	5.8946±0.0003	23.1964±0.0012	70.8998302
BaFe <sub>11.45</sub> Mn <sub>0.1</sub> Ti <sub>0.5</sub> O <sub>19</sub>	5.89184±0.00018	23.2252±0.0007	67.4872666
BaFe <sub>10.96</sub> Mn <sub>0.1</sub> Ti <sub>1</sub> O <sub>19</sub>	5.89217±0.00012	23.2949±0.0006	59.8471986

Figure 1 shows the DSC curves and Curie temperatures, as a result of the substitution of iron atoms with titanium and manganese atoms, it monotonically decreases compared to the initial value for barium hexaferrite. Substitution of ferrum cations for titanium ones leads to a decreasing in saturation magnetization (fig. 2), remanent magnetization, and coercivity.

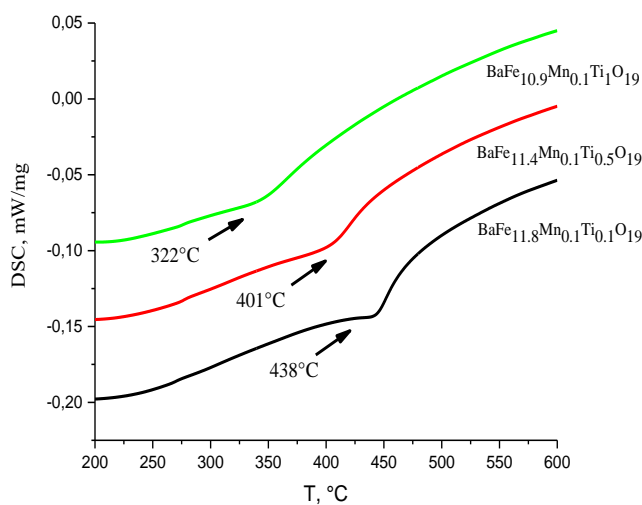


Figure. 1. DSC curves of the samples and Curie temperature

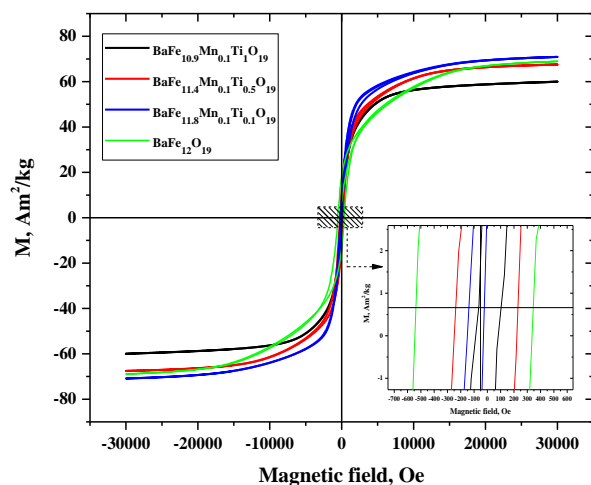


Figure. 2. Field dependences of the specific magnetization of ferrites at T = 300K

# Magnetic Properties of Broadened Landau Levels at the Saddle Point Energy of Two Dimensional Lattice

A. Nikolaev<sup>a,\*</sup>, M. Zhuravlev<sup>b</sup>

<sup>a</sup> Skobeltsyn Institute of Nuclear Physics, Lomonosov Moscow State University,  
119991, Leninskie gory 1, Moscow, Russia

<sup>b</sup> St. Petersburg State University, St. Petersburg, 199034, Russia

\*nikolaev@srd.sinp.msu.ru

Studying the magnetic characteristics of the two dimensional (2D) lattice (hexagonal, graphene-like [1] and the square one [2]) by solving numerically the exact system of discrete equations, which fully describes the broadening of Landau levels, we have found that the energy spectrum of the Landau level at the energy of the saddle point is principally continuous, so that even in a very small magnetic field this Landau level is always broadened in a miniband. In contrast to that, at other energies in a weak magnetic the spectrum of Landau levels is discrete. At the energy of the saddle point of the Brillouin zone (which is also known as a Van Hove peak) the corresponding density of states  $N(E_F)$  is formally infinite ( $N(E_F) \rightarrow +\infty$ ).

We then consider the 2D square lattice [2], used as a prototype electron system in which the Fermi level lies exactly at the Van Hove peak. According to the electron band treatment this could lead to a formally divergent paramagnetic susceptibility and an infinite electron contribution to the specific heat at zero temperature. Our accurate analysis shows that both values remain finite. Taking into account the electron spin polarization and the obtained numerical solution, we reproduce the temperature dependence of the induced magnetic moment proportional to the magnetic susceptibility, and the electron contribution to the specific heat. Both plots demonstrate unusual dependencies reflecting the “metal”-like or “insulator”-like structure of the Landau minibands in the neighborhood of the Fermi energy. At low temperatures all values display oscillatory behavior. We also prove rigorously that the fully occupied electron band has no contribution to the diamagnetic susceptibility and specific heat [1,2].

[1] A. V. Nikolaev, Physical Review B, **104**, 035419 (2021); Physical Review B, **105**, 039902 (2022).

[2] A.V. Nikolaev, M.Ye. Zhuravlev, Journal of Magnetism and Magnetic Materials, **560**, 169674 (2022).

## Magnetic Properties of Layered Ni/Cu Nanowires Depending on the Thicknesses of Cu-Layers

A. Rizvanova<sup>a,b</sup>, D. Bizyaev<sup>c</sup>, D. Khairtadinova<sup>a,b,\*</sup>, D. Zagorskiy<sup>a</sup>, I. Doludenko<sup>a</sup>, L. Panina<sup>b,d</sup>

<sup>a</sup> FSRC “Crystallography and Photonics” RAS, 119333, Leninskiy avenue 59, Moscow, Russia

<sup>b</sup> NUST MISIS, 119049, Leninskiy avenue 4, Moscow, Russia

<sup>c</sup> Zavoisky Physical-Technical Institute, FRC Kazan Scientific Center of RAS, 420029, Sibirskiy tract 18, Kazan, Russia

<sup>d</sup> Immanuel Kant Baltic Federal University, 236004, Nevskogo 14, Kaliningrad, Russia

\*hairtadr@gmail.com

Ferromagnetic nanowires (NWs) are elongated, one-dimensional nanoparticles that have specific magnetic properties due to their small size and high aspect ratio. The geometrical dimensions of NWs can be precisely controlled, which is important for applications in electronics and medicine. Layered NWs have additional spacing parameters to tune their magnetic properties.

In this work, arrays of NWs, consisting of nickel and copper layers were obtained by electrochemical deposition into the pores of the polymer track membranes with different diameters (30-100 nm). A series of samples where the height of the nickel layers was 400 nm, and the height of the copper layers varied from 25 to 400 nm were obtained. The hysteresis loops of the NW array were measured by vibrating sample magnetometry (VSM) and the magnetization processes in individual NWs were investigated by magnetic force microscopy (MFM). In addition, the samples were examined by scanning electron microscopy (SEM).

The study of NWs arrays by VSM showed that for 100 nm diameter NWs, with increasing the Cu layer height layer, the difference in hysteresis loops in two directions of the magnetizing field almost disappeared which may indicate a significant role of the dipole interaction between neighboring nanowires. The evolution of hysteresis loops in 30 nm diameter NWs was different because of stronger shape anisotropy and weaker dipole interactions. The coercive force is 150-200 Oe for Nws of 100 nm diameter and it increases to 300-650 Oe. for NWs with a diameter of 30 nm

For MFM investigation, isolated NWs were obtained. A suspension of NWs in a drop of water was placed on a glass substrate, and an alternating rotating magnetic field was applied. The MFM method was used to study remagnetization of NWs with a diameter of 100 nm in the presence of an external magnetic field varying from +160 Oe to -160 Oe (Fig.1). The change in the magnetization distribution of the two NWs occurred at -40 – -50 Oe, which indicates that the coercive force of this pair of NWs is about 40-50 Oe, which is considerably smaller than observed in NW array.

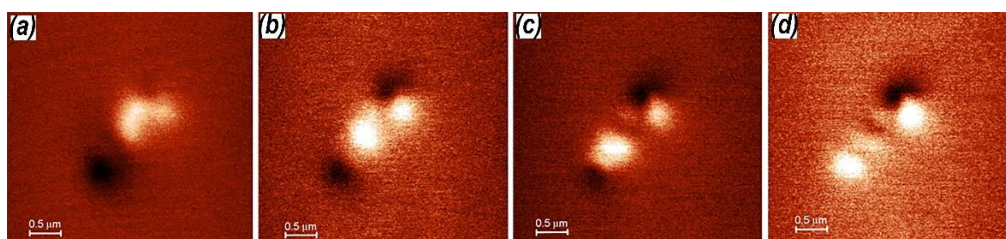


Fig.1 MFM images of NWs in the applied magnetic field with values a) 160 Oe; b) -40 Oe; c) -5 Oe; d) -160 Oe

Acknowledgements. The authors are grateful to Apel P.Yu. (Joint Institute of Nuclear Research, Dubna) for providing track membranes. The work was supported by the Russian Science Foundation, project no. 22-22-00983.

# Magnetic Properties of $\text{Ln}_{0.5}\text{Sr}_{1.5}\text{Ti}_{0.75}\text{Cu}_{0.25}\text{O}_4$ (Ln= Pr, Nd) layered perovskite

T. Gavrilova<sup>1a,\*</sup>, A. Yagfarova<sup>a</sup>, I. Yatsyk<sup>a</sup>, M. Cherosov<sup>b</sup>, R. Batulin<sup>b</sup>, Yu. Deeva<sup>c</sup>,

T. Chupakhina<sup>c</sup>, R. Eremina<sup>a</sup>

<sup>a</sup> Zavoisky Physical-Technical Institute, FRC Kazan Scientific Center of RAS, 420029, Sibirsky tract 10/7, Kazan, Russia

<sup>b</sup> Institute of Physics, Kazan Federal University, 420008, Kremlevskaya st. 18, Kazan, Russia

<sup>c</sup> Institute of Solid State Chemistry of RAS (UB), 620990, Pervomaiskaya St. 1, Ekaterinburg, Russia

\*tatyana.gavrilova@gmail.com

Layered perovskite structures with the chemical formula  $\text{A}_2\text{BO}_4$  (where A is a rare earth or alkaline earth element, and B is - d-metals of the IV period of the periodic table) belong to the Ruddlesden-Popper phases and they are widely known and intensively studied due to their multifunctional set of properties and promising practical applications. The scientific interest in  $\text{Ln}_{0.5}\text{Sr}_{1.5}\text{Ti}_{0.75}\text{Cu}_{0.25}\text{O}_4$  (Ln= Pr, Nd) compounds is caused by the following experimental fact. It is known from literature that the dielectric properties of these compounds differ significantly, although they have a similar crystal structure and morphology [1]. In this context, the study of magnetic properties is of particular interest. Here we present the detailed magnetometry and electron spin resonance measurements of  $\text{Ln}_{0.5}\text{Sr}_{1.5}\text{Ti}_{0.75}\text{Cu}_{0.25}\text{O}_4$  (Ln= Pr, Nd) oxides to investigate the possible realization of a complex magnetic structure due to the presence of two magnetic ions and the strong competition of different types of magnetic interactions.

$\text{Ln}_{0.5}\text{Sr}_{1.5}\text{Ti}_{0.75}\text{Cu}_{0.25}\text{O}_4$  (Ln= Pr, Nd) complex oxides with a layered perovskite structure were synthesized using the precursor method by the pyrolysis of metal-organic compositions. Magnetic properties were investigated using the magnetometry and electron spin resonance (ESR) methods. Magnetization measurements showed that the absolute value of the magnetization and effective magnetic moment for  $\text{Ln}_{0.5}\text{Sr}_{1.5}\text{Ti}_{0.75}\text{Cu}_{0.25}\text{O}_4$  (Ln=Nd) compound is much higher than in the case Ln=Pr (Fig. 1). A significant difference was also observed in the magnetization dependences on the external magnetic field and in the electron spin resonance spectra. This may be due to the presence of a magnetic moment of neodymium ions  $\text{Nd}^{3+}$  ( $4f^1$ ,  $S=1/2$ ) in contrast to the zero-magnetic moment of praseodymium ions  $\text{Pr}^{3+}$  ( $4f^0$ ,  $S=0$ ).

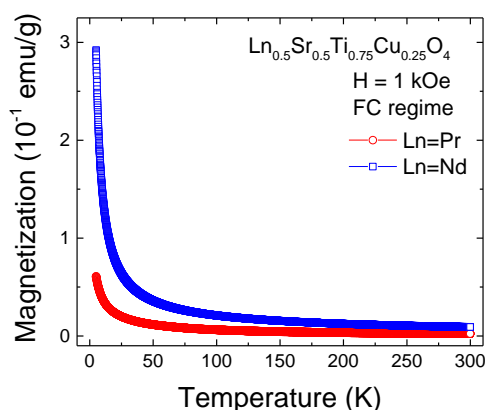


Fig. 1. Temperature dependence of magnetization for  $\text{Ln}_{0.5}\text{Sr}_{1.5}\text{Ti}_{0.75}\text{Cu}_{0.25}\text{O}_4$  (Ln= Pr, Nd) layered perovskites measured in FC regime in the external magnetic field  $H = 1$  kOe.

Finally, despite of the similar crystal structure these two compounds can exhibit various magnetic properties. One can assume that the observed difference in dielectric properties for these two compounds may be related to the difference in their magnetic properties.

[1] T.I. Chupakhina, et al. Mendeleev Commun. 29, 349 (2019)



## Magnetic properties of oxyborate with huntite structure

V. Titova <sup>a,b\*</sup>, I. Gudim <sup>a</sup>, E. Eremin <sup>a,b</sup>

<sup>a</sup>Kirensky institute of Physics, Federal Research Center KSC SB RAS, 660036, Krasnoyarsk, Russia

<sup>b</sup>Siberian Federal University, 660041 Krasnoyarsk, Russia

\* bb1995@mail.ru

Modern development of radio-electronic technology requires materials with high crystallographic perfection and purity.

Single crystals obtained by high-temperature methods have unique physical properties and are of great interest because of the potential for their practical application [1],[2].

The  $\text{Ho}_{1-x}\text{Nd}_x\text{Fe}(\text{BO}_3)_4$  family of crystals was chosen for research.

For the growth of  $\text{Ho}_{0.5}\text{Nd}_{0.5}\text{Fe}_3(\text{BO}_3)_4$  crystals, a melt-solution was chosen: 79% wt.  $\{\text{Li}_2\text{WO}_4 + 3,5\text{B}_2\text{O}_3 + 0,4(0,5\text{Nd}_2\text{O}_3 + 0,5 \text{Ho}_2\text{O}_3)\} + 21\%$  wt.  $\text{Ho}_{0.5}\text{Nd}_{0.5}\text{Fe}_3(\text{BO}_3)_4$ .

The grown single crystals of  $\text{Ho}_{0.5}\text{Nd}_{0.5}\text{Fe}_3(\text{BO}_3)_4$  were selected for measurements taking into account the possibility of their orientation with respect to the main crystallographic axes. Three samples were made for measurements:  $\perp c_3$ ,  $\perp a$ ,  $\perp b$ .

Measurements are carried out based on the PPMS-9 setup, which allows temperature measurements in the range of 5–350 K and magnetic fields up to 9 T.

Figure 1 shows the temperature dependences of the magnetization of  $\text{Ho}_{0.5}\text{Nd}_{0.5}\text{Fe}_3(\text{BO}_3)_4$  single crystals grown on the basis of lithium tungstate.

The temperature dependence of the magnetization  $M_{\parallel}$  and  $M_{\perp}$  was measured in a magnetic field of 0.1 T directed along the crystallographic c-axis and in the basal plane along the a-axis, respectively.

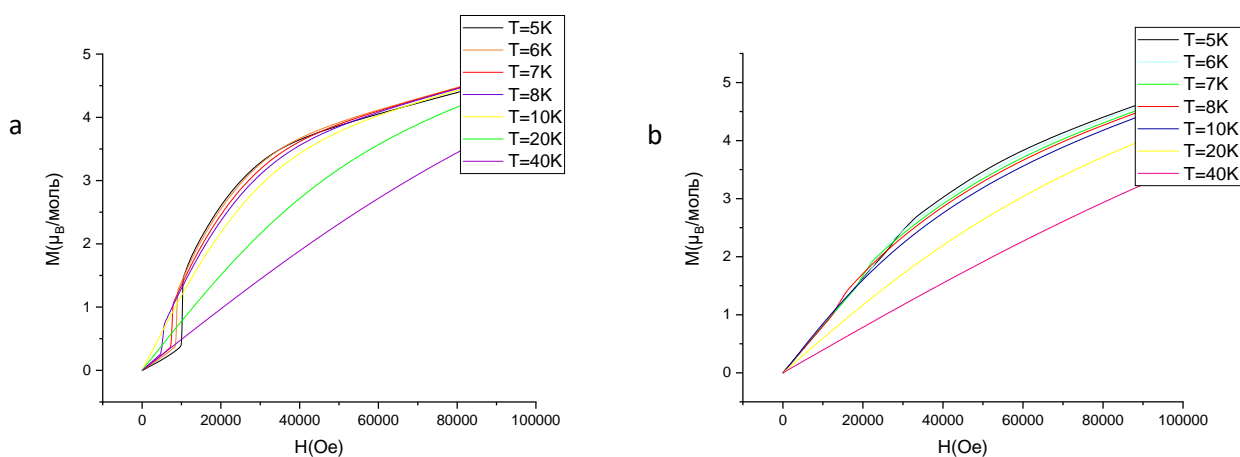


Figure 1 - Field dependence of the magnetization of the grown  $\text{Ho}_{0.5}\text{Nd}_{0.5}\text{Fe}_3(\text{BO}_3)_4$  crystal from a melt-solution based on lithium tungstate: a)  $\perp$  axis c, b)  $\parallel$  axis c, from a solution-melt based on lithium tungstate.

Support by RSF and KRFS № 22-12-20019 are acknowledged.

[1] Hinatsu Y., Doi Y., Ito K. et al. // J. Solid State Chem. 2003. V. 172. P. 438.

[2] Звездин А.К., Кротов С.С., Кадомцева А.М. и др. // Письма в ЖЭТФ. 2005. V. 81.

№ 6. P. 335.

## Magnetic properties of Ru/CoFe/Ru films

M. Kuznetsova<sup>a,\*</sup>, A. Prikhodchenko<sup>a</sup>, M. Bazrov<sup>a</sup>, A. Turpak<sup>a</sup>, A. Kozlov<sup>a</sup>

<sup>a</sup> Far Eastern Federal University, 690922, Russkii island, Vladivostok, Russia

\*kuznetcova.mal@dvfu.ru

The creation of new nanoscale materials is an urgent task of modern spintronics. In the present study, a non-magnetic metal (TM)/ferromagnet (FM) interface is used, in which it is possible to induce perpendicular magnetic anisotropy caused by the action of spin-orbit and dipole interactions. This approach makes it possible to use the Ru/CoFe/Ru thin film system as the basis for the manufacture of new generation magnetic recording devices.

The object of the study was a series of Ru(10nm)/Co<sub>90</sub>Fe<sub>10</sub>(0.45-10nm)/Ru(2nm) samples obtained by magnetron sputtering on a SiO<sub>2</sub> substrate with a variable thickness of the ferromagnetic layer. The layer thicknesses were selected in accordance with a previous study [1]. The value of the thickness of the film layers was registered using a quartz thickness gauge and additionally refined by X-ray reflectometry.

The magnetic parameters were studied based on the hysteresis loops M(H) using a vibromagnetometer (7410 VSM, LakeShore) in the directions of an external magnetic field applied in and out of the film plane. Based on the obtained magnetic characteristics, graphs of the dependence of the magnetic saturation moment, coercive force, effective anisotropy energy on the thickness of the Co-Fe ferromagnetic layer were plotted, as shown in Fig.1.

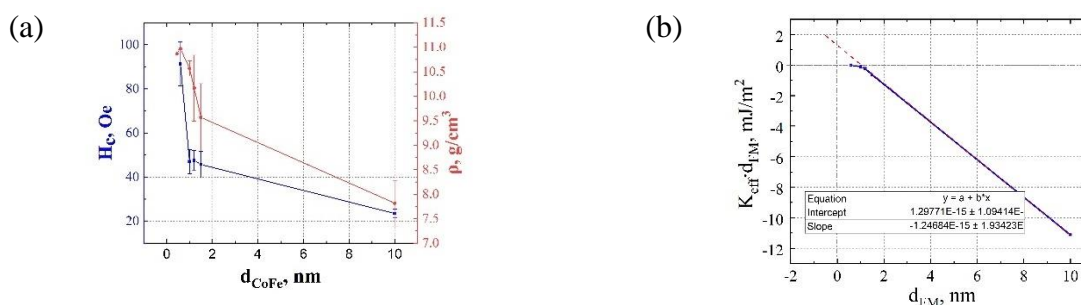


Figure 1. Dependences of Hc and layer density (a),  $K_{eff} \cdot d_{CoFe}$ (b) on the thickness of the Co-Fe alloy ferromagnetic layer

As a result of the study, it was revealed that the series is characterized by predominantly planar magnetic anisotropy, the behavior of magnetic parameters was explained taking into account the structure of the Ru/CoFe/Ru film layers.

### Acknowledgments

This research was supported by the grant of the Government of the Russian Federation for state support of scientific research conducted under supervision of leading scientists in Russian institutions of higher education, scientific foundations, and state research centers of the Russian Federation (Project No. 075-15-2021-607).

[1] Kolesnikov, Alexander G., et al. "Enhancement of perpendicular magnetic anisotropy and coercivity in ultrathin Ru/Co/Ru films through the buffer layer engineering." Journal of Physics D: Applied Physics 49.42 (2016): 425302.

## Magnetic Properties of the Impurity Sublattice of Semiconductor Crystals $\text{Cd}_{1-x}\text{Zn}_x\text{Te}$ ( $x = 0.05; 0.03; 0$ )

P. Podkur<sup>a,\*</sup>, I. Volchkov<sup>a</sup>, R. Morgunov<sup>b</sup>, V. Kanevskii<sup>a</sup>

<sup>a</sup> FSRC «Crystallography and Photonics» RAS, 119333, Leninskiy Prospekt 59, Moscow, Russia.

<sup>b</sup> Institute of Problems of Chemical Physics RAS, 142432, Chernogolovka, Russia

\*vverde85@yandex.ru

Progress in the area of semiconductor materials and technologies contributes to the widespread use of semiconducting crystals, in particular CdTe and  $\text{Cd}_{1-x}\text{Zn}_x\text{Te}$ , in electronics and energetics. These semiconductor crystals are the most promising materials for the development of X-ray and gamma radiation detectors operating at room temperature. In addition, thin films based on CdTe and  $\text{Cd}_{1-x}\text{Zn}_x\text{Te}$  are of interest, which can be used not only in the solar energy industry, but also in the field of semiconductor spintronics, like many  $\text{A}_{\text{III}}\text{B}_{\text{V}}$  and  $\text{A}_{\text{II}}\text{B}_{\text{VI}}$  compounds [1]. Due to this fact, it becomes important to study the magnetic properties of these semiconductor crystals. It should be noted that although the CdTe and  $\text{Cd}_{1-x}\text{Zn}_x\text{Te}$  crystals themselves are diamagnetic, their impurity sublattice is capable of exhibiting magnetic properties [2, 3]. Since doping of semiconductors is a standard way to achieve the necessary profile characteristics of semiconductors (such as electrical, optical properties, sensitivity to X-rays, etc.), it is also necessary to study the magnetic properties of the impurity sublattice.

CdTe and  $\text{Cd}_{1-x}\text{Zn}_x\text{Te}$  samples grown by the modified Obreimov-Shubnikov method at the FSRC "Crystallography and Photonics" RAS were used as the material under study. The impurity composition and structure of the samples were controlled by mass spectrometry by the iCAP Q ICP-MS (Thermo Scientific), EDX analysis by the JCM 6000 Plus (Jeol), and X-ray phase analysis by the X'PERT Pro MRD (Panalytical). Magnetic hysteresis was recorded by the SQUID MPMS XL (Quantum Design) magnetometer.

All samples under the study were diamagnets. However, the  $\text{Cd}_{1-x}\text{Zn}_x\text{Te}$  samples slightly deviated from the standard diamagnetic characteristic of a stoichiometric crystal. Moreover, it is interesting that this deviation was observed not only at 2K, but also, in a very small form, at 300K. The subtraction of the diamagnetic component of the crystal lattice made it possible to isolate the magnetic component of the impurity sublattice. In both cases, ferromagnetic hysteresis loops were observed. However, if on the  $\text{Cd}_{1-x}\text{Zn}_x\text{Te}$  ( $x=0.03$ ) sample they were insignificant, only slightly exceeding the measurement error, for the  $\text{Cd}_{1-x}\text{Zn}_x\text{Te}$  ( $x=0.05$ ) sample a pronounced ferromagnetic loop was observed.

An impurity analysis of the samples showed that, in addition to the Zn dopant, they contain minor amounts of Fe and Ni impurities (no more than 0.002 at %). However, this already turns out to be sufficient for the ferromagnetic ordering of the defect sublattice. Interesting that the greatest magnetic properties are performed not by the crystal ( $\text{Cd}_{0.97}\text{Zn}_{0.03}\text{Te}$ ) in which the concentration of magnetic impurities is maximum, but by the crystal containing the highest concentration of Zn ( $\text{Cd}_{0.95}\text{Zn}_{0.05}\text{Te}$ ). Possible reasons for the observed magnetic properties of the impurity sublattice are discussed, as well as the difference in the magnitude of the magnetic properties of crystals. The discovered magnetic properties suggest that the crystals  $\text{Cd}_{1-x}\text{Zn}_x\text{Te}$  are dilute magnetic semiconductors.

This work was performed within the State assignment of Federal Scientific Research Center "Crystallography and Photonics" of Russian Academy of Sciences.

[1] P.G. Baranov, et al. Physics-Uspekhi, 62, 795 (2019).

[2] Yu. V. Shaldin, et al., Semiconductors, 38, 288 (2004).

[3] P. Podkur, et al, Crystallography Reports, 68, 62 (2023).

# Magnetic State of Layered Cobalt Chalcogenides

## $\text{Co}_7\text{X}_8$ (X = Se, Te)

V. Ogloblichev<sup>a,\*</sup>, Yu. Piskunov<sup>a</sup>, A. Sadykov<sup>a</sup>, D. Akramov<sup>a,b</sup>, N. Selezneva<sup>b</sup>, N. Baranov<sup>a,b</sup>

<sup>a</sup> Mikheev Institute of Metal Physics of UB of RAS, 620108, S. Kovalevskoy 18, Yekaterinburg, Russia,

<sup>b</sup> Ural Federal University, 620002, Mira 19, Yekaterinburg, Russia

\*ogloblichev@imp.uran.ru

We are studying cobalt chalcogenides  $\text{Co}_7\text{Se}_8$  and  $\text{Co}_7\text{Te}_8$  belonging to cation-deficient layers compounds  $\text{M}_7\text{X}_8$ , where M are 3d transitional metal atoms and X are divalent Group VI anions S, Se, or Te. These compounds are characterized by vacancies in metallic layers and the formation of various superstructures caused by the ordering of vacancies and M atoms in layers. Vacancies in  $\text{M}_7\text{X}_8$  compounds with the NiAs structure are distributed in each second basic layer of transition metal atoms, which is the main principle of the formation of these superstructures. A well-known representative of this class of compounds is pyrrhotine  $\text{Fe}_7\text{S}_8$  [1, 2].

Structural and magnetic properties of the  $\text{Co}_7\text{Te}_8$  compound have been studied for the first time using X-ray, measurements of the magnetic susceptibility and  $^{59}\text{Co}$  nuclear magnetic resonance spectroscopy. The nuclear magnetic resonance study of  $\text{Co}_7\text{Se}_8$  selenide with the same structural type (NiAs) as  $\text{Co}_7\text{Te}_8$  has also been performed for the first time. The components of the magnetic shift and electric field gradient tensors at the location of  $^{59}\text{Co}$  nuclei have been determined from the NMR spectra. The analysis of these spectra has revealed a significant local charge and magnetic inhomogeneity of  $\text{Co}_7\text{Se}_8$  and  $\text{Co}_7\text{Te}_8$ . The hyperfine coupling constant  $H_{\text{hf}}$  in Co ions has been estimated from the temperature dependences of the shift and susceptibility in  $\text{Co}_7\text{Te}_8$  ( $H_{\text{hf}} = 188(5)$  kOe/ $\mu_B$ ). The hyperfine coupling constant for  $\text{Co}_7\text{Se}_8$  cannot be determined similarly because the shift in this compound is not proportional to the magnetic susceptibility in the entire temperature range. It has been found that the ordering of vacancies and Co atoms in cation layers is absent in the  $\text{Co}_7\text{Te}_8$  compound, and its crystal structure is more planar and is characterized by a significantly smaller ratio  $c_0/a_0$  compared to  $\text{Co}_7\text{Se}_8$ . This difference is apparently due to a larger polarizability of Te ions and to a higher degree of covalence of Co-Te bonds compared to Co-Se bonds. Since an increase in the interatomic distances from  $\text{Co}_7\text{Se}_8$  to  $\text{Co}_7\text{Te}_8$  occurs predominantly in the plane, it does not lead to a stronger localization of electrons or to the appearance of magnetic moments on Co atoms, as could be expected. The  $\text{Co}_7\text{Te}_8$  compound is even closer to classical Pauli paramagnets than  $\text{Co}_7\text{Se}_8$ . It has been shown that a nonmonotonic temperature-induced change in the magnetic susceptibility and the spin-lattice relaxation rate in the  $\text{Co}_7\text{Se}_8$  compound can be due to strong electron-electron correlations

This work was supported by the Russian Science Foundation (project no. 22-12-00220).

[1] C. I. Pearce, R. A. D. Patrick, D.J. Vaughan, Rev. Mineral. Geochem. 61, 127 (2006)

[2] H. Wang, I. Salveson, Phase Transition 78, 547 (2005)

[3] Yu.V. Piskunov et al., JETP Letters, 117, 54 (2023)

## Magnetization processes in Ni/Cu layered nanowires

S. Lukkareva<sup>a,\*</sup>, L. Panina<sup>a,b</sup>, I. Doludenko<sup>c</sup>, D. Zagorskiy<sup>c</sup>

<sup>a</sup> NUST MISIS, 119049, Leninskiy Avenue 4, Moscow, Russia

<sup>b</sup> Immanuel Kant Baltic Federal University, Kaliningrad, 236016 Russia

<sup>c</sup> FSRC “Crystallography and Photonics” RAS, 119333, Leninskiy Avenue 59, Moscow, Russia

\*lukkarevasa@gmail.com

Magnetic nanostructures in the forms of nanorods and nanowires are of great interest for research thanks to their unique properties due to their high aspect ratio. Such structures can be used in nanoelectronics, sensors, and in the biomedical field [1].

Heterogeneous nanowires contain layers of ferromagnetic material (Fe, Co, Ni) and metallic spacer (Cu, Ag, Au). With a certain combination of geometrical parameters (diameter and height) of the layers, it is possible to tune the alignment of the magnetization vector with respect to the NW axis. At a certain aspect ratio of ferromagnetic layers ( $AR = \text{height/diameter}$ ) and spacing between them, antiparallel alignment of magnetization in the neighboring layers or a vortex-like magnetization distribution can form, which leads to the formation of an artificial superparamagnetic state of a whole array of nanowires [2].

In this work, the synthesis and properties of such structures obtained by electrodeposition into the pores of ion-track membranes were studied. Technological regimes for producing Ni/Cu layered NW with given geometrical parameters were developed. The NW samples were characterized by scanning electron microscopy (SEM) methods, X-ray diffraction (XRD), and vibrating sample magnetometry (VSM).

The pore diameter of PETE ion track membranes varied from 30 to 200 nm with a predicted array length of 3  $\mu\text{m}$ . Nickel and copper layers were altered by changing the deposition potential and their length was controlled by the passed charge. SEM results showed that the heights of layers in 200 nm pores correspond to the calculations based on the passed charge. XRD data showed that NWs consist of three main phases: Ni, Cu, and NiCu. VSM results showed that there is a drastic change in the form of hysteresis loops (Fig.1) for different values of layers' thickness for all diameters. Arrays of Ni/Cu nanowires with different AR show magnetic anisotropy for wires with  $AR > 1$  with a high value of coercive force and remanence, while with  $AR < 1$  the loops show low values of coercivity and remanence. The results confirmed the existence of an easy magnetization axis in the parallel direction for all samples, which can be explained by high dipole interactions manifested between adjacent wires.

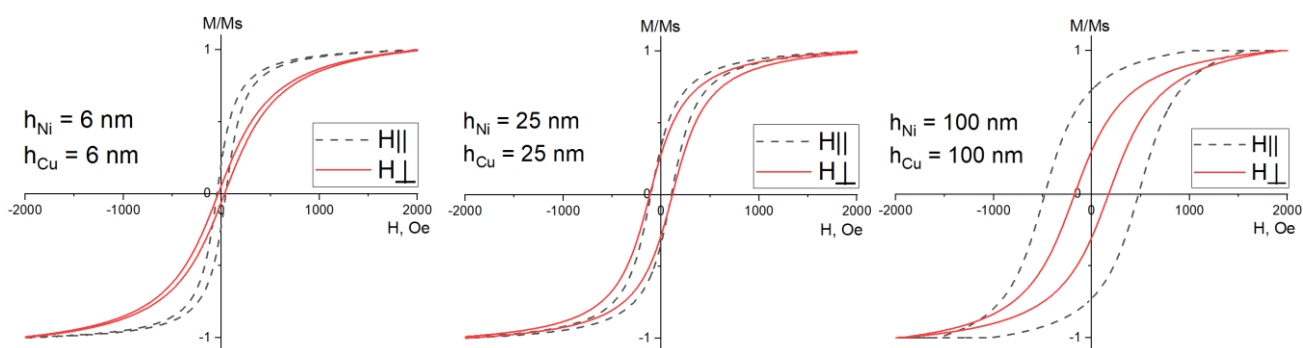


Fig.1. The hysteresis loops for layered nanowires with 30 nm diameter and various layer AR

[1] S. Sharko, Journal of Alloys and Compounds, 846(2020)

[2] C. Ezeh, Asian Journal of Applied Sciences 7, 4 (2019)

# Magneto-Impedance Tomography of Co-based amorphous wires

D. Bukreev\*, M. Derevyanko, A. Moiseev, A. Semirov

Irkutsk State University, 664003, Karl Marx 1, Irkutsk, Russia

\*da.bukreev@gmail.com

Direct study of the magnetic structure of the amorphous soft magnetic wires is difficult. However, it is possible to use the frequency dependences of the magnetoimpedance effect (MI) for this [1]. The higher the AC frequency  $f$ , the thinner the skin layer. Therefore, as the frequency increases, the inner regions contribution to the wire impedance  $Z$  decreases, while the surface regions contribution, on the contrary, increases. Thus, it is possible to reconstruct the distribution of magnetic parameters over the wire cross section by analyzing the frequency dependences of the MI. This method can be called magneto-impedance tomography (MIT).

MIT of the  $\text{Co}_{66}\text{Fe}_4\text{Ta}_{2.5}\text{Si}_{12.5}\text{B}_{15}$  amorphous wires with the radius of  $r_0 = 55 \mu\text{m}$  and the length of 90 mm was carried out according to the frequency dependences of MI, obtained using an automated complex of magnetoimpedance spectroscopy [2] in the frequency range of (0.01–100) MHz. The external magnetic field  $H$  was oriented along the wire length. Its maximum strength was  $H_{\text{max}} = \pm 12.3 \text{ kA/m}$ . MIT was performed as described in [3].

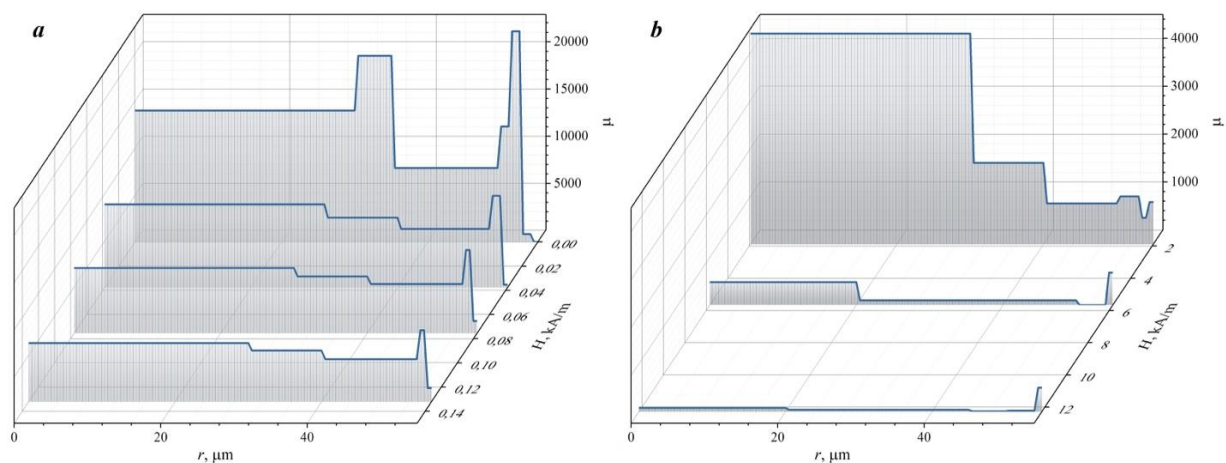


Figure 1. The radial distributions of the magnetic permeability  $\mu$  of the  $\text{Co}_{66}\text{Fe}_4\text{Ta}_{2.5}\text{Si}_{12.5}\text{B}_{15}$  wire reconstructed using MIT. The distributions are given for magnetic fields with intensity: a) 0, 0.04, 0.08, 0.13 kA/m; b) 1.9, 5.7 и 12.3 kA/m.

The magnetic permeability  $\mu$  of the wire outer layers ( $r > 52.5 \mu\text{m}$ ) in the zero external magnetic field is much lower than that of the inner layers. As  $H$  increases, the permeability of the outer layers first increases and then decreases. From this we can conclude that their magnetic anisotropy is predominantly circular.

The magnetic permeability of the inner regions at  $H = 0$  is more than 5000. With an increase in the magnetic field strength,  $\mu$  decreases, tending to 1 (Fig. 1). This behavior of  $\mu$  corresponds to predominantly axial magnetic anisotropy.

Support by RSF (project No 22-22-00709, <https://rscf.ru/project/22-22-00709/>) is acknowledged.

[1] L.V. Panina, K. Mohri, Appl Phys Lett. 65, 1189(1994).

[2] D.A. Bukreev, M.S. Derevyanko, A.A. Moiseev, A. V Semirov, P.A. Savin, G. V Kurlyandskaya, Materials 13, 3216 (2020).

[3] D.A. Bukreev, M.S. Derevyanko, A.A. Moiseev, A. V Svalov, A. V Semirov, Sensors 22, 9512 (2022).

## Magneto-optic YIG magnetometer for registration magnetic submicron particles

O. Lutsenko<sup>a,\*</sup>, P. Kapralov<sup>a,b</sup>, A. Leontyev<sup>a</sup>, N. Koshev<sup>c</sup>, M. Zharkov<sup>a,d</sup>, I. Radchenko<sup>a</sup>, M. Ostras<sup>a,b</sup>

<sup>a</sup> QLU, 121205, Bolshoy boulevard, 30, bld. 1, Moscow, Russia

<sup>b</sup> International Center for Quantum Optics and Quantum Technologies, 121205, Bolshoy boulevard, 30, bld. 1, Moscow, Russia

<sup>c</sup> Skolkovo Institute of Science and Technology, 121205, Bolshoy boulevard, 30, bld. 1, Moscow, Russia

<sup>d</sup> National Research Mordovia State University, 430005, Bolshevistskaya, 68, Saransk, Russia

\*o.lutsenko@rqc.ru

The field of nanomedicine is exploring a new approach called theranostics, which combines therapy and diagnostics to provide more personalized and precise care for patients with better outcomes. Magnetic nanoparticles such as [1,2] have shown potential in various diagnostic and therapeutic applications, making them ideal candidates for use in theranostic platforms. To support this, a new type of magnetometer has been developed that can detect magnetic nanoparticles and submicron particles in biological fluids and tissues.

The magnetometer uses a sensitive element made of a thin yttrium-iron garnet film grown on a garnet base and senses the magnetic state of the film using the magneto-optic Faraday effect. It can operate at room temperature and has a wide dynamic range, enabling measurements in unshielded environments.

In this study, various types of magnetic particles were explored: 1) submicron ‘nanospheres’ Fe<sub>3</sub>O<sub>4</sub> particles and submicron Fe<sub>3</sub>O<sub>4</sub> ‘rods’, which are promising for high remanence (fig.1); 2) magneto-electro nanoparticles CoFe<sub>2</sub>O<sub>4</sub>@BaTiO<sub>3</sub>, which show potential for medical applications. 25 μg of Fe of ‘nanospheres’ sample was registered.

Overall, this new magnetometer offers potential advantages for precise and quantitative detection of magnetic objects in biological samples, which could greatly improve theranostic capabilities.

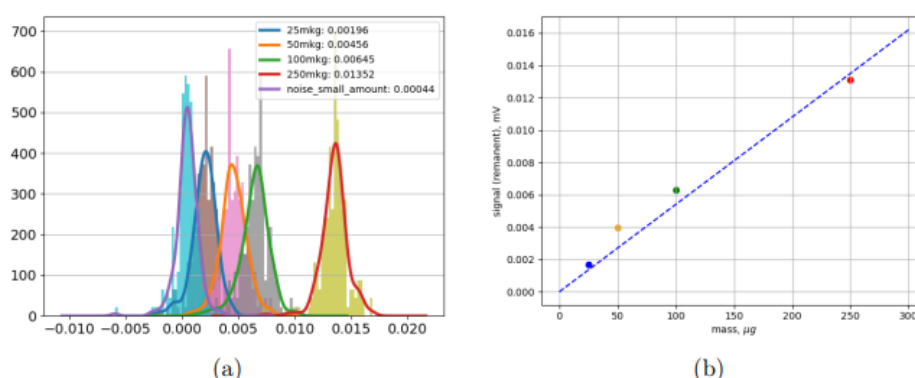


Figure 1. Remanent magnetization: (a) and (b) - histograms of measured signal, 200 measurements for every amount of ‘nanospheres’ sample for 25, 50, 100, 250 μg.

[1] Y.Huang, Langmuir 31, 1172–1179 (2015)

[2] E. Stimphil, Applied Physics Reviews 4(2):021101 (2017)

## Modification of colloidal CdZnSeS/ZnS alloyed quantum dots with thiols for application in analytical systems

P. Strokin, D. Drozd, A. Moshkov, I. Goryacheva

Saratov State University, 410012, Astrakhanskaya st. 83, Saratov, Russia

stropa99@mail.ru

Colloidal quantum dots (QDs) are luminescent semiconductor nanocrystals characterized by a narrow emission peak and a wide range of photoluminescence excitation. One-step synthesis and the possibility of controlled change in the wavelength of the photoluminescence maximum without changing the physical size of the nanocrystal are the main advantages of alloyed QDs [1]. The properties of alloyed QDs colloidal solutions have been studied to a lesser extent. Studies carried out in this direction demonstrate the potential for application of this type QDs in a number of analytical methods, including bioanalysis [2].

The object of this study is the CdZnSeS/ZnS alloyed QDs obtained by the method of one-step high-temperature organometallic synthesis. QDs obtained in this way are hydrophobic, which makes it impossible to use them in biological solution and necessitates their hydrophilization. In this work, the following hydrophilizing agents are used: dihydrolipoic acid (DHLA), thioglycolic acid (TGA), mercaptopropionic acid (MPA), 2-mercaptoethanol (BME). The dependences of the following properties of hydrophilized alloyed QDs on the applied modifier were studied: the photoluminescence quantum yield (QY), the periods of colloidal and optical stability, and cytotoxicity.

During hydrophilization with the use of BME, TGA and MPA, an increase in QY was noted. The maximum increase was observed when using BME and amounted to 51% relative to the original sample. A decrease in colloidal stability during long-term storage was noted for alloyed QDs hydrophilized with an excess of BME. This effect is less pronounced for TGA and MPA. As the storage temperature decreases, the stability of the samples under consideration increases. DHLA-modified alloyed QDs have lower toxicity than with other modifiers, which gives them an advantage in case of use in bioanalysis.

The reported study was funded by the Russian Science Foundation: project number 23-13-00380.

[1] Aubert, Tangi, et al. "Homogeneously Alloyed CdSe $_{1-x}$ S $_x$  Quantum Dots ( $0 \leq x \leq 1$ ): An Efficient Synthesis for Full Optical Tunability." *Chemistry of Materials* 25.12 (2013): 2388-2390.

[2] Lee, Ki-Heon, et al. "Highly efficient, color-reproducible full-color electroluminescent devices based on red/green/blue quantum dot-mixed multilayer." *ACS nano* 9.11 (2015): 10941-10949.



# New Magneto-optical Effects in One-Dimensional Magnetophotonic Crystal Induced by Broken Spatial Symmetry

T. Mikhailova <sup>a\*</sup>, D. Ignatyeva <sup>a,b,c</sup>, P. Kapralov <sup>c</sup>, S. Lyashko <sup>a</sup>,

V. Berzhansky <sup>a</sup>, V. Belotelov <sup>a,b,c</sup>

<sup>a</sup> V.I. Vernadsky Crimean Federal University, Simferopol, 295007, Russia

<sup>b</sup> Lomonosov Moscow State University, Moscow 119991, Russia

<sup>c</sup> Russian Quantum Center, 121205 Moscow, Russia

\* tatladismikh@cfuv.ru

Traditionally, magnetophotonic crystals (MPCs) are used to enhance the Faraday effect, which in classical observation geometry is linear in magnetization. However, as it turned out, simple one-dimensional MPCs are also capable of exhibiting other unusual magneto-optical properties, if conditions are intentionally introduced into the observation geometry for violation of spatial symmetry – an oblique incidence of electromagnetic wave with a mixed (s + p) polarization state. The broken spatial symmetry allows the appearance of asymmetric and intensity Faraday effects. The effects arise in the vicinity of resonant wavelength of a microcavity MPC and appear during remagnetization of MPC in opposite directions. In the case of asymmetric Faraday effect, the angles of Faraday rotation for opposite magnetic states differ not only in sign, but also in absolute value. The maximum observed value of the asymmetric Faraday effect is about 30% of the absolute value of Faraday rotation (Fig. 1, a). The intensity Faraday effect manifests itself in the change of transmission coefficient. Investigation have shown that the modulation of transmission coefficient of light reaches 6% (Fig. 1, b).

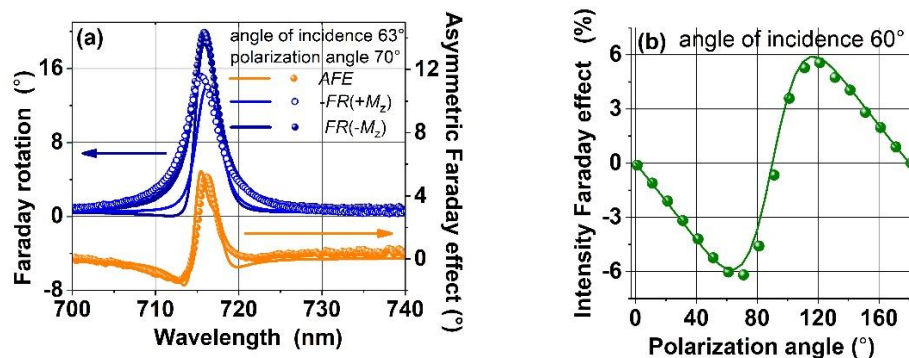


Figure 1. Spectra of asymmetric Faraday effect (a) and magneto-optical linear dichroism (b) of the MPC for the oblique illumination. Experimental data is presented by color spheres, while simulations – by solid curves.

The effects can be used in magneto-optical imaging, modulators and switches, magnonics and optomagnetism.

This work was financially supported by the Ministry of Science and Higher Education of the Russian Federation, Megagrant project N 075-15-2022-1108.

# Numerical modeling of the optical parameters of gold nanoparticles of different size

I. Kon<sup>a</sup>, D. Poltorabatko<sup>a</sup>, A. Zyubin<sup>a</sup>, I. Samusev<sup>a</sup>

<sup>a</sup>Immanuel Kant Baltic Federal University, 236004, Nevskogo 14, Kaliningrad, Russia

REC «Fundamental and Applied Photonics. Nanophotonics», Immanuel Kant Baltic Federal University

\*Correspondence author email: y.rainskon-70y@mail.ru

Nanoparticles of noble metals, in particular gold, are widely used for research in the field of nanoplasmonics. One of the characteristic features of the optical properties of gold nanostructures is the occurrence of localized surface plasmon resonance (LSPR) on them, which is induced on the surface by laser radiation. Gold-based nanocomplexes have a number of advantages: the ability to bind biomolecules [1], high absorption cross section [2], biocompatibility and low cytotoxicity [3], as well as plasmon excitation peaks in the visible light range. These properties can be used, for example, in such a promising field as optosensorics.

The main task in the study of nanoparticles and nanostructures is to find the optimal parameters for the frequency of the light pulse, media with different refractive indices, the geometry of nanoparticles, etc. The possibility of creating various nanostructures requires, first of all, a theoretical evaluation of the efficiency.

In this case, methods of mathematical calculation of the optical properties of nanostructures are used. In particular, for the purposes of nanoplasmonics, we use the Finite-Difference Time-Domain, (FDTD) method. The FDTD method is based on the discretization of Maxwell's equations, which have a differential form [4].

The aim of the work is to study the optical properties of gold nanoparticles by varying their parameters. By acting on a nanoparticle with a wide range of polychromatic waves. Such optical parameters of nanoparticles as the maximum values of the electric field strength  $E$ , scattering cross section, absorption cross section and extinction cross section are numerically obtained. The extinction cross section is the total attenuation parameter of the incident beam due to absorption and scattering near the surface of the nanoparticles.

Modeling is carried out in Ansys Lumerical software. To calculate the extinction cross section, a script is used that specifies access to the parameters of the scattering cross section, the absorption cross section, and the electric field profile  $E$  at its maximum intensity. The extinction cross section is found as:

$$\sigma_{\text{ext}} = \sigma_{\text{scat}} + \sigma_{\text{abs}} \quad (1)$$

The script calculates these parameters depending on the energy of the photon

Acknowledgements: Funding: Igor Kon was supported by Immanuel Kant Baltic Federal University, "Priority 2030" project number 122062100020-4.

References:

- [1] J. Heddle, *Catalysts*, 3 (2013).
- [2] C. Kim, et al., *ACS Nano* 4 (2010).
- [3] Y. Pan, et al., *Small*, 3 (2007).
- [4] K. Yee, *IEEE*. 14, 3 (1966)

## Optical and transport measurements of HgTe/HgCdTe semiconductor heterostructures in high magnetic fields

O. Surdin<sup>a,b,\*</sup>, Yu. Kudasov<sup>a,b</sup>, V. Platonov<sup>a,b</sup>, I. Makarov<sup>b</sup>, D. Maslov<sup>a,b</sup>, A. Korshunov<sup>b</sup>, I. Strelkov<sup>b</sup>  
R. Kozabaranov<sup>b</sup>

<sup>a</sup> Sarov Physics and Technology Institute, NRNU “MEPhI”, Sarov, Russia

<sup>b</sup> Russian Federal Nuclear Center – VNIIEF, Sarov, Russia

\*mossom1@rambler.ru

Most methods for studying the band structure of 2D systems are based on magnetotransport and magneto-optical experiments. The paper presents the technique and results of cyclotron resonance measurement in the temperature range 77–300 K in HgTe/Hg<sub>1-x</sub>Cd<sub>x</sub>Te heterostructures with quantum wells [1]. The measurements were carried out in pulsed magnetic fields up to 50 T at the SarPTI NRNU MEPhI high magnetic field facility [2]. The samples under the study differed in the width of the quantum wells, their number and the composition content. For these samples, cyclotron resonance lines were recorded (Figure 1a) for the first time at temperatures above 77 K [3]. It is shown that it is possible to measure simultaneously cyclotron resonance and the quantum Hall effect in the pulsed magnetic field (Figure 1b). The quantum Hall effect in several HgTe/Hg<sub>1-x</sub>Cd<sub>x</sub>Te heterostructures was studied at a temperature of 4,2 K.

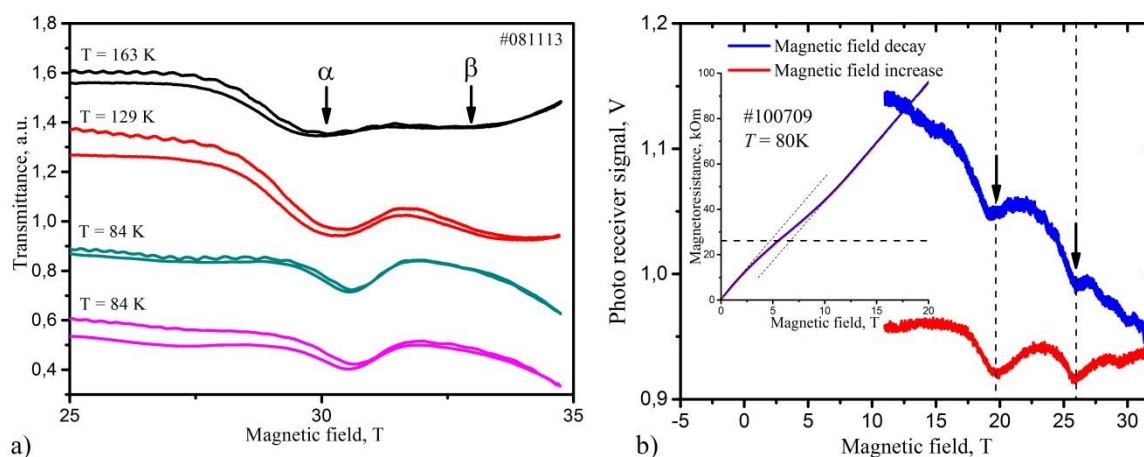


Figure 2. Cyclotron resonance and quantum Hall effect measurements in HgTe/Hg<sub>1-x</sub>Cd<sub>x</sub>Te heterostructures.

[1] S. Dvoretzky, N. Mikhailov, Y. Sidorov, et al. Journal of Elec Materi (2010) 39: 918. <https://doi.org/10.1007/s11664-010-1191-7>

[2] Y.B. Kudasov, I.V. Makarov, D.A. Maslov et al. Instrum Exp Tech (2015) 58: 781. <https://doi.org/10.1134/S0020441215050097>

[3] A.V. Ikonnikov, S.S. Krishtopenko, O. Drachenko, et.al. Temperature-dependent magnetospectroscopy of HgTe quantum wells, Pys. Rev. B 94, 155421 (2016).

## Orthogonal magnetic structures of Fe<sub>5</sub>O<sub>6</sub>: representation analysis and DFT calculations

V. Zhandun<sup>1\*</sup>, N. Kazak<sup>1</sup>

<sup>1</sup>Kirensky Institute of Physics - Federal Research Center “Krasnoyarsk Science Centre, Siberian Branch of the Russian Academy of Sciences”, 660036 Krasnoyarsk, Russia

\*e-mail: jvc@iph.krasn.ru

Iron oxides are attracting a lot of attention due to their complex structural properties and fundamental aspects from the point of view of the natural sciences and industrial applications [1,2]. In the last decade, studies at high temperatures and high pressures have revealed the existence of new binary iron oxides with unusual stoichiometry, such as Fe<sub>4</sub>O<sub>5</sub> [3] and Fe<sub>5</sub>O<sub>6</sub> [4]. The discovery of new classes of systems motivated the study of their physical properties and potential for innovative applications [2]. While structural information and some properties of the new oxides at atmospheric pressure are available, information on their electronic and magnetic properties under extreme pressure-temperature conditions is very limited. Knowledge of these properties is important for both solid state physics and the earth sciences. We have applied a combination of irreducible representation analysis and density-functional theory plus Hubbard U (DFT + U) calculations to analyze the ground magnetic state of Fe<sub>5</sub>O<sub>6</sub> at ambient pressure (Fig.1). For the parent space group *Cmcm* (#63), the total energies of the different spin configurations involving iron ions at all symmetry non-equivalent sites have been calculated. The spin structures with  $k = (0, 0, 0)$  propagation vectors can be realized. The ground state magnetic configuration corresponds to orthogonal structures with Fe spins in the 1D chains directed along the *b* axis and spins in the slabs aligned along the *c* axis. The evolution of magnetic moments under high pressure was studied and a site-dependent spin-state crossover was found.

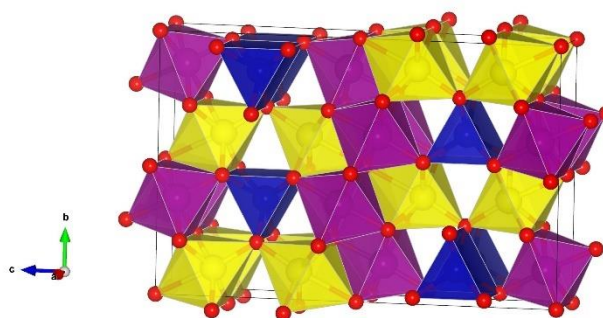


Fig. 1. The crystal structure of Fe<sub>5</sub>O<sub>6</sub>. The symmetry distinct iron sites are highlighted in purple (Fe1), yellow (Fe2), and blue (Fe3)

**Acknowledgements.** This research is funded by the Russian Foundation for Basic Research (project no. 21-52-12033).

- [1] C. Delacotte, et al. *Solid State Chem.*, **247**, (2017) 13–19.
- [2] S. V. Ovsyannikov, et al. *Nat. Commun.*, **9** (2018) 4142.
- [3] B. Lavina, et al. *Proc.Natl.Acad.Sci. U.S.A.*, **108** (2011) 17281–5
- [4] B. Lavina, Y. Meng, *Sci. Adv.*, **1** (2015) e1400260–e1400260.

## Perpendicular magnetic anisotropy in thin-film spin structures: growth and investigation

G. Kirichuk<sup>a\*</sup>, A. Grunin<sup>a</sup>, A. Goikhman<sup>a</sup>, K. Maksimova<sup>a</sup>

<sup>a</sup> REC "Functional nanomaterials", Immanuel Kant Baltic Federal University, 236004, Nevskogo 14, Kaliningrad, Russia

\*corresponding author email: [gv.kirichuk@gmail.com](mailto:gv.kirichuk@gmail.com)

Modern technology development has led to the creation of many devices that not only consume energy but also can generate it. As the number of such devices increases, the relevance and importance of the energy storage issue increases. Currently, lithium-ion batteries are the most common type of battery, and their components continue to be improved to enhance efficiency. However, in parallel, intensive research and development of alternative energy storage methods are underway to expand and improve the possibilities in this area and move from chemical energy sources to more advanced and environmentally friendly solutions.

The structure formation with a controllable spin state is an important step towards the development of a new type of battery - spin batteries [1]. A group of scientists led by Ya. Tserkovnyak has proposed a spin battery theoretical model, which consists of a bilayer thin film metal/magnetic insulator ring [2]. The main requirements for such a model are perpendicular (out-of-plane) magnetization in the metal layer and in-plane magnetization in the magnetic insulator layer. To validate the theoretical model, the FeCoB/Me(Mo, W)/NiO structure was designed (Fig. 1(a)).

This work focused on the perpendicular magnetic anisotropy (PMA) phenomenon in thin films FeCoB/Mo and FeCoB/W bilayer structures grown by pulsed laser deposition. The dependence of PMA on annealing temperatures and layer thicknesses was studied. Thin NiO films were deposited by RF magnetron sputtering. Based on the research results the presence of antiferromagnetism in NiO films was confirmed by exchange bias in the FeCoB/NiO structure. The main result was the formation of a functional structure FeCoB(1.3nm)/Mo(5.5nm)/NiO(10nm), in which PMA was observed, but without exchange bias (Fig. 1(b)).

Devices based on this concept will not be able to replace lithium-ion batteries. However, the implementation of a new energy storage technology will help expand the variety of technological solutions for devices that provide safe and long-term energy storage.

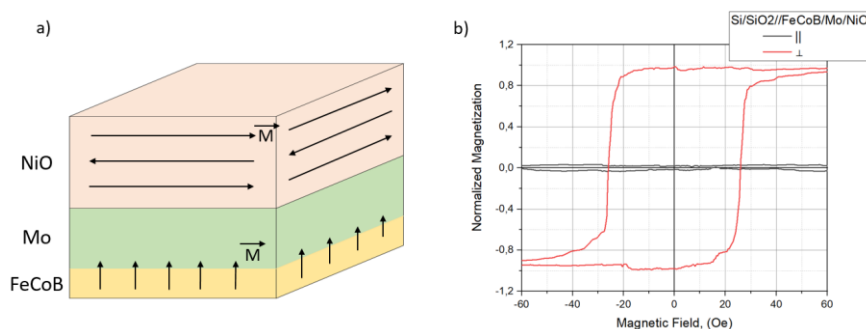


Fig. 1. (a) Thin-film functional structure concept of FeCoB/Mo/NiO. (b) The magnetic measurements results of the structure FeCoB/Mo/NiO.

### REFERENCES:

[1] - Hai P. N. et al. Electromotive force and huge magnetoresistance in magnetic tunnel junctions //Nature. – 2009. – T. 458. – №. 7237. – C. 489-492.

[2] - Jones D. et al. Energy storage in magnetic textures driven by vorticity flow //Physical Review B. – 2020. – T. 102. – №. 14. – C. 140411.

# Phase Diagram three-state Potts Model on the bcc Lattice

D. Kurbanova\*, M. Magomedov, M. Ramazanov, K. Murtazaev, A. Murtazaev

Amirkhanov Institute of Physics, Daghestan Federal Research Centre RAS, 367015, Makhachkala, Russia

\*d\_kurbanova1990@mail.ru

When studying the nature of phase transitions in the Potts model with a different number of spin states  $q$ , in most cases, systems with ferromagnetic interactions between nearest neighbors were considered. Depending on the number of spin states  $q$  and spatial dimension, the Potts model demonstrates a temperature phase transition of the first or second order. Originally, most studies of the Potts model focused on ferromagnetic interactions, and for that case the critical properties and phase diagram are well known [1,2]: at  $q > 4$ , the system exhibits a first-order phase transition, whereas at  $q \leq 4$ , the transition is continuous. For the three-dimensional case, it is known that at  $q > 3$ , a first-order phase transition is observed in the system. The behavior of the antiferromagnetic Potts model is more complicated because it strongly depends on the lattice microscopic structure. Another interesting point in the antiferromagnetic Potts model is that this model has a non-zero entropy of the ground state without frustration. The nonzero entropy of the ground state  $S_0 \neq 0$  is an important subject of statistical mechanics. One of the physical examples is spin ice.

In present work, on basis Wang-Landau Monte Carlo algorithm, we investigate the exchange interaction competition influence on phase transitions and thermodynamic properties of the antiferromagnetic 3-state Potts model on a body-centered cubic lattice.

Hamiltonian of the model:

$$H = -J_1 \sum_{\langle i,j \rangle, i \neq j} \cos \theta_{i,j} - J_2 \sum_{\langle\langle i,k \rangle\rangle, i \neq k} \cos \theta_{i,k} \quad (1)$$

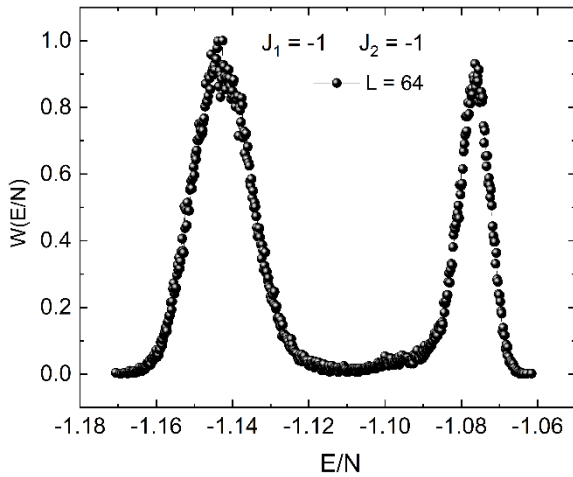


Fig. 1. Energy histograms at  $J_2 = -1$  with linear dimensions  $L = 64$ .

where  $J_1$  and  $J_2$  are the parameters of the exchange antiferromagnetic interactions for the first and second nearest-neighbors;  $\theta_{i,j}$ ,  $\theta_{i,k}$  are the angles between interacting spins  $S_i - S_j$  and  $S_i - S_k$ , respectively. The calculations were carried out for systems with periodic boundary conditions and linear dimensions  $2L \times L \times L = N$ ,  $L = 8 \div 64$  in the range  $-1 \leq J_2 \leq 0$ . A nature of phase transitions is estimated using the methods of the histogram analysis and the fourth order Binder cumulants. Fig. 1 shows histogram of the energy distribution for the case of  $J_2 = -1.0$  with linear dimensions  $L = 64$ . The presence of a double peak in the energy histograms is a characteristic feature of a first-order phase transition ( $T_N = 1.925(2)$ ) (the temperature is given in units of  $|J_1|/k_B$ ). Without taking into account the interaction of second neighbors

( $J_2 = 0$ ), a second-order phase transition is observed in the model under study.

This research was supported by the grant of the President of the Russian Federation for state support of young Russian scientists - PhD (№ MK-5223.2022.1.2).

[1] F.Y. Wu, Rev. Mod. Phys. 54, 235 (1982).

[2] R.J. Baxter, J. Phys. C 6, 445 (1973).

## Phase transitions in $R_2Fe_{14}B$ in magnetic fields up to 500 T

V. Platonov<sup>1,2</sup>, A. Bykov<sup>1</sup>, R. Kozabaranov<sup>1</sup>, A. Korshunov<sup>1</sup>, Yu. Kudasov<sup>1,2</sup>, I. Makarov<sup>1</sup>, D. Maslov<sup>1,2</sup>,  
P. Repin<sup>1</sup>, V. Selemir<sup>1,2</sup>, I. Strelkov<sup>1</sup>, O. Surdin<sup>1,2</sup>

<sup>1</sup> Russian Federal Nuclear Center – VNIIEF, Sarov, Russia, 607188

<sup>2</sup> Sarov Institute of Physics and Technology, NRU MEPhI, Sarov, Russia, 607186.

Materials based on rare-earth intermetallic compounds with the structure  $R_2Fe_{14}B$  are of great importance for industry and are of fundamental interest in connection with the problem of f - d interaction. Of great interest are such magnetic phenomena as spin-reorientation transitions and magneto-induced transitions manifested in high magnetic fields. These compounds have a sufficiently high magnetocrystalline anisotropy, high Curie temperature.  $R_2Fe_{14}B$  compounds are formed with all RZ ions, therefore it is possible to vary their magnetic properties with partial substitution.

To determine and optimize the functional magnetic properties of rare-earth transition metal intermetallics, it is important to know the parameters of the crystal electric field and exchange interaction. Directly, they can be determined by measuring the magnetization in super-strong magnetic fields. This paper presents the results of measuring the magnetization of  $R_2Fe_{14}B$  compounds in magnetic fields up to 500 T. Critical fields of spin-reorientation transitions are determined and additional jumps of magnetization in fields over 150 T are detected.

## Production of MXene film by vacuum filtration

Ya. Sokolov <sup>a,\*</sup>, S. Voronina <sup>a</sup>.

<sup>a</sup>I Siberian State University of Science and Technology named after Academician M.F. Reshetnev. Avenue named after the newspaper "Krasnoyarsky Rabochiy", 31, Krasnoyarsk, Krasnoyarsk Territory, 660137, Russia.

\* sokolovyaroslav2015@gmail.com

**Abstract.** Vacuum filtration is an effective method for obtaining MXene films from colloidal solutions, which are highly sensitive to changes in external parameters. This method allows for the production of films with specific thicknesses and structures, making them promising for use in various applications such as sensors, batteries, and supercapacitors.

**Introduction.** MXene films have attracted increasing attention in the scientific community due to their unique properties such as high conductivity [1], mechanical strength [2], and chemical stability [3]. To utilize these properties in various applications, it is necessary to develop efficient methods for producing MXene films with desired properties.

**Methods.** The object of this study is the process of obtaining MXene films by vacuum filtration, and the subject of the study is the investigation of the properties of the obtained film. Vacuum filtration is one of the most efficient methods for obtaining MXene films. It is based on filtering the MXene colloidal solution through a membrane under vacuum. This method allows for the production of MXene films with high purity and stability. However, the specific features of this method, such as the complexity of setting up and servicing the vacuum equipment, as well as the need for additional steps to remove residual solvents and transfer the film from the filtration element to the monitoring object, must be taken into account. To do this, it is necessary to ensure adhesion of the film to the material and then dissolve the filtration material. Vacuum filtration is an effective and promising method for producing MXene films with a uniform thickness distribution in laboratory conditions. However, this method has some limitations, such as the need for special equipment and difficulties in controlling the film thickness.

**Conclusion.** This work describes the process of obtaining MXene films by vacuum filtration. The main principles of this method, its advantages, and disadvantages compared to alternative methods of producing MXene films are presented.

**Acknowledgements.** This work was carried out by the team of the scientific laboratory "Smart Materials and Structures" under contract No. 322 dated 06/29/2023 for the implementation of the project: "Development of a digital sensor system for monitoring the pre-failure condition of rail lashes using nanomodified composite materials" by order of the Regional State Autonomous Institution "Krasnoyarsk Regional Fund for Support of Scientific and Scientific-Technical Activities" and open Joint Stock Company "Russian Railways"

[1] Liu P., Ding W., Liu J., Shen L., Jiang F., Liu P., Zhu Z., Zhang G., Liu C., Xu J., Surface termination modification on high-conductivity MXene film for energy conversion, *Journal of Alloys and Compounds* (2020)

[2] Zhang Z., Yao Z., Jiang Z. Fast self-assembled microfibrillated cellulose@MXene film with high-performance energy storage and superior mechanical strength. *Chin. Chem. Lett.* 32(11) (2021)

[3] Zhao, Z. Wang, S. Xu, H. Wang, Y. Li, and C. Fang Flexible bilayer Ti<sub>3</sub>C<sub>2</sub>T<sub>x</sub> MXene/cellulose nanocrystals/waterborne polyurethane composite film with excellent mechanical properties for electromagnetic interference shielding, *Colloids and Surfaces A: Physicochemical and Engineering Aspects*, 669, (2023)



## Quantum Acoustics of Dilute Magnetic Semiconductors

M. Sarychev<sup>a</sup>, I. Zhevstovskikh<sup>a,b</sup>, Yu. Korostelin<sup>c</sup>, V. Surikov<sup>d</sup>, N. Averkiev<sup>e</sup>, V. Gudkov<sup>a,\*</sup>

<sup>a</sup> Ural Federal University, Institute of Physics and Technology, 620002, Mira st. 21, Ekaterinburg, Russia

<sup>b</sup> Miheev Institute of Metal Physics, Ural Branch, Russian Academy of Sciences, Kovalevskaya st. 18,  
620137, Ekaterinburg, Russia

<sup>c</sup> Lebedev Physics Institute, Russian Academy of Sciences, 119991, Leninskiy prospect 53. Moscow, Russia

<sup>d</sup> Institute of Solid-State Chemistry, Ural Branch, Russian Academy of Sciences, 620090, Pervomayskaya st.  
91, Ekaterinburg, Russia

<sup>e</sup> Ioffe Institute, Russian Academy of Sciences, 194021, Polytechnicheskaya st. 26, St. Petersburg, Russia

\*v.v.gudkov@urfu.ru

The term “magnetic quantum acoustics” commonly relates to interaction of acoustic waves with nuclear spins and paramagnetic spin-phonon interaction [1]. However, Van Vleck [2] pointed out that spin-phonon interaction summand in spin Hamiltonian is closely related to the Jahn-Teller (JT) effect (JTE) (see, e.g., [3]). In doped crystals, the JT sub-system is formed by the complexes consisting of the JT ion and the nearest neighbors. In the case of small amount of dopant, the complexes do not interact with each other. Consequently, the JT sub-system is represented by the objects of the order of atomic size which are described in terms of quantum mechanics as quantum oscillators in the minima of the potential energy which are separated by the barriers. At low temperatures the complexes occupy the lowest energy levels and transitions between these levels in the nearest minima caused by an ultrasonic wave occur due to quantum tunneling. Therefore, anomalies in dispersion and the energy dissipation of an ultrasonic wave initiated by the JT sub-system, those are obtained in an experiment, relate to quantum acoustics absolutely to the same extent as the acoustic magnetic resonance phenomena (see also [4,5]). Manifestation of magnetism in the JTE can be studied if the dopant is not only the JT ion but the magnetic one as well. Consequently, investigation of semiconductors doped with magnetic ions those possess orbit degeneracy is of particular interest both in the fields of fundamental research and possible applications. Here we report the results of our experimental study of ZnSe:Cr<sup>2+</sup> (sphalerite crystal structure) and CdSe: Cr<sup>2+</sup> (wurtzite one) with small concentration of the dopant (the order of 10<sup>18</sup> 1/cm<sup>3</sup>). The experiments were carried out at High Magnetic Field Laboratory (Dresden, Germany) at the frequency of ultrasonic waves of about 30 MHz in magnetic field  $B = 0 - 17$  T at the temperatures  $T = 1.3 - 200$  K. Magnetic-field dependences of attenuation and phase velocity at fixed  $T$  and the temperature dependences at fixed  $B$  were obtained. Interpretation was given with account of magnetic-field variation of the adiabatic potential energy using spin Hamiltonian introduced in [6] and magnetic-field dependent tunneling through the potential energy barrier [7].

The study was supported by the Russian Science Foundation (project no. 22-22-00735).

[1] S. A. Al'tshuler, Zh. Eksperim. i Teor. Fiz. 24, 681 (1953); 28, 49 (1954)

[2] J. H. Van Vleck. J. Chem. Phys. 7, 72 (1939)

[3] I. B. Bersuker, *The Jahn-Teller Effect* (Cambridge University Press, Cambridge, 2006)

[4] E. B. Tucker in *Physical acoustics*, vol. IV A: *Application to Quantum and Solid State Physics*, ed by W. P. Mason (Academic Press, New York and London, 1966) p. 47-112

[5] D. I. Bolef in *Physical acoustics*, vol. IV A: *Application to Quantum and Solid State Physics*, ed by W. P. Mason (Academic Press, NY York and London, 1966) p. 113-182

[6] J. T. Vallin, *et al.* Phys. Rev. B 11, 4313 (1970)

[7] N. S. Averkiev, *et al.* Phys. Rev. B 96, 09443113 (2017)

# Research in the field of creating strain-sensitive sensors for large deformations

S. Voronina<sup>a</sup>, V. Vlasov<sup>b,\*</sup>

<sup>a</sup> Reshetnev Siberian State University of Science and Technology, 660037, Krasnoyarsky Rabochy Ave 31, Krasnoyarsk, Russia

<sup>b</sup> Yaroslavl State Technical University, 150999, Moskovskiy prospekt 88, Yaroslavl, Russia

\*Vlasovvv@ystu.ru

**Introduction.** The use of flexible sensors for medical applications, electronics and special purpose products is one of the global trends. Displacement sensors are especially in demand, having a minimum mass, inertia to environmental influences, capable of registering the movements of elements and structures to much greater values, compared to classical strain gauges. We have conducted a study in the field of monitoring the state of the structure to develop a strain-sensitive sensor element capable of recording deformations in the range up to 25%.

**Methods.** The basis of the strain-sensing element was silicone rubber, in which carbon nanomaterials were intervened using a special technology. The objects of study were samples based on silicone rubber by Wacker (Germany) with various concentrations (0.5, 1, 2, 3 wt.%) of single-wall carbon nanotubes – SWCNT and concentrate based on SWCNT - Matrix) manufactured by OCSiAl (Russia) and also Taunit-M (multiwalled nanotubes - MWCNT) manufactured by NanoTechCenter LLC (Russia). Test specimens were made from this obtained material (ISO 527-2:2012, Type 1). In order to determine the effect of sample deformation on its electrical resistance, we developed and constructed a special attachment for a tensile testing machine. The resistance of composites with different concentrations of carbon nanotubes was measured by the digital ohmmeter under different loads and depending on the number of loading cycles in real time. Each sample was subjected to 30 cycles at 25% strain. Based on the data obtained, the coefficient of tensoresistance ( $K$ ) was determined.

**Results.** Based on the research, a technology was proposed for mixing carbon nanomaterials with silicone under the action of ultrasound in combination with mechanical mixing according to a certain algorithm. This made it possible to obtain a homogeneous dispersion of nanomaterials without traces of agglomeration. However, it should be noted that a nanocomposite with a concentration of 3% or more could not be obtained due to a significant increase in viscosity and a decrease in the formability of the material. For the studied compositions of nanocomposites, the material with MWCNT 1% ( $K \approx 1$ ) has the highest value of the tensoresistance coefficient. Next is Matrix 2% ( $K \approx 0,7$ ), Matrix 0,5% ( $K \approx 0,65$ ), SWCNT 1% ( $K \approx 0,4$ ) and Matrix 1% ( $K \approx 0,25$ ). However, it is worth noting here that the electrical resistance of the studied samples of materials decreased with an increase in the Matrix dosage from 240-280 kOhm for Matrix 0.5% to 4.5-5 kOhm for Matrix 2%. At the same time, the lowest electrical resistance (about 350 Ohms) was observed in samples containing 1% SWCNT.

**Discussion.** Studies have shown that nanocomposites containing Matrix 2% and SWCNT 1% showed the best stability under repeated deformations. In addition, the materials obtained at these dosages had the best technological properties in the manufacture of test samples. The results obtained can be used in the manufacture of strain-sensitive elements for various applications.

**Acknowledgments.** This paper was carried out by the Ministry of Science and Higher Education of the Russian Federation project No. FEFE-2020-0015.

# Spin Current Magnetization Control in [Pd/Co/CoO]<sub>n</sub> Epitaxial superlattices

A. Kozlov<sup>a</sup>, A. Shishelov<sup>a\*</sup>, A. Turpak<sup>a</sup>, Zh. Namsaraev<sup>a</sup>

<sup>a</sup> Far Eastern Federal University, 690920,10, Ajax, Russkiy island, Primorsky Krai, Russia

\* shishelov.af@dvfu.ru

Spin current provides effective magnetization control in thin films, which makes it possible to use such structures in magnetic RAM with high speed and long service life [1-3].

The effect of current-induced spin-orbit torque (SOT effect) is the most powerful tool for magnetization control in heavy metal/ferromagnetic systems. The SOT effect, based on the bulk spin Hall effect, as well as on interface effects such as the Rashba effect, leads to a nonequilibrium spin distribution at the interface of ferromagnetic and nonmagnetic layers. The angular magnetic moment induced at the interfaces is transmitted to the volume of the ferromagnetic layer by exchange interaction. Oxidation of the ferromagnetic layer can be used as a tool to control the characteristics of the current-induced switching of magnetization and the SOT effect.

In our work we studied the thin epitaxial Cu/[Pd/Co/CoO]<sub>n</sub>/Pd superlattices were obtained by molecular beam epitaxy technique on the Si(111) substrate. The cross-like structures for current-induced switching of magnetization were obtained by electron beam lithography using a negative electron resist.

The effect of spin-orbital torque was estimated by the shift of the magnetization loop during magnetization switching in a hall structure with an alternating out-of-plane field  $H_z$ , fixed by a planar field  $H_x$  and a constant current [2]. The current creates an effective field with a perpendicular component, the direction of which depends on the orientation of the current, and this field is equal to the shift. Hysteresis loops of abnormal Hall voltage and changes in magnetization were received using Kerr microscopy.

The evolution of the domain structure from the magnetized state occurs by the generation of a single branched domain, which, when the coercive force field is reached, instantly spreads over the entire area of the ferromagnetic structure. When passing an electric current there is a narrowing of the hysteresis loop, which is explained both by the additional energy of the electric field and by the heating of the structure. However, a slight deviation from the center may indicate the existence of an SOT effect in the system. With a significant current, a dedicated direction appears in the ordering of the domain structure, the domains begin to stretch slightly in the direction of the applied electric field.

This work was supported by the Russian Ministry of Science and Higher Education for state support of scientific research (State Assignment No. FZNS-2023-0012).

[1] S. Woo, K. Litzius, B. Krüger, M.Y. Im, L. Caretta, K. Richter, M. Mann, A. Krone, R. M. Reeve, M. Weigand, P. Agrawal, I. Lemesh, M.A. Mawass, P. Fischer, M. Kläui, G. S. D. Beach. Observation of room-temperature magnetic skyrmions and their current-driven dynamics in ultrathin metallic ferromagnets // *Nature Materials*. – 2015. – № 15. – C. 501

[2] D.-Y. Kim, M.-H. Park, Y.-K. Park, J.-S. Kim, Y.-S. Nam, D.-H. Kim, S.-G. Je, H.-C. Choi, B.-C. Min, and S.-B. Choe. Chirality-induced antisymmetry in magnetic domain wall speed // *NPG Asia Mater.* – 2018. - № 10. – C. e464

[3] A. Fert, V. Cros, J. Sampaio. Skyrmions on the track // *Nature Nanotechnology*. – 2013. – № 8. – C. 152

## Strontium iridate thin films - material for superconducting cryoelectronics and spintronics

I. Moskal<sup>1</sup>, A. Petrzikh<sup>1</sup>, A. Shadrin<sup>1,2</sup>,  
Yu. Kisilinski<sup>1</sup> and G. Ovsyannikov<sup>1</sup>

<sup>1</sup>V.A. Kotelnikov Institute of Radio Engineering and Electronics Russian Academy of Sciences, Mokhovaya 11-7, 125009, Moscow, Russia;

<sup>2</sup>Moscow Institute of Physics and Technology (National Research University) 141701, Moscow region, Dolgoprudny, Russia;

\*e-mail: ivan.moscal@yandex.ru

Antiferromagnets are more promising materials for spintronics compared to ferromagnets since they are more resistant to disturbances of the external magnetic field and provide orders of magnitude faster dynamics of changing the direction of magnetization. Antiferromagnetic systems also have better scalability. At the same time, there are a number of obstacles to the widespread use of antiferromagnets, in particular, in many cases, when working with antiferromagnets, it is necessary to use more complex equipment than for ferromagnets, for example, to register vanishingly small macroscopic magnetization.

The Hall spin magnetoresistance (SMR) is a universal tool for studying the antiferromagnetic spin structure using simple experiments on electric charge transfer [1]. One of the promising materials for this area of research is strontium iridate  $\text{Sr}_2\text{IrO}_4$ , which acquires an antiferromagnetic order at temperatures below 240K. Iridates have a number of unusual properties, which, in particular, are associated with a strong spin-orbit interaction, which is on the order of 0.5 eV.

Superconductor -  $\text{SrIrO}_3$  heterostructures may be interesting from a practical point of view as low-resistance contacts with  $\text{YBa}_2\text{Cu}_3\text{O}_x$  for promising cryoelectronic devices.  $\text{SrIrO}_3$  also demonstrates interesting properties in the  $\text{SrIrO}_3/\text{La}_{0.7}\text{Sr}_{0.3}\text{MnO}_3$  bilayer.

Strontium iridate films of different compositions differ significantly, for example,  $\text{SrIrO}_3$  demonstrates the properties of a paramagnetic metal, and  $\text{Sr}_2\text{IrO}_4$  is an antiferromagnetic dielectric. A feature of the synthesis of thin films of iridates by laser ablation and cathode sputtering is the possibility of obtaining different phases, as well as their mixtures, from the same target. In a number of works from metal target  $\text{SrIrO}_3$  by laser ablation method films of composition  $\text{SrIrO}_3$ ,  $\text{Sr}_2\text{IrO}_4$  and  $\text{Sr}_3\text{Ir}_2\text{O}_7$  were obtained [2].  $\text{SrIrO}_3$ ,  $\text{Sr}_2\text{IrO}_4$  and  $\text{Sr}_3\text{Ir}_2\text{O}_7$  films were obtained from  $\text{Sr}_3\text{Ir}_2\text{O}_7$  target [3].

In this paper, the features of the synthesis of thin films of strontium iridate by direct current cathode sputtering are discussed. The electric transport characteristics of the obtained films are considered, the dependences of the resistivity on temperature and the activation energies calculated from them are given. Activation energy  $\Delta EA = d(\ln\rho) / d(1/T)$ , where  $\rho$  is the resistivity of the film, and  $T$  is the temperature.

The work was supported by the grant of the Russian Science Foundation, N 23-49-10006, <https://rscf.ru/project/23-49-10006/>

- [1] Kazunori Nishio, Harold Y. Hwang, *APL Mater.* 4, 036102 (2016);
- [2] Araceli Gutierrez-Llorente, Lucía Iglesias, *APL Materials* 6, 091101 (2018);
- [3] Stephan Geprägs, Matthias Opel *J. Appl. Phys.* 127, 243902 (2020);
- [4] I. E. Moskal, K. E. Nagornykh, A. M. Petrzikh, *Bulletin of the Russian Academy of Sciences: Physics*, 2023, Vol. 87, No. 3, pp. 374–378

# Study of structure and magnetic properties of multi-component $\text{BaFe}_{(12-x)}(\text{Al,Cr,Ga,In})_x\text{O}_{19}$ ( $x = 1-11$ ) solid solutions

A. Zykova<sup>a\*</sup>, V. Zhivulin<sup>a</sup>, S. Taskaev<sup>b</sup>, E. Trofimov<sup>a</sup>, D. Vinnik<sup>a</sup>

<sup>a</sup>South Ural State University, 454080, Lenin av. 76, Chelyabinsk, Russia

<sup>b</sup>Chelyabinsk State University, 454001, Bratiev Kashirinykh st. 129, Chelyabinsk, Russia

\*zykovaar@susu.ru

Interest in creating M-type hexaferrites remains strong due to the unique combination of their properties. Doping with various metals makes it possible to modify the crystal lattice and adjust the magnetic properties. Producing high-entropy solid solutions with the M-type hexaferrite structure might make it possible to create a material with controlled properties such as degree of uniaxial magnetic anisotropy, saturation magnetization, coercivity, and Curie point. In this study, substituted barium hexaferrites with a magnetoplumbite structure were obtained through solid-phase synthesis. Triple-charged, mainly diamagnetic  $\text{Al}^{3+}$ ,  $\text{Cr}^{3+}$ ,  $\text{Ga}^{3+}$  and  $\text{In}^{3+}$  cations were chosen as the dopants. The maximum degree of substitution was  $x=11$ .

Magnetization was measured using a SQUID magnetometer [1]. The magnetization area was studied from 3T to  $-3\text{T}$  at 50K–300K. The  $M_s$  saturation magnetization,  $M_r$  residual magnetization, SQR loop squareness, and  $H_c$  coercivity were extracted.

The  $M_s$  saturation magnetization, as expected, regularly and monotonously decreases with a decrease in the  $n$  content of iron cations.

The  $M_r$  residual magnetization increased up to  $n = 8$  at 50 K, and  $n = 9$  at 300K and then decreased with further doping by  $\text{Al}^{3+}$ ,  $\text{Cr}^{3+}$ ,  $\text{Ga}^{3+}$ ,  $\text{In}^{3+}$ . The values of  $M_r$  non-monotonically increased when ( $\text{Al}^{3+}$ ,  $\text{Cr}^{3+}$ ,  $\text{Ga}^{3+}$ ,  $\text{In}^{3+}$ )-doping concentration increased. The decrease in the  $M_r$  could be also attributed to weakening the  $\text{Fe}^{3+}\text{-O-Fe}^{2+}$  super-exchange interactions [2]. In general, for substituted  $\text{BaFe}_{12}\text{O}_{19}$ , the tendency to decrease the values of  $M_s$  and  $M_r$  as the degree of substitution increases is fixed.

The maximum coercivity is found for the  $\text{BaFe}_{8.22}\text{Al}_{0.84}\text{Cr}_{0.99}\text{Ga}_{1.11}\text{In}_{0.84}\text{O}_{19}$  composition with  $n = 8$  at 50 K. The maximum coercivity is fixed for the  $\text{BaFe}_{3.07}\text{Al}_{2.00}\text{Cr}_{2.27}\text{Ga}_{2.58}\text{In}_{2.07}\text{O}_{19}$  composition  $n = 3$  at 300 K. The value of the coercivity for all the investigated samples changes non-monotonically. The  $H_c$  is influenced by factors such as shape anisotropy, micro-strain, magnetic particles' morphology, size distribution, and the magnetic domain's size [3].

The temperature behavior of the  $M$  magnetization is measured in a field of 500 Oe. The magnetization firstly increases with an increase temperatures for the compositions  $n = 10-7$ . This effect can be related to the antiferromagnetic-ferrimagnetic state transition. For the samples  $n = 5-6$ , a similar phase transition can be also considered at temperatures below 50 K. The second phase transition for the samples  $n = 1-7$  from the ferrimagnetic state in the paramagnetic one, corresponds to the Curie temperature. In this work, differential scanning calorimetry (DSC) was employed to determine the Curie temperature (TC) above 300 K, of the compositions  $n = 8-11$ .

[1] S.V. Trukhanov, J. Exp. Theor. Phys. 100, 95 (2005). <https://doi.org/10.1134/1.1866202>

[2] M.M. Rashad, H.M. El-Sayed, M. Rasly, A.A. Sattar, I.A. Ibrahim, J. Mater. Sci.: Mater. Electr. 24, 282 (2013). <https://doi.org/10.1007/s10854-012-0740-7>.

[3] M.A. Darwish, V.A. Turchenko, A.T. Morchenko, V.G. Kostishyn, A.V. Timofeev, M.I. Sayyed, Z. Sun, S.V. Podgornaya, E.L. Trukhanova, E.Yu. Kaniukov, S.V. Trukhanov, A.V. Trukhanov, J. Alloys Compd. 896, 163117 (2022). <https://doi.org/10.1016/j.jallcom.2021.163117>.

# Synthesis and characterization of magnetite and silver nanocomposites

E. Kozenkova<sup>a,\*</sup>, A. Omelyanchik<sup>a</sup>, V. Rodionova<sup>a</sup>

<sup>a</sup> Immanuel Kant Baltic Federal University, 236004, Nevskogo 14, Kaliningrad, Russia

\*ekozenkova1@gmail.com

Magnetic nanoparticles have made a significant contribution to the field of nanomedicine as agents for theranostics of oncological diseases. In our work, we synthesized composites, which are aggregates consisting of magnetite and silver nanoparticles, as a potential system for targeted delivery to various cell organelles, including mitochondria [1, 2].

The Ag/Fe<sub>3</sub>O<sub>4</sub> magnetic composites were obtained by the co-precipitation method. First, colloidal silver particles were obtained from a solutions of silver nitrate and sodium citrate. Next, magnetite was obtained by co-precipitation using iron sulfate 2<sup>+</sup> and 3<sup>+</sup> in a ratio of 1:2, heated at 80°C for 2 hours. Subsequently, 20 ml of 3 M sodium hydroxide was added to initiate the co-precipitation reaction. Then, solutions of colloidal silver and magnetite were mixed with water and heated to evaporation. 2-Methylbutanol1 was used to create a stable suspension of Ag/Fe<sub>3</sub>O<sub>4</sub> aggregates.

According to magnetization measurements as a function of the external magnetic field at a temperature of 300 K, the samples exhibit superparamagnetic behavior with a saturation magnetization of 24 emu/g and almost zero residual magnetization. The lowering of this value compared to the magnetic iron oxides Fe<sub>3</sub>O<sub>4</sub> or  $\gamma$ -Fe<sub>2</sub>O<sub>3</sub> (80–92 emu/g) is associated with the presence of diamagnetic silver in the composite. The position of the maximum of the zero-field-cooled (ZFC) curve is proportional to the blocking temperature  $T_B$ , at which the transition from the blocked ferromagnetic state to the superparamagnetic state occurs. Consequently, we have successfully obtained a stable colloidal suspension of Ag/Fe<sub>3</sub>O<sub>4</sub> composites with superparamagnetic properties at room temperature, which will further be used in biomedical applications.

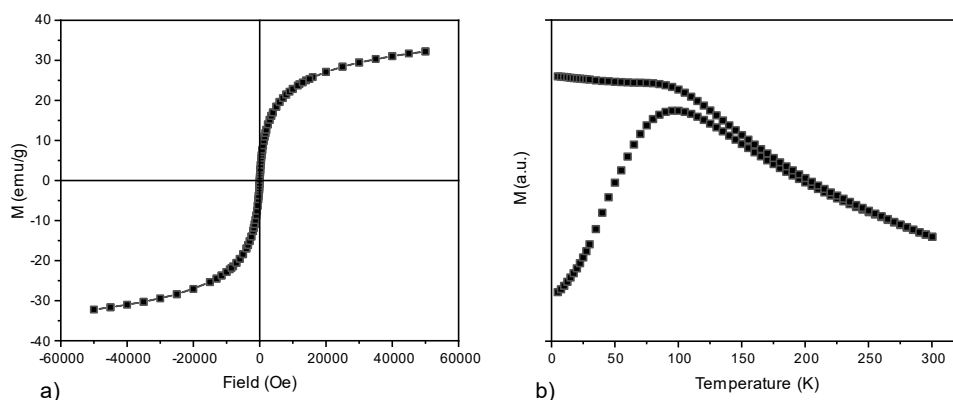


Figure 1 - Dependence of the magnetization on the external magnetic field, measured at 300 K (a) and temperature dependences of the ZFC and FC magnetizations (b) of Ag/ Fe<sub>3</sub>O<sub>4</sub> nanoparticles.

The authors are grateful to Professor of the Institute of Organometallic Chemistry of the Italian National Research Council Claudio Sangregorio.

Acknowledgments: This research was supported by funds provided through the Russian Federal Academic Leadership Program “Priority 2030” at the Immanuel Kant Baltic Federal University, project number 3312.

[1] D. Solomon, Synthesis and Study of Silver Nanoparticles Journal of Chemical Education. Vol. 84 (2), 2007.

[2] S. Raza, Biosynthesis of silver nanoparticles for the fabrication of non cytotoxic and antibacterial metallic polymer based nanocomposite system. Sci Rep 11, 2021.

# Synthesis and investigation of hexaferrite $\text{BaFe}_{12-x}\text{In}_x\text{O}_{19}$ ( $x = 0.25-1$ )

A. Punda<sup>a,\*</sup>, V. Zhivulin<sup>a</sup>, K. Pavlova<sup>a</sup>, S. Gudkova<sup>a,b</sup>, D. Vinnik<sup>a,b</sup>

<sup>a</sup> South Ural State University (National Research University), 454080, Lenin ave. 76, Chelyabinsk, Russia

<sup>b</sup> Moscow Institute of Physics and Technology (National Research University), 141701, Institutskiy per. 9, Dolgoprudny, Moscow Region, Russia

\*pundaai@susu.ru

This work describes the solid-state synthesis method and methods for studying the structure of barium hexaferrite doped with indium. Compared to iron ions, indium ions are larger, which can affect the crystalline lattice and magnetic properties of the resulting material. The iron substitution degree “ $x$ ” was range from 0 to to 1 with a step of 0.25. The structure analysis was conducted using the powder diffractometer Rigaku Ultima IV with X-ray phase analysis method. The results of electron microscopic analysis showed the production of monophasic samples.

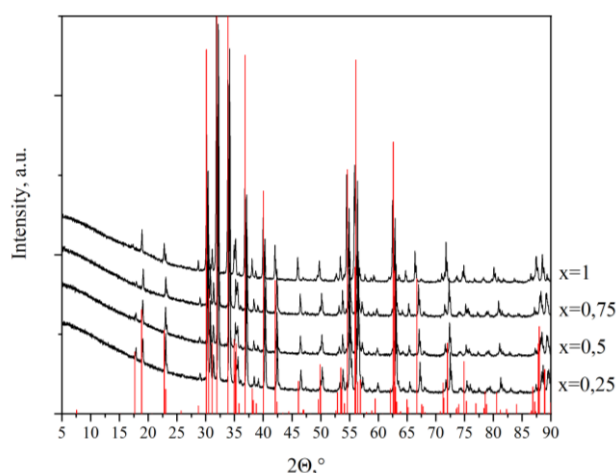


Figure. Experimental X-ray patterns for  $\text{BaFe}_{12-x}\text{In}_x\text{O}_{19}$  samples; red lines – literature data for initial  $\text{BaFe}_{12}\text{O}_{19}$  matrix [1]

The X-ray patterns (Figure) show that as the indium content increases from sample to sample, the reflections shift uniformly, indicating an increase in the crystalline lattice. The obtained type structure is close to the structure of pure barium hexaferrite [1]. The crystalline lattices were calculated (Table). Volume increases with increasing substitution due to larger ionic radius  $\text{In}^{3+}$  ions compared to  $\text{Fe}^{3+}$  ions with the same coordination number, e.g.  $\text{CN} = 4$ ,  $r(\text{In}^{3+}) = 0.76 \text{ \AA}$ ;  $r(\text{Fe}^{3+}) = 0.63 \text{ \AA}$  [3]. Using the solid-state synthesis method, we can choose the degree of substitution of  $\text{BaFe}_{12-x}\text{In}_x\text{O}_{19}$  with  $x$  up to 1 and control the indium content by varying the initial concentration of indium in the mixture.

Table

Lattice parameters for  $\text{BaFe}_{12-x}\text{In}_x\text{O}_{19}$  samples

Lattice parameters	Iron substitution degree “ $x$ ”					
	0 [1]	0 [2]	0.25	0.5	0.75	1
$a(\text{\AA})$	5.8945(5)	5.8929(4)	5.9035(2)	5.9177(4)	5.9266(19)	5.93213(18)
$c(\text{\AA})$	23.215(3)	23.1943	23.2652(12)	23.3384(16)	23.4171(9)	23.4402(10)
$V(\text{\AA}^3)$	698.5	697.54	702.19(5)	707.81(8)	712.32(4)	714.35(4)

1. Wong-Ng, W., McMurdie, H., Paretzkin, B., Hubbard, C., Drago, A., Powder Diffraction, 3, (1988), 249

2. Vinnik D.A., Zherebtsov D.A., Mashkovtseva L.A., Doklady Physical Chemistry, 499, (2013), 39-40

3. R.D. Shannon, Revised effective ionic radii and systematic studies of interatomic distances in halides and chalcogenides, Acta Crystallogr. A32 (1976) 751–767.

# Synthesis and Magnetic Properties of Solid Solutions Based on Co-Zn-Ni Ferrites

D. Sherstyuk<sup>a,\*</sup>, D. Vinnik<sup>a,b</sup>, V. Zhivulin<sup>a</sup>, E. Shipkova<sup>c</sup>, N. Perov<sup>c</sup>

<sup>a</sup> South Ural State University (National Research University), 454080, Lenin ave. 76, Chelyabinsk, Russia

<sup>b</sup> Moscow Institute of Physics and Technology (National Research University), 141701, Institutskiy per. 9, Dolgoprudny, Moscow Region, Russia

<sup>c</sup> Lomonosov Moscow State University, 119991, Leninskie gory 1, Moscow, Russia

\*sherstiuk@susu.ru

The results of the synthesis and magnetic properties investigation of ferrites with the general formula  $\text{Co}_{0.2}\text{Zn}_{0.8-x}\text{Ni}_x\text{Fe}_2\text{O}_4$  ( $x=0-0.8$ ) are presented. Materials of this type have magnetic resistance, chemical and thermal stability, high values of saturation magnetization, high electrical resistivity, etc. The samples were obtained by the solid phase reaction method. The starting reagents ( $\text{Ni}^{2+}$ ,  $\text{Zn}^{2+}$ ,  $\text{Co}^{2+}$  and  $\text{Fe}^{3+}$  oxides) were mixed to a homogeneous state, pressed, and placed in a high-temperature furnace. The exposure time and temperature were 5 hours and 1150°C, respectively.

Based on the data obtained as a result of elemental analysis (Jeol JSM 7001F, INCA X-max 80 electron microscope), it can be concluded that the given and actual formulas are in a good agreement. The surface morphology of the samples is a set of microcrystallites characteristic of the cubic system. The samples phase compositions were studied on a powder diffractometer Rigaku Optima IV. The diffraction patterns of the studied samples are shown in Fig. 1. All the observed peaks correspond exactly to the JCPDS 74-2397 card (blue line) [1] related to zinc ferrite with space group Fd3m. The magnetic characteristics were measured on a VSM Lakeshore 7400 vibrating magnetometer in fields up to 16 kOe and in the temperature range from 100 to 420 K.

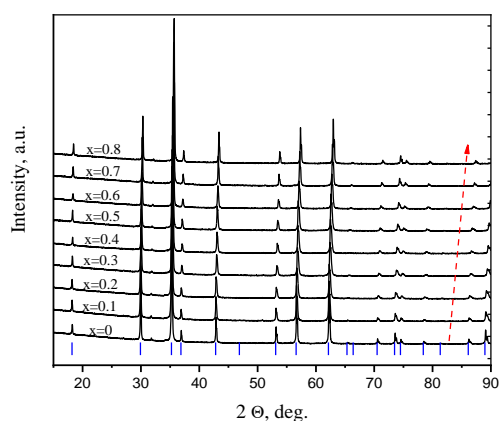


Figure 5. XRD patterns of the samples  $\text{Co}_{0.2}\text{Zn}_{0.8-x}\text{Ni}_x\text{Fe}_2\text{O}_4$

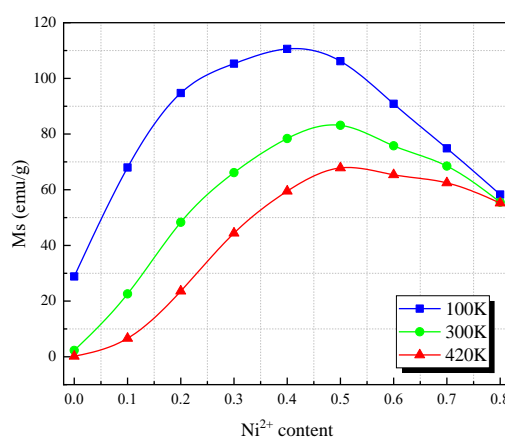


Figure 6. Dependence of saturation magnetization on  $\text{Ni}^{2+}$  content

The dependence of the saturation magnetization has a general character: with a  $\text{Ni}^{2+}$  substitution increasing  $M_s$  increases, then reaches a maximum and then decreases (see Fig. 2). That can be explained by the cations redistribution over the tetrahedral (A) and octahedral (B) positions of the spinel. It is known that Zn with a magnetic moment of 0  $\mu\text{B}$  preferentially occupies A positions, while Ni (2  $\mu\text{B}$ ) tends to occupy B positions. Thus, the magnetic moment of the sublattice (B) increases; therefore, an increase in the saturation magnetization is associated with an increase in the B-B interaction. The further decrease in  $M_s$  of the samples under study can be explained by a decrease in the A-B interaction, which causes ferrimagnetism.

[1] U. Koenig, G. Chol, J. Appl. Crystallogr., 1(1968)



# Synthesis and study of the properties of ferrites of the composition $\text{BaFe}_{12-x}\text{Cr}_x\text{O}_{19}$ .

D. Afansiev<sup>a</sup>, V. Zhivuli<sup>a, \*</sup>, D. Vinnik<sup>a</sup>

<sup>a</sup>South Ural State University (National Research University), 454080, Lenin ave.76, Chelyabinsk, Russia \*zhivulinve@mail.ru

Barium hexaferrite  $\text{BaFe}_{12}\text{O}_{19}$  and ferrites based on it are promising functional materials. The literature widely presents works on the preparation of ferrites in which  $\text{Fe}^{3+}$  atoms are partially replaced by atoms of other trivalent metals such as  $\text{Al}^{3+}$ ,  $\text{Ga}^{3+}$ ,  $\text{In}^{3+}$  [1–3]. The analysis of literary sources allows us to conclude that the substitution of iron in the structure of barium hexaferrite leads to a significant change in its magnetic and electrophysical properties. In this case, a proportional dependence of the change in the properties of ferrites depending on the concentration of the iron-substituting ion is observed. In the literature there are also known ferrites in which iron is replaced simultaneously by two or three substituents. Thus, by varying the iron-replacing element and its concentration, it is possible to controllably change and adjust the properties of the material to solve a specific engineering problem.

The purpose of this work was to develop the technology for obtaining ceramics of the composition  $\text{BaFe}_{12-x}\text{Cr}_x\text{O}_{19}$  by solid-phase synthesis and to study the physical properties of the obtained ferrites.

The oxides of iron ( $\text{Fe}_2\text{O}_3$ ), chromium ( $\text{Cr}_2\text{O}_3$ ), and barium carbonate  $\text{BaCO}_3$  served as starting materials for solid-phase synthesis. The initial oxides were weighed in a stoichiometric ratio, mixed, and ground with an agate mortar. The ground powder from the initial oxides was pressed into a tablet in a metal mold. The resulting tablet was placed on a platinum sheet and sintered at a temperature of 1400 °C for 5 hours. Thus, 13 samples were prepared, one of which was the original barium hexaferrite  $\text{BaFe}_{12}\text{O}_{19}$  and 12 samples of substituted barium hexaferrite of the composition  $\text{BaFe}_{12-x}\text{Cr}_x\text{O}_{19}$ , where  $x(\text{Cr})$  varied within 0.5–6 s with a step of 0.5.

Powder X-ray analysis revealed that all samples up to the degree of substitution  $x(\text{Cr}) = 4.5$  forms single crystalline phase. Samples with a higher degree of substitution have 2 crystalline phases, one of which belongs to the magnetoplumbite structure, and the second to iron oxide. X-ray diffraction analysis led to the conclusion that, as a result of the substitution of  $\text{Fe}^{3+}$  by  $\text{Cr}^{3+}$ , the crystal lattice parameters decrease monotonically with an increase in the  $\text{Cr}^{3+}$  concentration.

The Curie temperature of each of the samples was determined by differential scanning calorimetry (DSC). It was found that an increase in the concentration of  $\text{Cr}^{3+}$  ions leads to a monotonic decrease of the Curie temperature. The value of the initial magnetic permeability of the obtained ferrites was measured. The measurements were carried out at a frequency of 100 kHz by fixing the inductivity of the toroidal coil in which the ferrite was the core. The value of the initial magnetic permeability for the original barium ferrite  $\text{BaFe}_{12}\text{O}_{19}$  was  $\mu = 3$ . Substitution with chromium leads to a decrease in this value and for a sample of the composition  $\text{BaFe}_{12-x}\text{Cr}_{4.5}\text{O}_{19}$  it was  $\mu = 1.6$ .

[1] A.V. Trukhanov, Journal of Alloys and Compounds. 522, 791(2019)

[2] I. Bsoul, Jordan Journal of Physics 171, 3 (2009)

[3] S.V. Trukhanov, Journal of Magnetism and Magnetic Materials. 130, 417(2016)

# Temperature dependence of impedance of amorphous $\text{Co}_{66}\text{Fe}_4\text{Nb}_{2.5}\text{Si}_{12.5}\text{B}_{15}$ wires with different diameter

M. Derevyanko<sup>a,\*</sup>, D. Bukreev<sup>a</sup>, A. Moiseev<sup>a</sup>, A. Semirov<sup>a</sup>

<sup>a</sup> Irkutsk state university, 664001, K. Marx, Irkutsk, Russia

\*mr.derevyanko@gmail.com

The results of studies of the amorphous alloy  $\text{Co}_{66}\text{Fe}_4\text{Nb}_{2.5}\text{Si}_{12.5}\text{B}_{15}$  samples in the form of segments of cylindrical wires 30 mm long are presented. Samples diameter was 150 and 180  $\mu\text{m}$ . The wires are obtained by fast quenching technique from the melt.

The impedance modulus  $Z$  of the samples was measured in automated setup. Measurements of  $Z$  were carried out with an alternating current frequency range,  $f$ , of (0.1 – 100) MHz. The effective value of the current was 1 mA. The impedance measurements were carried out with decreasing temperature in the range from 510 to 295 K. In the same way, the magnetic hysteresis properties were studied by the inductive method.

The wires were subjected a heat treatment at a temperature of 520 K for 5 hours.

Figure 1a shows that the Curie temperatures of the as-quenched wires of different diameters differ slightly at a frequency of 0.1 MHz. At this frequency the thickness of the skin layer is commensurate with the radius of the wire. At a frequency of 10 MHz, there is no such difference. This is due to the presence of at least two magnetic phases with different Curie temperatures, which was discussed in [1].

After the heat treatment, the difference in the Curie temperatures becomes more significant and is observed in the entire volume of the wire (Fig. 1, b). The difference in the Curie temperatures of the heat-treated wires with diameters of 150 and 180  $\mu\text{m}$  is confirmed by the temperature dependences of their saturation magnetization (Fig. 2).

The dependence of the wire quenching rate on its diameter, and hence the radial distribution of internal quenching stresses [2], leads to a difference in the volume and concentration distributions of defects [3], as well as their evolution during the heat treatment. This may be the reason for the difference in the Curie temperatures of the wires with different diameters.

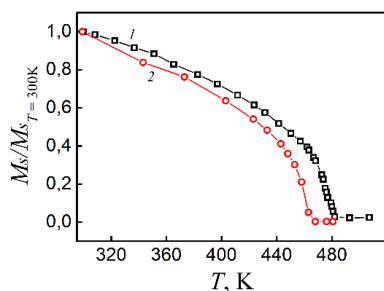


Fig. 2. Temperature dependences of the reduced saturation magnetization of the heat-treated amorphous wire: 1–180  $\mu\text{m}$  and 2–150  $\mu\text{m}$ .

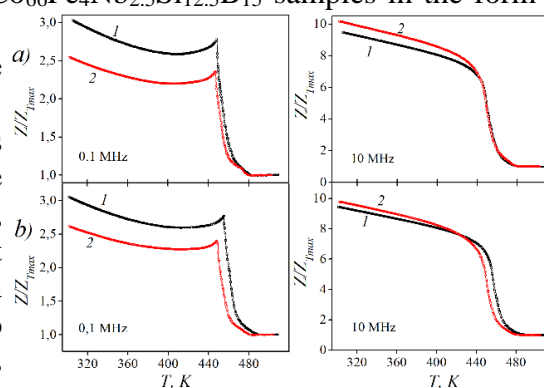


Fig. 1. Temperature dependences of the reduced impedance of amorphous  $\text{Co}_{66}\text{Fe}_4\text{Nb}_{2.5}\text{Si}_{12.5}\text{B}_{15}$  wires with a diameter of 180  $\mu\text{m}$  (1) and 150  $\mu\text{m}$  (2). The dependences were obtained at AC frequencies of 0.1 and 10 MHz before (a) and after (b) heat treatment.

[1] A.A. Moiseev, M.S. Derevyanko, D.A. Bukreev, G.V. Zakharov, A.V. Semirov, Phys. Met. Metallogr. 123, 874 (2022).

[2] A.S. Antonov, V.T. Borisov, O. V Borisov, V.A. Pozdnyakov, A.F. Prokoshin, N.A. Usov, J. Phys. D. Appl. Phys. 32, 1788–1794 (1999).

[3] Betekhtin V.I., Kadomtsev A.G., Kipyatkova A.Yu., Glezer A.M., Physics of the Solid State. 40, 74-78 (1998).

Supported by the Russian Scientific Foundation (grant no. 22-22-00709, <https://rscf.ru/project/22-22-00709/>).

# The influence of the length and applied magnetic fields to the behaviour of magnetic filaments with solvophobic, super-paramagnetic colloids

D. Mostarac<sup>a</sup>, E. Novak<sup>b,\*</sup>, S. Kantorovich<sup>a</sup>

<sup>a</sup> University of Vienna, 1090, Vienna, Austria

<sup>b</sup> Ural Federal University named after the first President of Russia B.N. Yeltsin, 620000, Ekaterinburg, Russia

\*ekaterina.novak@urfu.ru

The idea of smart, magneto-responsive materials has brought forth a surge of synthetic soft matter system designs, since magnetic fluids were first synthesized. Such materials, which are responsive to magnetic fields, can be made by combining magnetic micro- and nanoparticles with conventional soft materials, such as fluids or gels. Out of these systems, magnetic filaments first synthesized as micron-sized magnetic-filled paramagnetic latex beads forming chains, open up a plethora of new potential applications. They have been experimentally investigated as artificial swimmers for cellular engineering uses and biomimetic cilia designs. Even though synthesis techniques of magnetic filaments are nowadays rather diverse and powerful there is no clear recipe how to create a polymer-like, supracolloidal chain, that exhibits the desirable "polymeric" flexibility, and a significant magneto-responsiveness that supplants the magnetic response of the monomers - magnetic nanoparticles. Considering the length scales characteristic of single-domain nanoparticles used to create magnetic filaments, the magnetic nanoparticles can be both ferro- and super-paramagnetic. Moreover, steric or electrostatic stabilisation might not fully screen Van der Waals interactions.

In this work, using coarse-grained molecular dynamics simulations, we investigate the influence of susceptibility of super-paramagnetic magnetic nanoparticles, their number and central attraction forces between them, on the polymeric, structural and magnetic properties of magnetic filaments with varied backbone rigidity. In particular, we elucidate the implications of filament length, crosslinking approach, monomer susceptibility, and central inter-monomer attraction. We find that for a flexible backbone, where the rotational degrees of freedom between the monomers are decoupled, and the magnetic susceptibility of monomers is low, magnetic filaments assume collapsed conformations, with a close to a close packing of monomers - each monomer is surrounded by seven eight nearest neighbours, out of which, however, only two-three are favourable in terms of the dipole-dipole interaction energy. In such compact conformations the dipoles are forced into unfavourable alignment, which can hinder the magneto-responsiveness of magnetic filaments. The decrease in magnetisation is more pronounced, for more magnetically susceptible monomers: one might need to double the field strength in order to achieve magnetisation of magnetic filaments with no Van der Waals forces present. For a backbone with rigidity against bending, the additional correlations induced by the crosslinking notably enhanced the magneto-responsiveness of magnetic filaments in weak applied fields, particularly for highly susceptible monomers, where we observe less compact conformations.

This research has been supported by the Russian Science Foundation Grant No 19-72-10033.

# The magnetization reversal of the finite-size Co and Fe chains on Pt(664) surface: a comparison of the analytical and the computational results

A. Klavsyuk, S. Kolesnikov\*, E. Saprionova

Lomonosov Moscow State University, 119991, Leninskie gory 1, Moscow, Russia

\* kolesnikov@physics.msu.ru

An intensive study of magnetic properties of single-atomic chains has begun after the discovery of the giant magnetic anisotropy energy (MAE) of Co atoms and Co atomic chains on the Pt(997) [1,2]. Ferromagnetic Co chains can grow on the step edges of Pt(997) surface as a result of self-organization process at low concentrations of Co atoms and low temperatures. The analogous effect was observed for Fe atomic chains on the Cu(111) surface [3]. The applications of atomic chains in spintronics, quantum communications, quantum computing, and other fields have been discussed in literature. Strong DMI in atomic chains also can lead to some interesting phenomena. For example, biatomic Fe chains on the Ir(001)(5×1) surface have a DMI-induced noncollinear magnetic ground state [3]. Also DMI can significantly change the energies of excited states even if the ground state of an atomic chain is collinear. Using *ab initio* calculations the significant DMI in Co and Fe chains on Pt(664) surface has been predicted [4]. It has been shown that the infinitely long Co and Fe chains have the collinear ferromagnetic ground state, but DMI changes the energies of the excited states.

The magnetic properties of the atomic chains can be satisfactorily described in the framework of some effective theory including the exchange interaction, the magnetic anisotropy energy (MAE), DMI, and the interaction with the external fields. The parameters of the effective theory have been taken from Ref. [4]. For the numerical calculations the geodesic nudged elastic band (GNEB) method [5] is employed. For analytical calculations the continuous XY-model is used.

The main goal of the presented work is detailed comparison of the analytical results obtained in the framework of XY-model and the numerical results obtained with GNEB method. The following physical values are under the consideration: energy barriers for magnetization reversal, average magnetization reversal times [6] and coercivity of the finite-size Co and Fe chains. It is shown that the most of the numerical results can be satisfactorily explained in the framework of the XY-model. The limitations of the XY-model are also discussed. Finally, the influence of the long-range dipole-dipole interaction on the energy barriers for the magnetization reversal is investigated.

The research is carried out using the equipment of the shared research facilities of HPC computing resources at Lomonosov Moscow State University [7]. The investigation is supported by the Russian Science Foundation (Project No. 21-72-20034).

[1] P. Gambardella, A. Dallmeyer, K. Maiti, M. C. Malagoli, W. Eberhardt, K. Kern, C. Carbone, *Nature* 416, 301 (2002).

[2] P. Gambardella, S. Rusponi, M. Veronese, S. S. Dhesi, C. Grazioli, A. Dallmeyer, I. Cabria, R. Zeller, P. H. Dederichs, K. Kern, C. Carbone, H. Brune, *Science* 300, 1130 (2003).

[3] J. Shen, R. Skomski, M. Klaua, H. Jenniches, S. S. Manoharan, J. Kirschner, *Phys. Rev. B* 56, 2340 (1997).

[4] B. Schweflinghaus, B. Zimmermann, M. Heide, G. Bihlmayer, S. Blugel, *Phys. Rev. B* 94, 024403 (2016).

[5] P. F. Bessarab, V. M. Uzdin, H. Jonsson, *Comput. Phys. Commun.* 196, 335 (2015).

[6] S.V. Kolesnikov, E.S. Saprionova, *IEEE Magn. Lett.* 13, 2505905 (2022).

[7] V. Voevodin, et. al., *Supercomput. Front. Innov.* 6, 4 (2019).

# The Structural and Magnetic Properties of a Ferrocomposite: the Role of Polydispersity

A. Solovyova\*, D. Rudushnov, E. Elfimova

Ural Federal University, 620000, 51 Lenin Avenue, Ekaterinburg, Russia

\*corresponding author email: Anna.Soloveva@urfu.ru

This study is devoted to the theoretical investigation of the structural and magnetic properties of a ferrocomposite, taking into account the orientation anisotropy and polydispersity of system in the framework the bidisperse approximation. The process being modeled can be divided into two steps. In the first step, the sample's orientational structure is formed: in response to a magnetic field, particles move and rotate, changing the orientation of their magnetic moments and easy magnetization axes. Once thermodynamic equilibrium is reached, the orientational and rotational degrees of freedom of the particles are fixed. As a result, an orientational texture of the easy axes is formed in the ensemble of immobilized particles. In the second step, the ensemble of immobilized particles is placed in a magnetic field directed parallel to the field that was applied during the first step. Due to Neel relaxation, the magnetic moments of the particles change their orientation, resulting in the sample's magnetization. In the first step, the magnetic field  $\mathbf{h}_p$  with the intensity  $h_p$  is directed parallel to the axis  $Oz$ ; the magnetic field  $\mathbf{h}$  acting on the system in the second step has the intensity  $h$  and  $\mathbf{h} \parallel \mathbf{h}_p$ . The obtained analytical expressions make it possible to calculate the magnetization and distribution function of the easy axes of magnetic filler particles depending on the dispersion composition, the concentration of magnetic particles, the intensity of dipole–dipole interaction, and sample synthesis conditions.

The bidisperse systems were considered at fixed volume concentration  $\varphi = 0.125$ , corresponding to saturation magnetizations  $M(\infty) = 50$  kA/m. The fraction of small particles  $\nu_s = N/N_s$  took values 1, 0.8, 0.5, 0.2 and 0. For each bidisperse configuration, two sets of Monte-Carlo calculations were performed: the magnetization curve  $M(h_p)$  for system of the particles in a liquid carrier before polymerization and the magnetization curve  $M(h, h_p)$  for immobilized particles after polymerization. The magnetization results for bidisperse polymer were average over 10 independent configurations of positions and orientations. Typical polymer configurations obtained at the polymerization field  $h_p = 40$  kA/m are presented in Figure 1. Comparison of theoretical and numerical results shown a good agreement for both the magnetization and distribution function of the easy axes of magnetic filler particles.

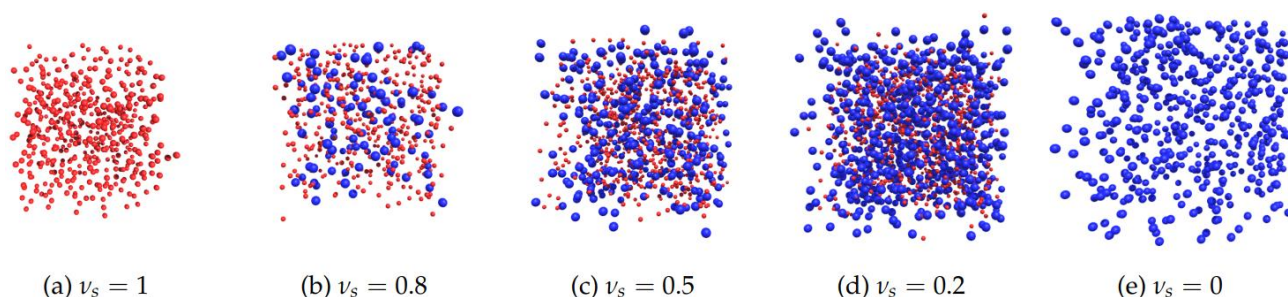


Figure 1. The bidisperse samples with total volume concentration  $\varphi = 0.125$  in the field  $h_p = 40$  kA/m and diferent value of small particle fraction  $\nu_s$ . Small particles are presented in red color; blue color demonstrates the large particle fraction.

The research was supported by the Russian Science Foundation, Grant No. 23-12-00039.

## The study of magnetic interactions in two-dimensional magnetoplasmonic crystals with Kerr magnetometry

Z. Grigoreva<sup>a,\*</sup>, D. Murzin<sup>a</sup>, V. Belyaev<sup>a</sup>, Ch. Gritsenko<sup>a</sup>, A. Kozlov<sup>b</sup>, A. Ognev<sup>b</sup>, V. Rodionova<sup>a</sup>

<sup>a</sup> Immanuel Kant Baltic Federal University, 236004, Nevskogo 14, Kaliningrad, Russia

<sup>b</sup> Far Eastern Federal University, 690922, Ajax Bay, Russky Island, Vladivostok, Russia

\*grigoreva-zoja@rambler.ru

The use of magnetic field sensors is relevant and in demand in various fields and applications. Despite all the variety of methods for magnetic field sensors fabrication in their development, special attention is paid to the increase of such characteristics as sensitivity, resolution, locality, and operating temperature range to improve conditions of use. Magnetoplasmonic crystals (MPICs) can be used as sensing elements in magnetic field sensors [1]. MPICs are nanostructures where the excitation of surface plasmon polaritons (SPPs) is observed. One of the prerequisites for SPP excitation is the structuring of metallic films, where the excitation of SPPs is triggered by the diffraction effects. Simultaneous detection of two orthogonal magnetic field components can be accomplished with two-dimensional MPICs. 2D structures possessing more reciprocal vectors can be used for simultaneous detection of two orthogonal magnetic field components by the additional flexibility of the surface plasmon resonance excitation via mutual orientation of plane of light incidence and reciprocal lattice of MPIC [3].

Two-dimensional diffraction gratings were fabricated by the electron-beam lithography. The samples represent nine 500x500  $\mu\text{m}$  areas each with two-dimensional lattices with the periods either of 500 nm, 600 nm or 700 nm. The exposure was performed with the beam current of 14 nA and doses ranging from 200 to 600  $\mu\text{C}/\text{cm}^2$  with the increment of 50  $\mu\text{C}/\text{cm}^2$ . The surface morphology of magnetoplasmonic crystals was investigated using a scanning electron microscope with the accelerating voltage of 30 kV. Magneto-optical properties of the samples were investigated with Kerr magnetometer. The NanoMOKE II setup was used for the investigation of samples' magnetization reversal. Magnetic field was applied in plane of the sample with respect to at angles of 0°, 45° and 90° during the experiment.

Increase of the exposure dose from 200  $\mu\text{C}/\text{cm}^2$  to 600  $\mu\text{C}/\text{cm}^2$  results in a double-step-like hysteresis behavior. This behavior corresponds to the alternate magnetization reversal of at least two ferromagnetic phases when applying the magnetic field at 0°, 45°, and 90°. Additionally, the mentioned increase in dose leads to a shift in the switching fields of the lower-coercive phase. The occurrence of magnetization reversal steps in hysteresis loops is likely a consequence of the presence of individual diffraction lattice elements.

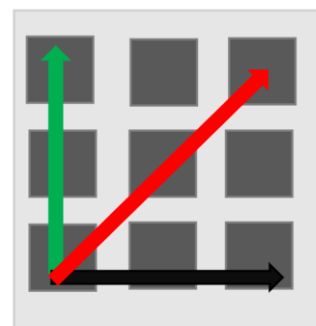


Figure 1. The direction of the applied magnetic field to the sample is indicated by the following colors: 0° (black curves), 45° (red curves), and 90° (green curves).

[1] Belyaev V. K. et al. // Scientific Reports. – 2020. – T. 10. – №. 1. – C. 7133.

[2] Murzin D. V. et al. // Japanese Journal of Applied Physics. – 2020. – T. 59. – №. SE. – C. SEEA04.

[3] Chetvertukhin A. V. et al. // Journal of Applied Physics. – 2013. – T. 113. – №. 17. – C. 17A942.

# Theoretical study of the cation and magnetic ordering in $\text{Ni}_x\text{Co}_{3-x}\text{B}_2\text{O}_6$

S. Sofronova<sup>a,\*</sup>, M. Pavlovskii<sup>a</sup>, A. Chernyshov<sup>a</sup>, E. Moshkina<sup>a</sup>, D. Velikanov<sup>a</sup>

<sup>a</sup> L. V. Kirensky Institute of Physics, Krasnoyarsk Scientific Center, Siberian Branch, Russian Academy of Sciences, 660036, Akademgorodok 50, b.36, Krasnoyarsk, Russia

\*ssn@iph.krasn.ru

We investigate the electronic structure, structural and magnetic properties of  $\text{Ni}_x\text{Co}_{3-x}\text{B}_2\text{O}_6$  ( $x = 0, 1, 2, 3$ ) using density functional theory calculation including spin-orbit coupling. The distribution of 3d-metal ions on crystallographic positions in  $\text{NiCo}_2\text{B}_2\text{O}_6$  and  $\text{Ni}_2\text{CoB}_2\text{O}_6$  were studied. The spin exchange interactions between the Ni(Co) ions were evaluated.

$\text{Ni}_x\text{Co}_{3-x}\text{B}_2\text{O}_6$  crystals belong to the  $\text{Pnmm}$  ( $D_{2h}^{12}$ ) space group (kotoite structure) [1,2]. The unit cell involves two formula units. Magnetic atoms are Ni (Co) occupying two nonequivalent crystallographic positions 2a and 4f. Thus, there are six magnetic atoms in the unit cell. The  $\text{Ni}_3\text{B}_2\text{O}_6$  and  $\text{Co}_3\text{B}_2\text{O}_6$  crystals are collinear with the easy magnetization axis directed along  $a$  axis for  $\text{Ni}_3\text{B}_2\text{O}_6$  and along  $c$  axis for  $\text{Co}_3\text{B}_2\text{O}_6$ [3]. In  $\text{Co}_3\text{B}_2\text{O}_6$ , in contrast to  $\text{Ni}_3\text{B}_2\text{O}_6$ , there is strong anisotropy of magnetization both above and below the temperature of the magnetic phase transition.

The calculations of energies of compounds  $\text{Ni}_x\text{Co}_{3-x}\text{B}_2\text{O}_6$  ( $x=1, 2$ ) in different cation ordered states showed that Ni and Co ions are not randomly distributed. In  $\text{Ni}_2\text{CoB}_2\text{O}_6$  Ni ions prefer to occupy crystallographic position 4f. In  $\text{NiCo}_2\text{B}_2\text{O}_6$  Ni ions prefer to occupy crystallographic position 2a. In agreement with experiment, these calculations reveal a strong magnetocrystalline anisotropy in  $\text{Co}_3\text{B}_2\text{O}_6$  with a magnetization easy axis directed along  $c$  axis. The anisotropy in  $\text{Ni}_3\text{B}_2\text{O}_6$  is weak with a magnetization easy axis directed along  $a$  axis. The calculated spin exchange interactions are similar for both crystals. There is the competition between the antiferromagnetic and ferromagnetic exchange in both crystals.

The research was funded by Russian Science Foundation and Krasnoyarsk Regional Fund of Science, project № 23-12-20012 (<https://rscf.ru/en/project/23-12-20012/>).

[1] R.E. Newnham, M.J. Redman and R.P. Santoro, Z. Krist, 121, 418 (1965).

[2] R.E. Newnham, R.P.Santoro, P.F. Seal, G.R. Sallings, Phys. Status.Solidi, 16, K17 (1966).

[3] L. N. Bezmaternykh, S. N. Sofronova, N. V. Volkov, E. V. Eremin, O. A. Bayukov, I. I. Nazarenko and D. A. Velikanov, Phys. Status Solidi B, 1–6 (2012)

# UHV Technological System for Synthesis and in situ Investigation of Nanostructures by Spectral Magneto-Optical Ellipsometry

D. Shevtsov<sup>a</sup>, S. Lyaschenko<sup>a</sup>, S. Varnakov<sup>a</sup>,  
S. Ovchinnikov<sup>a,b</sup>, O. Maximova<sup>a,b</sup>.

<sup>a</sup> Kirensky Institute of Physics SB RAS, 660036, Krasnoyarsk, Russia

<sup>b</sup> Siberian Federal University, 660041 Krasnoyarsk, Russia

\* e-mail:sdv@iph.krasn.ru

In recent decades, special attention has been paid to the methods of synthesis and investigation of nanoscale structures such as "ferromagnetic metal/semiconductor", where such elements as Ni, Mn, Co, Fe can be used as metal and Si, Ge can be used as semiconductor layer. One of the promising materials are ternary compounds based on oxygen-free ceramics, among which the MAX phases are considered. Such special layered nanostructures exhibit a unique combination of the most sought-after properties typical of both ceramics and metals [1].

When synthesizing these structures, it is very important to pay attention not only to their formation, but also to the composition and properties of the interlayer interfaces. Nondestructive diagnostics and control of nanosystems directly in the process of their creation offer great opportunities for investigation, allowing the synthesis of nanomaterials with controllable composition and desired characteristics, structure and properties on the atomic and subatomic level.

Reflectance spectral magnetoellipsometry, a non-destructive in situ method of surface analysis, makes this possible [2]. This polarization optical method makes it possible to obtain quantitative information about the structure and morphology of the surface of the sample under study, to find out its spectral-optical and magneto-optical parameters directly in the process of structure formation, as well as to perform magneto-optical analysis of thin films by placing a ferromagnetic sample in an external magnetic field. In situ ellipsometry and magneto-optical measurements at different temperatures are very interesting for studying solid-phase synthesis reactions, electronic structure, and phase transitions in ferromagnetic materials [3].

The developed ultrahigh-vacuum installation for obtaining thin films and multilayer materials from various elements is described, in which the combined use of in situ magnetoellipsometric method of analysis and systems of specimen temperature setting in a wide range with the application of an external magnetic field of a given value to it is implemented [4].

To demonstrate the capability of the created ultrahighvacuum complex, the Fe/SiO<sub>2</sub>/Si(100) structure was synthesized on a substrate surface with nondestructive in situ ellipsometric control and in situ studies of the obtained nanostructure by magnetoellipsometry in the temperature range 85-1005 K in one technological cycle.

The research was performed at the Magnetic MAX Materials Laboratory of the Kirensky Institute of Physics with the financial support of the Russian Science Foundation #21-12-00226, <http://rscf.ru/project/21-12-00226/>.

- [1]. M.W. Barsoum, T. E-Raghy, *Amer. Sci.* 89, 4336-345 (2001)
- [2]. O.A. Maximova, *Journal Of Magnetism And Magnetic Materials*. Volume 440, 196-198 (2017)
- [3]. I. A. Tarasov, *JETP Lett.* 99 (10), 565 (2014)
- [4]. D. V. Shevtsov, *Instruments and Experimental Techniques*. Volume 60, No. 5, 759–763 (2017)



# Unusual spin resonance in $\text{Nd}_3\text{Ga}_5\text{SiO}_{14}$ langasite: evidence of electroactive excitations

A. Kuzmenko<sup>a,\*</sup>, A. Mukhin<sup>a</sup>, V. Ivanov<sup>a</sup>, A. Tikhanovskii<sup>a</sup>,  
L. Weymann<sup>b</sup>, A. Shuvaev<sup>b</sup> and A. Pimenov<sup>b</sup>

<sup>a</sup> Prokhorov General Physics Institute of the Russian Academy of Sciences, Moscow, Russia

<sup>b</sup> Institute of Solid State Physics, Vienna University of Technology, Vienna, Austria

\* artem.kuzmenko.gpi@gmail.com

Rare earth langasites are well known piezoelectric crystals with trigonal crystallographic space group P321. Their symmetry also allows field-induced magnetoelectricity in langasites containing magnetic rare earths [1]. We studied spin resonance in  $\text{Nd}_3\text{Ga}_5\text{SiO}_{14}$ , where Nd subsystem remains paramagnetic up to the lowest temperatures. In this work, the transitions between the components of the ground Kramers doublet of  $\text{Nd}^{3+}$  were studied by terahertz quasi-optical spectroscopy in an external magnetic field up to 7 T. The ability to measure at a fixed frequency is provided by a backward wave oscillator (BWO) spectrometer, which allows tuning the frequency in a wide range from 50 to 1000 GHz using a set of BWO generators.

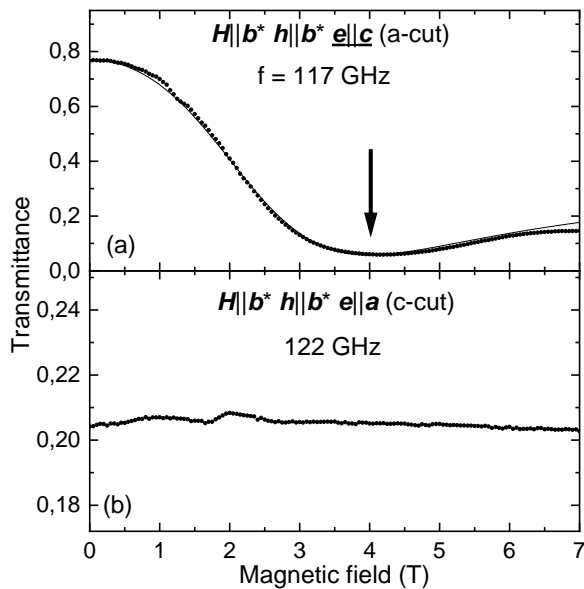


Fig. 1. Dependencies of transmittance on magnetic field  $H||b^*$  at temperature 1.8 K that demonstrate the electrical activity of the resonance mode in polarization  $e||c$  (see text). Points – experiment, line – theory.

An intense broad absorption line is visible in the  $h||b^* e||c$  polarization (Fig. 1a), but is absent in  $h||b^* e||a$  (Fig. 1b), which indicates that this line is excited by the  $e||c$  component. An intense phonon mode at a low frequency ( $\sim 600$  GHz) was observed in the same polarization  $e||c$ . Apparently, the electrical activity of the  $\text{Nd}^{3+}$  electron transition is related to the interaction between the phonon and paramagnetic resonance mode.

The frequency and magnetic dependences of the transmittance were simulated. The values of the frequencies and linewidths of the observed modes, as well as their contributions to the magnetic or dielectric permittivity were obtained.

Support by Russian Science Foundation (No. 22-42-05004) is acknowledged.

[1] L. Weymann et al., Npj Quantum Mater. **5**, 61 (2020).

Table 1. Observed excitation conditions of the resonance modes. The components that excite resonance in a given geometry are underlined. "No line" – no resonance line were reliably detected in this geometry.

		Magnetic field orientation		
		$H  a$	$H  b^*$	$H  c$
Polarization	$h  b^* e  c$	<u><math>e  c</math></u>	<u><math>e  c</math></u>	<u><math>h  b^* e  c</math></u>
	$h  c e  b^*$	<u><math>h  c</math></u>	<u><math>h  c</math></u>	no line
	$h  a e  b^*$	no line	no line	<u><math>h  a</math></u>
	$h  b^* e  a$	no line	no line	<u><math>h  b^*</math></u>

Plane-parallel samples cut perpendicular to the  $a$  ( $a$ -cut) and  $c$  ( $c$ -cut) crystal axes in various geometries of an external magnetic field  $H$  and  $ac$  magnetic  $h$  and electric  $e$  fields were studied. An analysis of the excitation conditions for all modes in various geometries (see Table 1) made it possible to establish that, in addition to the usual paramagnetic modes excited by  $h$ , the resonance is also excited by the  $ac$  electric component  $e||c$  for all investigated  $H$  orientations. An example of electroactive

# Wetting and spreading of Cu(Cr) melt over the Cr<sub>2</sub>AlC MAX phase

M. Gorshenkov<sup>a,\*</sup>, S. Zhevnenko<sup>a</sup>

<sup>a</sup> National University of Science and Technology MISIS, 119049, Leninskii pr. 4, Moscow, Russia

\*corresponding author email

Cr<sub>2</sub>AlC compound belongs to a new family of ternary layered compounds so-called MAX-phases [1]. The MAX phases are polycrystalline nanolaminated ternary carbides or nitrides [2]. These phases exhibit a unique combination of such properties as strength, ductility and toughness. The application of these materials involves the development of liquid-phase fabrication methods for composite materials [3] using MAX phases (in particular, Cr<sub>2</sub>AlC), the development of high-temperature brazing alloys, impregnating melts, etc. In the present work we have found good wetted Cu-based melts and have experimentally investigated the parameters of wetting and spreading over the sintered Cr<sub>2</sub>AlC MAX phase sample.

The wetting and spreading of Cu-based melts with addition of different element (Cr, Ti, B) over Cr<sub>2</sub>AlC MAX phase sintered sample were measured in 10<sup>-3</sup> Pa vacuum at 1150 °C. The measurements were carried out in-situ, by the dispensed drop method from a graphite dispenser. The good wettability of MAX phase surface by Cu (0.8 at.%Cr) melt at 1150 °C in vacuum was found. The contact angle of 35° was stabilized after 0.003 s. During this short time liquid metal spreading on a flat substrate can be described by a molecular kinetic model with a 2.2 Pa·s friction coefficient. Further wetting was accompanied by the active formation of a liquid phase based on Cu-Al inside the parent Cr<sub>2</sub>AlC phase with the retention of solid chromium carbide framework (presumably Cr<sub>3</sub>C<sub>2</sub>). The contact angles of the Cu (2 at.% B) and Cu (5 at.% Ti) melts on the MAX phase were found to be 138° and 91°, respectively. It is concluded that the melt containing Cr is suitable for brazing of Cr<sub>2</sub>AlC MAX-phase, which also gives a way for producing composites based on the MAX-phase by impregnation of a MAX-phase green body.

[1] S.E. Ziemniak *J. Chem. Thermodyn.* (2007)

[2] J.-M. Lihmann *J. Eur. Ceram. Soc.* (2008)

[3] E. Saiz et al. *Curr. Opin. Solid State Mater. Sci.* (2005)

# Author index

## A

Afanasyev K. ....	56
Afansiev D. ....	185
Akramov D. ....	164
Aksenov S. ....	14
Alberti S. ....	16
Albino M. ....	99
Alekhina Iu. ....	19
Aleroev A. ....	73
Alexandrov A. ....	96
Aliiev A. ....	36
Alina Y. ....	95
Aliya B. ....	95
Al-khadj Aioub A. ....	144
Amirov A. ....	120
Andreev N. ....	111
Andreiko M. ....	132
Andryushchenko T. ....	49, 125, 126, 129, 130
Anikin A. ....	91, 92, 99, 106, 107
Antonov I. ....	136
Astakhov V. ....	134
Avdeev M. ....	32
Averkiev N. ....	93, 177
Azarevich A. ....	100
Azarova L. ....	98

## B

Babkin A. ....	155
Babu P. ....	74
Bachurin V. ....	136
Baigutlin D. ....	66, 77, 105
Bakhtiarov A. ....	28
Balymov K. ....	131
Baraban I. ....	111
Baranov N. ....	164
Barucca G. ....	109
Baryshev A. ....	23, 56
Batulina R. ....	147, 160
Bazrov M. ....	162
Belotelov V. ....	27
Belyaev V. ....	91, 92, 99, 107, 115, 150, 190
Belykh S. ....	142
Bichurin M. ....	114
Biziaev D. ....	71
Bizyaev D. ....	159
Bobuyok S. ....	141
Boev N. ....	51, 138
Bogach A. ....	100
Bondarev M. ....	130
Borus A. ....	12

Bozhev I. ....	108
Bratschisch R. ....	150
Brodovskaya E. ....	144
Buchelnikov V. ....	66, 77, 105
Bukreev D. ....	166, 186
Bunge A. ....	21
Burmistrov I. ....	155
Bykov A. ....	175
Bykov V. ....	136

## C

Castagnotto E. ....	109
Chairetdinova D. ....	71
Chashin D. ....	88
Chechenin N. ....	154
Chekanova L. ....	135
Cherkasova N. ....	156
Chernousov N. ....	38
Chernov A. ....	104
Chernozem P. ....	39
Chernozem R. ....	39
Chernyshov A. ....	191
Cherosov M. ....	147, 160
Chichay K. ....	42
Chigarev S. ....	71
Chinenkov M. ....	117
Chirikov D. ....	26
Christianen P. C. M. ....	78
Chupakhina T. ....	160
Cima-Cabal M. ....	21

## D

Danil A. ....	95
Danilov Yu. ....	136
Darwish A. ....	112
Davkina A. ....	106, 107, 120
Davydenko A. ....	38
Deeva Yu. ....	147, 160
Demin G. ....	84
Demina P. ....	81, 124, 139
Denisova E. ....	135
Derevyanko M. ....	166, 186
Dikansky Yu. ....	133
Djuzhev N. ....	84, 117
Dolgova T. ....	45
Doludenko I. ....	71, 123, 143, 159, 165
Dorokhin M. ....	81, 124, 137, 139
Dorozhko D. ....	133
Draganyuk O. ....	17, 149
Drovorub E. ....	94
Drozd D. ....	168

# IBCM-2023

Dubrovskiy A. ....	57
Dudin Yu. ....	136
Dzhun I. ....	154

## E

Egorov S. ....	41
Elfimova E. ....	189
Eremin E. ....	76, 128, 161
Eremina R. ....	160
Eryzhenkov A. ....	48
Evstigneeva S. ....	31, 112

## F

Fattakhov I. ....	152
Fedina A. ....	84
Fedorova N. ....	18, 103
Fedulov F. ....	80
Fedyanin A. ....	4, 45, 108
Ferretti M. ....	16
Fetisov L. ....	80, 88
Fetisov Y. ....	88
Filipov V. ....	100
Filippov N. ....	117
Flachbart K. ....	100
Fomin L. ....	71
Fortuna A. ....	50
Fraerman A. ....	33, 46, 60
Frolov A. ....	45, 108

## G

Gabáni S. ....	100
Gamzatov A. ....	36
Gan'shina E. ....	79
García-Suárez M. ....	21
Gareev K. ....	75
Gaviko V. ....	119
Gavriliuk A. ....	14
Gavrilova T. ....	147, 160
Gerasimov E. ....	7, 119
Gerasimova Yu. ....	57
German S. ....	146
Gippius A. ....	143
Gladkikh D. ....	133
Glushkov V. ....	100
Goihman A. ....	145
Goikhman A. ....	173
Gonchar L. ....	85
Gorev R. ....	60, 137
Gorin D. ....	146
Gorshenkov M. ....	50, 111, 194
Goryacheva I. ....	53, 168
Goryacheva O. ....	53

Granovsky A. ....	20, 79
Grigoreva Z. ....	190
Grigoriev S. ....	98
Gritsenko Ch. ....	190
Grunin A. ....	173
Gubkin A. ....	119
Gudim I. ....	76, 127, 128, 161
Gudkov V. ....	93, 177
Gudkova S. ....	156, 183
Gusev N. ....	33, 68
Gusev S. ....	33

## H

Harin E. ....	52
Hodapp M. ....	69, 153

## I

Ignatov A. ....	24, 101
Ignatyeva D. ....	169
Ildus S. ....	95
Inishev A. ....	119
Iskakova L. ....	43
Iskhakov R. ....	40, 51, 135, 138
Ivanov S. ....	114
Ivanov V. ....	44, 148, 193
Ivanova A. ....	14

## J

Janson S. ....	75
Jovanović S. ....	92

## K

Kalachikova I. ....	143
Kalashnikova A. ....	6, 78
Kalentyeva I. ....	136, 137
Kalinin M. ....	131
Kaluzhnaya D. ....	63
Kaminskiy A. ....	5
Kanevskii V. ....	82, 83, 163
Kanevsky V. ....	140
Kantorovich S. ....	187
Kapralov P. ....	112, 167, 169
Karashtin E. ....	89
Karpenkov A. ....	72, 73
Karshieva S. ....	13
Kaspar C. ....	150
Kazak N. ....	172
Kern J. ....	150
Khairtdinova D. ....	123, 159
Khanadeev V. ....	91
Khantimerov S. ....	147

# IBCM-2023

Kharitonskii P.	75
Kholkin A.	39
Khoroshilov A.	100
Khutieva A.	97
Khutorskaya I.	144
Kichin G.	64, 102
Kikteva V.	64
Kirichuk G.	173
Kiryakov M.	45
Kiseleva K.	64, 102
Kislinski Yu.	180
Klavysyuk A.	188
Knyazev Y.	57
Koksharov Yu.	22
Kolesnikov S.	35, 188
Kolesnikova V.	111
Kolmychek I.	68
Komogortsev S.	40, 135
Kon I.	170
Konstantinova E.	154
Koptsev D.	39
Korneva N.	105
Korostelin Yu.	93, 177
Korovushkin V.	155
Korshunov A.	65, 171, 175
Koshelev I.	140
Koshev N.	112, 167
Kostishyn V.	134, 155
Kostiuchenko T.	70
Kotychkov A.	69, 153
Koudan E.	13
Kovaleva A.	103
Kovaleva P.	13
Kozabaranov R.	65, 171, 175
Kozak V.	18, 103
Kozenkova E.	182
Kozlov A.	38, 145, 162, 179, 190
Kozlova E.	15
Kramarenko E.	8
Krasikov K.	100
Kravtsov E.	46
Kriukov R.	136
Krivoshapkin P.	61
Krylov A.	128
Kryuchkova A.	61
Kryukova O.	51, 138
Kudasov Yu.	65, 118, 171, 175
Kudrin A.	136, 139
Kudyukov E.	131
Kulikova D.	23, 56
Kurbanova D.	174
Kurganskaya A.	72
Kuzmenko A.	44, 148, 193
Kuznetsov Yu.	139
Kuznetsov Yu.	81, 137

Kuznetsova M.	162
Kvartalov V.	82, 83

## L

Ladygina V.	51
Lapine M.	11
Laptash N.	57
Laureti S.	109
Leontyev A.	167
Lepalovskij V.	131
Lesnikov V.	81
Levada K.	92, 99, 106
Levin A.	13
Li O.	51, 138
Litvinova L.	92
Lobanov D.	28
Lobanov I.	42, 54, 86, 122
Logunov M.	65
Lomov A.	152
Lomova M.	25
Lukkareva S.	165
Lukoyanov A.	74
Lukyanenko A.	12, 49, 59, 130, 151
Lupandin L.	143
Lushnikov S.	72
Lutsenko O.	31, 112, 167
Luzan N.	12
Lyadov N.	147
Lyaschenko S.	49, 125, 126, 129, 130, 192
Lyashko S.	169
Lysenko E.	141
Lyubutin I.	14
Lyubutina M.	14

## M

M. Ostras.	112
Magomedov E.	55
Magomedov K.	37, 107
Magomedov M.	174
Makarin R.	19
Makarov I.	65, 171, 175
Makarova L.	19
Maksimova K.	145, 173
Mamian K.	108
Marqués-Fernández J.	21
Martínez-García J.	21
Maslov D.	65, 118, 171, 175
Matyunina M.	66, 105
Maximova O.	126, 192
Maydykovskiy A.	29
Mazaletsky L.	152
Mikhailova T.	169
Mikhashenok N.	127

# IBCM-2023

Mironov V. ....	60
Mironovich A. ....	14
Mohov A. ....	40
Moiseev A. ....	166, 186
Moiseeva E. ....	146
Molokeev M. ....	127
Morchenko A. ....	132, 134, 155
Morgunov R. ....	82, 83, 163
Morozova T. ....	50
Moshkina E. ....	191
Moshkov A. ....	168
Moskal I. ....	180
Mostarac D. ....	187
Mostovshchikova E. ....	67
Motorzhina A. ....	92, 99, 106
Mukhin A. ....	44, 148, 193
Murtazaev A. ....	174
Murtazaev K. ....	174
Murzin D. ....	106, 107, 115, 150, 190
Murzina T. ....	29, 68
Musatov V. ....	80, 88
Mushnikov N. ....	7, 119
Musikhin A. ....	110

## N

Namsaraev Zh. ....	179
Nemtsev I. ....	135
Neskoromnaya E. ....	155
Nesterov V. ....	154
Nezhdanov A. ....	136
Nikitin P. ....	9
Nikitov S. ....	65
Nikolaev A. ....	158
Nikolaev E. ....	141
Nikolaev S. ....	20
Nikolaeva E. ....	51, 138
Novak E. ....	187
Novikov I. ....	45, 69, 70, 153
Novikov V. ....	68

## O

Ogloblichev V. ....	164
Ognev A. ....	190
Olshevskaya J. ....	103
Omelyanchik A. ....	107, 109, 111, 182
Omelyanchik S. ....	55
Oreshkin G. ....	117
Orlova A. ....	137
Ostras M. ....	167
Ovchinnikov S. ....	18, 49, 103, 126, 129, 192
Ovchinnikova T. ....	103
Ovsyannikov G. ....	180

## P

Pakhomov A. ....	104, 116
Pakhomova A. ....	132
Panina L. ....	31, 71, 91, 92, 99, 123, 159, 165
Pankrats A. ....	127
Parafin A. ....	136
Pashenkin I. ....	46, 68
Pashenko A. ....	38
Patel A. ....	74
Pavlova K. ....	157, 183
Pavlovskii M. ....	191
Pavlyuk M. ....	82, 83
Peddis D. ....	16, 21
Pernice W. ....	150
Perov N. ....	19, 87, 184
Perova N. ....	79
Petrov S. ....	13
Petrov Yu. ....	33
Petrzhik A. ....	180
Pilati V. ....	21
Pimenov A. ....	193
Pisarev R. ....	78
Piskunov Yu. ....	164
Platonov V. ....	65, 171, 175
Podkur P. ....	82, 83, 140, 163
Poltorabatko D. ....	170
Polushkin N. ....	46
Popov A. ....	152
Popov V. ....	45, 108
Potkina M. ....	122
Presnov D. ....	154
Prihodchenko A. ....	162
Pripechenkov I. ....	79
Prosnikov M. ....	78
Prudnikov P. ....	94
Prudnikov V. ....	94
Pryanichnikov S. ....	67
Pshenichnikov S. ....	92, 99
Pshenichniy K. ....	98
Punda A. ....	183
Pyankov V. ....	51, 138
Pyataev N. ....	112, 144
Pyatakov A. ....	5

## R

Radchenko I. ....	112, 167
Raikher Yu. ....	24, 62, 101
Ralin A. ....	75
Ramazanov M. ....	174
Rautskii M. ....	59, 130, 151
Repin P. ....	175
Reznikova P. ....	140
Rivas M. ....	21, 111

# IBCM-2023

Rizvanova A. ....	159
Rodionova V. 24, 55, 91, 92, 99, 101, 106, 107, 111, 115, 120, 150, 182, 190	
Rudenko R. ....	59
Rudushnov D. ....	189
Ryapolov P. ....	63
Rybkin A. ....	48
Rylkov V. ....	20

## S

Sadovnikov A. ....	97
Sadykov A. ....	164
Salnikov V. ....	91
Salvador M. ....	21
Samusev I. ....	170
Sangregorio C. ....	91, 99
Sapozhnikov M. ....	33, 46
Sapronova E. ....	35, 188
Sarychev M. ....	93, 177
Savelev D. ....	80, 88
Selemir V. ....	65, 175
Selezneva N. ....	164
Semirov A. ....	166, 186
Senatov F. ....	13
Sergienko E. ....	75
Setrov E. ....	75
Sgibnev E. ....	23
Shadrin A. ....	180
Shanmukharao Samatham S. ....	74
Shapeev A. ....	69, 70, 153
Shcherba K. ....	132
Sheftel E. ....	52
Shelaev A. ....	23
Shendrikova L. ....	152
Sherstyuk D. ....	157, 184
Shevtsov D. ....	49, 126, 129, 192
Shevyrtalov S. ....	111
Sheydaev T. ....	75
Shilov N. ....	106, 107
Shilov R. ....	55
Shipkova E. ....	184
Shishelov A. ....	179
Shitsevalova N. ....	100
Shlyapkina V. ....	144
Shubin A. ....	18, 103
Shuleiko D. ....	154
Shuvaev A. ....	193
Shvets P. ....	145
Sidane I. ....	16
Simakin S. ....	136
Sitnikov A. ....	20
Skidanov V. ....	47
Skirdkov P. ....	64, 102, 104
Skorobogatov S. ....	127

Skorokhodov E. ....	60
Slimani S. ....	16, 109
Sluchanko N. ....	100
Sobolev I. ....	151
Sobolev K. ....	106, 107
Sobolev V. ....	55
Sofronova S. ....	191
Sokolov A. ....	12
Sokolov O. ....	114
Sokolov Ya. ....	176
Sokolov E. ....	63
Sokolovskiy V. ....	66, 77, 105
Solizoda I. ....	156, 157
Solovyova A. ....	189
Stepanov G. ....	28, 110
Sterkhov E. ....	67
Stognij A. ....	65
Stolbov O. ....	24, 62, 101
Stolyar S. ....	40, 51, 138
Storozhenko P. ....	28
Strelkov I. ....	65, 171, 175
Strokin P. ....	168
Struzhkin V. ....	14
Sukhachev A. ....	59
Sukhorukov G. ....	112
Surdin O. ....	65, 171, 175
Suresh K. ....	74
Surikov V. ....	177
Surmenev R. ....	39
Surmeneva M. ....	39

## T

Tananaev P. ....	23
Tantardini C. ....	69, 153
Tarasov A. ....	18, 48, 59, 103, 130, 151
Taskaev S. ....	157, 181
Tataeva S. ....	37
Tatarskiy D. ....	33, 60, 137
Tedzheto V. ....	52
Temiryazev A. ....	29, 33
Temiryazeva M. ....	29
Terentev P. ....	119
Tereshina I. ....	72, 73
Tikhanovskii A. ....	44, 148, 193
Timin A. ....	112
Titova V. ....	76, 128, 161
Tkachenya A. ....	132
Tkachev A. ....	143
Tomilin F. ....	18, 103
Trofimov E. ....	181
Troyan I. ....	14
Trushin O. ....	152
Tsepanin P. ....	134
Turcu R. ....	21



# IBCM-2023

Turpak A. .... 38, 162, 179

## U

Urakova A. .... 39  
Usachev P. .... 58  
Usmanova G. .... 52  
Uspenskaya L. .... 41  
Utesov O. .... 98  
Uzdin V. .... 42, 54, 122

## V

Varnakov S. .... 18, 49, 59, 103, 125, 126, 129, 130, 192  
Vas'kovskiy V. .... 131  
Vashenina I. .... 135  
Vasilchenko D. .... 15  
Vasiliev A. .... 30  
Vazquez M. .... 111  
Ved M. .... 81, 124  
Vedyayev A. .... 96  
Velikanov D. .... 51, 57, 138, 191  
Verbetsky V. .... 72  
Vetoshko P. .... 112  
Vikhrova O. .... 136, 137  
Vinnik D. .... 156, 157, 181, 183, 184, 185  
Vlasov V. .... 178  
Volchkov I. .... 82, 83, 123, 140, 163  
Volkov N. .... 59, 151  
Volkova O. .... 90  
Volochaev M. .... 59  
Voronina S. .... 176, 178  
Vorotynov A. .... 51, 57, 138

## W

Weymann L. .... 193

## Y

Yagfarova A. .... 160  
Yakobson D. .... 144  
Yakovlev I. .... 49, 59, 125, 126, 129, 151

Yankovskii G. .... 23  
Yashchenok A. .... 146  
Yashin M. .... 79  
Yatsyk I. .... 147, 160  
Yerin C. .... 142  
Yudanov N. .... 31, 132  
Yunin P. .... 136  
Yurasov A. .... 79  
Yurlov V. .... 104, 116

## Z

Zabluda V. .... 12  
Zabotnov S. .... 154  
Zagorskiy D. .... 71, 159, 165  
Zagorsky D. .... 143  
Zagrebin M. .... 66, 77  
Zakharov D. .... 152  
Zamay G. .... 12  
Zamay S. .... 12  
Zamay T. .... 12  
Zamkova N. .... 17  
Zdoroveyshchev A. .... 81, 124, 137, 139  
Zdoroveyshchev D. .... 81, 124, 136, 137, 139  
Zeynalov R. .... 37  
Zhandun V. .... 17, 149, 172  
Zharkov M. .... 112, 144, 167  
Zhevnenko S. .... 194  
Zhevstovskikh I. .... 93, 177  
Zhigalina O. .... 71  
Zhivuli V. .... 185  
Zhivulin V. .... 156, 157, 181, 183, 184  
Zhuravlev M. .... 96, 158  
Zhurenko S. .... 143  
Zhurenok A. .... 15  
Zimina A. .... 13  
Zirnik G. .... 156  
Zubarev A. .... 26, 43, 110  
Zvezdin A. .... 116  
Zvezdin K. .... 64, 102, 104, 116  
Zykova A. .... 181  
Zyubin A. .... 170